Risk-based Optimization of Reservoir Emergency Operations

Pablo Sánchez Gómez

Source: Alberto Sánchez Gómez

Technische Universiteit Delft

TU Delft

Risk-based Optimization of Reservoir Emergency Operations

by

Pablo Sánchez Gómez

to obtain the degree of Master of Science
at the Delft University of Technology,
to be defended publicly on December 14^{th}, 2018 at 13:00 PM.

Student number:	4619781
Project duration:	February 1, 2018 – November 19, 2018
Thesis committee:	Prof. Dr. ir. S.N. Jonkman
	Dr. J.D. Bricker
	Prof. Dr. ir. P.H.A.J.M. van Gelder
	Dr. A.G. Sebastian
	Dr. ir. K.T. Lendering
	Dr. ir. E.C. van Berchum

TU Delft

Executive Summary

Dam-reservoir systems will never provide complete protection against flooding, but, when their capacity of storing excess water is properly managed, they can play an important role in flood-plain management. They are responsible for reducing the risk of loss of life and economic damages in downstream regions by temporarily retaining water during storms and releasing it afterwards at admissible non-damaging rates. Generally, dams are designed to safely retain the local runoff from minor and moderate flood events, maximizing the storm peak attenuation at downstream locations. However, as soon as the inflows are predicted to exceed the capacity of the reservoir, dam operators face an operational dilemma: how much water to release and at what rate. Although their priority is to ensure the integrity of the structure, so as to prevent catastrophic damages downstream, maximizing the use of the control storage is also desired.

As continued development in areas protected by such large-scale infrastructures coincides with changes in extreme rainfall patterns and watershed runoff characteristics, the incidence, and cost of downstream flooding can be expected to rise. As such, now, more than ever, it is crucial to be prepared to operate a reservoir under extreme circumstances, when the consequences of an operational error could be very serious. This graduation project aims to improve existing methods for developing emergency operation schedules by including the concept of risk into the optimization of flood control operations. To address this topic, the research is divided into: (1) development of a methodology for including reservoir operation effects in the risk analysis of dam-reservoir systems; (2) combination of the risk analysis procedure with an optimization algorithm to devise optimal risk-based emergency operation schedules; and (3) application of the proposed framework to a case study of the Barker Reservoir in Houston, Texas.

In Phase I, a novel procedure for conducting risk analysis applied to dam-reservoir systems is presented. The suggested approach quantitatively includes the effect of dam operations within the risk estimation process. Based on a Monte Carlo simulation technique, the methodology provides the insight required to move away from the volume-duration-frequency-based empirical analysis towards a more realistic framework for estimating risk in dam-reservoir systems. The total risk of the system is assessed as a set of structural (Ultimate Limit State) and non-structural (Serviceability Limit State) failure scenarios, each of which has a probability and a economical consequence. The serviceability limit state risk includes all those non-structural failure scenarios which may end up flooding structures from the upstream and downstream areas during normal or emergency operations, whereas the ultimate limit state refers to the risk posed by the dam due to the collapse of the structure. By using a simple hypothetical example, the importance of including dam operation as an essential component in the definition of risk is illustrated. The results demonstrate that the approaches currently use in engineering practice oversimplify the complex processes associated with dam-reservoir system operations, ultimately leading to incorrect estimations of the overall levels of risk.

Phase II focuses on combining the simulation approach for risk analysis developed in Phase I

with an optimization algorithm following a Parametrization-Simulation-Optimization technique. The suggested framework starts with the shape of an operating rule defined by four parameters responsible of dividing the reservoir into three storage zones and determining the releases at each time step. These parameters are then evaluated according to the weighted sum aggregation of minimizing flooding risks at the upstream region, minimizing flooding risk at the downstream area and minimizing the risk attributed to the structural failure of the dam. A simplified example is used to demonstrate that changing the emergency operation of reservoirs can be an efficient non-structural risk mitigation measure. Furthermore, the results reveal that the optimal operation of reservoirs depends on the characteristics of the dam structure, the upstream and downstream regions attributes, and the reservoir storage capacity. Although the optimal operations are strictly dependent on the particular system under study, similarities can be recognized between different systems. In cases in which high pool levels dictate the overall risk of the system, opening operation strategies with higher outflow rates are optimal, leading to higher risk mitigation. Meanwhile, when releases exceeding downstream channel capacities dominate the total risk of the system, flood control strategies that maximize the storm peak attenuation by closing the gates during the flood event are preferred.

The thesis culminates with a case study in which the emergency operations are optimized for the Barker Reservoir system in Houston, Texas. Susceptible to Hurricanes like Hurricane Harvey (2017) and intense precipitation events such as Tax Day (2016), the Barker system presents an operational dilemma requiring trade-offs between released flows and stored volumes. Over the lifetime of the structure, changes in extreme rainfall patterns and urban development have increased the vulnerability and exposure of both upstream and downstream communities to flooding. While release policies have been modified during the reservoir's service life in response to encroachments in the floodplain downstream of the dam, flooding of more recent commercial and residential development adjacent to publicly owned reservoir lands has also become a major concern. Using the methods developed in Phase I and II of this thesis, the flood risk analysis shows that a change in the operational strategy would contribute greatly to reducing the total risk of the system. Under extreme hydrological events, an operation strategy with releases starting at the first stages of the flood event display a reduction of almost a 32% on the total risk of the system as compared with the current operation strategy, including a 40% decrease on the ultimate limit state risk. The new operating policy, however, increases the frequency of downstream damages during non-structural low frequency failure scenarios. Therefore, an increase of the downstream channel capacity along Buffalo Bayou and adequate measures to strengthen the dam are recommended to reduce downstream damaging flooding and diminish the failure probabilities of the structure.

Acknowledgments

First of all, I would like to thank my committee members, Dr. S.N. (Bas) Jonkman, Dr. P.H.A.J.M. van Gelder, and Dr. J.D. Bricker, who have provided invaluable feedback and mentorship throughout this research; my project supervisors Erik van Berchum and Kasper Lendering for always having time for my doubts and questions; and Antonia Sebastian, probably the person to whom I am most grateful to for her dedication and for the encouraging words she always has had towards me. I would like to express my most sincere appreciation to all of them not only for the opportunity of conducting this graduation project, but also for giving me the change of visiting other institutions.

I would equally like to thank my mentors and professors at Delft University of Technology, at the Karlsruhe University of Technology and at the Polytechnic University of Madrid because a piece of everybody has been reflected within this project. I would also like to dedicate a few words to thank the professors and students at Rice University in the Department of Civil and Environmental Engineering for hosting my during the cold summer of Houston. Ferne and Connie for all those great memories and Dr. P. Bedient for making it happen.

To my colleges from Delft and Karlsruhe, with whom I have shared city, studies, coffee, lunches and ideas. Berta, Guille, Adrián, Álvaro, Cristino, Sam, Radu, Jibbe, Nacho Embid, Nacho Legorburo, Enrique, Santi and Xavi, thanks for making me feel like home and for all those good moments together. Particularly, I would like to thank my best friends and flat-mates Nacho and Alberto, without whom this work would have never been possible. For their constant support, advice and confidence, thank you so much.

Thanks also to my friends from Madrid, because even in the distance, one can always rely on them. Especially to Jaime, Fernando, Victor and Jorge for being there when needed and for putting up with labor and personal lamentations.

Last but not least, I would like to thank my parents, Eloy and Alicia, my sister, Carolina, and my brother, Alberto, for being my family and support throughout this graduation period. To my mother, because nobody takes better care of me; to my father and sister, who offered kind words and understanding during the lasts couple of months; and to my brother, for his undoubtedly help on making this report look as it is today. Their care, love, spirit, teaching and help makes them as the best mirror to look at.

"The first step is to establish that something is possible; then probability will occur"

Elon Musk

Contents

List of Figures

List of Tables

Nomenclature

Acronyms and abbreviations

Acronym	Description
APF	Annualized Probability of Failure
ALARP	As Low As Reasonably Practicable
ALL	Annualized Life Loss
ANCOLD	Australian National Committee on Large Dams
APA	Aggregated Parameter Approach
CDF	Cumulative Density Function
DP	Dynamic Programming optimization method
EAD	Expected Annual Damage
EOS	Emergency Operation Schedules
ESO	Explicit Stochastic Optimization method
FCL	Flood Control Level
FEMA	Federal Emergency Management Agency
FERC	Federal Energy Regulatory Commission
HCFCD	Harris County Flood Control District
IO	Inflow-Outflow reservoir operation strategy
ISO	Implicit Stochastic Optimization method
LP	Linear Programming optimization method
NLP	Nonlinear Programming optimization method
NOAA	National Oceanic and Atmospheric Administration
PDA	Pareto Domination Approach
PDF	Probability Density Function

PFMs	Potential Failure Modes
PSO	Parametrization-Simulation-Optimization methodology
ROMEO	Risk-based Optimization Model for Emergency Operations
SDP	Stochastic Dynamic Programming
SLS	Serviceability Limit State
SPANCOLD	Spanish National Committee on Large Dam
SUFRI	Sustainable Strategies of Urban Flood Risk Management
TCP	Top of the Conservation Pool
ULS	Ultimate Limit State
USACE	United States Army Corps of Engineers
USBOR	United States Bureau of Reclamation
USGS	United States Geological Survey
VDF	Volume-Duration-Frequency method
VEM	Volumetric Evaluation Method
WSE_{max}	Maximum Water Surface Elevation

Greek Symbols

Symbol	Description	Units
α	Generalized Extreme Value scale parameter	–
γ	Set of reservoir physical constraints	–
μ	Expected value	–
μ_{reg}	Expected value for the linear regression analysis	–
σ	Standard deviation	–
σ_{reg}	Standard deviation for the linear regression	–
θ	Set of operational constraints	–
θ_{opt}	Balance optimum solution	–
ε	Pattern search algorithm mesh size	–
ξ	Generalized Extreme Value location parameter	–

Roman Symbols

Symbol	Description	Units
a	Plotting position parameter	–
B	Breakage peak flow	m^3/s

CC	Downstream channel capacity	m^3/s
c_d	Crest overflow discharge coefficient	–
c_o	Outlet conduits discharge coefficient	–
c_s	Spillway discharge coefficient	–
d	Storm hydrograph duration	days
D_i	Potential economic consequence for scenario i	$
$D_{SLS,h}$	Damages caused by reservoir pool levels	$
$D_{SLS,O}$	Damages caused by reservoir releases	$
$D_{SLS,B}$	Damages caused by dam breach	$
D_z	Sub-critical region for the characteristic damage variable	–
$\hat{D}_i$	Supercritical region for the characteristic damage variable	–
F_H	Cumulative distribution function for initial reservoir levels	–
F_i	Cumulative distribution function of i	–
$FO(K)$	Objective function for the optimization model	–
$F_{Q,V}$	Joint cumulative distribution function of volumes and peaks	–
$f_{Q,V}$	Joint probability density function of volumes and peaks	–
F_Z	Cumulative distribution function of the characteristic damage variable	–
$g(.)$	Function accounting for the interaction between the dam structure, the operations and the external hydrologic variable	–
h	Reservoir water surface elevation or pool level	m
H_0	Initial reservoir level	m
H_{res}	Elevation of upstream residential properties	m^3/s
H_{spill}	Spillway elevation	m
h_w	Reservoir pool level at breakage	m
I	Inflow discharge entering the reservoir	m^3/s
K	Vector of decision variables for multi-objective optimization models	–
A_o	Outlet conduits cross sectional area	m^2
L_d	Dam crest length	m
L_s	Dam spillway length	m

m_1	Proposed parameter for reservoir emergency operations	–
m_2	Proposed parameter for reservoir emergency operations	–
N_i	Number of potential human lives lost for scenario i	lives
O	Outflow discharge from the reservoir	m^3/s
O_{max}	Maximum permitted released flows	m^3/s
$p_{f,h}$	Conditional structural failure probability	–
$p(h)$	Reservoir stage occurrence probability	–
$p(B,h)$	Conditional probability of breakage flows given a reservoir pool level	–
$p(O,h)$	Conditional probability of reservoir outflow given a reservoir pool level	–
p_i	Occurrence probability of scenario i	1/yr
$p_{nf,h}$	Conditional non structural failure probability	–
$p(O)$	Released flow rate occurrence probability	–
Q	Unregulated peak inflow discharge	m^3/s
$q(K)$	Constraint for a multi-objective optimization	–
$R_{SLS,h}$	Serviceability limit state risk related to upstream flooding	\$/yr
$R_{SLS,O}$	Serviceability limit state risk related to downstream flooding	\$/yr
R_T	Overall risk of a dam-reservoir system	\$/yr
$R_{ULS,B}$	Ultimate limit state risk	\$/yr
S_1	Proposed separation limit between storage zones	hm^3
s_1	Proposed parameter for reservoir emergency operations	–
S_2	Proposed separation limit between storage zones	hm^3
s_2	Proposed parameter for reservoir emergency operations	–
R^*	Combination of active storage and inflow	hm^3
S	Reservoir storage	hm^3
S_A	Expected inflow storage for emergency operation schedules development	hm^3
S_{max}	Maximum reservoir storage for emergency operation schedules development	hm^3
S_C	Critical storage for emergency operation schedules development	hm^3
s_i	Flooding scenario i	–

S_0	Initial reservoir storage	hm^3
T	Target demand for the standard linear operating rule	m^3/s
T_s	Exponential recession constant	days
T_Z	Return period of the characteristic damage variable	yr
V	Inflow hydrograph volume	hm^3
V_w	Reservoir volume at breakage point	hm^3
w_i	Weight associated to each objective in an aggregated parameter approach	hm^3

Chapter 1

Introduction

1.1 Problem Statement

In words of Professor Jim Blackburn from Rice University's Baker Institute, Hurricane Harvey clearly revealed what many people already knew for a long time: "Houston and the Houston - Galveston region have major flooding problems [1]". Geographically prone to severe tropical weather, Harris County has a long history shaped by chronic flooding. To an extent that diverse sources have described the city of Houston as America's Flood Capital [2]. According to Houston-based Weather Research Center [3], there have been at least twenty six events that flooded homes in the Houston metro area since the mid 1970s. Among others, historic Tropical Cyclones like Claudette (1979), Allison (2001) and Ike (2008), and recent precipitation events such as Memorial Day (2015) and Tax Day (2016) undoubtedly exemplify Houston's flood vulnerability. But above all, Hurricane Harvey (2017), the most significant tropical cyclone rainfall event in United States history both in scope and peak rainfall amounts [4], underscored a new reality for America's fourth-largest city.

In addition to extensive riverine inundation along Houston's creeks and bayous, the city's two main flood retention reservoirs, Addicks and Barker, were overwhelmed by inflows from upstream tributaries [5] [6]. These two dams, reclassified in 2009 as two of the six most dangerous dams in the United States, were designed and constructed in the 1940s to protect downtown Houston and the west side along Buffalo Bayou from flooding. After several days of extreme rainfall, the U.S. Army Corps of Engineers (USACE) was forced to activate the emergency operation schedules, releasing higher-than-normal rates for first time in the reservoirs' service life. By performing such controlled releases, these emergency actions avoided dam failure and uncontrolled discharges over the emergency spillways. However, they also exacerbated flooding downstream of the reservoirs [7] releasing a volume of water six times larger than Buffalo Bayou's non-damaging channel capacity and flooding approximately 9.000 homes.

When their capacity of storing excess water is properly managed [8] [9], dam-reservoir systems like Addicks and Barker, play an imperative role in flood management plans, offering an efficient means of flood control and protection [10] [11]. They reduce the risks of loss of life and property damage in downstream regions by dampen the storm's peak and delaying its appearance until the storm has passed. However, as pointed out by Valdes and Marco [12], dams are also responsible for introducing important risk factors into the system, such as dam failure or inducing flooding due to flawed outlet works operation.

The problem associated with the operation of a reservoir in the case of a flood event is fundamentally multi-objective. It involves a compromise between the released flows and the stored volumes, to neither damaging the urban areas downstream and upstream of the dam, nor endangering the safety of the structure [13]. In those situations, gate management stands as a

great challenge for the dam operator, who must make decisions in an extremely short time frame under uncertain conditions and with limited information [14]. For instance, if an operator conducts emergency releases during a storm event and later learns that the reservoir's flood pool never filled, then the operator would have unnecessarily aggravated downstream flooding conditions. On the other hand, if emergency releases are not carried out and the storage capacity is then exceeded, flood damages could occur on a much larger scale [15].

The adequate definition of flood operating rules is therefore an essential component of flood risk management in dam-reservoir systems [16]. In current practice, reservoir operators usually follow rule curves, which stipulate the amount of water to be stored and released at any time conditioned on the state of the reservoir, the downstream conditions and the future inflows entering the reservoir. Figure 1.1 represents the simplest of the reservoir operating policies. Also known as the standard linear operating policy, the rule specifies the releases as a function of the target demands, T, and the available storage capacity. It is inferred from the figure that in cases in which there is no space left in the reservoir, releases should be equal to all the water in excess of maximum storage capacity to preserve the integrity of the structure.

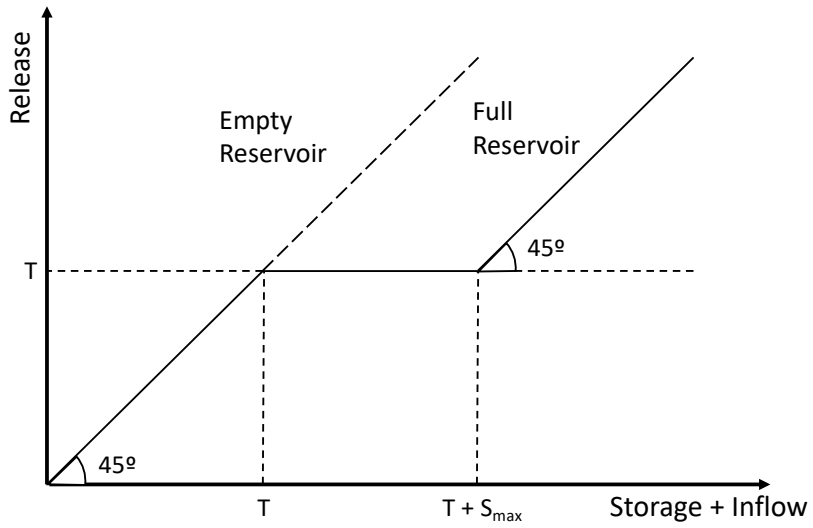

Figure 1.1: Graphical representation of the Standard Linear Operating Rule

Rule curves are typically constructed from simulation models that reproduce the reservoir responses to predefined operation constrains. Since there are often a large number of feasible policies, mathematical optimization techniques may help with the identification of the best one. The water resources literature includes a wide range of studies concerning developed mathematical optimization and simulation models [17] [18] [19]. However, most of the developed reservoir management techniques fail to address the specificities of flood control operations which are usually dealt with as a constraint to a primary conservation, hydropower or irrigation objective [20]. Furthermore, as stressed by Rivera [15], the majority of those that do focus on flood control operations, emphasize the normal rather than the emergency conditions.

Despite the increasing importance of applying risk analysis to inform dam safety decision-making [21] [22], very little research has been published related to the optimization of release and store operations using the combination of probabilities and consequences. While this was partially addressed by Rivera [15] and Rivera and Wurbs [23], an appropriate methodology for optimal risk-based reservoir operations during floods is still lacking. The standard method for developing emergency operating schedules currently in use by the USACE [24] is based on deterministic estimates of expected minimum inflow volumes and does not fully represent the

complexity of the problem regarding future inflows uncertainty. Moreover, the methodology relies on reservoir surface water levels and it lacks on mechanisms for evaluating and balancing the potential risks associated with the storage and release decisions.

According to the study on natural and technical disasters developed by Santella et. al [25], the probability of facing flooding conditions requiring emergency releases in reservoirs is still relatively small. Nonetheless, as continued development in areas protected by such large-scale infrastructure [11] coincides with changes in extreme rainfall patterns [26] and in the watershed runoff characteristics [27], now, more than ever, it is crucial to be prepared to operate a reservoir under extreme circumstances.

1.2 Research Question & Objectives

Under the title *Risk-based Optimization of Reservoir Emergency Operations*, this graduation project aims to improve existing methods for developing emergency operations schedules using a novel risk-based optimization framework. The study is based on the idea that operational decisions during extreme hydrological events should be built around the concept of risk rather than on critical water levels or downstream channel capacities. With this regard, the proposed framework should combine the simulation procedures for risk analysis of dam-reservoir systems with an optimization algorithm to create an operating rule that minimizes risk under extreme circumstances. While looking for the optimal release and storage strategy, the effect dam operations have in the total risk of a dam-reservoir system is to be investigated. These effects are a key component for the optimization framework and should be quantitatively included within the risk assessment of dam-reservoir systems.

The methodology is to be applied to the Barker Reservoir located in Buffalo Bayou Watershed of the San Jacinto River basin, approximately 25 kilometers west of downtown Houston, Texas. Together with the Addicks reservoir, the two structures form a parallel system responsible for the protection of downtown Houston and the west side of the city along Buffalo Bayou from flooding. The increase of intense rainfall events along the Texas coast [28] [29] combined with the rapid urban development along the lowlands adjacent to Harris County's bayou systems [30] highlight the necessity of adapting the emergency operation schedules of the chosen example by directly including the term risk within the operation decisions.

In view of the concerns related to the flood management and mitigation plans of dam-reservoir systems like Barker; and in order to overcome the limitations presented by the current methodologies dealing with the development of emergency operation schedules, this study seeks to answer questions such as: *How does the dam operation influence the risk? Could then total risk of a dam-reservoir system be effectively mitigated by optimizing its flood control operation? If so, what dam operation strategies minimize risk?*

In answering these questions, the research will achieve the following objectives:

1. Develop a risk assessment procedure which integrates the effect of predefined operating rules within the risk identification and estimation processes of dam-reservoir systems.

2. Develop a risk-based optimization framework for reservoir emergency operations considering downstream flooding, upstream flooding and dam failure risk as conflicting operation criteria and taking into account the stochastic nature of dam operation.

3. Utilize the framework to develop an optimal operating rule that minimizes the overall risk of the Barker Reservoir System during extreme events.

In order to cope with the objectives of the project, a Risk-based Optimization Model for Emergency Operations (ROMEO) is to be developed. The model should combine the simulation procedures for risk analysis with a optimization algorithm based on a parametrization-simulation-optimization methodology (PSO). This optimization procedure has been successfully applied in the literature [31] [32] and allows for the incorporation of inflow uncertainties into the optimization process. In their evaluation of stochastic reservoir operation optimization models, Celeste and Billib, highlighted the advantages presented by the PSO to obtain optimal rule curves [33]. The suggested approach will follow three phases: (1) parameterizing a predefined rule curve for emergency operations (2) quantifying the overall risk of the system for a given set of operation parameters using a simulation model, and (3) finding the optimal combination of parameters that assures minimum overall risk of the system by means of a pattern search algorithm.

1.3 Reading Guide

This report is comprised of six chapters. Chapter 1 provides a brief description of the problem, identifies the study area, and presents the research question, the research objectives and the research approach. Chapter 2 reviews the literature associated with the different approaches on reservoir operations during floods as well as their optimization, paying special attention to those models that account for the hydrologic variables uncertainties. Chapter 2 also reflects flood risk analysis and flood risk management and their application in the field of dam safety. The literature gaps found and covered by the project are briefly discussed at the end of Chapter 2 and more deeply analyzed at the introductory sections of Chapter 3 and Chapter 4.

An overview of Chapter 3, Chapter 4 and Chapter 5 is shown in Fig. 1.2. First, Chapter 3 presents a novel procedure for risk assessment applied to dam-reservoir systems which integrates the effects of predefined operating rules within the risk identification and estimation processes. Chapter 3 is explanatory in nature and seeks to illustrate the importance of retaining structure operations for the estimation of the total risk of the region. A simple hypothetical example is employed in order to highlight how specific assumptions in the traditional and widely used dam risk assessment methodologies could lead to over- and underestimation of the overall flood risk. The structure of the risk-based optimization framework proposed in this research is described in Chapter 4 where a closer look into the model set-up and the mathematical framework is provided. Then, the parametrization of the emergency operating rule based on the concepts of storage zoning and the relationships between inflows, outflows and storage is discussed in Chapter 4 also discusses. The chapter ends up with an evaluation of the suggested operation as a non-structural risk mitigation measure to minimize the risk of the system.

Once the proposed risk analysis methodology and risk-based optimization framework are explained, Chapter 5 addresses the implementation of the methodology in the Barker Reservoir. In addition to carrying out a quantification of the overall risk of the system given the current operation schedules, Chapter 5 also evaluates the adequacy of the suggested parametric emergency operation schedule by comparing its performance against the current operating rules. Finally, Chapter 6 summarizes the important results and addresses future challenges of the proposed framework.

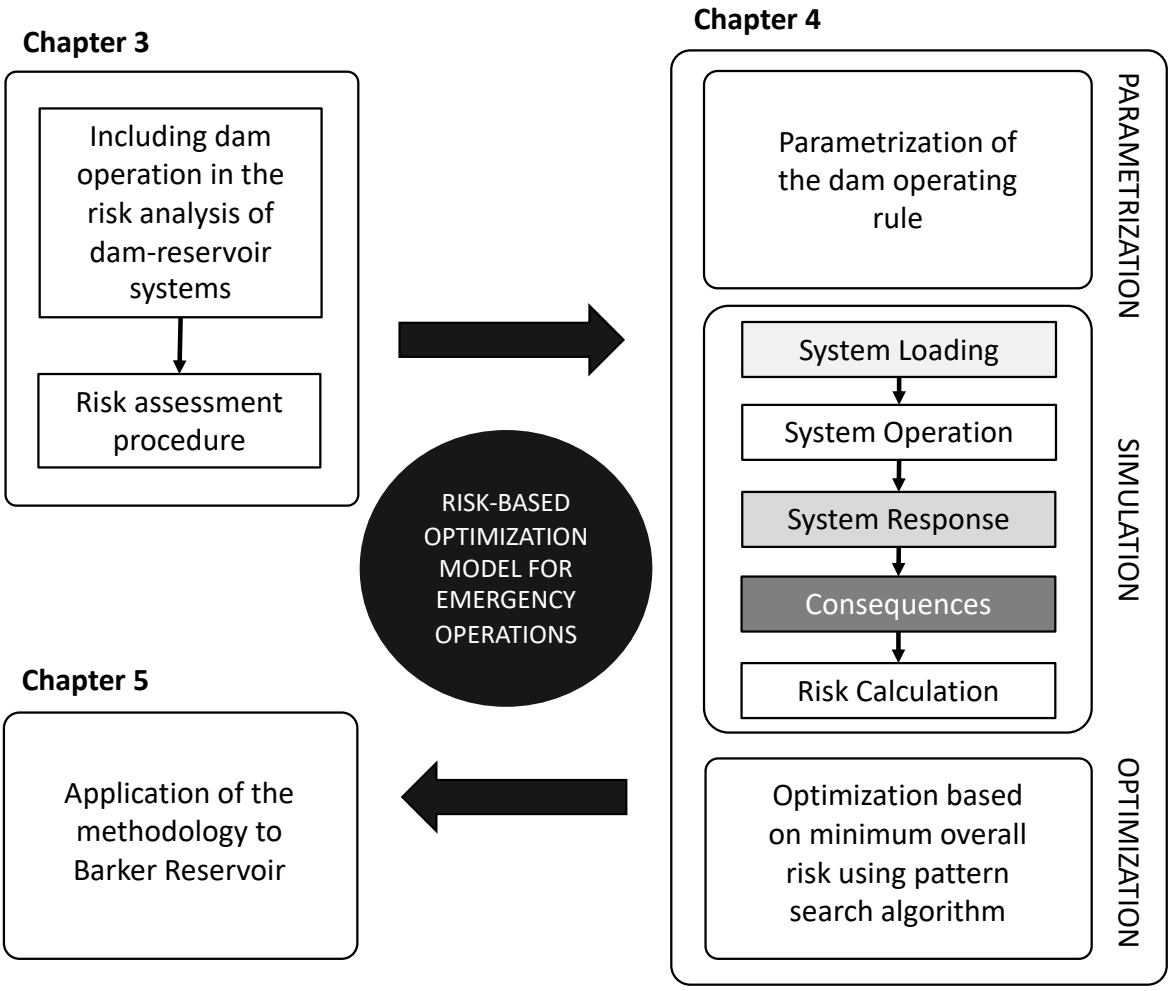

Figure 1.2: Overview of the report structure

Chapter 2

Background & Literature Review

Floods are a global problem which may result in serious socio-economic impacts, loss of life, and damage to the environment, services and properties. They remain among the most frequent and damaging natural disasters worldwide [34]. An analysis of global statistics carried out by Jonkman in 2003 [35] concluded that inland floods caused 175,000 fatalities and affected more than 2.2 billion people worldwide from 1975 to 2002. Hurricane Harvey (2017) is one example among many of their destructive nature. In fact, as reported by the U.S. Billion-dollar Weather and Climate Disaster analysis developed by the National Oceanic and Atmospheric Administration (NOAA) [26], during 2017 alone, the United States of America experienced 13 separate billion-dollar flood-related disasters.

Dam-reservoir systems cannot provide a complete protection against flooding, but they do help with its control and mitigation by using their available storage capacity to attenuate and delay storm peaks. The magnitude of the attenuation largely depends on their operation policies [16]. Generally, dams are designed to safely retain the local runoff from minor and moderate floods maximizing the protection at downstream locations. However, when facing extreme events, dam operators must also ensure the integrity of the structure. This situation poses an important conflict of objectives since maximizing the use of the control storage is also desirable. On one hand, simulation and optimization models provide good means of analyzing and evaluating different systems' operating procedures to select that one that better satisfies the demands of the structure; on the other hand, risk analysis to inform dam safety decision-making can be used to determine those decisions that may end up increasing or decreasing the risk to the reservoir area and the downstream floodplain occupants.

This chapter comprises an inclusive background and literature review of the most relevant topics of the project. First, the dam-reservoir system, its components and the most relevant variables are introduced. Second, in the context of *Reservoir Operation*, explanations are provided regarding the different strategies typically utilized for the operation of reservoirs during floods, stressing the operational conflict that emerges during extreme events. Since this project does not look for a random operation, but for the one that implies less risk to the system, a review of the current reservoir operation *Simulation-Optimization* models is presented. Special attention is paid to those models that account for the hydrological uncertainties. Finally, a *Risk-based* approach requires of the performance of risk analysis of the system. As such, a description of the terms risk, risk management and risk analysis is provided. Furthermore, current methodologies concerning risk assessment applied to dam safety management are detailed.

2.1 Dam-Reservoir System

The construction of a dam implies a great deal of changes in the river system. The watershed is divided into two regions, the *upstream* and the *downstream area*, connected to each other through a new element, the *dam structure* which temporarily stores water behind it creating a *reservoir*, and later release it to a *downstream channel* using the *outlet works* and *spillways*. Altogether, these components shape a new river scheme, the so-called dam-reservoir system. Figure 2.1 displays a cross-sectional view of the dam-reservoir system summarizing the components and variables described throughout this section.

In its broadest sense, a dam-reservoir system aims at regulating the natural streamflow. The temporal and spatial availability of water is managed following a set of *operating rules* which specify the amount of water to be stored and released at any time depending upon (1) reservoir characteristics, like the release capacity of the outlet works or the storage capacity of the reservoir; (2) the available storage capacity given by the reservoir state, (3) the available downstream capacity given by the information recorded at downstream control points; (4) the level of demands, and (5) the given information regarding future inflows into the reservoir.

2.1.1 Continuity Equation of the System

The relationship between releases, inflows and storage in a given time period can be mathematically expressed through the continuity equation of the system or mass balance equation:

$$S(t) = S(t-1) + I(t) - O(t) \tag{2.1}$$

where $I(t)$ is the total inflow volume during the time period t; $O(t)$ $[m^3]$ is the water released from the reservoir; $S(t)$ $[m^3]$ is the *reservoir storage* at the end of the period t; and $S(t-1)$ $[m^3]$ refers to the prior state of the reservoir at the time $t-1$. Depending upon the purpose of the reservoir, the forecast accuracy and the regulation policy, the time scale t can vary significantly. The continuity equation can be solved in time scales of years, months, weeks, or days. For instance, during floods, when a more precise definition of the storages, releases and inflows is required, control operations time scales are reduced to hours or even minutes.

The process of solving the continuity equation and determining the outflow hydrograph and the reservoir state for a given inflow hydrograph and known reservoir characteristics is called *reservoir routing*. Routing of hydrographs can be accomplished using many methods ranging from simplified mass balance to detailed watershed routing models. A thorough review of available numerical solutions for the reservoir routing equation is presented by Fiorentini and Orlandini [36]. The authors evaluate the robustness of three popular numerical methods: (1) the Laurenson-Pelgrim method [37] [38], (2) the fourth-order Runge-Kutta method [39], and (3) the fixed order Cash-Karp method [40]. They also acknowledged that the simplified pool routing method [39] is adequate in most of the cases giving errors non exceeding the 10%. Due to its absence of complication, the latter has been utilized for this research.

Also known as the storage indication method, the technique solves the mass balance equation considering that the reservoir has a flat surface. The time horizon is broken into intervals of duration Δt and the continuity equation shown in Eq. (2.1) is integrated over each time interval. In order to simplify the equation, a common procedure is to assume a linear variation of inflow and outflow over each time interval. The storage at any time can be then expressed as:

$$S_{t+1} = S_t + \frac{I_{t+1} + I_t}{2} \cdot \Delta t - \frac{O_{t+1} + O_t}{2} \cdot \Delta t \tag{2.2}$$

In order to complete the reservoir routing and solve the continuity equation, operation rules and the characteristics of the system need to be specified.

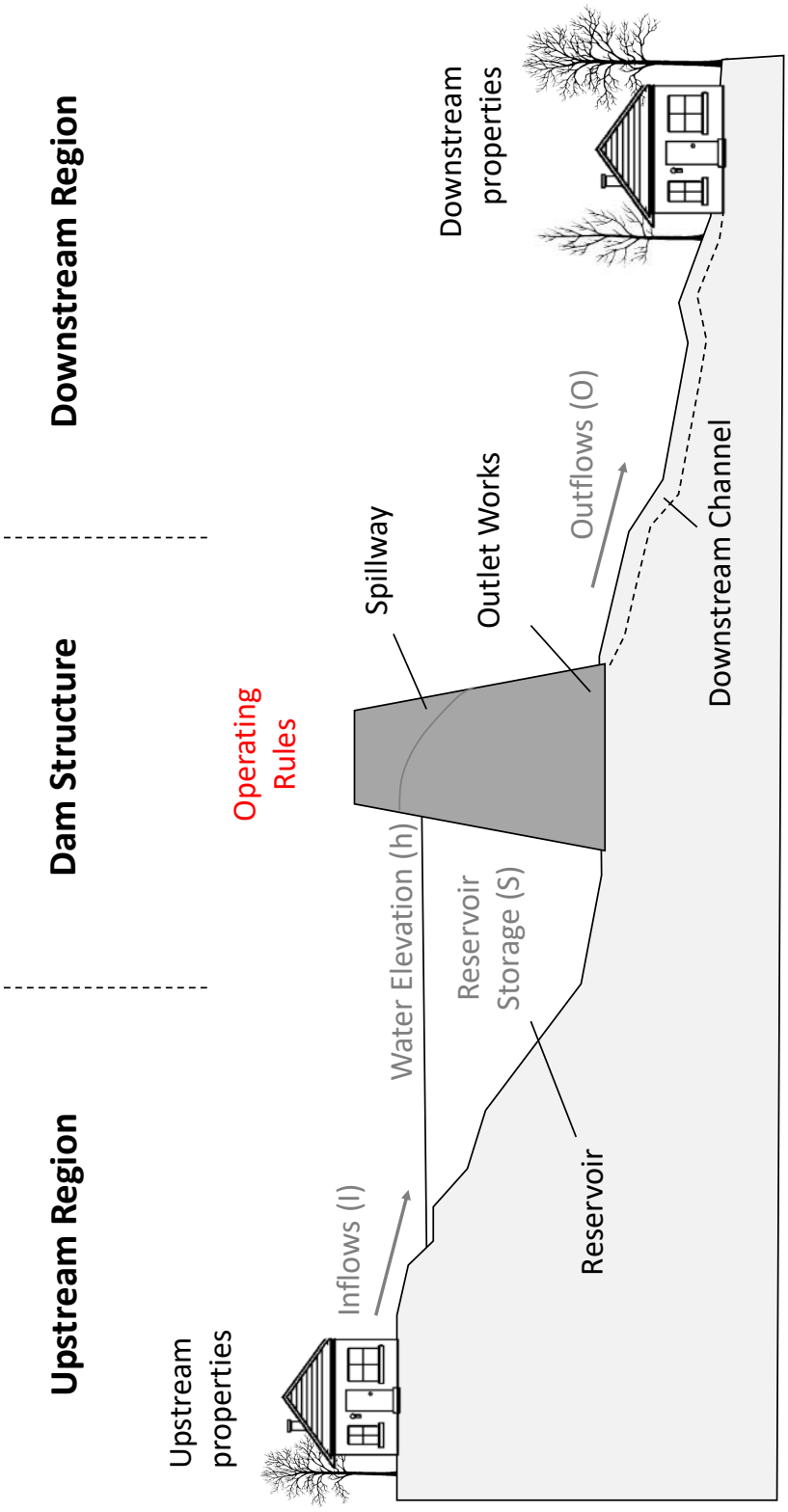

Figure 2.1: Graphical representation of a dam-reservoir system

2.1.2 System Variables and System Representation

Although the residual storage and the downstream conditions can always be known, the uncertainty regarding the inflow volumes makes reservoir regulation a challenging task. The most common way of representing the inflows is by means of *storm hydrographs* which display the flow rate entering the reservoir as a function of time. Figure 2.2 illustrates an example of inflow hydrograph in which its different components are displayed. Direct runoff begins at B, peaks at C, and ends at D. The segment BC is called the rising limb, whereas CD is the falling limb.

In practice, a watershed may have various shapes of flood hydrographs. The study of the external hydrological loads required for the design of dam-reservoir system relies on the analysis of the inflow hydrographs main characteristics: peakflows, Q_p, hydrograph volumes, V, and duration, d. Determination of flood duration involves establishing times for the start and end of flood runoff. Normally, time boundaries of a flood are marked by a rise in stage and discharge from base flow and a return to base flow. By noting the periods of times when the streamflow hydrograph coincides with the normal baseflow, the points where direct runoff begins and ceases can be identified.

A variety of techniques have been suggested to find points B and D from Fig. 2.2. One of the oldest is the normal depletion curve described by Horton [41]. Also known as the master baseflow recession curve, the normal depletion results from superimposing many of the recession curves observed on a given stream. Recession curves often take the form of exponential decay:

$$Q(t) = Q_0 \cdot e^{-(t-t_0)/T_s} \tag{2.3}$$

where Q_0 is the flow at time t_0 and T_s is an exponential decay constant having dimensions of time. With a known streamflow runoff hydrograph, the decay constant can be determined by plotting the curve of the logarithm of $Q(t)$ versus time on a linear scale as shown in Figure 2.2.

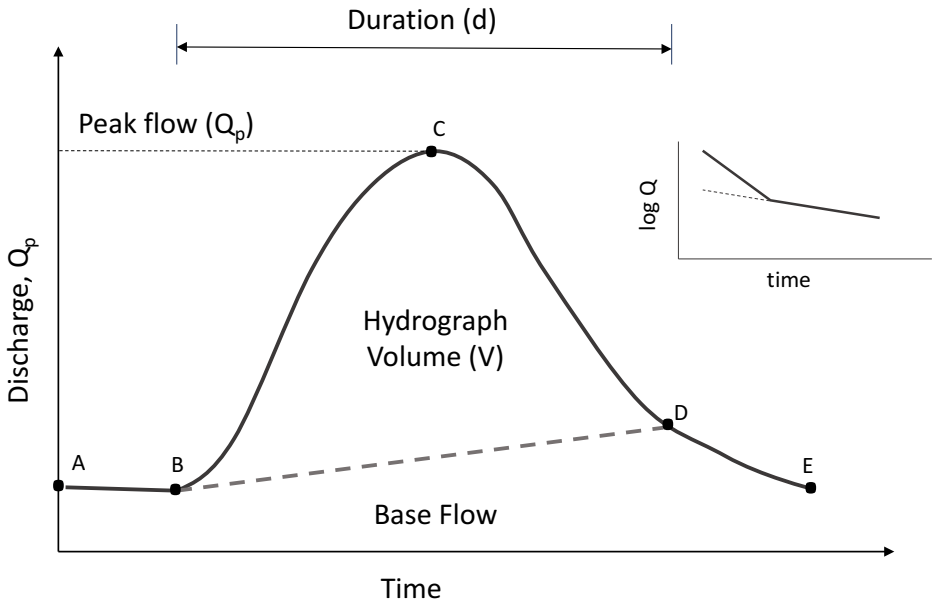

Figure 2.2: Components of the streamflow hydrograph including the separation between run-off and baseflow volumes

Other methods based on specified durations or specified flow thresholds are suggested in the literature [42]. Among them, the USGS HYSEP [43] recommends the use of three approaches proposed by Pettyjohn [44]: hydrograph-fixed interval, sliding interval, and local minimum.

These baseflow separation techniques stand out because they simplify the practical application and can be described conceptually as algorithms that systematically draw connecting lines between the low points of the streamflow hydrograph. The sequence of these connecting lines defines the separation between the baseflow and the runoff hydrograph.

Assuming that the inflows I_{t+1} $[m^3/s]$ are being forecasted and that both the current storage level in the reservoir, S_t $[m^3]$, and the outflow rate, O_t $[m^3/s]$, are known, operating rules dictate the increased in water releases, $\Delta O = O_{t+1} - O_t$ $[m^3/s]$, based either on downstream conditions or on the reservoir conditions. The downstream conditions depend to a large extent on the available non-damaging channel capacity which dictates the amount of water that can be released without contributing to flows spilling over the channel banks. Meanwhile, the upstream conditions are characterized by the *reservoir water surface*, h, which is directly related to the probability of failure of the structure and the flooding conditions upstream of the dam.

Reservoir releases to the river or channel below a dam are made through spillways and outlet works. These release structures might be gated or ungated depending upon the objective pursued with the construction of the dam. Controlled release structures allow for the adjustment of outflow rates maximizing the control and mitigation of floods. Whereas, with uncontrolled spillway or outlet conduits, the outflow rate is a function of the water surface elevation and the properties of the appurtenant structure. This relationship follows the classical hydraulic formulation reported by many authors in the technical literature [39]. Finally, since outflows involve extremely high velocities, stilling basins or other types of energy dissipation structures are required to prevent catastrophic erosion damage to the downstream river channel and dam.

In practical applications, the complexity of the system is circumvented by curves which represent the relationship between different variables. Two examples are presented in Fig. 2.3. On one hand, Fig. 2.3a depicts the reservoir stage - outflow relationship or *outlet rating curve*. The curve symbolizes the maximum release potential at every reservoir stage. In cases in which the opening rate of the outlets can be controlled, the gray area represents the possible discharges that can be made at each pool level. On the other hand, Fig. 2.3b displays the *capacity curve* of the reservoir. That is, the relation between elevation and storage. The relationship is usually obtained using Geographic Information System (GIS) tools for terrain data processing and are used to determine the total volume of water that the structure is able to hold.

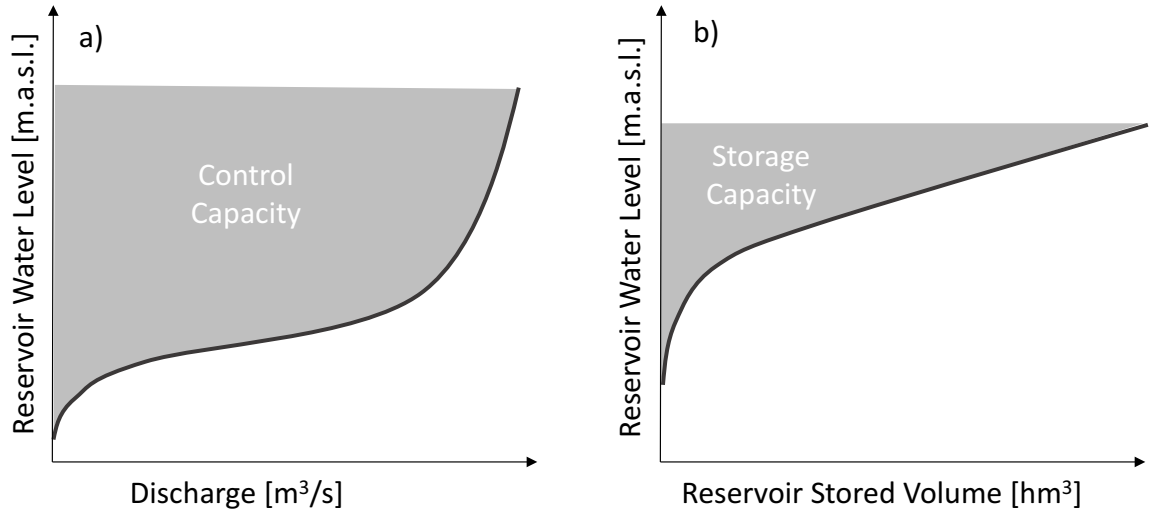

Figure 2.3: Hypothetical (a) Outlets rating curve (b) reservoir capacity curve

2.2 Dam-Reservoir System Operations

A wide variety of operating policies are presently in use throughout Texas, the United States, and the world. According to the comparative evaluation of generalized river-reservoir systems carried out by Wurbs in 2005, two main reservoir system operations are highlighted in the literature: (a) operations during **normal hydrologic conditions** and (b) operations during **hydrologic extremes** [13]. Minor and moderate floods are to be considered under normal hydrologic conditions, that is, the more frequent, low-magnitude flood events, whereas, hydrologic extremes refer to rare extreme floods which can result in storages exceeding the capacity of a reservoir and threaten the integrity of the structure.

In case of single purpose reservoirs, the operation problem consists of deciding whether the releases should be made so that the benefits for that purpose are maximized. For instance, conservation demands are best served when the surplus water is stored in the wet season and released in a future dry season. In contrast, the flood control purpose requires empty storage space in order to absorb and moderate the incoming floods to permissible limits. This is achieved by releasing water before and after a storm and storing it during the event. When different purposes are to be attended, conflicts in space, time and discharge arise among demands of various purposes.

2.2.1 Storage Zoning and Rule Curves

Reservoir operating policies typically involve dividing the total storage capacity into designated pools. This is known as *storage zoning*. A typical reservoir cross section is conceptually separated into *operational pool* and *surcharge pool* by an imaginary horizontal plane, the *maximum Flood Control Level (FCL)*. The reader should note that the terminology within the technical literature is not unique and other terms such as static full pool or discharge pool may be used to appoint the flood control level and the surcharge pool respectively. The vocabulary employed in this report is in accordance with the U.S. Army Corps of Engineers engineering manual for "Management of Water Control Systems" [24].

The operational pool contains the water volume that can be controlled by the dam operator. This is the volume between the minimum level at which controlled releases can be made and the flood control pool. For multipurpose dams, the operational pool is subdivided into conservation and flood control pools. Figure 2.4 illustrates the typical storage zoning in case of multi-purpose and flood control reservoirs. This conceptual division stems from the way a reservoir must act to fulfill its objective. As mentioned above, the maximum possible empty space is desirable for flood control, whereas water storage is required for the other objectives such as water supply, irrigation, navigation, or hydroelectric power. To satisfy all the possible purposes, the reservoir water surface is maintained at or as near as possible to the designated *Top of the Conservation Pool (TCP)* elevation. The flood control pool remains empty most of the time except when flood waves arrive to the reservoir. The top of flood control level is often set by the crest of an uncontrolled emergency spillway, with releases being made through other outlet structures. Occasionally, gated spillways allow the top of flood control pool elevation to exceed the spillway crest elevation as shown in Fig. 2.4.

The surcharge pool refers to uncontrolled storage capacity above the flood control pool and below the *maximum design water surface* (WSE_{max}). Hydrologic extremes may end up exceeding the capacity of the flood control pool encroaching into surcharge storage. The maximum design water surface profile is established during project design from the perspective of hydrological dam safety. Reservoir design and operation is based on assuring that the reservoir pool level will never overpass the designated maximum design water surface elevation. For the majority of

retaining structures, particularly embankments, the *crest level* is set above the top of surcharge pool. The difference is known as *freeboard* and provides an additional safety factor against overtopping.

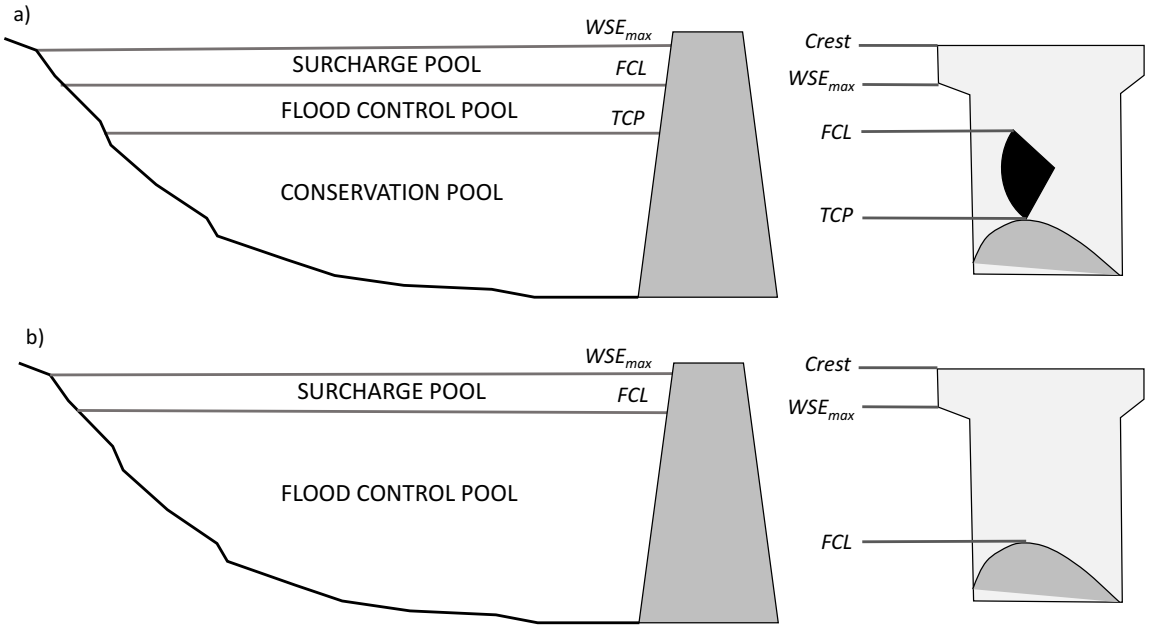

Figure 2.4: Reservoir storage zoning (a) multi-purpose reservoirs (b) flood control reservoirs

To ensure that the reservoir satisfies its purposes and benefits, the water control manual provides operating guidelines for the flood control pool and the conservation pool. A type of management frequently used is based on rule curves [33]. Rule curves are decision tools in form of equations or graphs relating the outlet and spillway gate openings to reservoir state parameters. By following these operation schemes, releases are made as a function of water surface, preceding outflows and inflow rates. Alternatively, inflows can also be expressed as a rate of rise of the water surface that can be measured at the dam itself. The latter is operationally safer [12].

2.2.2 Reservoir Flood Control Operations

Once the water levels reach the flood control pool, dam operators face an operational dilemma. On one hand, flood control operations should minimize flood damages at downstream locations; on the other hand, operations must ensure the integrity of the structure by preventing the reservoir water levels from reaching the maximum flood control storage capacity and, above all, the maximum design water surface. Finally, in some cases, urban development upstream from the reservoir also poses a limiting constraint to be considered during flood control operations. Consequently, as pointed out by Bianucci et. al [16], the problem associated with the operation of reservoirs during floods is to be seen as multi-objective in nature.

The conflicting nature of these objectives is not always easy to see. For instance, in case of small floods, dam safety is of little concern, given that dams are designed to safely withstand floods of a certain magnitude. According to Wurbs [45], flood control reservoirs operated by the USACE are able to contain in many cases floods greater than the 100-year recurrence interval without making any releases that would contribute to downstream flooding. However, during extreme events, when the storage capacity has a higher probability of being exceeded, dam managers

must prioritize the safety of the dam over the downstream impact of dam spillage, since a dam failure would cause a much greater damage.

Depending on whether or not the reservoir storage capacity is expected to be exceeded, two distinct operational schemes are used interchangeably among reservoirs all over the world. The *normal operations scheme* is followed when enough storage capacity is available to regulate a flood event. Alternatively, as soon as the storage capacity is limited and inflows are expected to exceed the residual storage capacity, the *emergency operations schemes* are activated.

Figure 2.5 illustrates the differences between the mentioned schedules. Consider that the figure represents a flood control reservoir constructed in a flood prone area where flood damages occur if flows exceed a critical level or downstream channel capacity symbolized by the lower dotted horizontal line. Two different outflow hydrographs, gray lines, are obtained when routing the same inflow hydrograph, represented by the black curve, through the dam following the two operation schedules. Furthermore, the releases are limited by the maximum released capacity of the outlet works represented by the upper dotted line.

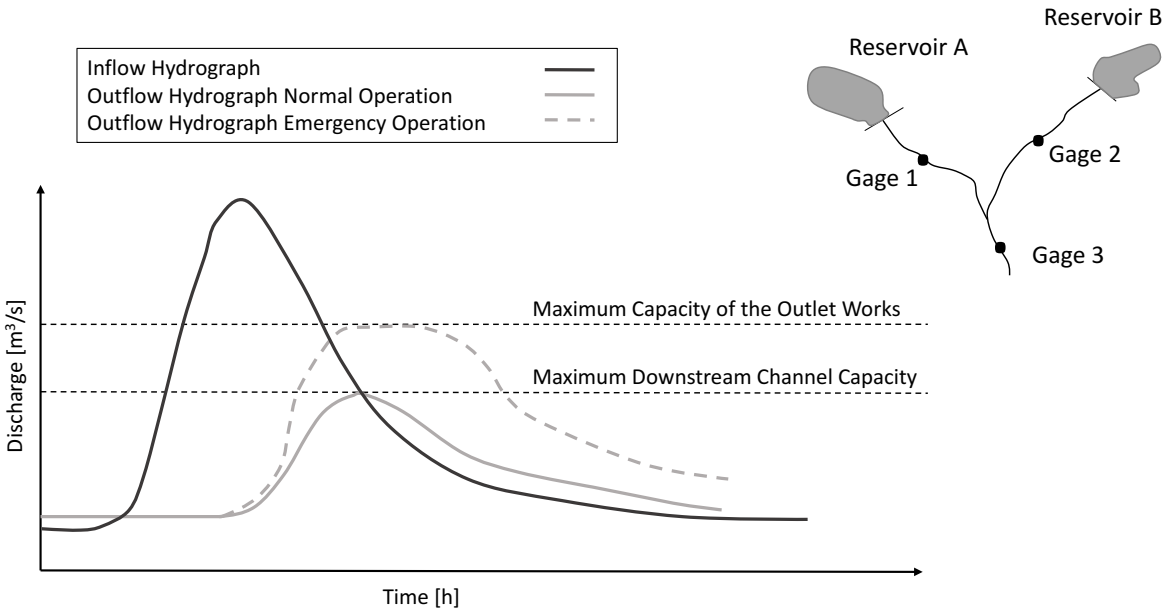

Figure 2.5: Normal and emergency flood control operations of reservoirs

Under normal operations, the reservoir uses the available storage capacity to contain the inflow volume in the rising limb of the inflow hydrograph and release it gradually later. By doing so, the flood damages downstream from the reservoir are minimized. It can be seen in the figure that the releases made following the normal operation are based on the downstream channel capacity which it is not to be exceeded. Comparing the two schedules it seems clear that the emergency schedule entails larger releases implying also lower reservoir pool levels.

In those cases in which two reservoirs are constructed to protect a joint downstream location from flooding, their combined releases should not exceed the established maximum channel capacity at common control points during normal operations (e.g. Gage 3 in Fig. 2.5). In order to maximize the protection objective, release decisions should aim at maintaining equal available flood storage in each reservoir. In other words, releases are to be made from the reservoir with the greatest percentage of used storage.

Another important consideration when making operational choices based on downstream conditions is the possible runoff contribution from uncontrolled areas. If rainfall occurs after a

release has been made but within the water travel time to a control point, reservoir releases, although lower than the non-damaging capacity, may be combined with the uncontrolled runoff exacerbating downstream damages.

Under emergency operations, the primary objective is the protection of the dam. Contrary to the normal operations, release decisions are no longer based downstream conditions but on the current state of the reservoir. Therefore, channel capacity may be exceeded at some downstream locations so that the reservoir will not be completely filled before the entire flood has passed (Fig. 2.5). This type of operation relies on the idea that moderately high damaging releases beginning before the flood control storage is full are preferable to waiting until a full reservoir requires of higher releases to avoid overtopping.

Although, in general, both operating schemes attenuate the peak, delay its appearance in time and extend the duration of the inflow hydrograph, as pointed out by Windsor [46], normal or emergency, "a fixed release rule" is unable to make the best use of the available storage for the entire range of possible flood conditions. For instance, following the normal operations scheme during a major flood event could result in flooding upstream structures, dam overtopping, and in a worse case, a dam collapse. On the contrary, the application of emergency schemes may result in higher releases for lesser floods, and larger flooding periods.

2.2.3 Development of Emergency Operation Schedules

A common practice in reservoir management is to develop emergency operation schedules. These operating rules, in the form of equations or graphs, provide the required guidance to the reservoir operators in charge of making real-time release decisions with limited available data during extreme events. The importance of these curves has been acknowledged by the entire water management community. For instance, Valdes and Marco described them as "crucial for flash flood control" [12] since they can be used by reservoir managers in complete isolation at the dam, a common situation under emergency conditions.

Diverse emergency operation schedules are available in the technical literature. This section focuses exclusively on the procedure for developing emergency operation schedules proposed by the USACE [24]. The methodology determines the required releases to be made in order to limit the storage to the available capacity. This is done by estimating the expected inflow volume under the premise that the inflow hydrograph has just crested. The process of elaborating the curves has five steps:

1. Define the recession constant T_s
2. Calculate the inflow storage S_A
3. Calculate the critical storage S_C
4. Determine the tentative maximum allowable pool elevation WSE_t
5. Adjust each tentative maximum starting reservoir elevation WSE_t

The first step in the procedure is to analyze the recession characteristics of inflow hydrographs to obtain the recession constant, T_s, that can be used to predict the minimum expected inflow volume. With the aim of obtaining conservative results, the USACE method assumes a rapid recession rate, that is, the recession from a large flood cause by a short period of intense rain. The spillway-design flood (SDF) satisfies these demands. Using the simple exponential decay function showed in Section 2.1, the flow after a time period Q_t can be predicted given a initial discharge Q_0, and a recession constant T_s as shown in Eq. (2.4):

$$Q_t = Q_0 \cdot e^{-t/T_s} \tag{2.4}$$

As inferred from Eq. (2.4), the recession constant T_s, is defined as the time required for the discharge to decrease from any value, say Q_1, to a value Q_2, where Q_2 equals Q_1/e, being $e \simeq 2.7$. Expressing that in mathematical terms, the time t required for the inflow to recede until equalizing the release may be solved by:

$$t = T_2 - T_1 = -T_s \cdot ln(Q_2/Q_1) = T_s \cdot ln(Q_1/Q_2) \tag{2.5}$$

Once T_s is known, the second step consists of determining the volume of water to be stored. Given an inflow peak and an outflow rate, the available volume results from the subtraction of the volume under the recession limb and the outflow volume. Figure 2.6 illustrates the total inflow volume that will be stored during the reminder of a flood, S_A given that the outflow rate remains constant. Q_1 represents the inflow, Q_2 represents the constant outflow rate, and T_s may be defined as the sum of stored V_s and released V_r volumes during time required for inflow to recede to match outflow:

$$T_s = \frac{V_s + V_r}{\Delta Q} = \frac{(S_A/c) + Q_2 t}{Q_1 - Q_2} = \frac{S_A + cQ_2 t}{c(Q_1 - Q_2)} \tag{2.6}$$

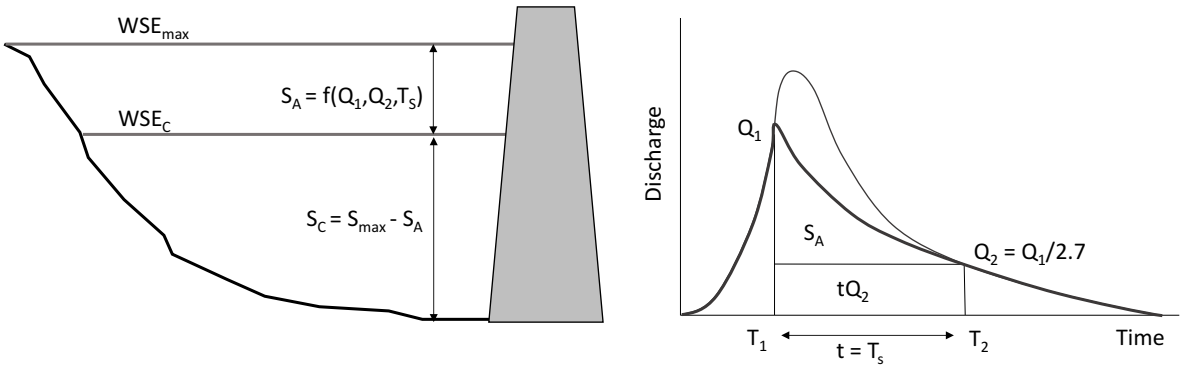

Figure 2.6: Schematic hydrograph and reservoir with USACE standard method notation

Substituting Eq. (2.5) into Eq. (2.6) and rearranging:

$$S_A = cT_s[Q_1 - Q_2 - Q_2 \cdot ln(Q_1/Q_2))] \tag{2.7}$$

$$S_A = cT_s[Q_1 - Q_2(1 + ln(Q_1/Q_2))] \tag{2.8}$$

where c is the conversion constant. If the stored volumes are expressed in hm^3, the T_s in days and the discharges in m^3/s, c is equal to 0.0864. The above equation is solved for a series of inflow and outflow rates to obtained the volume of water that must be stored in each situation. The third step in the procedure is to obtain the critical storage level at which releases should start to be able to retain the entire volume without exceeding the maximum reservoir capacity:

$$S_C = S_{max} - S_A \tag{2.9}$$

The fourth step implies using the reservoir capacity curve to determine the tentative maximum allowable pool (WSE_t) corresponding to each S_C. The complete regulation schedule is obtained by plotting the WSE_t corresponding to various outflows using the inflows as changing

parameters. Finally, the regulation curves are adjusted according to the reservoir rating curve. The outflow-storage pair must be within the permissible limits given by the maximum released capacity at each reservoir stage. Sample calculations of this methodology has been applied to the simple dam-reservoir example presented in Chapter 3 and Chapter 4.

2.3 Dam-Reservoir Systems Simulation and Optimization Models

In many cases, the damaging effects of floods can be mitigated by adequate emergency management of reservoirs [16]. It is inferred from previous sections, though, that reservoir operation during extreme events is not an easy task. Dam managers face an operational dilemma. Although the priority under extreme conditions is to ensure the integrity of the dam, maximizing the use of the flood control storage to minimize downstream damages is also desired. In order to deal with the multi-objective nature of the problem and trying to predict the behavior of the reservoir under statistically possible future extreme events, the water resources literature includes a wide range of studies concerning simulation and optimization models [18] [17] [47].

A number of systems analysis techniques combining simulation and optimization algorithms have been developed and applied over the last several decades. Wurbs et al. [17] and Yeh [18] were the first to present extensive lists of references and in-depth reviews on the use of these models for various reservoir system analyses. In his state-of-art review, Yeh [18] put a strong emphasis in the available mathematical optimization techniques (linear programming, nonlinear programming, and dynamic programming) for their application in reservoir management. Reservoir optimization and simulation models were also reviewed by Wurbs [17] [19] who, rather than focusing on the analysis of the mathematics, evaluated the usefulness of each optimization approach for different decision support situations. His technical reports on the matter provided a great basis for practitioners regarding the selection of the appropriate model for each particular situation. Labadie [47], in his revision on optimal operations of multi-reservoir systems, addressed the gap between the theoretical development and the real-world implementation, suggesting as a solution the need to improve the linkage of optimization models and simulation models to diminish the skepticism of dam operators.

In addition to the traditional optimization methods, more recently, Rani and Moreira [48], acknowledged the stochastic nature of many of the variables playing a role in the operation and optimization of reservoir policies, and reported the use of computational intelligence techniques, such as, evolutionary computations, fuzzy set theory and artificial neural networks, in reservoir system operation studies. Finally, following that same line of thinking, Celeste and Billib [33] realized the mathematical complexity pointed out by Labadie [47] of explicit stochastic optimization models. In their work, the authors investigated the performance of implicit stochastic programing and parametrization-simulation-optimization approaches to define optimal operating policies. Their research concluded with a clear statement addressing their superior overall performance as compared with a neuro-fuzzy explicit stochastic programming approach.

2.3.1 Simulation Models

A simulation model can be described as a mathematical representation of a system that is able to predict and reproduce its behavior under predefined characteristics and external hydrological conditions. In a pure simulation model, reservoir releases are determined using predefined operating rules. The simulations models, therefore, help answer *what if* questions regarding the performance of alternative operational strategies [47]. Simulation models associated with reser-

voir operation are usually based on the mass balance equation and represent the hydrological behavior of reservoir systems using inflows and other operating conditions.

Application of simulation techniques to water resources planning and management started with simulations of the Missouri River conducted by the U.S. Army Corps of Engineers (USACE). The famous Harvard Water Program applied simulation techniques to the economic design of water resources [49]. The simulated model reproduced the behavior for power generation, irrigation and flood control. Since then, simulation models have been routinely applied by water resources development agencies responsible for planning, construction, and operation of reservoir projects [19]. A detailed comparative evaluation of user-oriented generalized river/reservoir simulation–optimization models, modeling capabilities and related issues are reviewed in a report by Wurbs [13]. Among the most important and widespread generalized simulation models, the author highlighted:

- RIBASIM - River Basin Simulation Model (Deltares) [50]
- HEC - REsSim / HEC-5 [51]
- MIKE 11 (Danish Hydraulic Institute) [52]
- RES-J - Hydrologic Software Engineering Branch (Riverside Technology Inc.) [53]

In spite of the large number of optimization techniques available in the literature, simulation models still remain the primary tool for reservoir planning and management studies. The reason behind this is attributed to the fact that simulation models provide a more detailed and faithful representation of the system [31]. Moreover, they can be easily combined with synthetically generated streamflow sequences. The synthetic generation of inflow hydrographs and stochastic prediction of flood events allows the ensemble of inputs to be representative of extreme flood events and permits consideration of the uncertainty associated with the input variables [54] [55].

Figure 2.7 illustrates the main components of a simulation model. First, stochastic models capture streamflow variability by generating ensembles of scenarios of plausible streamflow values, and then reservoir operation models rout the generated inflows through the reservoir solving the mass balance equation according to a series of operational and physical constraints. The final objective of these kind of models is to compute storage levels and discharges for a given set of hydrologic inputs, system demands, and operating rules.

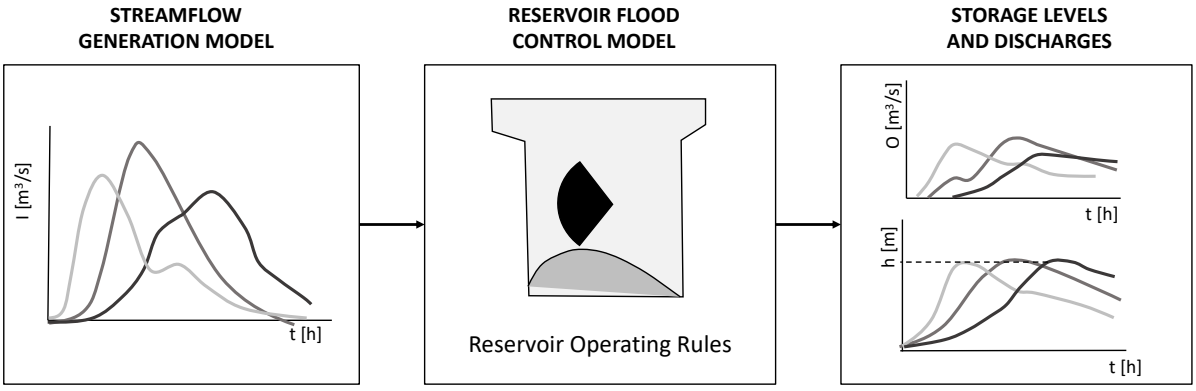

Figure 2.7: Reservoir flood control operation simulation model scheme including (1) streamflow generation model, (2) reservoir flood control model, and (3) results in terms of storage levels and discharges

2.3.2 Optimization Models

Prescribing the best operating procedures based on trial and error using simulation models can be, however, a challenging task. To overcome this difficulty, researches generally combine them with optimization models [19], which offer the possibility of systematically select optimal storage and release policies [47]. Optimization is described as a mathematical formulation in which a formal algorithm computes a set of decision variable values that minimize or maximize an objective function subject to constraints [45].

Various kinds of mathematical optimization algorithms have been proposed in the literature to improve the performance of reservoir systems [56]. The selection of the most appropriate depends upon the characteristics of the dam-reservoir system, the available data and the constraints and optimization objectives [13]. Linear programming (LP) is considered as the simplest and widely use technique [57]. Nonlinear programming (NLP) presents an advantage over LP since it can be applied when either the objective function or constraints are nonlinear [58]. Dynamic programming (DP) divides a multistage decision process into stages with individual decisions [59]. Stochastic dynamic programming (SDP) is an extension of DP which introduces the stochastic features of the flow conditions [55]. Finally, Genetic Algorithms have been suggested to search optimal operations due to its capacity of handling objective functions in any type [60] [61]. An extensive application of these methodologies can be found in Yeh [18], Labadie [47], Wurbs [13], and Rani and Moreira [48].

General Mathematical Formulation

Optimization models are based on clearly defined goals (objective functions) as criteria for the evaluation of the control decisions; and constraints as limitations during optimization [62]. According to Labadie [47], "Objective functions used in reservoir optimization models should incorporate measures such as efficiency (i.e. maximizing current and future discounted welfare), survivability (i.e. assuring future welfare exceeds minimum subsistence levels), and sustainability (i.e. maximizing cumulative improvement over time)". Generally, the objectives surrounding the optimizations deal with economic, social and environmental issues [13]. Let consider the objective function $FO_i(K)$ which deals with diverse objectives $FO_i(K)$ where K is the vector of decision variables and $q_i(K)$ are constraints that define the feasible solutions. In mathematical terms, the optimization model tries to maximize or minimize the objective function:

$$FO(K) = [FO_1(K), FO_2(K), FO_3(K), ..., FO_n(K)) \tag{2.10}$$

Subject to constrains

$$q_i(K) \leq 0 \quad i = 1, 2, 3, ..., n \tag{2.11}$$

The typical constrains in a reservoir optimization model include the conservation of mass or continuity equation used while routing the floods through the reservoir, specific upper and lower bounds on storage, upper and lower limit on reservoir releases, and constraints in the elevations defined by the maximum and minimum permissible water level. Other constraints may be applicable depending upon the objective of the optimization. For instance, Ngo [62] implemented a constraint on hydropower generations for the multi-objective optimization of flood control strategies of a hydropower reservoir, or Prakash et. al [20] included channel routing equations for its multi-objective flood mitigation framework.

In the last decades, a large number of methods addressing the optimization of the multi-objective problem generated during flood control operations have been developed. According to Khu and Madsen [63], two main approaches are highlighted in the literature: Aggregated Parameter

Approach (APA), and Pareto Dominance Approach (PDA). In the former, the various objectives are aggregated into a single scalar objective function using penalizing and weighting coefficients. Mathematically, the objective function is given by Eq. (2.12):

$$\text{Minimize:} \quad F(X) = \sum_{i=1}^{N} w_i g_i(F_i(X)) \tag{2.12}$$

where w_i is the weight associated to the i_{th} objective and $g_i(.)$ are the transformation function assigned to each objective function. The priority of each objective function can be specified by using different weights. Cheng and Chau [64] presented a fuzzy iteration methodology for the assessment of the objective weights and relative membership degree of flood control alternatives. Meanwhile, Can and Houck [65] applied a goal programming approach based on physical operating criteria to avoid the complexity of penalty-benefit functions.

Acknowledging the difficulties of determining the relative importance of the weight coefficients in the traditional penalty function approaches, some authors have suggested the multi-objective optimization frameworks based on Pareto solutions to find the optimal operation of dam-reservoir systems [48]. Ngo [62] optimized the flood control strategies of a hydropower reservoir using the Pareto dominance approach. The author applied the methodology to the Hoa Binh reservoir in Vietnam and found that the equally weighted solution provided a good compromise between the two objectives. A few years later, Prakash et. al [20] proposed a multi-objective simulation optimization framework for optimal mitigation operations focusing on three different objectives. Another multi-objective approach was proposed by Malekmohammandi et. al [66]. In their research, the authors included the expected damages in the objective function formulation. The framework presented in this thesis is based on a similar concept as Malekmohammandi et. al [66], however, the formulation applied as objective function also considers the effects of dam operations on expected annual damages.

Optimization Modeling Techniques

Each mathematical optimization technique can be applied using deterministic or stochastic hydrologic inputs. If optimization is performed using a deterministic approach, the obtained operating rules may not be optimal for hydrologic situations that differ from those used as inputs of the model. Implicit stochastic optimization methods, also known as Monte Carlo optimization, optimize over long continuous series of historical or synthetically generated inflow time series, or several shorter equally likely sequences. This allows the stochastic nature of the problem to be implicitly included. Alternatively, explicit stochastic optimization procedures attempt to operate directly on probabilistic descriptions of random streamflow processes rather than deterministic hydrologic sequences. Optimization is thus performed without perfect knowledge of future events. Figure 2.8 and Fig. 2.9 display an adapted version form Labadie [47] of the general scheme for the explicit and implicit stochastic optimization procedures respectively.

Although theoretically ESO application to reservoir system optimization is more appealing, some authors in the literature have pointed out its greater operational inconveniences and limited computational feasibility [67]. Furthermore, some comparative studies have found ISO methods to be better than ESO's, as they can be formulated to represent the operational problem more closely [68]. As previously mentioned, Celeste and Billib [33] in their evaluation of stochastic reservoir operation optimization models demonstrated the superior performance of ISO-based optimization procedures. They authors also introduced the advantages of a different type of technique, the Parametrization-Optimization-Simulation (PSO) method. Formally presented by Koutsoyiannis and Economou [32], Parametrization-Simulation-Optimization yields solutions that are not inferior to those of ISO and ESO methods and, simultaneously, presents several theoretical, computational, and practical advantages [69].

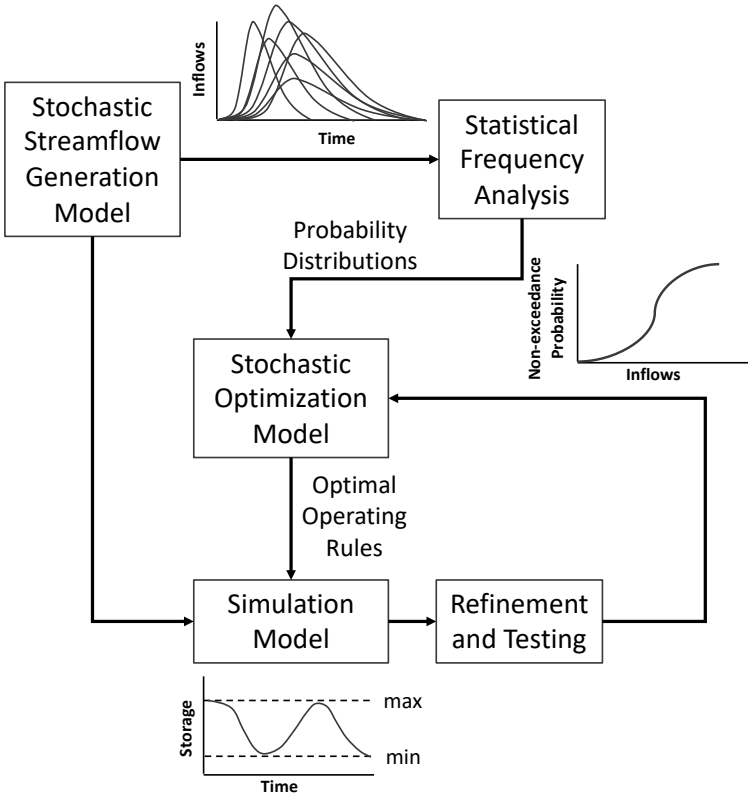

Figure 2.8: Explicit stochastic optimization (ESO) procedure [47]

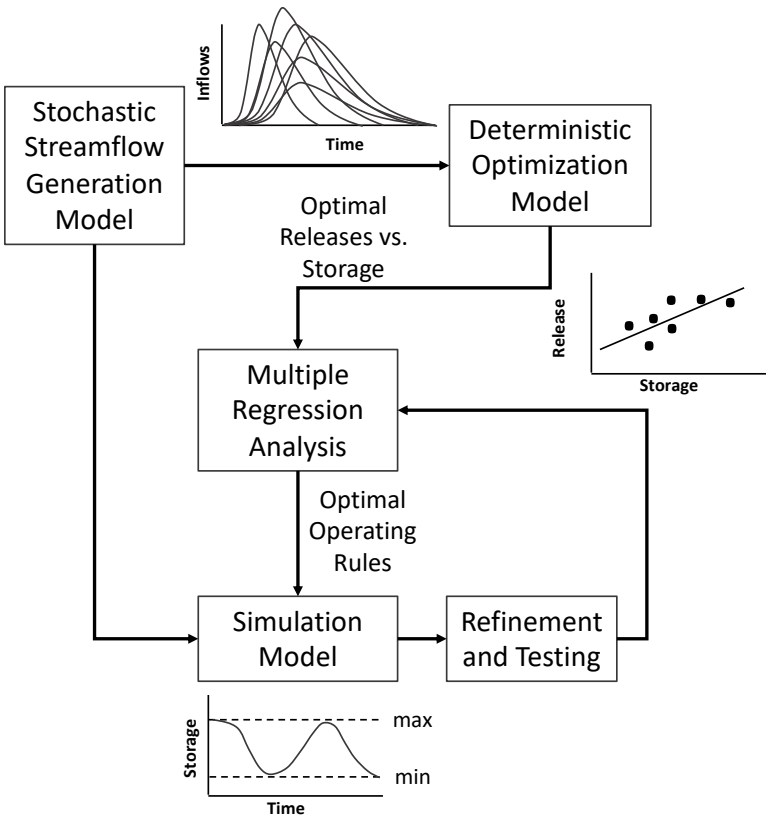

Figure 2.9: Implicit stochastic optimization (ISO) procedure [47]

2.4 Flood Risk Analysis and Management

As a result of past flood events and their consequences, the development of effective strategies to prevent or to reduce flood damages has become a paramount issue in the field of water resources management [70] [71]. To fight against such natural events, flood management policies, based on flood risk analysis procedures, include a large variety of risk mitigation measures which aim at either reducing the probability of flooding or its consequences [72]. In general, these measures can fall into two categories: structural and non-structural. According to the systematization proposed by the project FLOOD-ERA [73], structural measures refer to any physical construction that reduces or avoids possible impacts of floods (e.g. engineering measures or construction of protective infrastructures). As a result, non-structural measures may include all other interventions, mainly focused on acting on potential consequences [74]. Among the structural solutions, dams, levees and dikes are the most commonly means used to stop excess water in flood prone areas. According to the latest reports from the World Commission on Dams, at least 45,000 large dams were constructed during the twentieth century [75], 13% of which have flood management as primary function.

2.4.1 Risk, Hazard and Vulnerability

The terminology within the technical literature concerning the natural flood risk assessment is not unique. The most comprehensive definition was given by Gouldby and Sammuels [76], who described the term as a combination of the four components shown in Eq. (2.13): the nature and probability of a source of *hazard*, the degree of *exposure* of the receptors to the hazard, the *susceptibility* of the receptors to the hazard, and the *value* of the receptors:

$$Risk = Hazard \cdot Exposure \cdot Susceptibility \cdot Value \tag{2.13}$$

As inferred from the above definition, in order to have risk, a source which may result in harm and a valuable receptor susceptible to such initiator are required. With this regard, while the term *hazard* refers to that source of danger or initiator event, *exposure*, *susceptibility* and *value* relate to the potential consequences in case of an event. Other sources in the literature may combine the concept of susceptibility and value into a unique term, the *vulnerability*, which includes characteristics of the system describing its potential to be harmed. Therefore, instead of Eq. (2.13), the definition of risk can also be given as in Eq. (2.14):

$$Risk = Hazard \cdot Exposure \cdot Vulnerability \tag{2.14}$$

Exposure is related to people, properties, or any valuable element present in hazard zones that are thereby subject to potential losses. In practice, both exposure and vulnerability are mostly captured in the assessment of the *consequences*. In the field of Civil Engineering, an often-used definition of risk refers to the description of Kaplan and Garrick [77]. They introduced risk as "a set of scenarios, s_i, each of which has a probability, p_i, and a consequence, D_i". This report follows this last interpretation of risk, from which one can quantify and depict the total risk expressing the value of the expected damage $E(D)$ for a set of discrete scenarios as in Eq.(2.15):

$$R = f(s_i, p_i, D_i) \quad | \quad E(D) = \sum_{s_i=1}^{N} p_i \cdot D_i \tag{2.15}$$

In flood risk analysis, *probabilities* are often referenced to a specific time frame, for example, annual exceedance probability. Furthermore, they include not only the occurrence of potential hazards, but also the conditional probabilities of the system response given such hazard. For instance, the probability of failure of a flood defense structure given a certain water level. The

second risk component, *consequences*, can be classified according to their direct and indirect impact [78]. They are commonly expressed quantitatively in terms of economic damages or loss of human lives. In the case of considering potential economic impacts, the term *economic* risk is to be used. Whereas, when relating the consequences to loss of life, the concepts of *individual risk* or *societal risk* are utilized [79].

Although the expected annual damage (EAD) is widely applied in practice, it should be noted that there is an important difference between "risk" and "expected value of damage" [80]. As explained by Jonkman et.al [81], the expected value neither gives an insight in the magnitude of probability and consequences nor an understanding in the contribution of individual scenarios. In order to get a quantitative and comprehensive picture of the flood risk in a certain area, the risk curves or Frequency-Damage curves, such as the *FN* and the *FD* curves, are preferred.

As defined by the ISO International standard IEC/FDIS 31010 [82] for risk management and risk assessment techniques, the risk curves are a graphical representation of the probability of events causing a specific level of harm to specific valuable receptors. *FN* curves are related to the societal risk and show the cumulative frequency F at which N or more members of the population will be affected. Similarly, *FD* curves illustrates the estimated level of economic damages D being the area under the curve the economic risk of the studied system. Figure 2.10 depicts an example of Frequency Damage curve developed by Escuder-Bueno et.al [83] for an hypothetic urban case study. The figure compares three situations with and without any protections and exemplifies the effect of structural and non-structural measures on flooding risk.

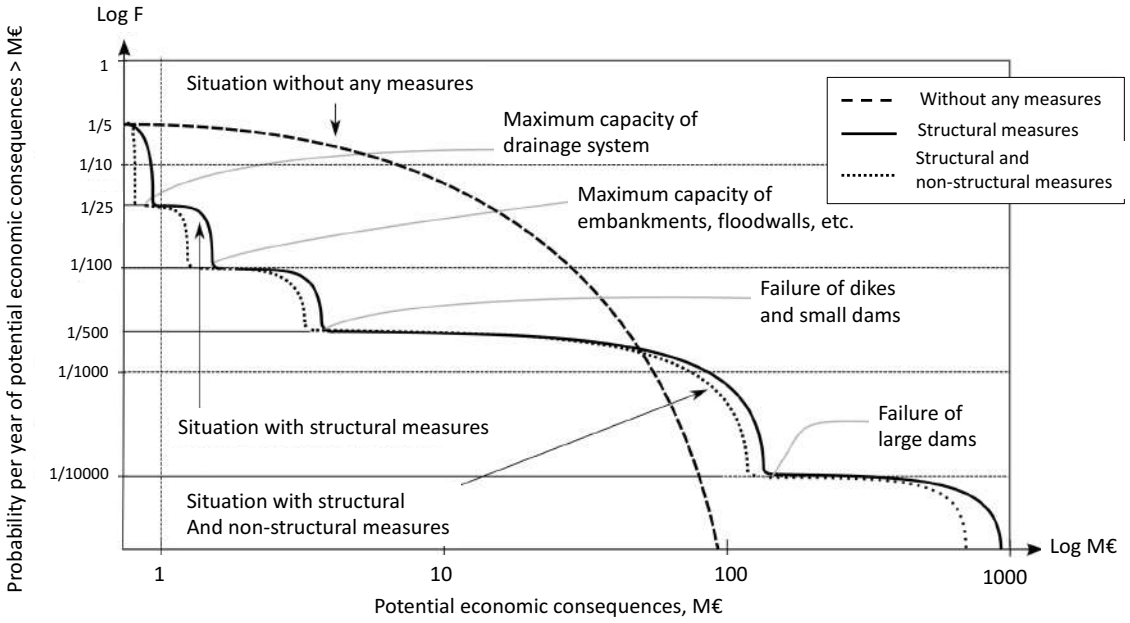

Figure 2.10: Example of FD-curve for a hypothetic urban case study [84]

2.4.2 Flood Risk Management and Flood Risk Analysis

Flood risk management is defined as an approach to systematically identify, analyze, evaluate, control and manage the flood risk in a given system. To put it another way, in addition to the assessment and evaluation of the level of risk, flood risk management policies consider the implementation and maintenance of structural and non-structural measures which aim at reducing the expected consequences and their probabilities of occurrence.

Flood risk analysis is the process of objectively determining risk by analyzing the possible hazards affecting a system and combining their probabilities and consequences. Generally, four phases are distinguished in the literature [85] in the process of risk analysis: a) definition of the system and setting the scope and objectives of the analysis; b) qualitative analysis of undesired events; c) quantitative analysis of the flood risk; and d) risk evaluation.

As in any other type of study, the first step of a Risk Analysis consists of *defining the system*, determining the scope and setting the objectives of the analysis. According to Castillo-Rodriguez et al. [86], a system encloses the assembly of natural, human and social elements which define the area under study. Depending on the complexity of the system and the level of detail pursued by the analysis, flood risk can be carried out analytically or by means of more sophisticated software tools. In this regard, dam safety risk models like DAMRAE or iPresas, will be analyzed in the coming sections.

Following the pre-assessment preparations, the risk of the system is identified and estimated. While the *qualitative analysis* comprises the identification and description of hazards, failure modes and scenarios, the *quantitative analysis* determines the response of the system to the previously defined events, assessing their probabilities and consequences. In the end, the risk of the system is represented by a number or a graph.

With the aim of performing risk calculations, the combination of different scenarios, probabilities and consequences require of the use of event trees [71] [87]. Event trees are extensive representations of all the events, scenarios and possibilities that can lead to risk within the studied area. Figure. 2.11 depicts a simplified example of an event tree for a system with a flood defense. Each of its branches comprises a possible flood event with related conditional probabilities of failure of the structure and the potential consequences. In the coming section, an example of event tree applied to a dam-reservoir system is deeply discussed.

Finally, the *risk evaluation* involves interpreting risks according to the existing societal tolerances to inform decisions and actions for flood risk management [88]. Virjling and van Gelder [89] proposed a framework in which risk can be evaluated based on three criteria. First, limit the individual risk to prevent that certain people are exposed to disproportionately large risks. Second, limit the societal risk to restrict the risks of large scale accidents with many fatalities. Third, optimize the economics to balance investments in risk reduction.

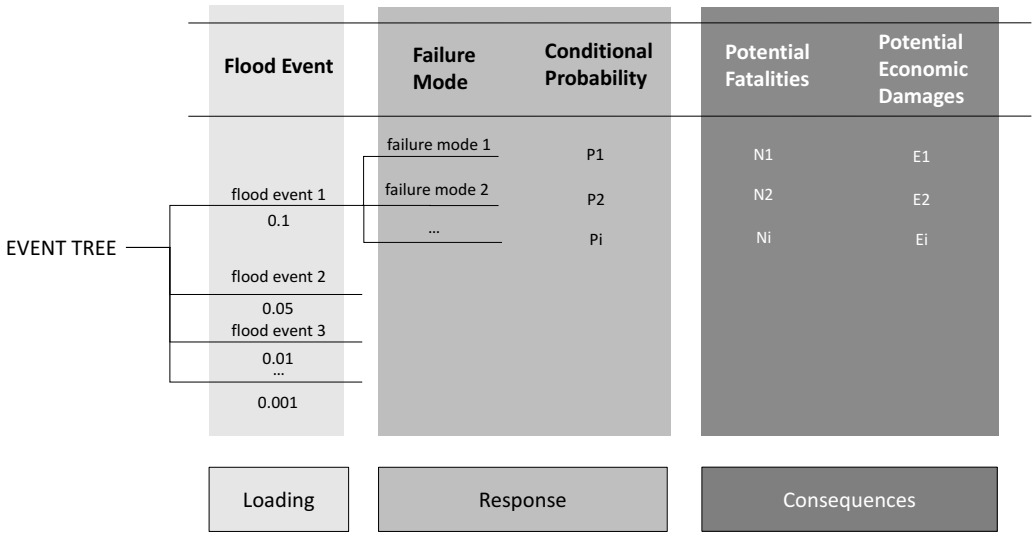

Figure 2.11: Generic event tree for a system with flood defense

2.5 Risk Management Applied to Dam Safety

Since the failure of Teton Dam (USA) in 1976 [90], the technical literature recognizes a significant evolution in the understanding of floods, dams and other critical infrastructures [91]. Prior to that moment, dams and reservoir safety and management had always been based on remarkably deterministic approaches. Risks were primarily controlled by certain rules and practices dictated by experience, or by safety factors that were understood as conservative measures of prudence [92]. Those that analyze, evaluate, and manage risks found in risk-based analysis the rigorous and systematic process required for decision-making in the field of dam safety. In words of Dr.ir. Escuder-Bueno, head of the Spanish National Committee on Large Dams: "when it comes to dam safety and flooding, methodologies to support decision making should be based on a much broader concept like risk rather than on existing margins to structural collapse [93]".

Although initial development work in this area started shortly thereafter the mentioned event with the development of *The Federal Guidelines for Dam Safety* in 1979 [94], it was not until the mid-1990's that the Bureau of Reclamation (USBOR) began using risk analysis for dam safety decision-making as an additional tool to combine with traditional approaches [95] [96]. Following that tendency, the USACE along with the USBOR and the Federal Energy Regulatory Commission (FERC), came up with a common risk management framework that included an interim version for tolerable risk guidelines [88] [21]. This change in the methodology has also been reflected in the European Directive on Floods of 2007 (2007/60/CE) [70], the European Directive of Protection of Critical Infrastructures of 2008 (208/114/CE) [71] and other country-based international entities like the Australian National Committee on Large Dams (ANCOLD) [97] [98] and the Spanish National Committee on Large Dams (SPANCOLD) [92].

Dam safety management can therefore be seen as a overarching activity which uses *risk analysis* and *risk evaluation* to inform dam safety decision making. It encompasses activities related to making risk-informed decisions and prioritizing risk reduction activities including the potential structural and nonstructural actions on a given dam or project. All of the above-mentioned international regulations acknowledge risk analysis utility and advices its use as an indispensable management tool. The current state-of-the-practice for analyzing dam safety risks is presented in the "Best Practices in Dam and Levee Safety Risk Analysis" [22], a document which summarizes the overall philosophy, methods and approaches.

2.5.1 Incremental, Non-Breach and Residual Risk

As shown in Section 2.4, risk can be interpreted as the combination of three concepts: *what can happen*, *how likely it is to happen* and *what are its consequences* [99]. When the long-established science of risk analysis is adapted for its application in the field of dam safety management, what can happen refers to all those scenarios that lead to dam failure; how likely it is to happen is the combination of the probability of occurrence of certain loads and the conditional probabilities related to the response of the system given those loads; and the consequences are the impacts resulting from failure, including, economic consequences and loss of life.

The reader should note that within the scope of risk analysis applied to dam safety, the concept of failure is not limited exclusively to the catastrophic breakage of the dam, but includes any event that might produce adverse consequences like induced flooding due to flawed outlet works operations. As such, failure also comprehends all those situations beyond which specified service requirements resulting from the planned use are no longer met. In Chapter 3, the terms *Serviceability Limit State Risk (SLS)* and *Ultimate Limit State Risk (ULS)* are introduced to illustrate these two types of risk. Meanwhile, in this literature review, following the standard notation from the technical literature, the terms failure and breakage are interchangeable, whereas non-failure risk is confined to non-breach scenarios.

In order to better understand these two components of the overall risk and the concept of system failure, it seems convenient to first identify under what conditions water being held by the dam might end up causing damages. These conditions are called inundation scenarios. According to the "Safety of Dams - Policy and Procedures" guidelines from the U.S. Army Corps of Engineers [21], the risk associated with a dam can be expressed in terms of the four inundation scenarios shown in Fig. 2.12. These include:

1. Structural failure of the dam prior to overtopping
2. Structural failure of the dam due to overtopping
3. Inundation resulting from malfunction or misoperation of dam components
4. Spillway flow without breach of the dam or overtopping without breach

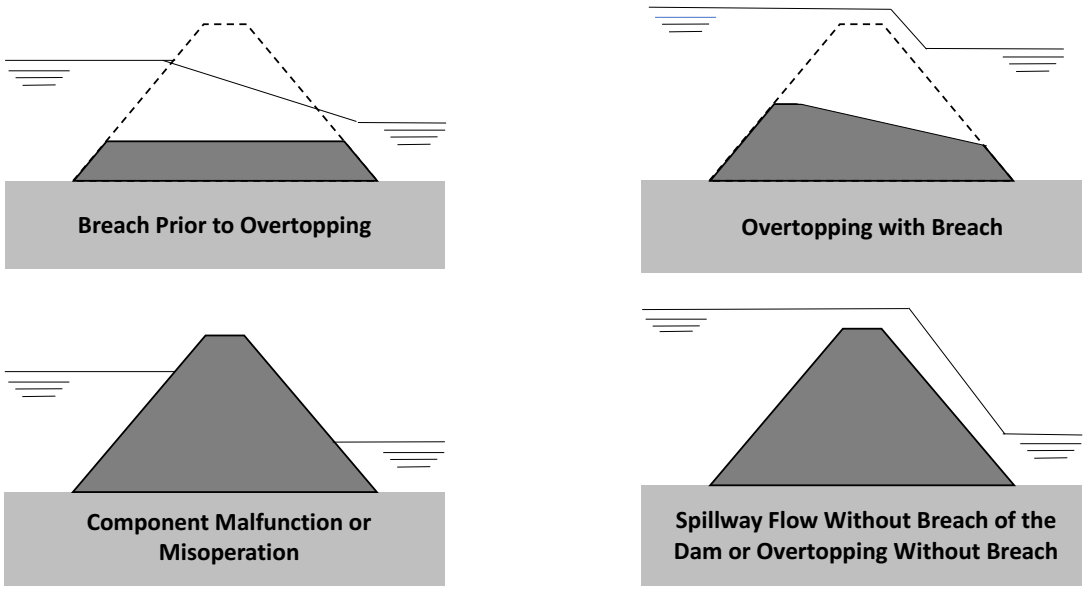

Figure 2.12: The four inundation scenarios for dam safety [21]

There are several forms of representing risk. In some occasions it is useful to reduce the concepts of *what can happen*, *how likely it is to happen* and *what are its consequences* to just one figure, the expected annual damage. In the technical literature, that overall risk is referred to as "residual risk" [21] and it can be numerically expressed as:

$$R_T = \sum_l p(l) \cdot [p(f|l) \cdot C(l,f) + p(nf|l) \cdot C(l,nf)] \tag{2.16}$$

where $p(l)$ is the probability that certain loads may occur (**system loading**); $p(f|l)$ and $p(nf|l)$ are the conditional probability of failure and non-failure given those loads (**system response**); and $C(l,f)$ and $C(l,nf)$ symbolize the consequences in cases of failure and non-failure respectively (**consequences**). It is inferred from the equation that the residual risk associated with a dam-reservoir system consists of two components: the *Non-breach Risk* associated with the probability of non-structural failure, and the *Incremental Risk* related to dam breach or dam component malfunction.

On one hand, the incremental risk is the risk to the reservoir area and downstream floodplain occupants that is attributed to the first, second and third inundation scenarios. To put it another way, any structural failure leading to damages in the upstream and downstream regions. Conceptually, that structural failure probability can be defined through the following equation:

$$P_f = \sum_l p(l) \cdot p(f|l) \tag{2.17}$$

Risk Analysis methodologies are not limited to one single failure mode but instead they study all the possible ways in which a dam could fail. Each of them is called failure mode. Thus, the total failure probability is the sum of the probabilities of each failure mode. Once the total failure probability is defined, the incremental risk, R_Δ, is obtained by subtracting from the consequences of the dam failure the ones that would have happened anyway, $C_\Delta(l, f)$:

$$R_\Delta = \sum_l p(l) \cdot p(f|l) \cdot C_\Delta(l, f) = \sum_l p(l) \cdot p(f|l) \cdot [C(l, f) - C(l, nf)] \tag{2.18}$$

On the other hand, even if the dam functions as intended and the structure does not collapse, the reservoir area and the downstream affected floodplains may be in a state of high risk. This risk is due to normal and emergency flood operations. The non-breach risk is largely dependent on the downstream channel capacity and the elevation at which houses start being inundated in the upstream region:

$$R_{nf} = \sum_l p(l) \cdot p(nf|l) \cdot C(nf, f) \tag{2.19}$$

The analysis and evaluation of each individual potential failure mode and inundation scenario can lead to an improved understanding of the effects different system variables have on the overall economic, societal and individual risk of the system. It can also provide insights that can lead to the identification of both structural and non-structural risk reduction measures. This process is known as *Risk Assessment*.

2.5.2 The Process of Risk Assessment

In order to assess risk, David S. Bowles, Professor and Director of Utah's Water Research Institute for Dam Safety Risk Management, identifies four steps: (a) pre-assessment preparation, (b) risk identification, (c) risk estimation, and (d) risk evaluation [100]. Similar to the outline proposed by Jonkman et. al [85] and discussed in the previous section, Fig. 2.13 illustrates the risk assessment procedure described in the 2013 guidance document of the UK Environment Agency "Guide to risk assessment for reservoir safety management" [101].

A risk analysis should commence with a clear definition of its purpose and a exhaustive analysis of all the information required. Then, similar to the afore-described quantitative flood risk analysis, the second step aims at identifying the causes and sources of the hazards, the potential failure modes of the structure (PFMs) and the receptor susceptible to the hazard. Once the loads, failure modes and consequences are identified, the risk of the system is to be quantified. In this part of the analysis, the frequency of occurrence of the loadings that could initiate potential failure and then cause adverse consequences are estimated.

The risk analysis is initially conducted on the existing condition of the dam-reservoir system which establishes the perfect baseline for the evaluation of structural (e.g., raise dam crest elevation, or increase spillway capacity) and non-structural risk reduction measures (e.g., increase warning time, or enhance evacuation planning). Finally, the significance of the estimated risks for both, the baseline case and applying the risk reduction measures is to be evaluated.

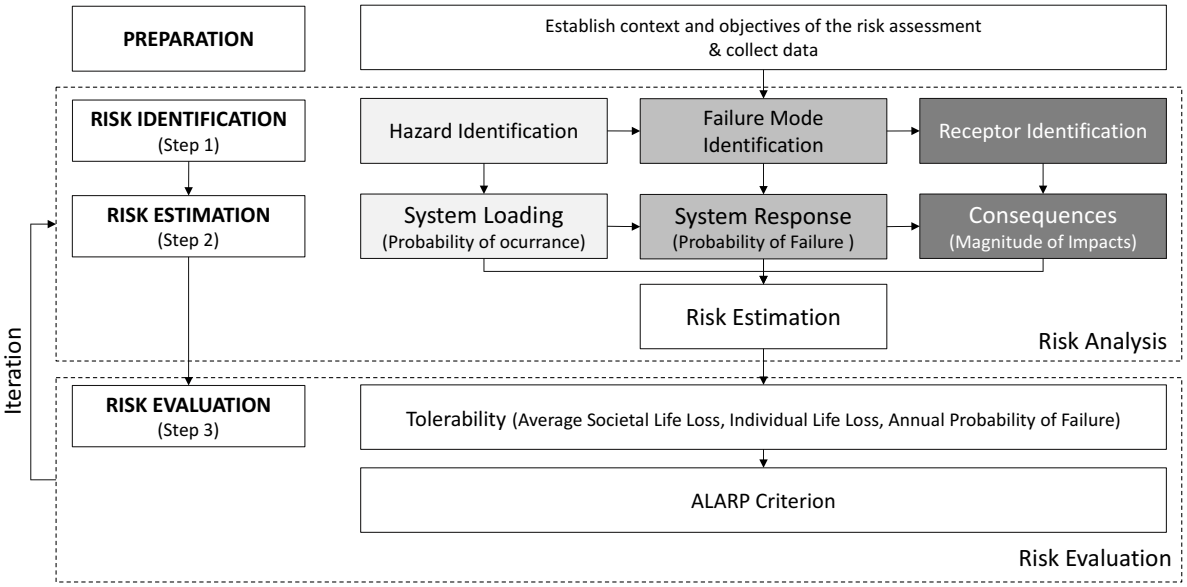

Figure 2.13: The dam risk assessment process [101]

To date, the international panorama includes a wide variety of tolerable risk guidelines. Above all the existing recommendations, the USBOR [102], ANCOLD [97] and USACE [88] guidelines are the ones mostly used in engineering practice. In addition to these three, the procedures employed in The Netherlands [89] and the British guidelines [103] are to be mentioned since they were precursors of the current approaches applied in risk evaluation. For instance, the concepts unacceptable risk, tolerable risk and broadly acceptable risk established by The Health and Safety Executive provide the basis for all the international recommendations on tolerability.

The USACE Interim tolerable risk guidelines [88] includes a two-step evaluation process. A level of risk is to be considered tolerable when both the tolerable risk limits and the ALARP criterion are satisfied. To begin with, the total estimated risk for all failure modes and all the loading scenarios leading to failure is compared against the tolerable risk limit values:

- A total Annual Probability of Failure (APF) limit value of 0.0001 per year
- A total Annualized Life Loss (ALL) limit value of 0.001 lives per year. The guideline also states that in those cases in which the total ALL value is greater than 0.01 lives per year, urgent actions to reduce risk are to be taken.
- An Individual Risk (IR) limit value of 1 in 10,000 years as a measure of life-safety risk expressed as the probability of life loss for the identifiable people most at risk. This value has been represented as a point on Fig. 2.14.
- A Societal Risk (SR) expressed in probability distribution of potential life loss is limited by the sloping line in the FN chart shown on Fig. 2.14.

Second, the ALARP requirement determines whether a risk has been reduced to be As Low As Reasonably Practicable. This evaluation should consider, among others, the level of risk in relation to the tolerable risk limits, the disproportion between the efforts in terms of money and time in implementing the risk reduction measures and the subsequent risk reduction achieved, and the cost-effectiveness of the risk reduction measures.

	Acceptable	Unacceptable	
		actions	urgent actions
Annualized Life Loss (lives/year)	ALL< 0,001	0,01 > ALL > 0,001	ALL > 0,01
Annual Probability of Failure (per year)	APF < 0,0001	APF > 0,0001	

Table 2.1: USACE risk tolerability limits for ALL and APF

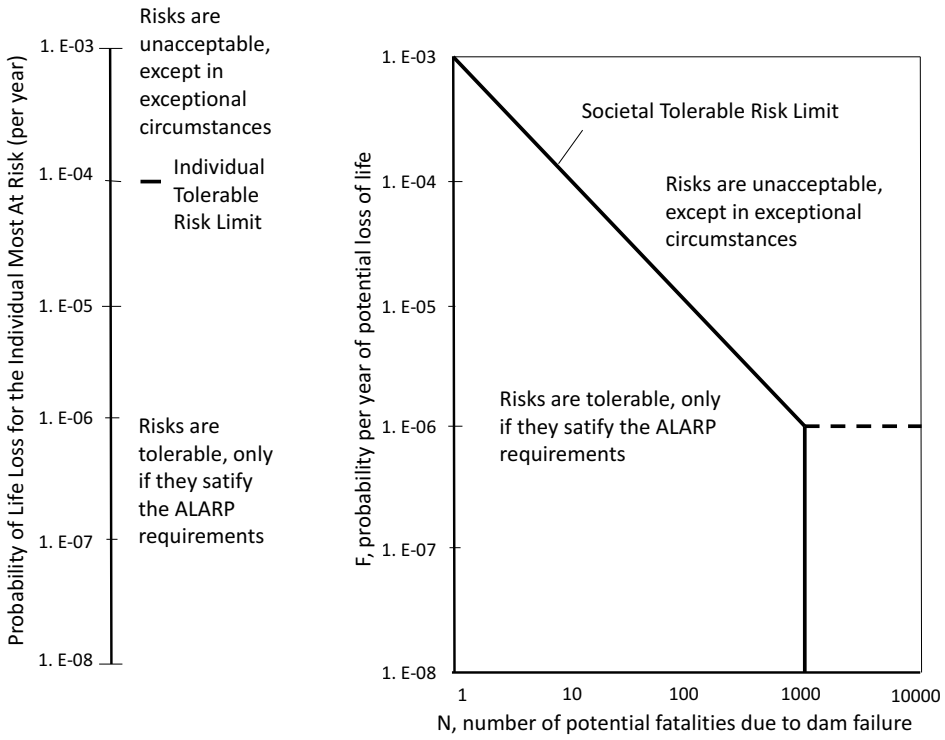

Figure 2.14: (a) Individual risk guidelines and (b) societal risk guidelines for existing dams [88]

2.5.3 Risk Assessment Methodologies

Current efforts on flood risk investigations applied to the management of dam safety aim at establishing methodologies and tools to assess the existing flood risk of dam-reservoir systems [104] [84]. In the last decade, various dam owners and agencies have been developing computer-supported risk assessment and management softwares, so-called "risk models". A risk model is described by many authors [105] [93] [86] as a robust and complete means of performing quantitative risk analysis of complex systems.

Diverse risk models can be found in the technical literature. Among others, *ResRisk*, developed by Utah State University and RAC Engineers & Economists for a large UK dam owner [106], *PAMS* developed for the Department for Environment, Food and Rural Affairs (Defra) and Environmental Agency [107] for flood risk management in the UK, or *DAMRAE* with its latest update *DAMREU* developed for the U.S. Army Corps of Engineers [91] [108] [109]. The *iPresas* risk assessment software developed by the company iPresas in close collaboration with the Technical University of Valencia, Spain, is also worth mentioning. The model is an expansion of Serrano-Lombillo's doctoral thesis [105] and comprises the main source utilized by the SPANCOLD for the elaboration of their technical guidelines on dam safety [92].

To obtain the risk associated with a dam-reservoir system, the risk models usually disaggregate the calculations into various scenarios, depending on how the failure is originated. For instance, failure can be motivated by flooding or by an earthquake, and it is convenient to do those calculations in a separate way, each situation being called loading scenario. According to the ANCOLD guidelines [97], the most common loading scenarios are: (a) Normal scenario, (b) Hydrological scenario, (c) Seismic scenario, and (d) Other scenarios.

The hydrological and seismic scenarios deal with unusual events. On the contrary, a normal scenario deals with the normal day-to-day situation, in which no flood nor earthquake is considered. Meanwhile, the category of other scenarios includes actions of sabotage, vandalism [110] or any other situation that does not fall into the previous categories. Figure 2.15 provides a graphical representation of the typical "source-pathway-receptor" for dam safety risk analysis in case of hydrological loading scenario. The figure has been divided in three sections that correspond with the three terms of the risk equation:

- **System Loading** : What is the chance of flooding?
- **System Response**: Will the dam withstand the loading?
- **Consequences** : Who and what can be harmed?

A description of the standard procedure for risk estimation in case of a hydrologic loading scenarios is discussed in the following paragraphs. Following the scheme presented in Fig. 2.15, the analysis of loading probabilities, the use of fragility curves representing the response of the system, and the damage curves for the assessment of consequences are explained. In doing so, attention is directed to the implicit assumptions made about the relationships between inflows, outflows and water levels. Current engineering practices base their calculations on assuming that those relations are unique, when in actuality they are not. The non uniqueness arises when a multivariate analysis of all the important characteristics defining a flood scenario is performed. Combination of different initial water surfaces, inflow peaks, inflow volumes and hydrograph shapes leads to cases in which, for instance, the same inflow peak result in completely different reservoir stages. As a result, a value of the peakflow cannot be directly associated with a pool level and consequently cannot be related with the probability of failure of the structure.

In the relatively recent literature, some authors have been applying the multivariate analysis for the determination of the risk of failure of hydraulic structures. De Michelle et al. [111] were the first to check the adequacy of a dam's spillway under a bivariate hydrological load. Since then, the use of copulas and distributions functions with finite support for the combined analysis of peakflows and volumes have been used to address the design of flood control systems [112] and the generation of synthetic design hydrographs [113]. In 2010, Mediero et. al [114] formalized the idea that the return period of a failure of a structure depends on the structure of interest, and therefore the interaction between the hydrological loads and the structure should be taken into account when fixing the return period of the event. This "structure-based approach" has been later expanded by Jimenez [115] and Volpi and Fiori [116] which expressed the return periods of flood events as their probability of exceeding a certain water level in the reservoir. This definition of return period is further explained in Chapter 3.

System Loading

When the source of hazard is hydrologic in nature, the loading event is usually a flood. Floods are mostly represented by storm hydrographs obtained from rainfall-runoff models, or from scaling up representative hydrological shapes based on historic events, design events or balanced hydrograph methods. In the standard engineering approach, these obtained hydrographs are characterized by a unique environmental variable. A common way to proceed is through the

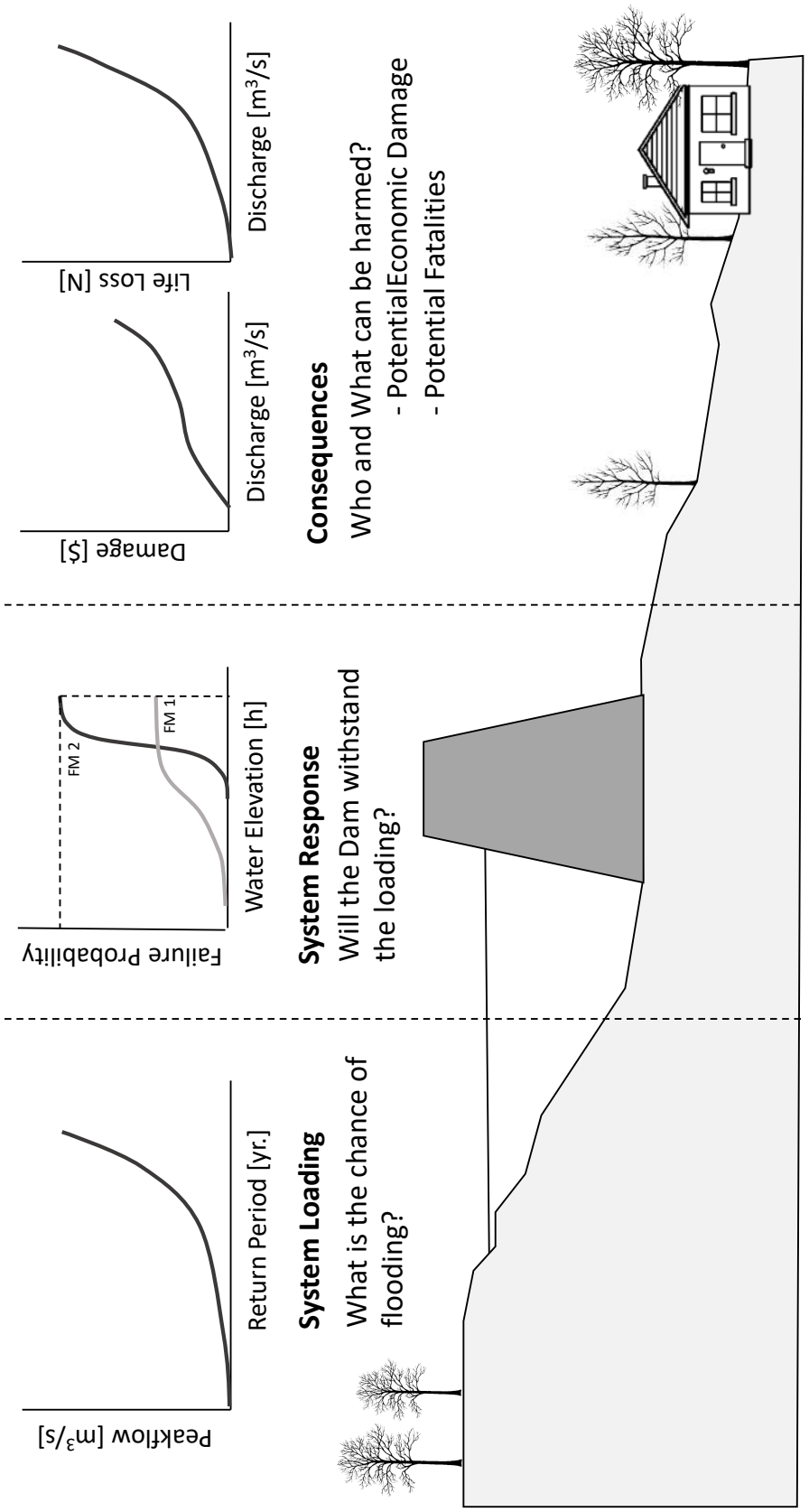

Figure 2.15: Risk Framework applied to a Dam-Reservoir System

univariate analysis of peak discharges, which can be associated to a certain probability of occurrence, defined by its annual exceedance probability.

The generated hydrographs are then routed to obtain their corresponding water surface stages and peak outflow rates which are assumed to have the same frequency of the variable characterizing the hydrograph. Figure 2.16 illustrates a hypothetical example of patterned hydrographs characterized by their peak flows frequencies. The reader should note that the reservoir routing is achieved assuming that the initial water level in the reservoir is at the bottom of the flood control pool, which, as pointed out by Goldman [117] is "the simplest and most defensible approach."

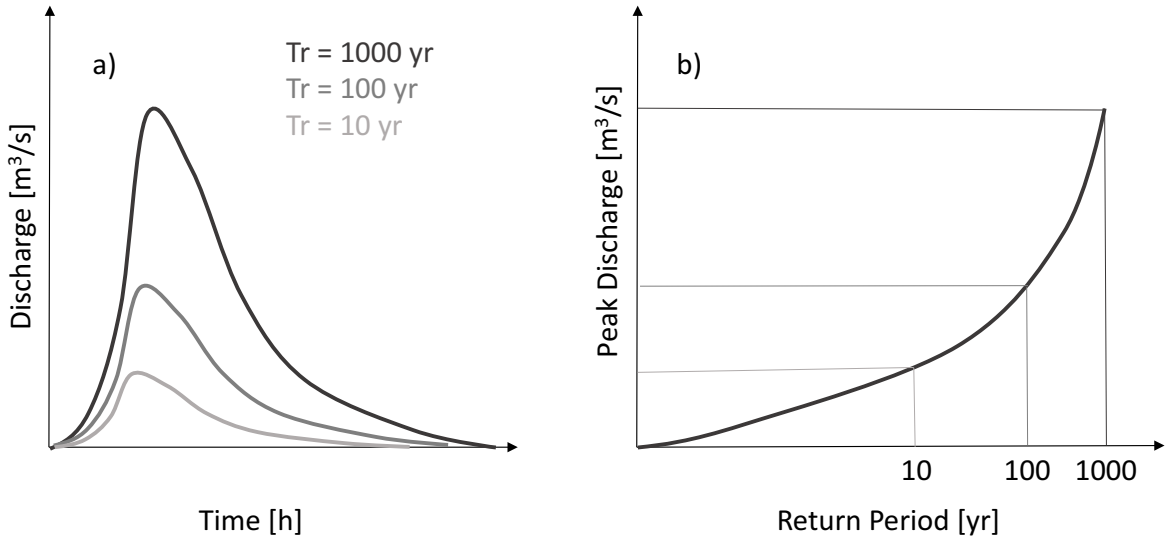

Figure 2.16: Example of patterned hydrographs showing the range of hydrologic loading for reservoir routing and their associated peakflow frequency curve

The "Best Practices in Dam and Levee Safety Risk Analysis" manual [22] sets out a great variety of streamflow-based and rainfall-based methods for estimating the magnitudes and probabilities of extreme events. Several authors have been able to obtain, for instance, accurate maximum peak-inflow frequency curves within Monte Carlo frameworks and extend the recorded series of data with historical, regional and paleoflood information [118] [119] [120] [121]. Acknowledging that the magnitude of a flood and its consequences does not depend only on the peakflow but also on the volume, duration and temporal distribution of the hydrograph, in the last decades, multivariate probabilistic approaches have increasingly been gaining importance [122] [123] [124] [125].

Indeed, in cases in which the reservoir storage capacity is large enough to alter the relationship between peak flow, peak stage and peak outflow, the current risk assessment guidelines recommend the used of additional methods based on volume duration frequency analysis (VDF) [126] [117]. First, the estimation of volume-duration-frequency (VDF) relationships is performed. Second, after analyzing inflow-outflow data and performing reservoir routing studies, the critical inflow duration that leads to the largest peak annual regulated flows is estimated. Third, a relationship between unregulated inflow volume and peak outflow for the critical inflow duration is developed. Finally, this relationship is used to translate an inflow volume of a given frequency to peak outflow of the same frequency. In this way, the regulated flood frequency is estimated from the inflow volume frequency. Similar procedures are applied for the estimation of inflow volume to peak stage relationship.

System Response

The following step in the risk assessment procedure is the analysis of the response of the system to the loading conditions. This is normally done by identifying and estimating the most probable failure modes of the structure. The objective is to obtain a curve that relates the water level in the reservoir with the annual failure probability of the structure. Since water level frequency curves are directly correlated to the frequency of the flood events, the probability of failure for a given water level can also be expressed in terms of inflow volumes or peakflows.

Figure 2.17a displays two fragility curves for two different failure modes: overtopping and internal erosion/piping. The light gray fragility curve represents the failure due to piping and the black line the failure due to overtopping. It can be seen that the probability of failure of a structure can be high even though the water levels never reach the crest level. This means that emergency schedules which only focus on ensuring the integrity of the structure against overtopping may be underestimating the level of risk posed by dam failure.

In those cases in which the probability of failure is non-zero, the dam breach hydrograph is to be estimated. Nowadays, a broad range of hydraulic numerical models that allow for the simulation of breach scenarios and their corresponding hydrographs are available in the literature. Wahl [127] compiled the different models that have been developed with both a parametrical and physical basis. A very simple way of estimating the characteristics of a breach hydrograph relies in the use of empirical equations that relate peak discharges at failure with one or several parameters of the dam or the reservoir, for instance, the water surface elevation (Fig. 2.17b). Among the most renowned formulations, the one developed by Fröhlich [128] based on a simple regression analysis of 22 past failure events is widely used in the engineering practice. The equation estimates the breakage peak discharge B as a function of the reservoir volume V_w and its height h_w:

$$B = 0.607 \cdot V_w^{0.295} \cdot h_w^{1.24} \tag{2.20}$$

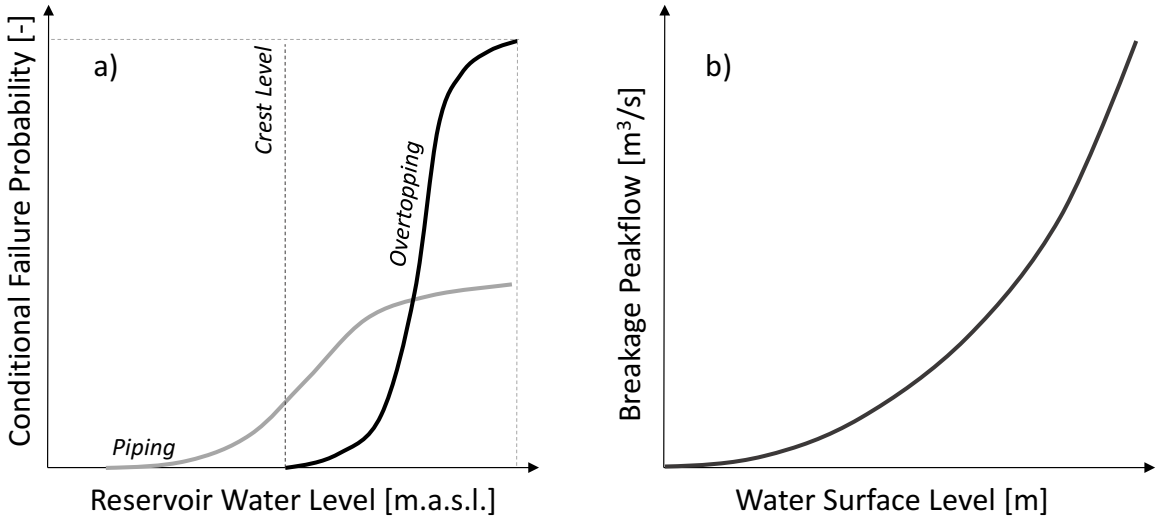

Figure 2.17: (a) System response curves, and (b) breakage peak flow curve

Consequences

The estimation of consequences derived from each scenario is normally based on predefined relations with the output hydrographs obtained from flood routing and dam failure modeling. The

so-called damage curves. These curves indicate the consequences in terms of monetary values, $M\$$, or number of lives loss, N, associated with a specific characteristic of the hydrograph. The peak discharge is usually employed since larger discharges flood larger areas, with higher depths and heavier costs.

For the development of the damage curves, several floods with different maximum peak discharges must be considered. This study consists of (a) routing the hydrograph through the floodplain assisted by hydraulic models to compute the depths at each parcel, and (b) the elaboration of depth-damage curves for the area under study that relate the depth with the percentage of structural damages in different types of land uses including agriculture, residential, commercial, transport, or industrial. Figure 2.18a sketches an example of depth-damage curve for residential structures according to the 2017 JRC European Commission Report on global flood depth-damage functions [129]. It can be inferred from the figure that at a depth of 6 meters, a maximum damage value is reached.

Different shapes of damages curves may result from the study of consequences. Specifically, the flood damage function caused by peak flow can be linear (Curve A) convex (Curve B), concave (Curve C) or piece wise linear with thresholds (Curve D) as illustrated in Figure 2.18b [130]. These shapes depend on the topography of the region as well as the geometry of the streams. For instance, a consequences curve can rise almost vertically if from a certain value of discharge the flood overtops a levee of population protection.

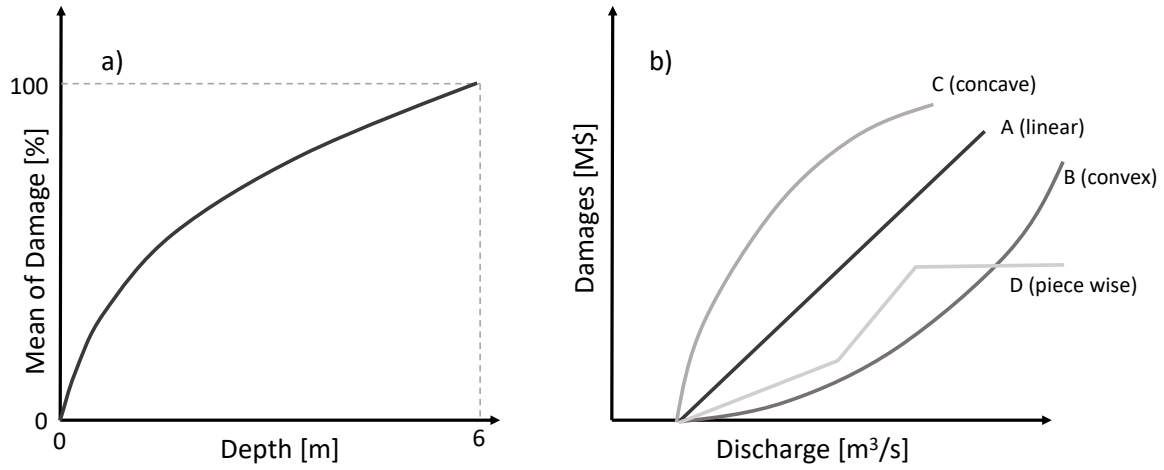

Figure 2.18: (a) Depth-damage curve, (b) damage curve shapes in terms of peak outflows

2.5.4 Hydrologic Event Tree Construction

The quantitative assessment of the risk associated with a dam-reservoir system is commonly performed using event trees. Event trees associate consequences with system performance and loading conditions, providing a qualitative representation of all the possible scenarios leading to failure of the system. They consist of a sequence of interconnected nodes and branches. Every random or discrete variable of the system is represented by a node. For instance, a certain water level in the reservoir. Branches originating from each node symbolize all possible events or states of nature that can occur. Following the prior example, a certain water level can derive in a failure or no failure of the structure. A probability is associated for each branch to represent the likelihood for each event or condition. These probabilities are conditional on the occurrence of the preceding events to the left in the tree. The conditional structure of the event tree allows

the probability for any sequence of events to be computed by multiplying the probabilities for each branch along a pathway. The branching structure of the event tree, which requires that all branches originating from a node be mutually exclusive and collectively exhaustive, allows for the computation of the combined probability of all the events leading, for example, to structural failure, by summing branch probabilities across multiple pathways.

An example of a hydrologic event tree adapted from the generalized computational framework DAMRAE is shown in Fig. 2.19. The figure displays the typical shape of a hydrologic event tree. It is comprised of nodes and branches distributed over seven levels of complexity. Furthermore, the event tree recognizes two possible failure modes: dam overtopping and piping, and considers two different exposure scenarios: day and night. Level 1 contains a *continuous branch* representing a continuous stochastic variable, the flood peakflows, which values can be related to their annual exceedance probability. Levels 2 and 3 are *state function branches*. A state function branch represents the deterministic relationship among variables in a event tree. In the presented example, Level 2 and 3 compute the peak pool and the peak outflow related to the peakflow values of Level 1. Level 4 contains the *failure branches* for the system response curves in cases of dam overtopping and piping, and the non-failure branch. As mentioned above, only one exposure scenario has been included in this example, the time of the day. This type of exposure scenario is very important for the calculation of loss of life consequences. However, if the risk analysis focus exclusively on structural damages, the time of the day won't affect the results. Finally, the estimated magnitudes of life-loss and economic consequences for combinations of the various types of initiating events, failure modes and exposure conditions are assigned to the *consequence branches* represented in Levels 6 and 7.

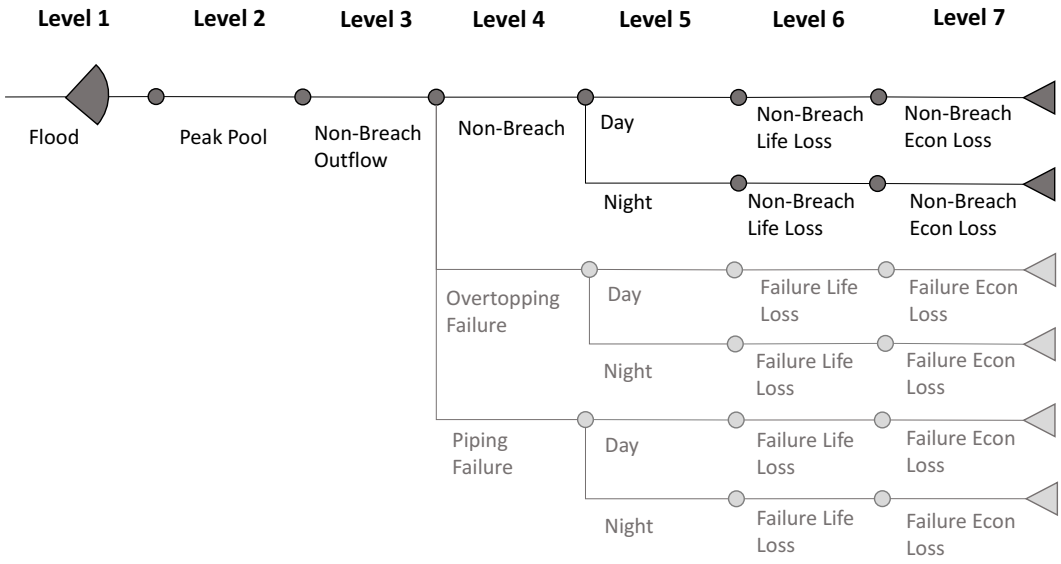

Figure 2.19: Example of flood event tree [109]

As previously stated, the reader should note that by including, for instance, the peak outflow as a state function, a direct relation between reservoir inflow and outflow is assumed. The dam operation is therefore implemented as a deterministic variable which gives unique values of outflow for each inflow value. Chapter 3 demonstrates that these assumptions are seriously limited and which might lead to under and overestimation of the total risk. When the stochastic natures of the initial water levels, the inflow volumes and the inflow peaks are taken into account, the dam operation is to be seen as stochastic in nature. In other words, the same peakflow can derive into different peak outflow values.

2.6 Conclusions

As a result of past flood events and their consequences, flood management policies, include a wide range of risk mitigation measures which aim at either reducing the probability of flooding or its consequences. Among the structural solutions, one of the most common means of retaining excess water in flood prone areas is the construction of dam-reservoir systems [10] [11]. Their competences on flood control and mitigation largely depend on the management of their available storage capacity [16]. The method currently recommended by the USACE for developing operation policies is based on conservative estimates of future inflow volumes and focuses exclusively on critical water surface elevations. The application of these strategies could lead to operations which might be distant from the optimal. Furthermore, from a risk point of view, the dam could be posing high levels of risk to the downstream floodplain occupants even if the crest of the structure is never exceeded. This should also be considered in the development of the operating schedules.

Alternatives to the deterministic approach from the USACE are available in the literature. In the following chapters, **a combined simulation-optimization model will aim to improve the existing methods for developing emergency operation schedules**. Simulation models help answer *what if* questions about the performance of different operational strategies, whereas optimization models might assist with the identification of the best one according to a series of constraints and objectives. To guarantee that the operational policies display fitting behavior for a wide and representative ensemble of flood events, an **stochastic approach would allow the array of inputs to be representative of minor, moderate and major flood events**.

Implicit Stochastic Programming and Explicit Stochastic Programming optimization techniques are often used by researches to include the uncertainty of future inflows within the optimization process. However, the complexity of these methods increases the gap between theory and practice [47], especially when stochasticity is explicitly included [33]. To facilitate the application of the framework to different case studies and simplify the problem, **the Parametrization-Simulation-Optimization technique could be utilized**. The method parametrizes the flood control operations reducing the dimensions of the typical optimization models to **a handful set of variables**. The parametrized rule is then linked to a simulation model which enables the evaluation of the performance of the system for given parameter values; and to heuristic strategies to look for the optimal balance solution.

Finally, **risk assessment procedures could be used to determine those operational decisions that may end up increasing or decreasing the levels of risk**. Despite the increasing importance of risk-informed management of dam-reservoir systems, there is a scarce literature treating the combined use of probabilities and consequences for flood control operations. One of the reasons limiting its use might be related to the absence of an appropriate methodology to include the effects of dam operations within the risk estimation of dam-reservoir system. Current practices for risk assessment are largely dominated by simplified assumptions which reduce the dam operation to a simple deterministic relation between inflow volumes and outflow peaks, leaving the effects of the dam operation on the overall risk out of the calculations. **For the correct optimization of the flood control operations based on risk, the effects of predefined operating rules should be quantitatively included within the risk assessment process**

Chapter 3

Including Reservoir Operation in the Risk Analysis of Dam-Reservoir Systems

In this chapter, a simple hypothetical example is employed to illustrate the importance of including dam operational effects in the risk analysis of dam-reservoir systems. Despite the crucial role operating rules have in the mitigation of damages during floods, to date, their effect on the overall risk of the system has not been quantified nor directly included in the standard risk assessment procedures. The current methodologies used in the engineering practice are largely dominated by simplified assumptions made about the relationships between unregulated inflow volumes, peak regulated outflows and peak reservoir stages. These shortcomings reduce the dam operation to a simple deterministic relation between inflow volumes and outflow peaks which can lead to incorrect estimations of the overall level of risk.

In light of this challenge, the chapter presents a procedure for conducting risk analysis applied to dam-reservoir systems which integrates the effect of predefined operating rules by including the *system operation* as an essential component in the definition of risk. When the statistical variability of the reservoir initial state, the inflow peaks, and the inflow volumes are taken into account, a set of operational constraints can lead to situations in which similar inflow volumes or inflow peaks result in significantly different peak pool elevations and peak outflows.

Although the example presented in this research does not represent the full complexity of the problem, it reveals how specific assumptions widely used in the current engineering practice concerning inflow-outflow and inflow-pool level relationships could end up in an over and underestimation of the overall risk. The chapter, therefore, provides the insight required to move away from the volume-duration-frequency-based empirical analysis towards a more realistic framework for estimating risk in dam-reservoir systems. Simultaneously, the difficulties in fully addressing the influence of important hydrological system characteristics such as different hydrograph shapes are acknowledged and, consequently, future work to improve the underlaying statistical dependence between the variables of the system is advocated.

The chapter is organized as follows: it begins with a brief description of the problem followed by a thorough literature review of the current methodologies for risk assessment. The introductory section concludes setting up this chapter's objectives. Then, the new definition for the overall risk of a dam-reservoir system is presented, where explanations regarding the different components of risk as well as the inclusion of operational effects in their quantification are provided. The results obtained from the implementation of the methodology into a hypothetical dam-reservoir system are exposed and properly discussed in the results and discussion section. The chapter concludes with a summary of the findings and recommendations for future research and chapters.

3.1 Literature Review

Although reservoirs are not designed to provide complete protection against floods, a proper use of their storage capacity can efficiently attenuate incoming storm peaks and minimize the damages in downstream regions [131] [9]. The degree of control and protection offered by the retaining structures largely depend on their operation policies [16]. The temporal and spatial availability of water in the reservoir is managed following a set of operating rules which specify the amount of water to be stored and released during a storm. These operating rules are predominantly influenced by diverse system variables including the residual storage capacity at the time of the flood wave arrival, the downstream conditions during the storms, the characteristics of the reservoir, and the release capacity of the outlet structures. Other factors pertain to the dynamics of the incoming flood waves and are characterized by their total water volumes, their peaks and their distribution over time.

The manner in which all these factors combine determines how the dam should be operated. What is not well known is how these operation decisions modify the overall risk in the long term and how to best include their effects in the risk analysis procedures. Despite its practical significance, there is limited literature that discusses this topic. Several authors such as Ayalew et. al [132], Mediero et.al [114], and Volpi and Fiori [116] have explored the effects of reservoirs on peak released flows and peak reservoir stages frequencies. Nonetheless, a methodology addressing all these impacts for their inclusion in the assessment of risk is still lacking.

Currently, the risk estimation procedures recommended by the USACE [126] [21] and other international guidelines [92] [97] for risk-informed dam safety management are based on implicit assumptions made about the relationships between inflow volumes, outflow peaks and peak reservoir stages. These relationships allow for the definition of the risk in terms of single variables associated with the external loading such as inflow hydrograph peaks or volumes. To determine the inflow volume to peak outflow and the inflow volume to peak reservoir stage relationships, historical flood events are scaled up and routed through the reservoir in accordance with the operation schedules. The obtained peak reservoir stages and peak outflow rates are then related to their corresponding inflow volume assuming that they all have the same frequency. As a result, the probability of structural failure given by the reservoir stage and the probability of having damaging outflows are known from the frequency analysis of the inflow volumes.

During the last decade, some authors in the literature have been questioning this traditional procedure. For example, Ayalew et. al [132] demonstrated by means of a simple hydrological example that the assumption of the unique relation between inflow volumes and peak outflows is erroneous. Furthermore, they proved that it can lead to the underestimation of the peak regulated outflows and ultimately to an underestimation of risk at downstream regions. The authors pointed out that when the stochastic nature of the reservoir's water level at the time of flood wave arrival and the dam operation are considered, it is impossible to determine an event-based unique curve relating inflow volume to peak outflow. For instance, they highlighted how a high-frequency inflow volume that occurs when the reservoir is full can lead to a low-frequency peak outflow. Gabriel-Martin et. al [133] arrived to a similar conclusion in their study concerning the influence of the initial reservoir level in dam safety analysis, The authors indicated that the implementation of an initial variable water level increases the estimated downstream river safety in comparison with common design practices.

The work from Ayalew et. al [132] provided insight into the steps necessary to move away from the volume-duration-frequency-based empirical analysis towards a more realistic framework for estimating risk at downstream regions from reservoirs. However, they did not include dam breach scenarios in their simplified example. When facing low-frequency events, the authors suggested that the inflows were equal to the outflows. Contradicting this assumption, Mei [56]

explained that in the low-frequency tail of reservoir outflows, downstream discharges are larger than inflows due to dam failure.

In recent literature, some authors have proposed probabilistic approaches for describing the hydrological phenomena simultaneously considering multiple variables [122] [123] [124] [125]. This has allowed the practitioners to estimate multivariate return periods of the hydrological loads. Gräler et.al [134] presents a state-of-art review of different approaches differentiating between multivariate return periods based on regression analysis, bivariate conditional distributions, bivariate joint distributions, Kendal and survival Kendall distribution functions. De Michelle et al. [111] were the first to check the adequacy of a dam's spillway under a bivariate hydrological load. Since then, other studies proposed the use of multivariate hydrological design events according to different definitions of multivariate return periods [135] [136] [137].

More recently, Mediero et. al [114], while simultaneously accounting for storm peakflows and runoff volumes, formalized the idea that the interaction between the hydrological loads and the structure should be taken into account when fixing the return period of a flood event. As such, the authors altered the concept of a unique design hydrograph towards a family of events that all reach the same water level in the reservoir, and thus, pose to the structure the same level of risk. Following the same idea, Requena et al. [138] attempted to verify the assumption of a multivariate hydrological design event by comparing the multivariate return period of the hydrological loads to the structure return period proposed by Mediero et. al [114]. The results highlighted that differences exist among the return periods of flood hydrographs and that of dam overtopping. This "structure-based approach" was later expanded by Jimenez et. al [139] who studied the effect of different spillway lengths and reservoir capacities and Volpi and Fiori [116] who mathematically expressed the method.

A novel procedure for conducting risk analysis applied to dam-reservoir systems is formulated in this chapter. The approach provides an alternative to overcome the two main limitations of current risk assessment methodologies: (1) the multivariate analysis of the hydrological loading, and (2) the inclusion of the effects of the dam operation in the estimation of risk. To address this challenge, the proposed method is based on two ideas: one relating to the interpretation of the hydrologic loading return period using the structure-based approach; and the other, to the representation of the probabilistic dependence between water levels and peak outflows through their joint distribution function. Based on a generalized event tree framework, the potential economic damages to the upstream and downstream regions are related with their probability of occurrence through a Monte Carlo simulation technique. To illustrate the important features of the new interpretation of risk, a simple hypothetical example is employed. At the same time, the example is used to demonstrate that the current procedures use in the engineering practice oversimplify the complex processes associated with dam-reservoir system operations, leading to incorrect estimations of the overall risk.

3.2 Proposed Methodology

According to the definition of risk proposed by Kaplan and Garrick [77] and Kaplan [99], risk is to be interpreted as a combination of *what can happen*, *how likely is to happen* and *what are the consequences*. It was previously explained in Chapter 2 how the science of risk analysis has been adapted for its application to the field of dam safety management. Risk encompasses all those scenarios in which the water held by the structure could cause damages, the probability of occurrence of the loads leading to those scenarios, and the magnitude of the damages resulting from those loads. Acknowledging the influence the operation of the system has on those three components, the definition of risk presented in this chapter includes the question *how is the system operated* as an essential element in the risk assessment process (Fig. 3.1).

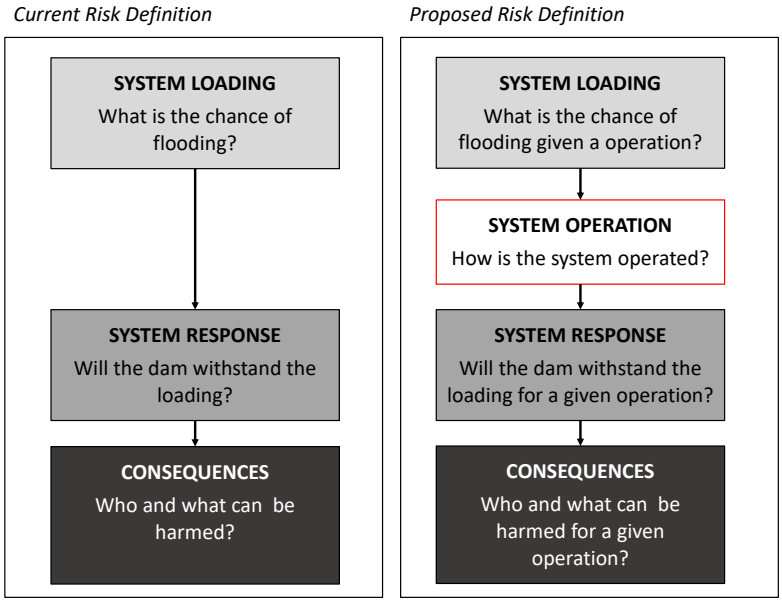

Figure 3.1: Difference between the current and the proposed risk definition which includes system operation as an essential component in the estimation of risk

Within the scope of risk analysis applied to dam-reservoir systems, the concept of risk should not be limited exclusively to the catastrophic breakage of the structure, but must also include any event that might produce adverse consequences in the reservoir area and downstream floodplain. As such, the total risk of the system, R_T, is assessed as a summation of the set of structural (Ultimate Limit State) and non-structural (Serviceability Limit State) failure scenarios, each of which has a probability of occurrence and a economical consequence:

$$R_T = R_{SLS} + R_{ULS} \tag{3.1}$$

The ultimate limit state refers to the risk posed by the dam due to the collapse of the structure. Inundation scenarios resulting from the structural failure of the dam prior to overtopping and the structural failure of a dam due to overtopping fall into this category. When a breach is generated in the dam structure, large uncontrolled volumes of water flow towards downstream floodplains causing enormous damages. The breakage flows in those situations depend upon the stage of the reservoir at the time of the breach as well as the total volume of water held by the dam at the breaching stage [128]. Since larger discharges flood larger areas with higher depths and heavier costs, a well-accepted approach consists of elaborating consequence curves relating the damages to the *breakage peakflows*, B [92].

The serviceability limit state includes all those scenarios which may end up flooding structures from the upstream and downstream areas during normal or emergency operations. Downstream flooding due to malfunction or misoperation of outlet works, release rates above the non-damaging capacity of downstream channels, uncontrolled flows over emergency spillways, and pool levels inundating structures upstream of the reservoir are to be considered in this group. Leaving out the flooding risk resulting from malfunction of gates, which is out of the scope of this research, serviceability limit state damages can be related to the reservoir stages, $h(t)$, and the reservoir released flows, $O(t)$, at any time. In a simplified way, the maximum damage caused by each flood event can be expressed in terms of the *maximum water level* reached, h, and the *maximum released flow*, O.

The risks posed by the the external hydrological loads to downstream and upstream areas can therefore be characterized by different *characteristic damage variables* depending upon the failure scenario: peak released flow, O, peak reservoir stage, h, and peak breakage flow, B. Equation (3.1) is thus rewritten as the summation of the risk of flooding upstream structures should the dam not break, $R_{SLS,h}$, the risk of releasing flow rates larger than the downstream non-damaging capacity should the dam not fail, $R_{SLS,O}$, and the risk to the downstream floodplain occupants and structures that is attributed to dam failure, $R_{ULS,B}$:

$$R_T = R_{SLS} + R_{ULS} = R_{SLS,h} + R_{SLS,O} + R_{ULS,B} \tag{3.2}$$

The reader should note that throughout this chapter the term failure adopts two different meanings: the failure of the structure refers to the breach of the dam, whereas the failure of the system comprehends both the ultimate and the serviceability limit states. Figure 3.2 illustrates an schematic of the different failure scenarios to be included in the estimation of risk, the potential economic damages, and their occurrence probability.

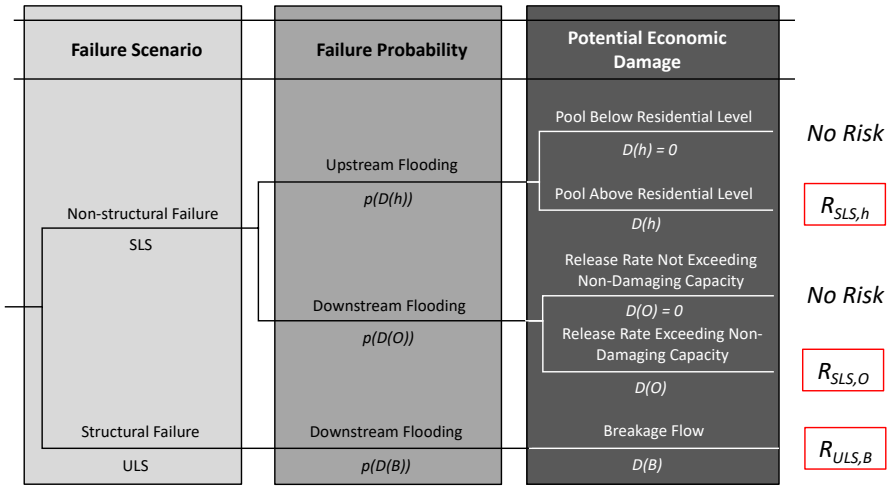

Figure 3.2: Plot illustrating an schematic of the different failure scenarios; the potential economic damages, $D(h)$, $D(O)$, $D(B)$; and their occurrence probabilities, $p(D(h))$, $p(D(O))$, $p(D(B))$

To include the effects of dam operations, the proposed method incorporates two ideas to the current approaches for dam-reservoir system risk assessment: one relating to the interpretation of the hydrologic loading return period using the structure-based approach developed by Mediero et. al [114], mathematically expressed by Volpi and Fiori [116], and explained in detail in Appendix A; and the other, to the representation of the probabilistic dependence between water levels and peak outflows through their joint distribution function. Finally, based on a generalized event tree framework, the potential damages to the upstream and downstream regions are related with their probability of occurrence through a Monte Carlo simulation technique. Figure 3.3 provides a graphical representation of the source-path-receptor scheme for the suggested dam safety risk analysis in case of hydrological loading scenario. The figure has been divided in four sections that corresponds with the new definition of the risk equation.

- **System Loading** : What is the chance of flooding given a dam operation?
- **System Operation** : How is the system operated?
- **System Response** : Will the dam withstand the loading for a given dam operation?
- **Consequences** : Who and what can be harmed for a given dam operation?

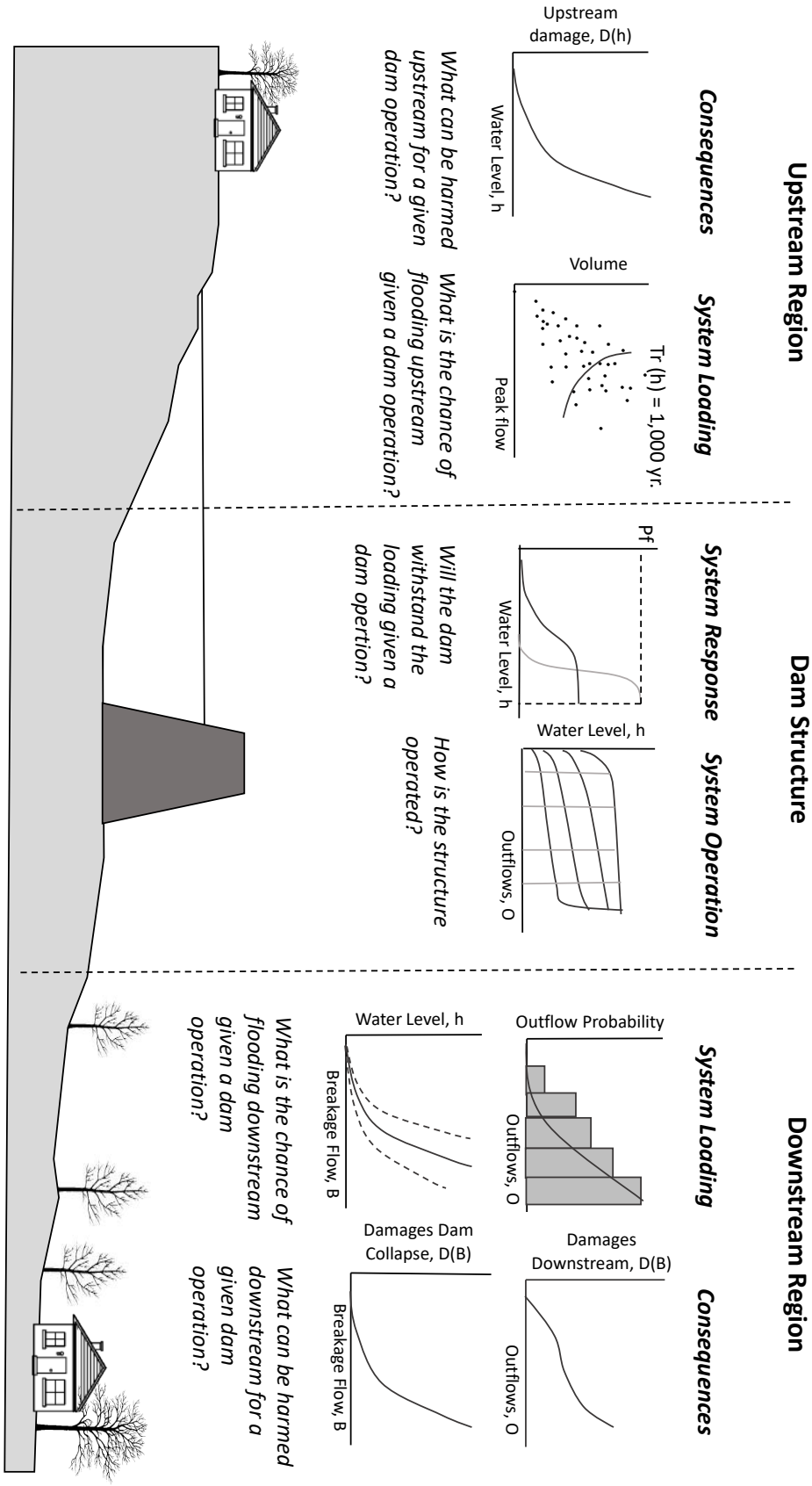

Figure 3.3: Risk Framework including Dam Operation applied to a Dam-Reservoir System

3.2.1 Components of the Overall Risk of the System

To estimate each one of the overall risk components presented in Eq. (3.2), the probability of occurrence of each characteristic variable, its associated expected value of the damage, and the response of the system in terms of structural failure probability (for ULS) and structural non-failure probability (for SLS) need to be taken into consideration. In the following, explanations are provided regarding the risks posed by the construction of a retaining structure to the upstream and downstream area including the influence the dam operation has on them through:

1. Simultaneous analysis of initial reservoir levels, inflow peaks and inflow volumes.
2. Interpretation of the multivariate return period using the structure-based approach.
3. Study of the statistical dependence between peak reservoir stages and peak outflows.

Serviceability Limit State Risk of Upstream Flooding, $R_{SLS,h}$

The serviceability limit state risk of upstream flooding, $R_{SLS,h}$, is given by the probability of reaching certain maximum water level, the probability of non-failure given that peak reservoir stage and the flooding damages in the reservoir area caused by those water levels:

$$R_{SLS,h} = \sum_{h} p(h) \cdot p(nf|h) \cdot D_{nf,h} \tag{3.3}$$

where $p(h)$ is the probability that the variable of characterization, h, may occur; $p(nf|h)$ is the conditional probability of non-failure of the structure given a peak reservoir stage; and $D_{nf,h}$ symbolizes the consequences derived from the maximum water levels reached. Figure 3.4 displays a non-structural upstream flooding failure scenario with its respective dam-reservoir system cross section. Diverse operational, θ, and physical constraints, γ, limit the system operation. Its interaction with the characteristics of the flood event, i.e. the peak inflow Q, the hydrograph volume V, and the initial reservoir level H_0, lead to different reservoir water levels that might cause damages in the upstream region.

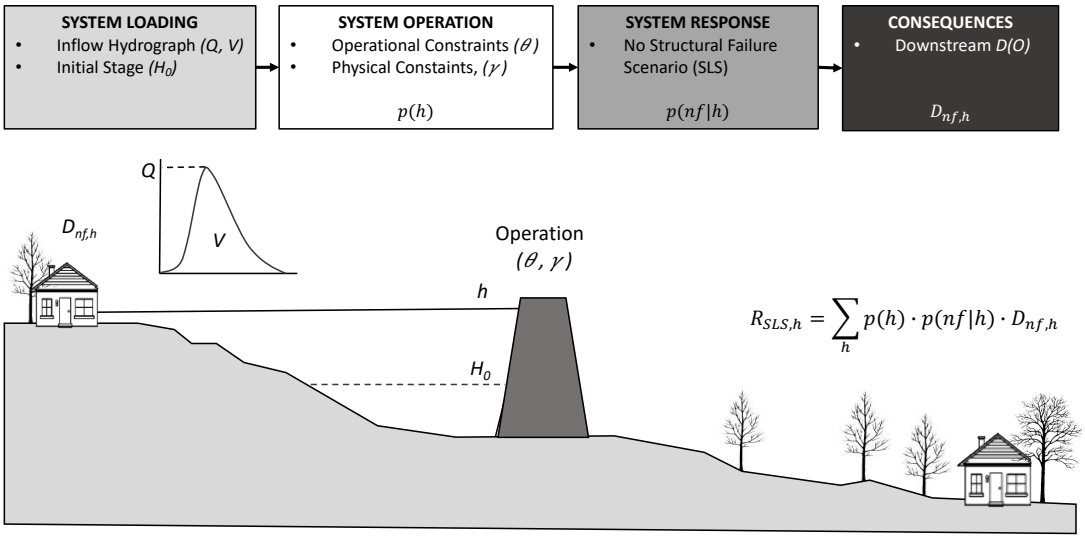

Figure 3.4: Influence diagram representing the interrelation between external loads, operation of the structure and characteristic damage variables for non structural failure scenarios

Following the structure-based approach described in Appendix A, the flood events affecting the system are characterized by their probability of reaching a predetermined water level which is directly associated with the potential upstream damages and the serviceability limit state risk of upstream flooding. Applying that return period definition, a family of hydrographs which generate the same maximum reservoir level and thus cause similar damages and pose the system to the same level of risk is obtained [115].

Serviceability Limit State Risk of Downstream Flooding, $R_{SLS,O}$

Similar to the serviceability limit state risk in the upstream region, the second term from Eq.(3.2), corresponding to the serviceability limit state risk for the downstream region, $R_{SLS,O}$, is estimated by combining the probability of occurrence of the peak outflows $p(O)$, their associated damages $D_{nf,O}$ and the conditional probability of non structural failure given a value of the peak outflow, $p(nf|O)$:

$$R_{SLS,O} = \sum_{h} p(O) \cdot p(nf|O) \cdot D_{nf,h} \tag{3.4}$$

Nonetheless, although the peak outflows associate the external loads with the damages downstream of the dam, they are not the direct cause of the failure of the structure which is indeed driven by the reservoir stage. When applying the definition provided in Eq. (3.4), it is assumed that the probability of non-failure of a structure is related to the probabilities of having a certain peak outflow. To put it another way, it is assumed that there is a unique relation between peak stages and peak outflows. Is that assumption realistic? What should be expected based on general reasoning?

Consider the problem of constructing a flood control reservoir with gated outlet conduits and uncontrolled spillways. A conceptual answer to both raised questions is displayed in Fig. 3.5a, which shows the expected shape of the relationship between peak outflows and peak water surface elevations. The black and gray envelope lines represent the maximum and minimum releases at each reservoir stage. The figure shows that at the elevation of 2.5 m, the maximum release capacity of the outlets is achieved. Flows over the spillways are expected at 4.5 m.

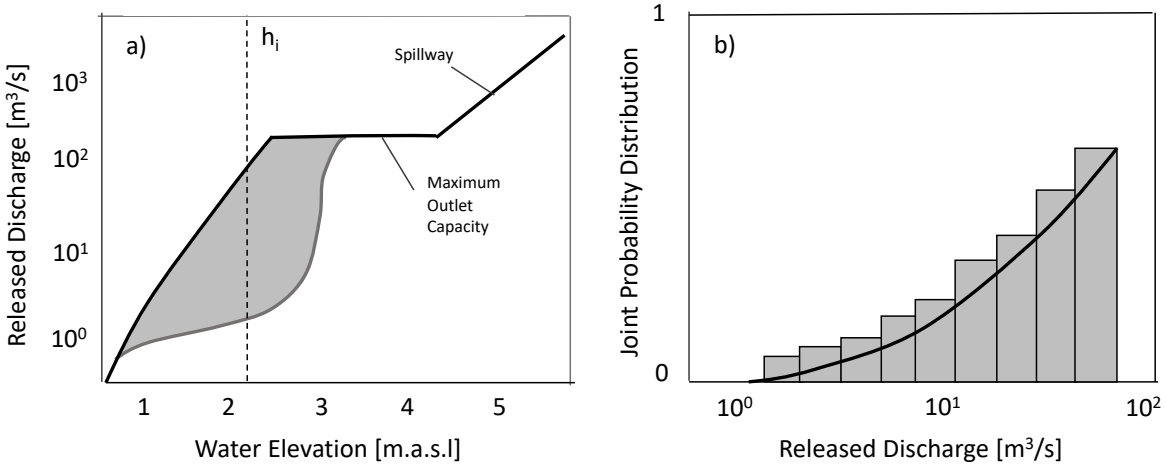

Figure 3.5: Plot representing the hypothesized (a) relationship between outflow peaks and maximum water surface elevations where the gray area includes all possible combinations; and (b) the probability of having an outflow rate for the reservoir stage, h_i

For low water levels, which correspond to high probability of exceedance, changing the outflow would not be desirable due to the environmental considerations associated with the low-flow regime of the river stream. Consequently, the relationship between outflows and reservoir levels will be equal to the rating curve, as are their frequencies. For higher reservoir levels for which the maximum release capacity could potentially lead to downstream flooding, reducing the outflow peaks as appropriate is desirable. Therefore, the associated outflows will have values lower than the maximum releases. However, as water levels increase inside the reservoir, the potential of reducing the outflows is diminished because the remaining storage capacity is limited. Finally, there will be a point at which the control structures can no longer regulate the outflows because the maximum release capacity is required to avoid uncontrolled releases over the spillways or to ensure the integrity of the structure. The last part of the graph represents the releases over the spillways which are not controlled in this example.

The degree of departure from the maximum release line depends on the future inflow volumes and the initial state in the reservoir at the time of flood wave arrival which determines the rates of gate opening during the flood event. In this research is hypothesized that all combinations of peak stages and peak outflows within the colored area are possible due to the stochastic nature of all the external variables affecting the reservoir operations. These combinations, however, are not equally likely. This is why the relationship between peak stages and peak outflows should be represented by their joint distribution function, expressing the outflows through conditional probabilities given a certain water level (Fig. 3.5b). By applying the new concepts, Eq. (3.4) is rewritten as:

$$R_{SLS,O} = \sum_{h} p(h) \cdot p(nf|h) \cdot \left\{ \sum_{O} p(O|h) \cdot D_{nf,O} \right\} \tag{3.5}$$

where $p(h)$ is the occurrence probability of reaching certain water level in the reservoir and $p(nf|h)$ is the conditional probability of failure for the attained reservoir stage. The last term of the equation represents the sum of the expected damages resulted from having a certain water level. In other words, the peak outflow probabilities expressed through their conditional probability for the given reservoir stage, $p(O|h)$, and their associated damages $D_{nf,O}$. Figure 3.4 displays a non-structural downstream flooding failure scenario with its respective dam-reservoir system cross section.

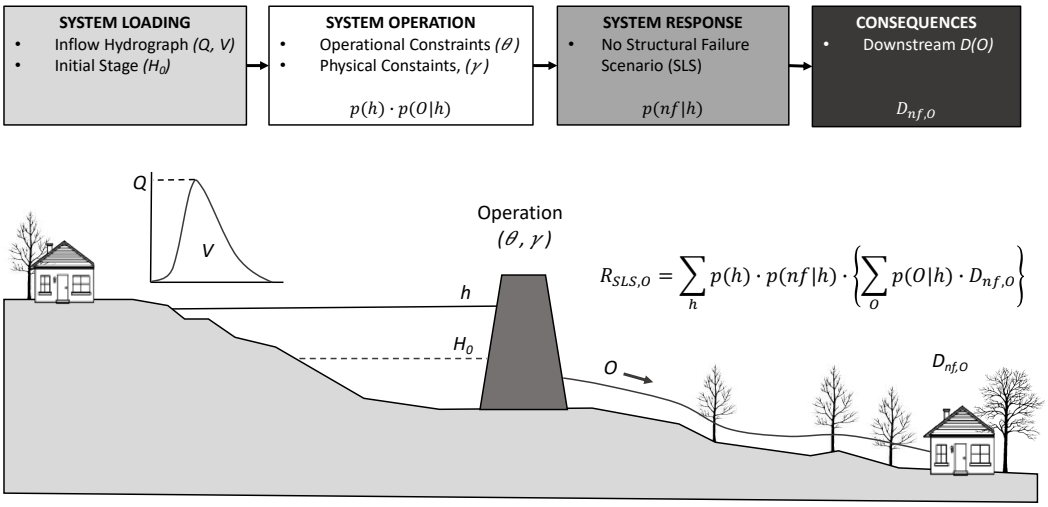

Figure 3.6: Influence diagram representing the interrelation between external loads, operation of the structure and characteristic damage variables for non structural failure scenarios

Ultimate Limit State Risk, $R_{ULS,B}$

Finally, the ultimate limit state risk, $R_{ULS,B}$ is estimated as the multiplication of the damages caused by dam breach and the probability of occurrence of a breakage flow. The latter is the combination of the probability of structural failure of the dam and the probability of having a certain magnitude of the breakage flow. Similar to the non-breach outflow peaks, the breakage peakflows are not directly related to the failure of the structure, but are, indeed, a consequence of it. A very simple way of relating the breakage peaks with the water surface elevation at the reservoir is through the empirical formulation of Fröhlich [128].

However, it is important to understand the nature of the information being used and the uncertainties inherent in it. The linear regression proposed by Fröhlich based on the analysis of 22 past failure events, presents a standard error of the predicted natural logarithm of B equal to $s_B = 0.4198$. For that reason, rather than assuming a deterministic relation, within this thesis the relationship between breakage peakflows and reservoir stages is considered as a conditional probability $p(B|h)$, with a mean equal to the result of the regression equation and a standard deviation equal to the residual variance of the regression:

$$R_{ULS,B} = \sum_h p(h) \cdot p(f|h) \cdot \left\{ \sum_B p(B|h) \cdot D_{f,B} \right\} \tag{3.6}$$

where $p(f|h)$ is the probability of structural failure of the dam for a given reservoir level and $D_{f,B}$ the damages associated to the breakage peakflow values. Figure 3.4 displays a downstream flooding scenario motivated by the structural failure of the dam with its respective dam-reservoir system cross section.

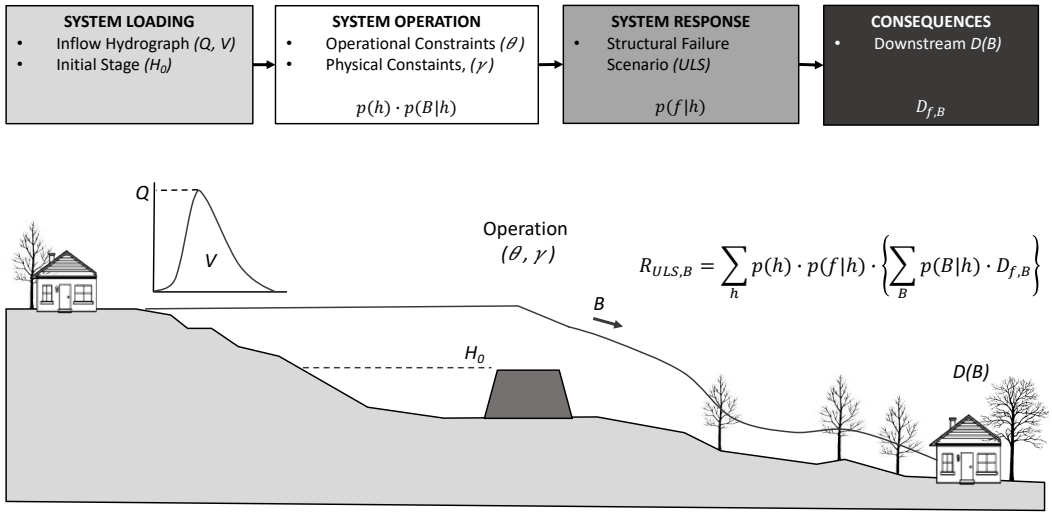

Figure 3.7: Influence diagram representing the interrelation between the external loading, the operation of the structure and the breakage peak flow for dam breach scenarios

3.2.2 Estimation of the Overall Risk of the System

In the end, the proposed methodology expresses the overall risk in terms of probability of exceeding a specific reservoir level, which is directly related with the structural failure of the dam, and the conditional probability of having peak outflows and breakage peak flows given that reservoir level, which are connected with the probability of having damages downstream of the dam. In this sense, the procedure accounts for both the influence the system operation has

on the frequencies of the loading, and the controlling effects of the dam which depend upon the hydrological variables and the structure characteristics. Once all the components of the overall risk are referred to the maximum reservoir stages, the total risk yields:

$$R_T = \sum_h p(h) \cdot \left\{ p(f|h) \cdot \left(\sum_B p(B|h) \cdot D_f(B) \right) + p(nf|h) \cdot \left[\left(\sum_O p(O|h) \cdot D_{nf}(O) \right) + D_{nf}(h) \right] \right\} \tag{3.7}$$

With the aim of combining all possible scenarios, their probabilities and consequences, the methodology suggests the use of the event tree depicted in Fig. 3.8. It is comprised of nodes and branches distributed over five levels of complexity. Furthermore, the event tree recognizes two possible failure mechanisms: overtopping (failure mode 1) and piping (failure mode 2).

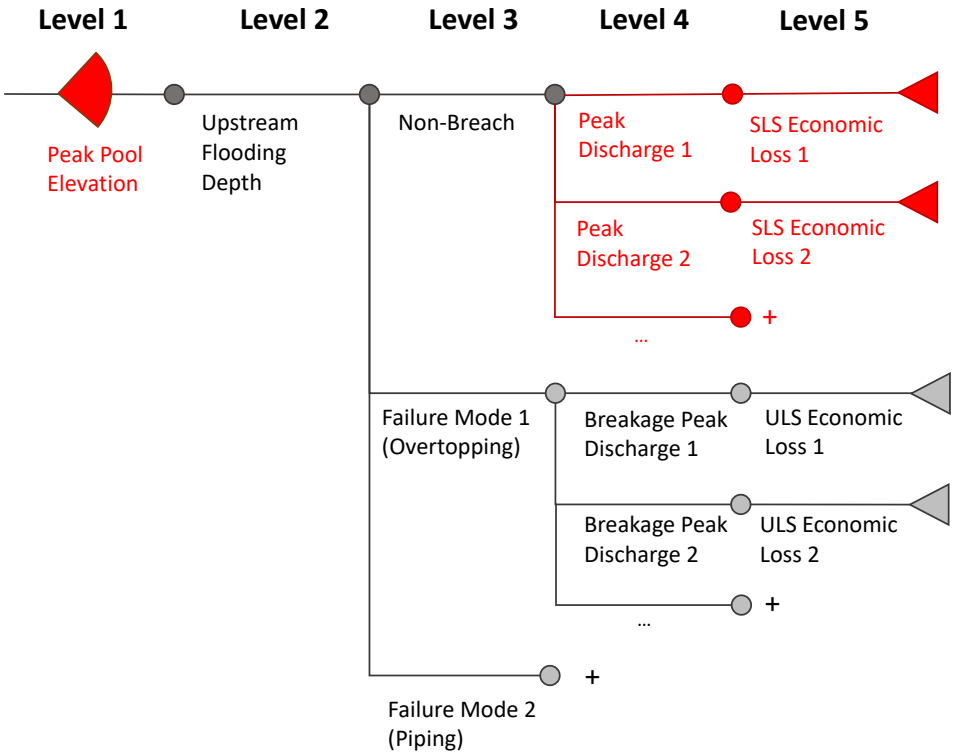

Figure 3.8: Flood risk assessment event tree for controlled water surface elevations marking in red all those branches affected by the dam operation effects

The principal differences with the hydrologic event trees currently in use by the USACE in the engineering practice resides in Level 1 and Level 4. These nodes and branches are affected by the dam operation and have been marked in red. The event tree starts with a continuous branch representing the peak reservoir stage, in which the values can be related to their annual exceedance probability. According to the structure-based approach, the return period of a flood event is calculated as the inverse of the probability of exceedance of the maximum water level that was attained while routing that hydrograph following a pre-specified operating rule. On the other hand, although in the hydrologic event tree described in Chapter 2, both, the breakage peak discharge and the non-breach peak outflow were considered as state function branches. The methodology proposed in this chapter, taking into account the probabilistic relation between the variables, describes Level 4 as random branches which relation with the branches on the left is based on conditional probability estimates. To put it another way, similar values of reservoir levels can lead to different values of peak outflows.

3.3 Implementation of the Methodology

Based on a Monte Carlo simulation framework, the proposed methodology suggests the use of the event tree shown in Fig. 3.8 for the estimation of the overall economic risk of single dam-reservoir systems. In order to implement the definition of risk and to simulate all the possible scenarios leading to the failure of the system, a stochastic flood scenario generator has been coupled to a reservoir flood control model and a risk estimator model. To guide the reader through the submitted approach, a scheme of the process is shown in Fig. 3.9. The two first components represent the system loading and system operation respectively and deal with the generation of all the data necessary for the quantification of risk. The statistical analysis of the characteristic damage variables and their combination with the system response and the damage magnitudes is carried out in the last part herein denoted as risk estimator model.

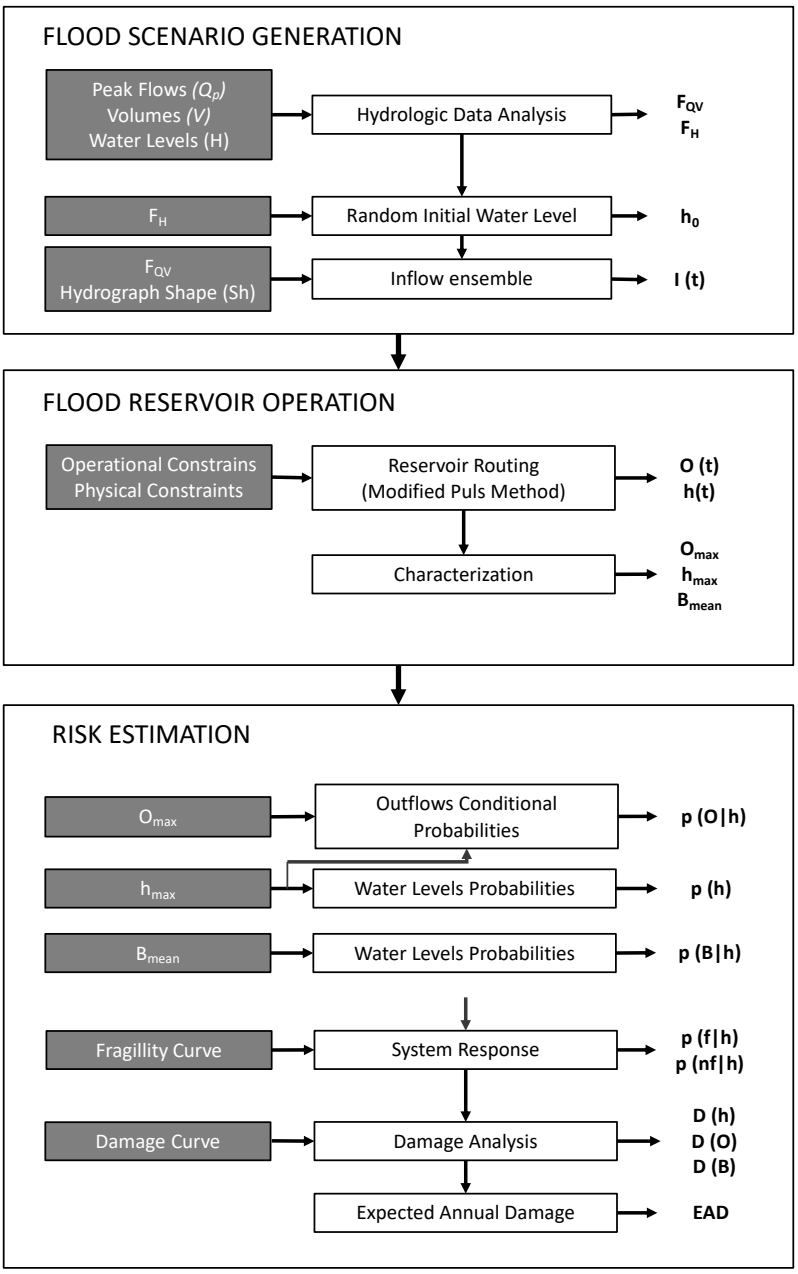

Figure 3.9: Simulation approach scheme for the implementation of the proposed methodology

3.3.1 Stochastic Flood Scenario Generation

As the probability of exceedance for high return periods is low, a large number of flood scenarios is required to accurately estimate the overall risk, the frequency law of the maximum water levels and the joint probability density function between peak reservoir levels and peak outflows. Therefore, inflow hydrographs and initial reservoir stages must be generated to extent the streamflow and reservoir level observations. A stochastic flood scenario generation model has been developed to study the response of the system under a long and statistically homogeneous ensemble of flood scenarios.

To cope with the generation of events, sample values for the initial reservoir level, the hydrograph peak and the hydrograph volume have been generated and associated using a Monte Carlo technique. The ensemble of simulated inflow flood hydrographs and initial water levels is assumed as being representative of the expected annual maximum hydrologic forcing of the dam. Consequently, the event tree branches are expressed in yearly probabilities, being the final overall risk assessed in dollars per year. Figure 3.10 depicts a simplify scheme of the entire process for flood scenarios generation which consists of four steps:

- Generation of a set of synthetic peak flows
- Generation of a synthetic volume for each synthetic peak
- Generation of a hydrograph shape for each synthetic pair of peak and volume
- Generation of a random initial reservoir stage for each inflow hydrograph

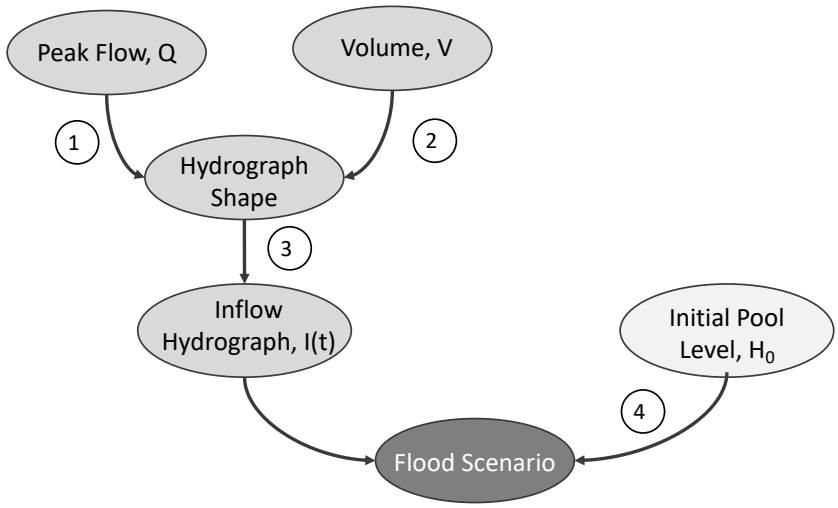

Figure 3.10: Stochastic Flood Scenario Generation scheme: (1) Synthetic generation of peak flows, (2) synthetic generation of hydrograph volumes, (3) generation of a hydrograph shape for each peak flow - volume pair, and (4) random generation of initial water levels

Synthetic Hydrograph Generation

The first step comprises the generation of random samples of peak inflows arriving to the reservoir in accordance with their marginal distribution function. Following the synthetic hydrograph generation procedure applied by Mediero et. al [8], the annual maximum analysis has been adopted for the implementation of the method. The reader may refer to Appendix B for more details regarding the estimation of the parameters, the goodness of fit tests and the selection of the most adequate flood frequency distribution function for each particular case.

The second step deals with the generation of a synthetic volume for each generated peak. The methodology adopted takes into account the statistical dependence between the maximum peakflows and hydrograph volumes through their joint distribution function. A synthetic volume could be estimated from a synthetic peak with a regression equation between them. This procedure, however, would lead to a perfect linear relationship ignoring the variability between the variables. According to the works carried out by Jimenez et. al [115], the conditional distribution of the volume with respect to the flow follows a log-normal distribution function when the residuals of the regression equation are normally distributed in the log-log space.

A normal randomization can be performed for each peak flow, with a mean equal to the result of the regression equation, μ_{reg}, and a standard deviation equal the 67% confidence interval of the regression equation, σ_{res}. The method proposed by Jimenez et. al [115] requires of a proper analysis of the relationship between the peak flow and the hydrograph volumes which may imply not only a local but also a regional analysis of the data. Figure 3.11 represents the synthetic generation process of a volume given a peak discharge and a linear regression analysis between the variables.

$$\mu_{reg,j} = V_j = 10^{a_j} \cdot Q_j^{b_j} \tag{3.8}$$

where V_j and Q_j are the hydrograph volume and peak flow of the j^{th} year, and a and b are parameters defined by the linear regression analysis.

$$\sigma_{reg,j} = \sqrt{\frac{\sum_{i=1}^{n}(log_{10}(V_j) - log_{10}(V_j'))^2}{n_j - p - 1}} \tag{3.9}$$

where V_j is the volume obtained through the regression, V_j' is the observed value at the gage station, n the length of the data series and p is the number of variables used in the regression analysis, which in this case is one.

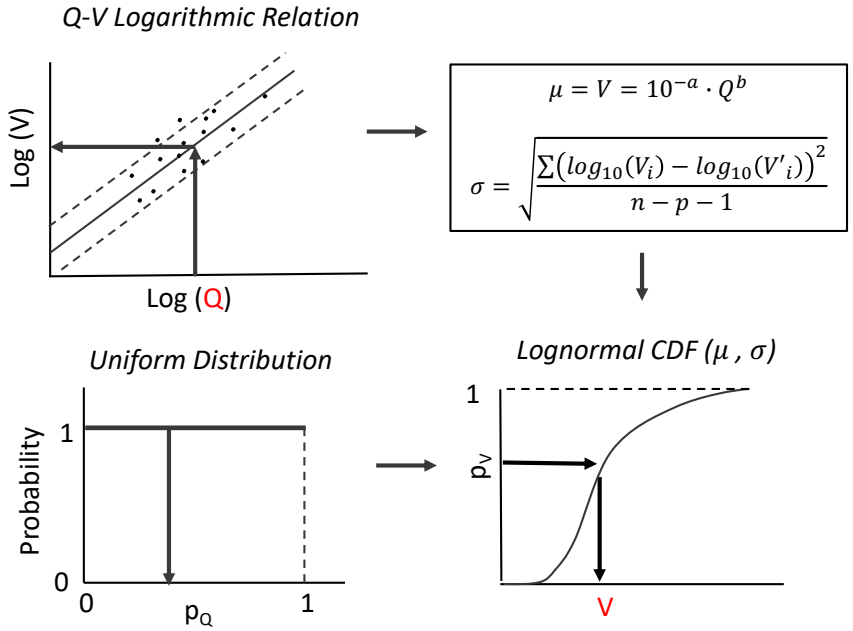

Figure 3.11: Schematic illustration showing the generation process of inflow volumes given a peak flow value and a regression analysis between peakflows and volumes

The third step refers to the transformation of each peak-volume pair into a inflow hydrograph. In practice, a watershed may have various shapes of flood hydrographs depending upon the intensity of the events, the prior moisture state or the urban development within the study area. Although different methods for the transformation of peaks and volumes into discharge time series have been proposed in the literature [140], a broadly accepted approach consists of scaling up design hydrographs or historical events to reproduce the shape of the hydrograph for low frequency events [22]. Figure 3.12 displays a hypothetical example of a rescaled hydrograph. In case of using more than one design hydrograph, first, the ratio between peak and volume is to be computed, and the hydrograph shape with the most similar ratio is selected [8].

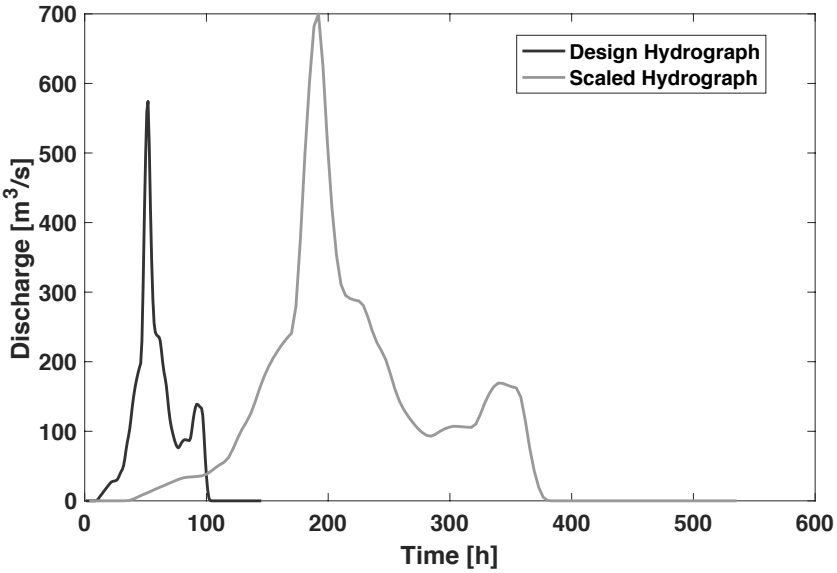

Figure 3.12: Hypothetical scaled hydrograph

Random Selection of Initial Water Levels

Finally, the variability of the initial water level is also considered. Following the procedure recommended by Carvajal et. al [141], the implementation of the methodology relies on the statistical analysis of prior water levels in the reservoir. The data is ordered in an increasing order and the empirical cumulative distribution function is obtained applying Eq. (3.10). Once the empirical cumulative density function of the prior pool elevations is known, a random water level based on the Monte Carlo technique is generated.

$$F_{H,n} = \frac{i_n - 1}{N - 1} \tag{3.10}$$

where $F_{H,n}$ is the non exceedance probability for a pool n, i_n is the order of the pool level n within the series of data and N is the length of the series [92].

3.3.2 Reservoir Flood Control Model

Coupled with the stochastic flood event generator, a reservoir flood control model simulates the routing of the ensemble of inflow hydrographs through the dam where each simulation starts at its corresponding random initial pool level. The mass balance equation is solved using the Modified Puls Method [39] and limited by an outflow-stage curve and a storage-elevation relationship (physical constraints). Furthermore, a predefined operating rule should be included

to complete the routing procedure (operational constraints). Each routed event is characterized by its peak outflow and its peak stage. Finally, for those cases in which the probability of failure is non zero, the peak stage is used to obtain a mean value for the breakage peak flow using the empirical equation formulated by Fröhlich [128]. A schematic describing the entire model is shown in Fig. 3.13.

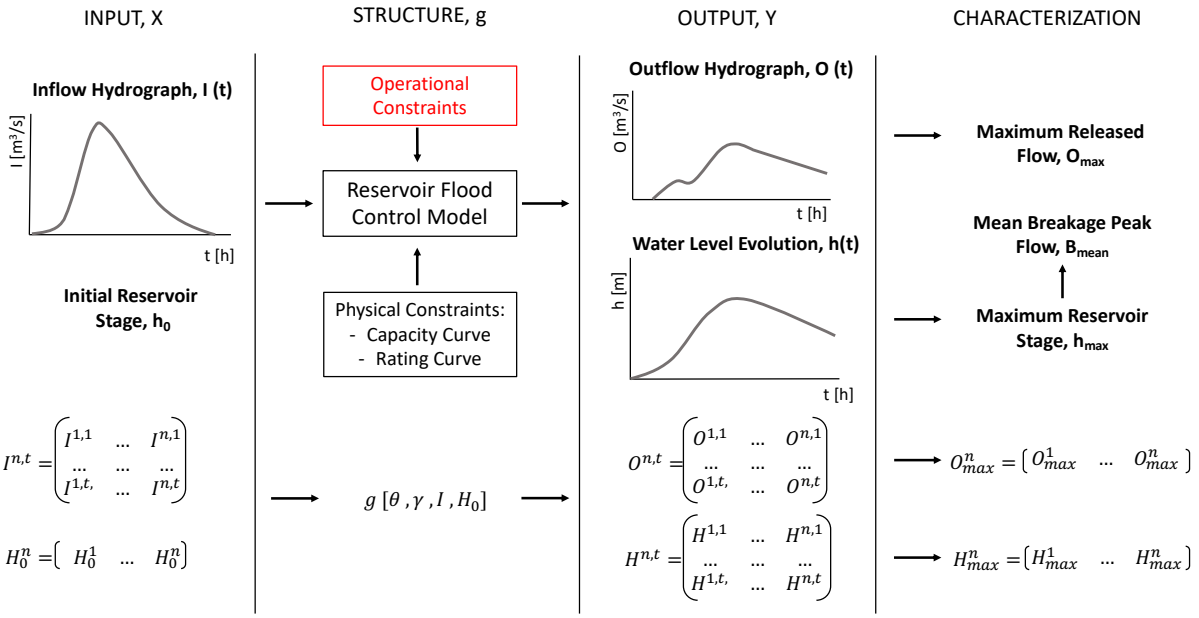

Figure 3.13: Reservoir Flood Control Model scheme

As described by Bianucci et. al [16], from a mathematical point of view, a reservoir flood control model is to be seen as an function g which transforms an input X into an output Y. The output is then characterized by an operator ϕ to obtain the characteristic damage variables. For the implementation of the methodology, the input X of the model is represented by the generated vector of initial reservoir levels, H_0^n, and the inflow hydrograph matrix, $I^{n,t}$, with $n = 1, 2, ..., N$, and $t = 1, 2, ..., T$, being N the total number of events generated and T the maximum flood event duration. The output Y is represented by means of the released flows matrix, $O^{n,t}$, and the reservoir stage matrix, $H^{n,t}$. Since the model depends on a set of operational parameter θ and a set of physical constraints γ, its behavior can be expressed by:

$$g[\theta, \gamma, X] = Y \tag{3.11}$$

where $\theta = \{\theta_1, \theta_2, ..., \theta_i\}$ comprises operational constraints. Among others, limitations regarding downstream channel capacities, maintaining the rate of outflow increase within acceptable limits, or the emergency operations activation levels fall within this type of constraints. The set of physical constraints $\gamma = \{\gamma_1, \gamma_2\}$ includes both, the maximum storage-outflow relation and the storage-elevation relationship.

It is inferred from Eq. (3.11) that for an equal input, that is, for the same initial water level and the same inflow hydrograph, the model provides different outputs according to the predefined set of parameters θ and γ. When the operating rules are changed, two equal flood scenarios result in disparate outflows and reservoir stages at each time step. The same applies when the storage-elevation relationship is modified. The described procedure is sketched in Fig. 3.13 where the input, structure function, output and characterization process are displayed.

Once the structure function g transforms the inflow hydrographs into release and stage time series, an operator ϕ is employed for estimating the maximum water levels and the outflow peak from each event. The hydrological loads must therefore be converted into the characteristic damage variables in order to assess of the overall risk of the system. The reader should note that, as a result of the multivariate approach taken for the implementation of the methodology, different combinations of the variables defining the external hydrological loads can lead to similar characteristic damage variables. This situation has been represented in Fig. 3.14 and is what Jimenez et. al [139] denoted as family of flood scenarios.

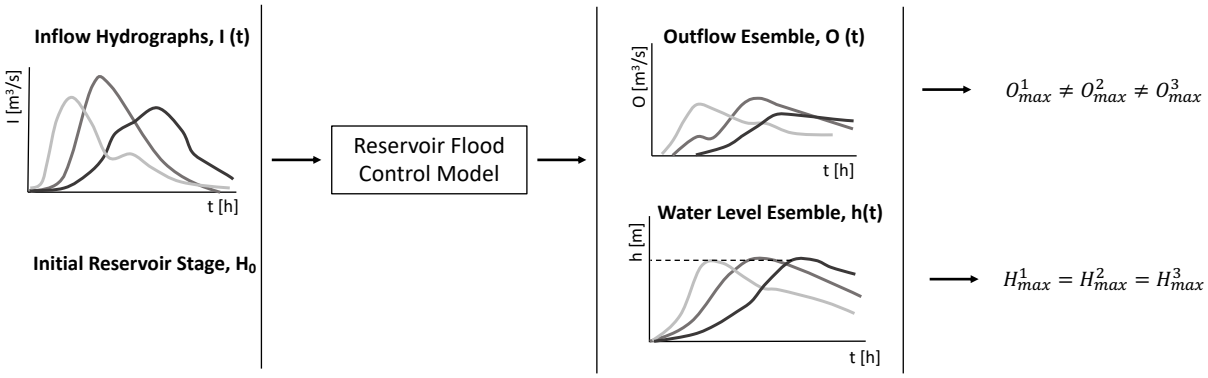

Figure 3.14: Family of hydrographs resulted from the reservoir flood control model

To transform inflow hydrographs to outflow hydrographs the continuity equation of the system is solved. The Modified Puls Method, also known as Level Pool Routing method [39], has been employed for the implementation of the proposed overall risk definition. The Level Pool Routing calculates outflow hydrograph from a reservoir with horizontal water surface given its inflow hydrograph and storage-outflow characteristics. The relationship between storage and water level is usually obtained using Geographic Information System (GIS) tools for terrain data processing. The rating curve is described by the set of equations which follow the weir and submerged flow formulas. Furthermore, as recommended by the SPANCOLD technical guidelines for dam safety [92], that in the simulations, flow over the entire crest of the dam should be computed according to the weir equation for broad-crested spillways. The relation between maximum release capacity and reservoir stage yields:

$$O(t,h) = \begin{cases} c_o A_o \sqrt{2gh}, & 0 < h < H_{spill} \\ c_o A_o \sqrt{2gh} + c_s L (h - H_{spill})^{3/2}, & H_{spill} < h < H_{crest} \\ c_o A_o \sqrt{2gh} + c_s L (h - H_{spill})^{3/2} + c_d L_d (h - H_{crest})^{3/2}, & h > H_{crest} \end{cases} \tag{3.12}$$

where c_o, c_s and c_d are the discharge coefficients, A_o the orifice cross-sectional area, L_s the spillway length, L_d the crest length, and H_{spill} and H_{crest} are the reservoir spill and crest elevation respectively. In addition to the previous set of equations, two different reservoir operating rules have been specified in order to complete the reservoir routing study: a normal flood control operation and an emergency operation schedule. The normal rule is a very simple operation strategy in which the outlet gates limit the outflow to the non-damaging downstream channel capacity. In this cases, the reservoir regulates the flow based on the non-linear storage-discharge relationship presented in Eq. (3.12) until reaching the maximum capacity threshold. On the other hand, the emergency operation schedules will maintain the gates closed until certain reservoir levels are reached in the reservoir.

3.3.3 Risk Estimator Model

Following the methodology explained in the previous section, the flood scenarios are characterized according to their capacity to reach certain water levels. To put it another way, their exceedance probability is assessed by the statistical analysis of the maximum peak stages attained while routing the inflow hydrographs through the reservoir. Peak outflows and maximum water levels are then related by their joint distribution function. Finally, a predefined system response curve and under given hypothetical damage curves at the upstream and downstream regions, the overall risk is estimated from the summation of three components: (1) serviceability limit state risk upstream of the dam motivated by high pool levels, (2) serviceability limit state risk downstream of the reservoir due to outflow rates larger than a non-damaging downstream capacity, and (3) the failure risk associated with failure of the structure.

$$R_T = R_{SLS,h} + R_{SLS,O} + R_{ULS,B} \tag{3.13}$$

To illustrate the entire process of risk assessment, Fig. 3.15 displays an event tree example in which a water level interval has been evaluated. For simplicity, the number of possible paths has been reduced to four: two different outflows for cases of non breach and two possible breakage peak flows. The probabilities of each branch as well as the expected value of each event at every node has been included. Furthermore, in the end nodes, the damages corresponding to each scenario have been implemented.

Branch probabilities within a particular level of the event tree can be summed to obtain an aggregate probability associated with a set of related events. For instance, the event tree in Fig. 3.15 illustrates the summation of the potential structural failure probability for the water level interval 1. Total annualized damages can be obtained by multiplying the the failure probability and associated consequences for each end branch and then summing across the end branches. A system failure path related to the serviceability limit state risk of downstream flooding ($R_{SLS,O}$) has been marked in red for illustrative purposes. The final probability of failure caused by the average value of the outflow interval 2 yields:

$$P_{SLS,O_2} = p(O_2|h) \cdot p(O_2|nf) \cdot p(h) = 0.2 \cdot 0.999 \cdot 0.4 = 0.07992 \tag{3.14}$$

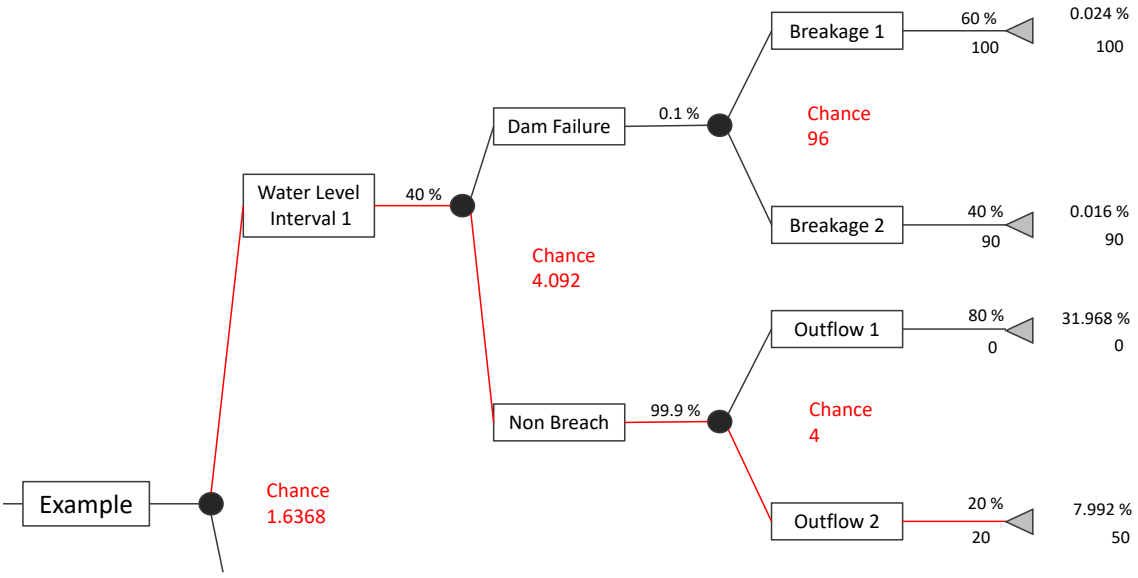

Figure 3.15: Total probability of system failure for water level interval 1

Statistical Analysis of Simulated Peak Stages and Peak Outflow Time Series

In order to assess the system failure probabilities, the outcomes from the stochastic flood scenario generator and the reservoir flood control model are to be analyzed statistically. The reader should note that the frequency estimations as well as the statistical relationships between the characteristic damage variables refer to a unique reservoir operating rule, reservoir capacity curve and outlet rating curve. Should one of these physical or operational constraints change, the results from the reservoir flood control model, their occurrence probabilities and their probabilistic dependence would be modified. The statistical analysis of simulated peak stages and peak outflow time series follows three steps:

1. Occurrence probability of water level intervals, $p(h)$
2. Conditional probability of peak outflow with respect to reservoir water levels $p(O|h)$
3. Conditional probability of peak breakage flow with respect to reservoir water levels $p(B|h)$

Occurrence Probability of Water Level Intervals, $p(h)$

The exceedance probability of the maximum reservoir levels is computed by sorting the flood control model outcomes in descending order, ranking the data from 1 to n, and computing the annual exceedance probability for each value using the following equation:

$$AEP = \frac{i - a}{N + 1 - 2a} \tag{3.15}$$

where i is the rank, N is the total number of values and a is the plotting position parameter. A wide range of plotting position parameters can be found in the literature. Cunnane [142] and Stedinger et. al [143] published a very comprehensive review of the existing formulas. In this research, due to its higher degree of acceptance and its adequacy for all types of parent distributions, the Weibull plotting position formula has been used for the estimation of the water level annual exceedance probability (AEP). This implies that in Eq. (3.15) a equals zero [142].

The maximum water level is a continuous variable. As such, when modeling the risk through the event tree shown in Fig. 3.8, it must be discretized to represent the different branches, each of which symbolizes a range of water levels the variable can adopt. The probability of each branch is, therefore, the probability of falling within any of the values of the range. Since the empirical cumulative distribution function has been already computed, the probability of the branch i can be calculated as $F_{i+1} - F_i$, where $i = 1, 2, ..., m$ being m the number of intervals into which the water level is divided. For ulterior damage estimations associated with each water level interval, a representative value of the branch needs must be selected. A common practice is to choose the average value [92].

Figure 3.16 illustrates an example of discretization of the water levels in the reservoir. The reservoir pool levels have been divided into m equidistant water intervals. The non-exceedance probability goes from $F_0 = 0$ for the minimum water level in the reservoir to $F_m = 1$ for the maximum water level attained during the routing of the flood events. The red points represent the average value of each interval to which the posterior damages are to be attributed. The probability of the event tree branch i represented by the water interval $\Delta h_i = h_{i+1} - h_i$, is the subtraction of the non-exceedance probabilities $p(i) = F_{i+1} - F_i$.

Conditional Probability of Peak Outflow with Respect to Reservoir Water Levels $p(O|h)$

Once the water levels are discretized in a finite number of intervals with their corresponding occurrence probabilities, the statistical relationship between the peak reservoir stages and the

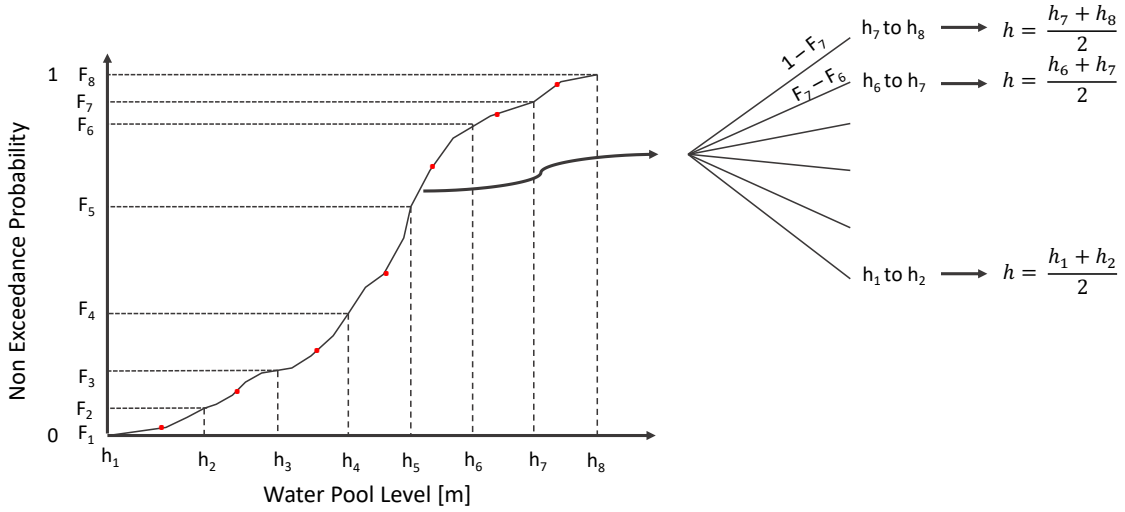

Figure 3.16: Example of the discretization of reservoir water levels into seven intervals characterized by their mean magnitudes represent with red points and their probability of occurrence $F_{i+1} - F_i$

remaining characteristic damages variables is computed. Similar to the procedure followed for the elaboration of the empirical cumulative density function of the water levels, the peak outflows resulted from the simulations and associated with maximum pool levels within each water level interval are ranked in increasing order. The annual non-exceedance probability for each value can be estimated using Eq. (3.10).

The variable under study is again continuous and a discretization is required for its inclusion in the event tree. Figure 3.17 represents an example of the discretization process for a number of peak outflows obtained for a water level interval. On the left side, the empirical cumulative distribution function is displayed. The non-exceedance probability goes from zero for the minimum peak outflow value to one for the maximum released obtained by simulation and associated with a reservoir level within the studied interval. On the right side, the probabilities of occurrence of the different peak outflow intervals for a given reservoir level are depicted.

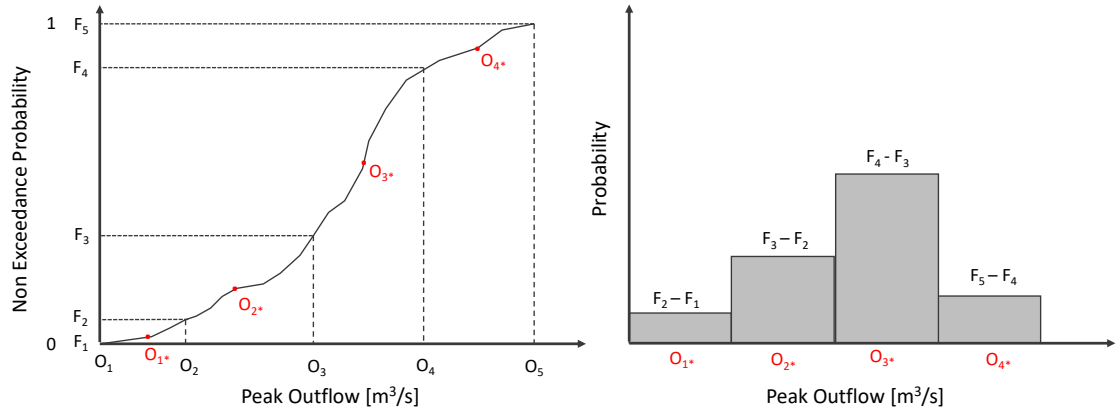

Figure 3.17: Example of the discretization of reservoir outflows for a given reservoir stage into four intervals characterized by their mean magnitudes represent with red points and their probability of occurrence $F_{i+1} - F_i$

Conditional Probability of Peak Breakage Flow with Respect to Reservoir Water Levels $p(B|h)$

The conditional probability for peak breakage flows has been implemented following the results from the multiple linear regression analysis performed by Fröhlich [128] whose empirical formulation has been utilized for relating the reservoir water levels to the peak breakage flows. A normal randomization is performed for each obtained value of the maximum water levels, with a mean equal to the result of the regression equation and a standard deviation equal to the residual variance of the regression.

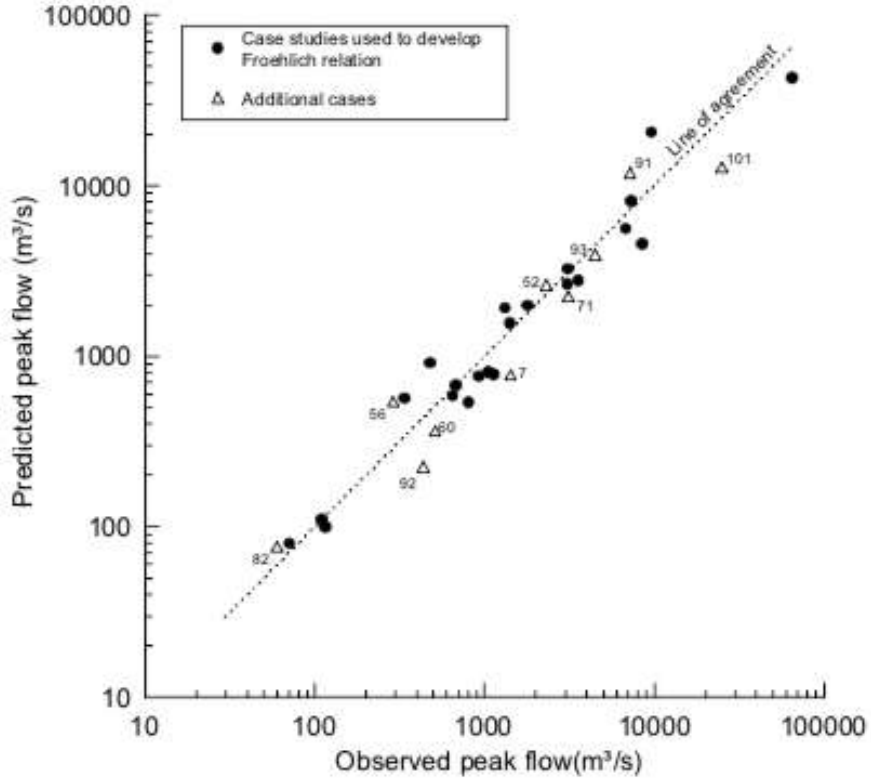

Figure 3.18: Observed peak discharges vesus predicted peak discharges using Fröhlich equation [128] including additional cases to those used by the author [92]

System Response to the Hydrological Loading, $p(f|h)$

According to the report on dam failure statistics developed by the International Commission on Large Dams (ICOLD) [144] and the works from Zhang et. al [145] presented in the First International Symposium on Geotechnical Safety and Risk celebrated in Shanghai in 2007, piping and overtopping comprise the two most frequent causes of embankment dam failure. As such, both failure mechanisms are included and combined through a common caused adjustment for the evaluation of the system response against the external hydrological loading [146].

First, the overtopping failure probability has been included using the fragility curves shown in Fig. 3.19. The image represents the conditional probability of structural failure against overtopping for three different types of dams. The curves are the outcome from a international joint effort carried out in Lausanne in 2015 during the "13^{th} ICOLD Workshop on Probability of Failure of Embankment Dams due to Slope Stability and Overtopping" [147] [148] [149]. Meanwhile, the piping failure probability has been assessed using a Monte Carlo probabilistic approach. The methodology follows the procedures contemplated by Jonkman [81] in which the piping failure is considered as a parallel system comprised of uplift, heave and piping.

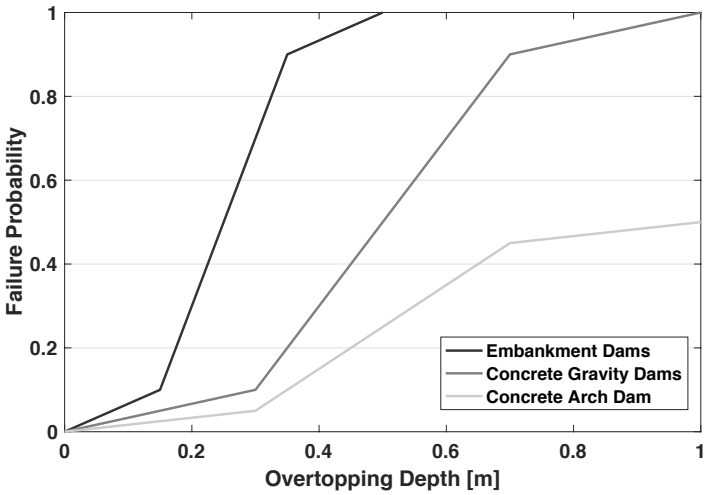

Figure 3.19: Overtopping fragility curves for different types of dams [149]

Within this implementation procedure, the simplified approach proposed by Hill et. al [146] for adjusting the system response probabilities for each potential failure mode has been followed. The method, as described by the "Best Practices in Dam and Levee Safety Risk Analysis" [22], redistributes the "correlation" between failure modes originated from a similar cause. The magnitude of the redistribution is proportional to the estimated probability of failure for each potential failure mode. As such, the mechanisms with larger probabilities of failure receive a larger portion of the "overlapping" area between mechanisms. The approach is implemented using the following equation, Eq. (3.16):

$$p'_j = p_j \cdot \frac{1 - \prod_{i=1}^{n}(1 - p_i)}{\sum_{i=1}^{n} p_i} \tag{3.16}$$

where p_j is the unadjusted probability of failure for potential failure mode j and p'_j is the adjusted probability of failure. The sum of the adjusted probabilities results in the correct total probability of failure indicated in Eq. (3.17):

$$P_f = p_j \cdot \frac{1 - \prod_{i=1}^{n}(1 - p_i)}{\sum_{i=1}^{n} p_i} \tag{3.17}$$

Damages in the Upstream and Downstream Regions, $D_{nf,h}$, $D_{nf,O}$, $D_{f,B}$

Structural damages in the upstream, $D_{nf,h}$, and downstream regions, $D_{nf,O}$, have been related to the reservoir water surface and the peak outflows through predefined damage curves. When the peak discharge and the peak reservoir stage exceed the channel capacity, CC, and the upstream properties elevation, H_{res}, respectively, damages start occurring. However, there is a critical threshold at which the total damage does not grow further. This limit is predefined by the maximum overtopping depth a dam can withstand without collapsing. According to the literature, that limit lies 0.5 m above the crest level for earthfill embankments and could be expanded to 1 m for concrete dams (Fig. 3.19).

Furthermore, given that the dam could collapse, a damage curve in terms of million of dollars per breakage peakflow has also been included. The analysis of consequences consists of three parts: estimation of the failure peak discharge, study of the flood through hydraulic modeling and estimation of the economic consequences which include direct economic consequences produced by the flood wave, $D_{f,B}$ and the dam reconstruction costs, D_{rec}.

3.4 Case Study

A hypothetical single reservoir, constructed with the main purpose of flood mitigation, has been employed to illustrate the influence of dam operation on the overall risk. The system is comprised of three components: a 150 m long earthfill embankment dam rising 9.5 m above the original stream bed; a downstream region where flooding occurs if flows exceed the non-damaging channel capacity of CC = 200 m^3/s; and an upstream region where residential properties are susceptible to flooding when a pool elevation of H_{res} = 7.5 m is reached. A summary of the characteristics of this hypothetical dam-reservoir system has been included in Table. 3.1. Moreover, Fig. 3.20 displays a schematic view of the system and its loading conditions.

DAM-RESERVOIR CHARACTERISTICS

DOWNSTREAM CHANNEL CAPACITY	200 m3/s		*REPRESENTATIVE FLOODS*	[m3/s]	[hm3]
			Design Flood	1800	310
DAM			*OUTLET WORKS*		
Type	Embankment dam		Spilway length	50 m	
Height (above stream bed)	9.5 m		Orifice outlet area	30 m2	
Length	150 m				
	Elevation	Storage			
RESERVOIR	[m]	[hm3]	FLOOD SCENARIOS		
Spillway	8,0	181,0	Peak Inflows	Gumbel (400 , 200)	
Urban Limit	7,5	154,0	Inflow Volumes	Normal (V , 0.1V)	
Top of the dam	9,5	243,0	Initial Reservoir Level	Normal (2 , 0.5)	

Table 3.1: Hypothetical Dam and Reservoir Characteristics

The flood scenarios considered for the example have been generated using the described Monte Carlo framework. To begin with, the peak inflows maximum yearly values are assumed to fit a Generalized Extreme Value Type I distribution function with location and scale parameters equal to $\xi = 400$ and $\alpha = 200$. To account for the statistical dependence between peak inflows and inflow volumes, a normal randomization has been performed for each synthetic peak flow, with a mean proportional to the peak and the relation between the design volume and peak, and a 10% standard deviation. Finally, the variability of the initial water level has been addressed by assuming that follows a normal distribution function with mean value, μ = 2 m and a standard deviation, σ = 0.5 m. Figure 3.21 displays the main statistical characteristics of the generated flood scenarios. Furthermore, the formulas below show the main form of a Gumbel and a Normal Probability Density Function (PDF) and Cumulative Density Function (CDF).

$$f(q) = \alpha^{-1} \cdot \exp\{-(q-\xi)/\alpha\} \exp[-\exp\{-(q-\xi)/\alpha\}] \tag{3.18}$$

$$F(q) = \exp[-\exp\{-(q-\xi)/\alpha\}] \tag{3.19}$$

where $f(q)$ symbolizes the probability density function, $F(q)$ the cumulative density function for a peak streamflow value q.

$$f(h) = \frac{1}{\sqrt{2\pi}} \cdot \frac{1}{\sigma} \cdot e^{\{-(h-\mu)^2/2\sigma^2\}} \tag{3.20}$$

$$F(h_0) = \Phi\left(\frac{h_0 - \mu}{\sigma}\right) \quad | \quad \Phi(h_0) = \int_{-\infty}^{x} f(h_0) dh_0 \tag{3.21}$$

where $f(h_0)$ symbolizes the probability density function, $F(h)$ the cumulative density function for a initial water level value h_0.

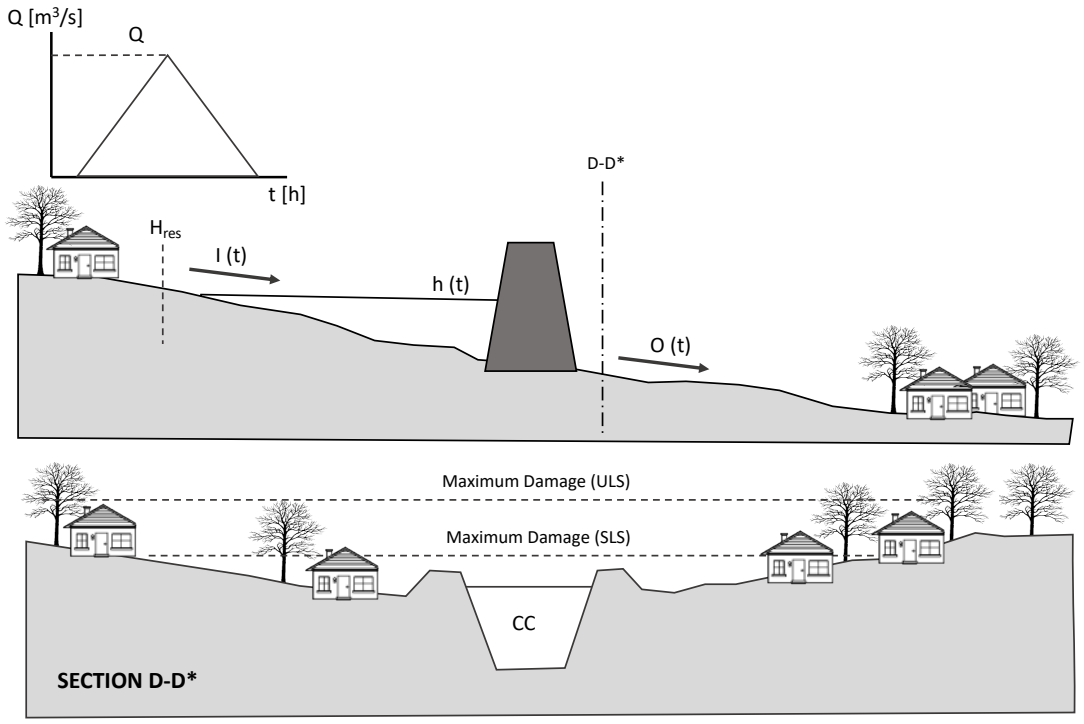

Figure 3.20: Schematic view of the hypothetic dam-reservoir system

For the sake of simplicity, following the first-order approximation utilized by De Michelle et. al [111], a symmetrical triangular-shaped hydrograph has been considered, where the base time is $t_b = 2V/Q$, the time of rise equals $t_p = t_b/2.67$, and the time of regression is equal to $1.67t_p$. The flood hydrograph $I(t)$ yields:

$$I(t) = \begin{cases} 1.335\dfrac{Q^2}{V} \cdot t & 0 \leq t \leq t_p \\ 1.6Q - 0.8\dfrac{Q^2}{V} \cdot t & t_p \leq t \leq t_b \end{cases} \tag{3.22}$$

The relationship between storage and water surface elevation has been fitted to a potential function. The assumption has been made following the example used by Sordo-Ward et al. [150], who studied the flood abatement effects of reservoir using simplified models. Based on this relation, the reservoir has capacity for 243 hm^3. It was further assumed that the retaining structure is provided of gated outlets with an orifice outflow area of 30 m^2 and a uncontrolled spillway with a weir length of 50 m. For the calculation of the rating curve according to Eq. (3.12), typical values of 0.7, 2.1 and 1.704 have been taken for the orifice coefficient, the spillway coefficient and the overtopping coefficient respectively [151].

In addition of the previous physical constraints, two distinct cases of reservoir operating rules have been specified in order to complete the reservoir routing: a normal flood control operations in which the downstream channel capacity determines the outflow; and emergency operation schedules in which the operation depends on the state of the reservoir. The emergency operation schedule has been developed in accordance with the guidelines of the USACE explained in Chapter 2.2.3. The methodology determines the releases to be made in order to limit the storage to the available capacity. Taking a Flood Control Level equal to the spillway elevation of 8 m and a recession constant T_s of 1.25 days, a set of five curves has been developed. The value of the recession constant was determined by assuming a hypothetical design hydrograph

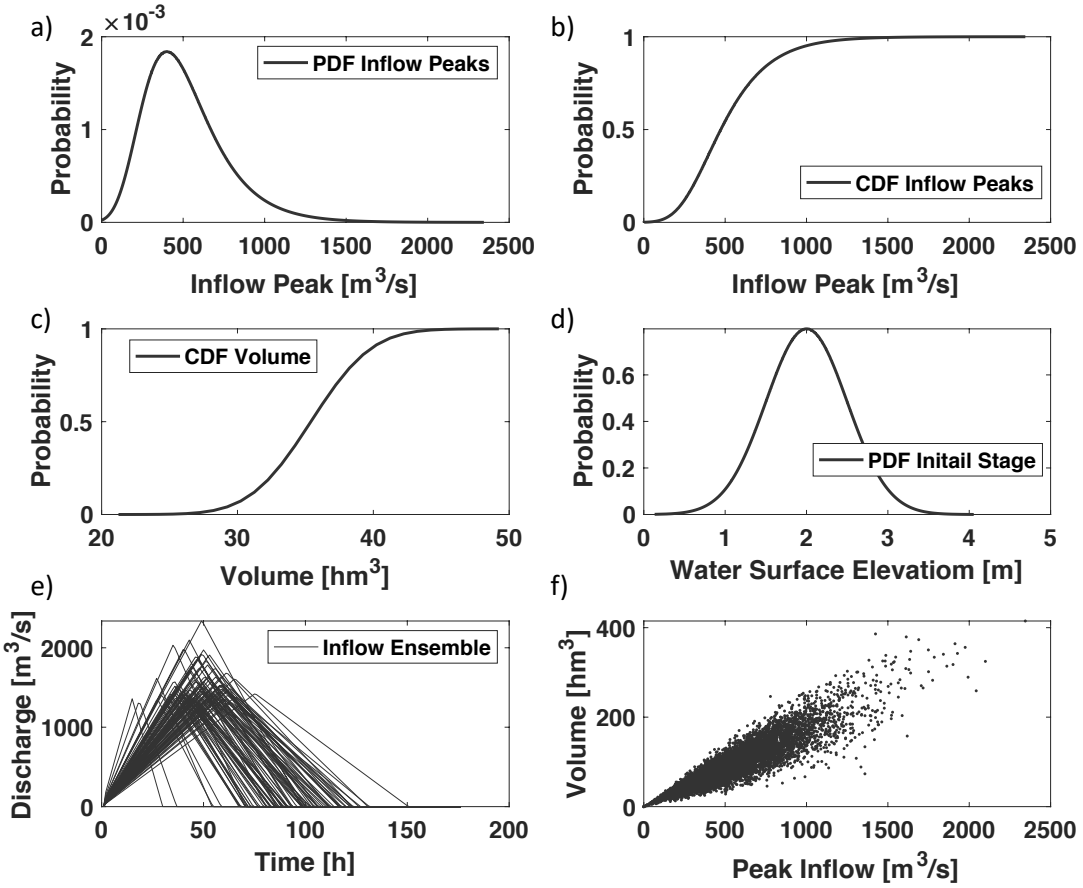

Figure 3.21: Stochastic flood scenario generation: (a) Probability Density Function of the Inflow Peaks, (b) Cumulative density Function of the Inflow Peaks, (c) Cumulative Density Function of the hydrograph volumes, (d) Probability Density Function of the initial reservoir stage, (e) Example of hydrograph ensemble, and (f) Simulated flood scenarios represented in the discharge-volume plane

with Q1 = 1800 m^3/s and Q2 = 667 m^3/s and a duration of $d = 96$ h. The values for the maximum initial stages at which the reservoir outlet can remain closed have been calculated for a series of combinations between inflow and outflow rates. An example of the computation for inflows equal to 300 m^3/s and 600 m^3/s is presented in Table 3.2. The shapes of the regulation curves displayed by Fig.3.22 show how the required releases increase with the initial reservoir state and the inflow rates. This increasing pattern continues until the required releases are limited by the rating curve.

The damages have been assumed to be linearly dependent with respect to the characteristic damage variables, i.e. breakage peakflow B, outflow peak, O, and peak stages, h. The damage functions yield as follows:

$$D_{f,B} = \begin{cases} D_{max,B} \cdot \dfrac{B_i - CC}{B_{max} - CC} + D_{rec}, & \text{for } CC < B_i < B_{max} \\ D_{max,B} + D_{rec} & \text{for } B_i > B_{max} \end{cases} \tag{3.23}$$

where $D_{max,B}$ is the maximum potential damage caused by the breakage peak flow resulted from dam breach assuming an overtopping depth of 0.5 m, CC is the the downstream channel capacity, B_{max} is the breakage peak flow at which the maximum damage is reached, and D_{rec}

	Initial Inflow Q1 in m3/s					
	300			600		
Q2 [m3/s] (1)	**SA [hm3] (2)**	**SC [hm3] (3)**	**WSEc [m] (4)**	**SA [hm3] (5)**	**SC [hm3] (6)**	**WSEc [m] (7)**
0	33	148	7,39	65	116	6,69
10	28	153	7,48	60	121	6,82
20	25	156	7,55	56	125	6,91
30	22	159	7,60	52	129	6,98
40	20	162	7,64	49	132	7,05
50	17	164	7,68	46	135	7,11
60	16	165	7,72	44	137	7,16
70	14	167	7,75	41	140	7,21
80	12	169	7,78	39	142	7,26
90	11	170	7,80	37	144	7,30
100	10	171	7,82	35	146	7,34
110	9	172	7,84	33	148	7,38
120	8	173	7,86	31	150	7,42
130	7	174	7,88	30	152	7,45
140	6	175	7,90	28	153	7,48
150	5	176	7,91	26	155	7,51
160	4	177	7,92	25	156	7,54
170	4	177	7,94	23	158	7,57
180	3	178	7,95	22	159	7,59
190	3	178	7,96	21	160	7,62
200	2	179	7,96	20	161	7,64
Notes:	Q1 represents the inflow rates					
	Q2 symbolyzes the constant outflow					
	Col. (2) and (5) = 2Ts[Q1 - Q2(1+ln(Q1/Q2))]					
	Col. (3) and (6) = Smax - SA					
	Col. (4) and (7) represent the tentative maximum allowable pool elevation					

Table 3.2: Emergency Operation Schedules using USACE method explained in Chapter 2.2.3

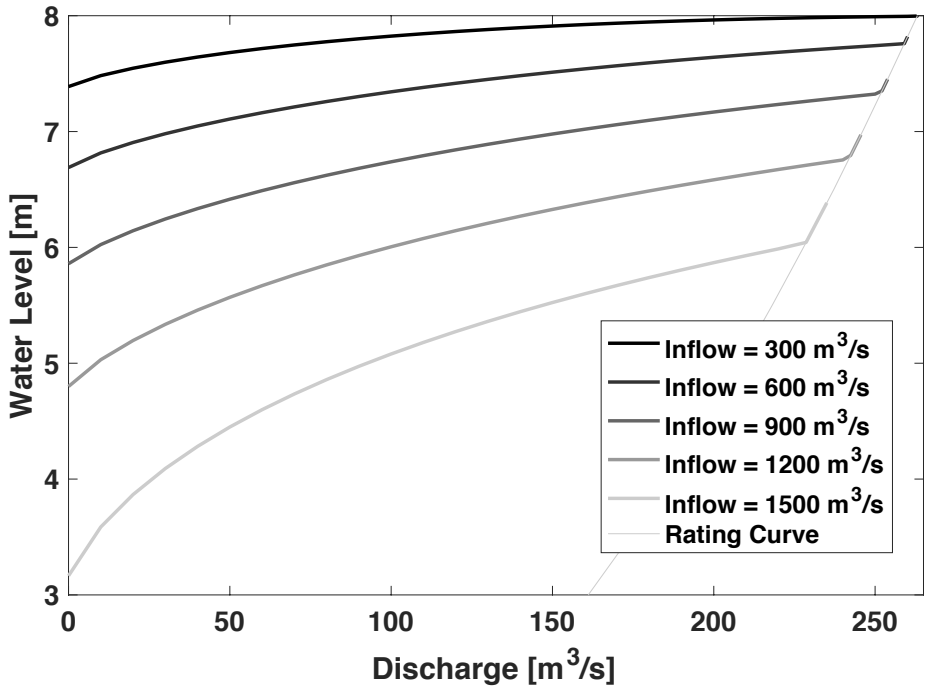

Figure 3.22: Emergency Operation Curves using the USACE method explained in Chapter 2.2.3

are the reconstruction cost of the dam. Accounting for the reconstruction of the dam and the large breakage peak flows, damages in case of dam breach reach a maximum of M$ 100 (including reconstruction of the embankment). This assumption follows the hypothetical example of Escuder-Bueno et. al [84] presented in Chapter 2 for small dam failure. In this example, lower maximum damages have also been established for the serviceability limit state scenarios. In the downstream region maximum releases obtained at an elevation of 9.5 m caused M$ 30 in structural damage, whereas in the upstream region maximum damages have been set to M$ 10. Both functions yield:

$$D_{nf,O} = \begin{cases} D_{max,O} \cdot \dfrac{O_i - CC}{O_{max} - CC}, & \text{for } CC < O_i < O_{max} \\ D_{max,O} & \text{for } O_i > O_{max} \end{cases} \tag{3.24}$$

$$D_{nf}(h) = \begin{cases} D_{max,h} \cdot \dfrac{h_i - H_{res}}{H_{max} - H_{res}}, & \text{for } H_{res} < h_i < H_{max} \\ D_{max,h} & \text{for } h_i > H_{max} \end{cases} \tag{3.25}$$

where H_{res} symbolizes the elevation at which residential buildings upstream from the reservoir start flooding and H_{max} the pool level 0.5 m above the crest level. Figure 3.23 sketches the three damage curves utilized in this case study.

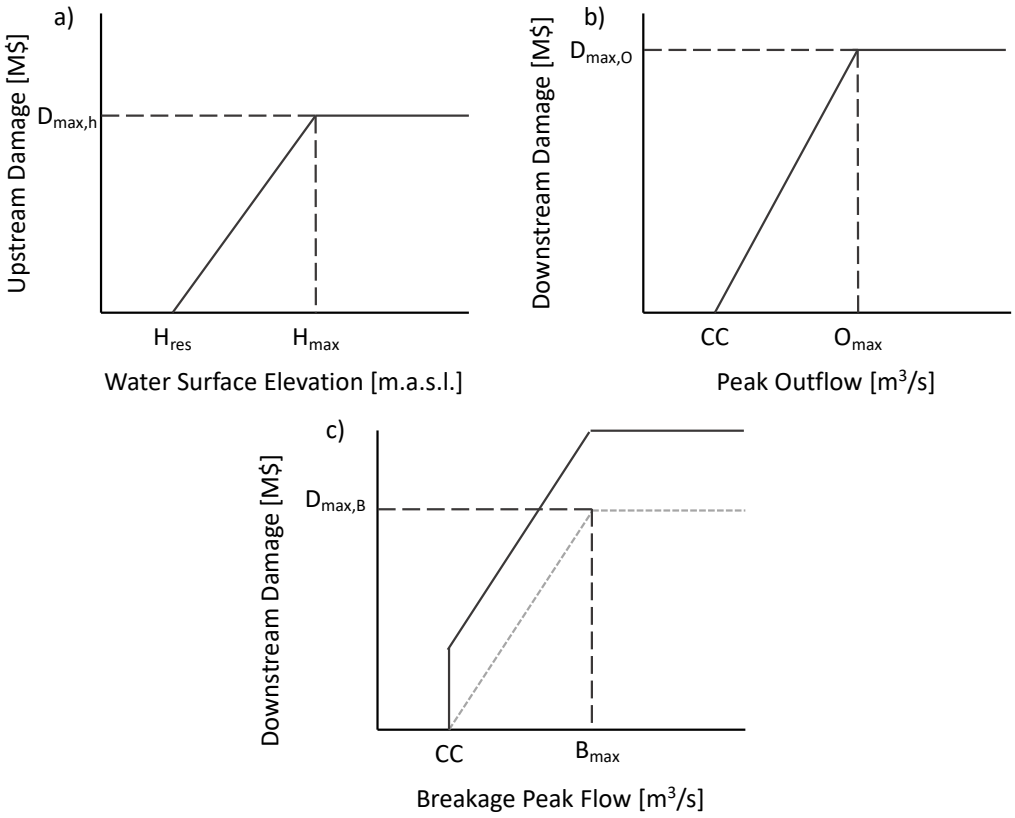

Figure 3.23: Hypothetical Damage Curves: (a) Upstream damage curve, (b) Downstream damage curve for non-structural failure scenarios, and (c) Downstream damage curve for structural failure scenarios

3.5 Results and Discussion

The risk assessment methodology presented in this chapter has been applied to a hypothetical single-purpose dam-reservoir system. The example aims to illustrate the importance of including the dam operation effects within the risk analysis. Additionally, this simplified example is used to demonstrate that the assumptions made by the current risk assessment procedures concerning the relationships between inflow volumes, outflow peaks and peak reservoir stages are erroneous, ultimately leading to incorrect estimations of the risk posed by the structure to the reservoir area and downstream floodplains.

3.5.1 Normal versus Emergency Flood Reservoir Operation

In order to illustrate the effects the dam operation has on the overall risk, two reservoir flood control operation strategies have been considered: normal flood control operation and emergency flood control operation. In the normal flood control case, the gate of the reservoir has been kept partially open throughout the entire simulation time releasing rates below the non-damaging capacity of the downstream channel. In contrast, in the emergency flood control operation scenario, the opening rates have been managed in accordance with the rule curves displayed in Tab. 3.2 and Fig. 3.22. Analysis of both sets of results have shown that **the peak reservoir as well as the peak outflow frequencies largely depend on how the reservoir is operated**.

Table 3.3 summarizes the risk values obtained for the upstream and downstream regions. The results reveal that for the studied case, the overall risk of the system is higher when the reservoir is managed following the emergency operating rules. The main difference between the two operation policies resides in the component of risk related to downstream flooding during non-structural failure scenarios. When reservoir releases exceed the non-damaging rate of 200 m^3/s, residential properties downstream of the reservoir start flooding. The higher than normal reservoir outflows conducted using emergency operations exacerbate the risk of downstream flooding as compare to the normal flood control strategy. Furthermore, the results have also disclosed important effects regarding the ultimate limit state risk, showing higher values for the normal operation schedules.

	NORMAL OPERATION [M$/yr]	EMERGENCY OPERATION [M$/yr]
$R_{SLS,H}$	0,0530	0,1769
$R_{SLS,O}$	0,0614	0,3778
$R_{ULS,B}$	0,0269	0,0035
R_T	0,1412	0,5582

Table 3.3: Serviceability limit state risk, ultimate limit state risk and overall risk in case of normal and emergency flood control operations

Figure 3.24 displays the annual exceedance curves of the reservoir water levels (Fig. 3.24a) and the reservoir released flows (Fig. 3.24b) when emergency and normal flood control operation strategies are adopted. The frequency curves of the former are represented in black, whereas the exceedance probabilities of the latter are depicted in light gray. The reader should note that the frequency curves herein refer to the probabilities of the characteristic damage variables and do not represent the exceedance probabilities of the damages.

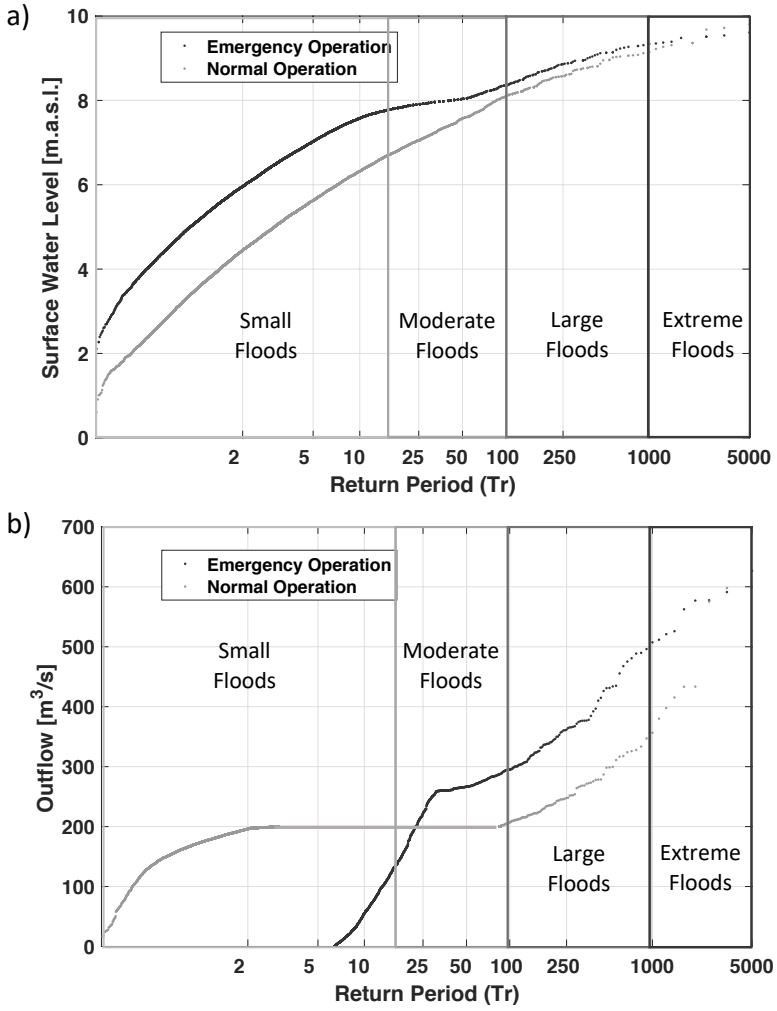

Figure 3.24: (a) Maximum water surface elevations frequency curves and (b) peak outflow frequency curves for normal and emergency operation schedules

To address the analysis of the frequency plots and to provide an explanation into the obtained results, the generated flood events have been classified into four categories: (1) small floods ($Tr < 20yr.$), (2) moderate floods ($20yr. < Tr < 100yr.$), (3) large floods ($100yr. < Tr < 1000yr.$) and (4) extreme events ($Tr > 1000yr.$). It should be pointed out that, as explained throughout this chapter, this characterization does not relate to the magnitudes of single external hydrological variables but to the combined capacity of initial reservoir levels, inflow volumes, inflow peaks and operational constraints to reach certain water levels in the reservoir. To help the reader understand the analysis, Fig. 3.25 depicts the event-to-event relationship between the peak outflow and the peak reservoir stage.

1. **Small Floods:** Releases starting at lower reservoir stages are observed during the normal flood control operation. Meanwhile, the emergency operation schedule is activated when the water surface elevation reaches 6.5 m. Despite the discrepancies, these high frequency events do not have an influence on the overall risk outcomes because none of the operational strategies lead to values of pool elevations or released flows exceeding the thresholds of upstream and downstream flooding.

2. **Moderate Floods:** Figure 3.24 clearly illustrates that following the emergency operation

schedules during moderate flood scenarios can lead to larger serviceability limit state risks due to higher pool elevations and higher peak releases frequencies. Before reaching the spillway level at 8 m, the normal operation releases are maintained at the downstream capacity of 200 m^3/s whereas the emergency schedule tries to avoid uncontrolled spills.

3. **Large Floods:** In comparison to the emergency schedules, the exceedance probability of peak releases and maximum reservoir levels is still lower for normal operations. This is explained by the fact that during normal operations, the volumes of water released prior to the activation level of the emergency operation are higher than the total outflow volumes discharged when the emergency operation schedule is applied.

4. **Extreme Floods:** The results show an interesting aspect for extreme events, maintaining the release rate equal to the downstream channel capacity results in higher pool elevations and higher total releases due to dam crest overflows. Consequently, higher values of the ultimate limit state risk are expected under normal operation schedules. These outcomes have nicely confirmed the fact that **in cases of extreme events, releases at higher rates earlier in the event are required to guarantee the safety of the structure**.

The results from Tab. 3.3 have been represented in Fig. 3.25. The figure depicts the Frequency-Damage curves of the system applying both operation strategies. The curves are in accordance with the plots of Fig. 3.24 and suggest lower levels of overall risk for small, moderate and large floods adopting the normal flood control schedules. However, in the high damage - low frequency tail of the curves, the emergency operation schedules reduces the risk with respect to the normal flood control operation strategy.

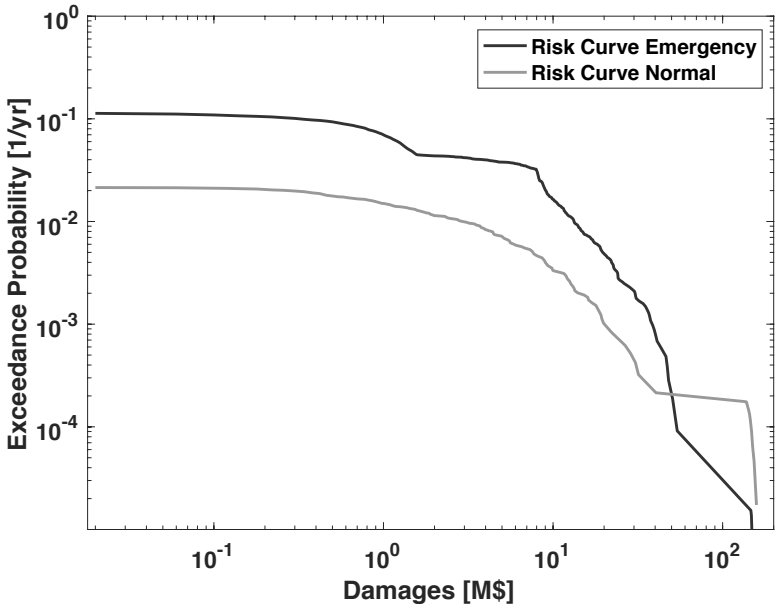

Figure 3.25: Frequency-Damage curves comparing the risk under normal (in light gray) and emergency flood control schedules (in black)

3.5.2 Connecting the Results to the Traditional Method of Estimating Risk

As discussed throughout this chapter, little research has been published related to the quantification and inclusion of the effects of reservoir operations in the standard risk analysis procedures for dam-reservoir systems. First, it is argued that the traditional method used by the USACE

and described in Chapter 2 is insufficient, due to the implicit assumption made about the relationship between inflow volumes, peak outflows and peak reservoir stages. The current methodologies assume that these relationships are unique for a critical duration, when in actuality they are non-unique. The non-uniqueness arises because: (1) the inflow volumes and the inflow peaks are not perfectly correlated variables; (2) the initial reservoir water level is a stochastic variable; and (3) the operating rule is a function of the three mentioned variables, which implies that it is also a random variable. Consequently, there are instances when similar values of any of the variables characterizing the external conditions lead to different peak outflows and different peak reservoir stages. Hence, the use of a single inflow volume to peak outflow and inflow volume to peak reservoir stage relationship produce incorrect risk estimations.

The non-uniqueness is confirmed using the results from the Monte Carlo simulations. Figure 3.26a displays the obtained event-to-event relationship between peak inflows and peak reservoir stages. Depending on the interaction between the external variables and the operation of the structure, a similar maximum reservoir level is reached by different peak inflow values. Another questionable conjecture in the volume-duration-frequency-based traditional approach arises from the assumption that peak reservoir stages and unregulated inflows share the same probability of occurrence. As discussed previously, a given inflow volume leads to a maximum water level that has a probability of occurrence either higher or lower than the probability of occurrence of the inflow volume. Figure 3.26b illustrates how a peak inflow of a given exceedance probability could lead to a peak reservoir stage that has a range of exceedance probabilities.

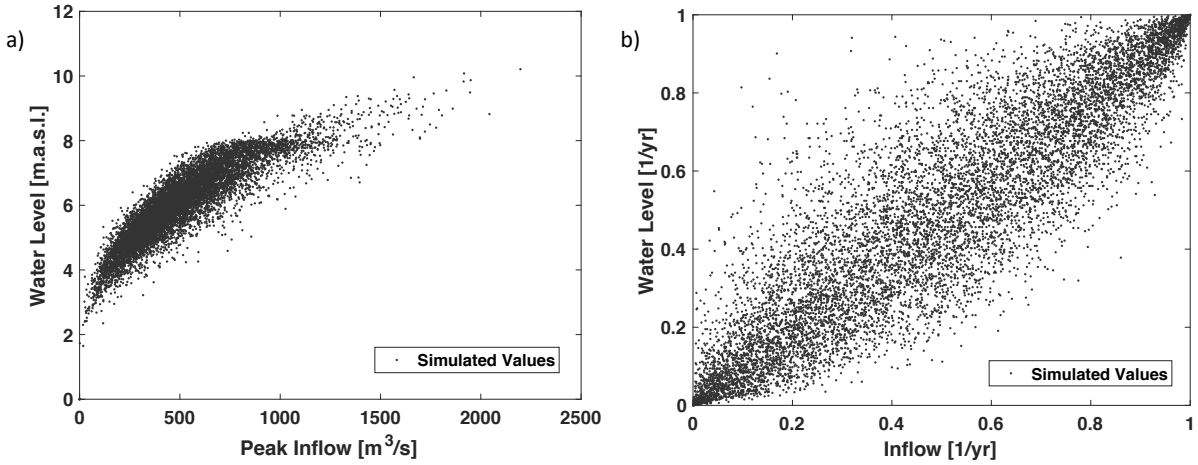

Figure 3.26: Plot of an event to event relationship between (a) peak inflow and peak reservoir stage, and (b) peak inflow and peak reservoir stage exceedance probabilities

Similar results have been obtained for the event-to-event relationship between the inflow peaks and the outflow peaks. It is inferred from Fig. 3.27 that neither the magnitudes nor the frequencies of the inflow and outflow peaks show a strict correlation. The results also contrast with the conclusions from Ayalew et. al [132]. The authors stated that the flood frequency of unregulated and regulated flows converge for low-probability flood events. However, Fig. 3.27 does not show that convergence. The difference has been attributed to the fact that, in the considered case study, the maximum release capacity through the outlets, the spillways and the overflows is not equal to the maximum inflow rates arriving to the reservoir. Whereas in the works from Ayalew et. al [132] inflows equalizing the outflows were assumed when reservoir stages reach the crest level.

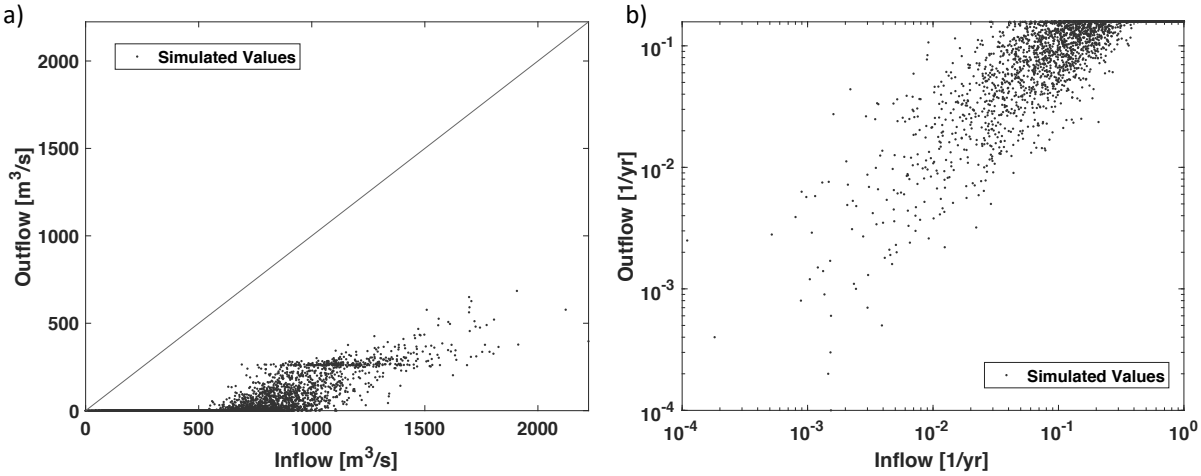

Figure 3.27: Plot of an event to event relationship between (a) peak inflow and peak outflows, and (b) peak inflow and peak outflow exceedance probabilities

Furthermore, the hypothesis made about the relationships between peak reservoir levels and peak outflows (Fig. 3.5) has been confirmed by the simulations. Figure 3.28a displays the event-to-event relationship between peak reservoir stages and peak outflow rates. The illustration shows that there is a non-unique relation among the pair of characteristic damage variables when reservoir stages remain within the flood control pool. Thus, defining a conditional probability of structural failure in terms of peak outflows could lead to an under or over estimation of the ultimate limit state risk. Nonetheless, both figures also present an interesting characteristic for low frequency events. When the maximum flood control level is reached (uncontrolled spillway elevation), the frequency of uncontrolled releases converges to the frequencies of reservoir stages.

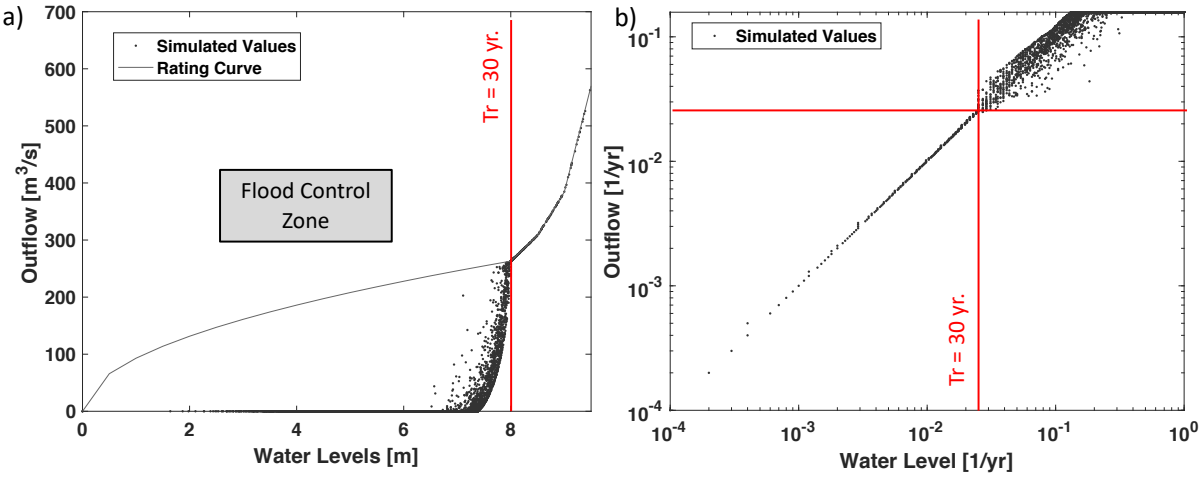

Figure 3.28: Plot of an event to event relationship between (a) peak reservoir stages and peak outflow, and (b) peak reservoir stage and peak outflow exceedance probabilities. The red line indicates the end of the flood control zone

In addition to exploring the dynamics of the water reservoir level to peak outflow relationship, **the example has also revealed that the quantile-quantile relationship between peak reservoir stage and peak reservoir release is unique for a given reservoir operation**. The quantile-quantile plot corresponds to pairs of reservoir storage-peak outflow values, such as

h_i versus q_j, for which the exceedance probabilities coincide. This is $P(H_i > h_i) = P(Q_j > q_j)$. The reader should note that this relationship does not assume the same exceedance probability for values attained during the same event but symbolizes the curve of equally likely peak reservoir stages to peak outflows. To put it another way, the curve represents the most likely outflow rate for each reservoir level. To illustrate this, three independent realizations of 10.000 yearly maximum flood events have been simulated. The event-to-event relationships has been plotted in Fig. 3.29a. It has been found that their quantile-quintile curves fall on top of each other as depicted in Fig. 3.29b. Using this relationship could reduce the amount of computations and may speed up the optimization framework proposed in the next chapter.

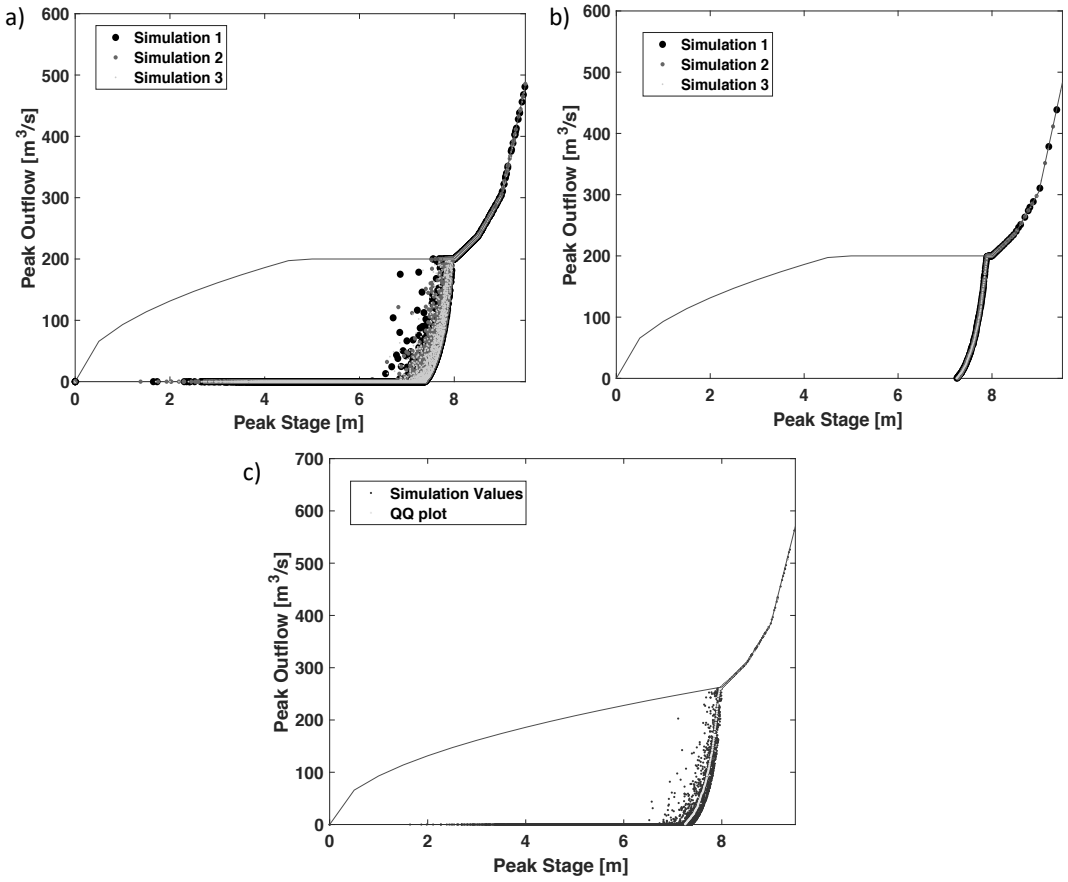

Figure 3.29: Plot of the peak annual reservoir stage and outflow relationship for (a) three independent realizations of 10.000 year reservoir stage-outflow time series; (b) their quantile-quantile plot following the same operating rule; and (c) a comparison between the simulated and the most likely relationship represented by the quantile-quantile curve

Finally, the maximum water level frequency estimates that would be calculated using the traditional method have been compared with the frequency estimates including the effect of dam operations. It was found that the traditional methodology largely depends on the chosen critical flood duration leading to an over- and underestimation of the serviceability limit state risk as well as the ultimate limit state risk. The results have been plotted in Fig. 3.30. The univariate statistical approach based on the peak inflows have been represented in gray. Assuming a critical duration of 120 hours, the frequency estimates are described by the dark gray curve; whereas in black, the frequency curve obtained by applying the structure-based approach is displayed.

The Frequency-Damages curves presented in Fig.3.31 show the difference between assessing the

risk of the system through the volume-duration-frequency-based methodology and the suggested approach where the system operation is included in the analysis using the Monte Carlo simulation. This former method would lead to an incorrect perception of flood risk for locations in the reservoir area and the downstream region. The reader should note that this overestimation could change if a different critical duration value is selected leading in some cases to an underestimation of the risks. However, the generalization of this conclusion would require a more sophisticated study in which each of the components of the estimation framework (stochastic streamflow generation, reservoir routing and operation, and risk estimation) are closer approximations to realistic conditions.

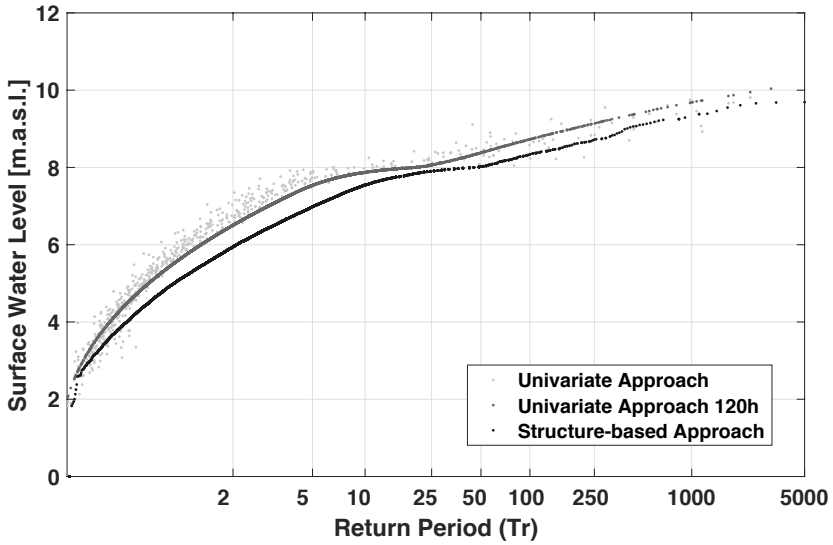

Figure 3.30: Maximum reservoir level frequency curve following a univariate analysis, a univariate analysis for a single flood event duration and accounting for the routing of the flood events through the reservoir (structure-based approach)

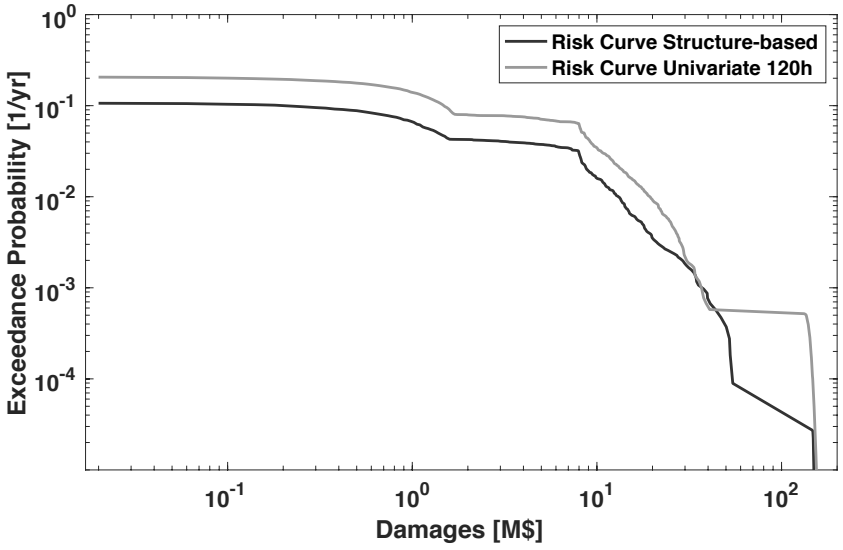

Figure 3.31: Frequency-Damage curve following a univariate analysis and accounting for the routing of the flood events through the reservoir (structure-based approach)

3.6 Conclusions

A Monte Carlo simulation approach has been used to investigate the effects dam operations have on the overall risk of dam-reservoir system. The simulation was necessary to study the interaction between the external hydrologic forcing and the structure as well as the statistical dependence between the different variables associated with upstream and downstream damages of the system. By limiting the scope of the simulation approach to simplified system response curves, damage curves and known cumulative distribution functions describing the hydrological variables affecting the reservoir, the complexities related to those three important issues have been avoided. These simplifications, however, do not compromise the generic insights gained in this chapter concerning the influence of the dam operations on the assessment of the overall risk of a dam-reservoir system.

Two distinct cases of reservoir operation rules have been analyzed: (1) normal flood control operations in which the downstream channel capacity determines the outflow, and (2) emergency operation schedules in which the operation depends on the state of the reservoir. Analysis of the two cases revealed that both the reservoir stage frequency and the peak outflow frequency highly depend on the operation procedure, ultimately affecting the overall risk of the system. In addition, the results revealed that although diminishing the ultimate limit state risk associated with the structural failure of the dam, the emergency operation schedule presents a worse overall performance, in terms of risk, as compared to the normal operation schedule. A detailed study of other operating rules as well as other reservoir storage and outlet characteristic might further reveal additional properties of the effects of the different operational decisions on the overall risk. Moreover, further investigation is advocated to study the influence of diverse hydrograph and damage curve shapes and to improve the underlying statistical relationships between the variables of the system.

By using a simple hydrologic example, this study has also shown that the traditional methodology used in current engineering practice by the USACE could lead to an under- or overestimation of the different components of the overall risk. These estimates are primarily motivated by the assumptions made about the relationship between inflow volumes, outflow peaks and peak reservoir stages. In the current methodology for risk assessment, it is assumed that the relationship between the variables is unique, when, as shown in this chapter, in actuality is non-unique. This non-uniqueness arises when the stochastic nature of all the external variables affecting the dam operation are simultaneously taken into account. Consequently, there are instances in which the same inflow volume leads to different peak reservoir stages and peak outflow rates leading to different estimates of risk.

Finally, it has been demonstrated that the quantile-quantile plot for the reservoir water level and outflow rate remains constant for a unique set of operational parameters. Instead of looking for the conditional probability of outflows for each water level interval considered in the event tree, the use of this curve simplifies the risk assessment procedure, speeding up the optimization of reservoir operations to be investigated in the next chapter.

Chapter 4

Risk-based Optimization Framework for Reservoir Emergency Operations

Despite the increasing importance of applying risk analysis to inform decision-making in the field of dam safety management, there is scarce literature treating its application on flood control operations. Although theoretically sound, the standard methodology currently in use by the U.S. Army Corps of Engineers for the development of emergency operation schedules does not fully represent the complexity regarding the uncertainty of future inflows. To define how much water to release as a function of the state of the reservoir, the method establishes a conservative estimate of expected minimum inflow volumes assumed to be appropriate under all flooding situations. Moreover, the approach lacks on mechanisms for evaluating and balancing the potential risks associated with the storage and release decisions. The application of these strategies, thus, could lead to operations which might be distant from the optimal.

In light of this challenges, this chapter presents a novel procedure for the development of optimal emergency operation schedules applied to single dam-reservoir systems. Rather than on critical water levels or reservoir states, the suggested framework is based on the idea that the operational decisions during extreme hydrological events should rely on the concept of risk. As such, the methodology combines a simulation approach for conducting risk analysis with an optimization algorithm following a Parametrization-Simulation-Optimization technique. The optimization framework uses a handful of control variables defining a simple operating rule that is valid throughout the entire control period and determines the releases at each time step. These parameters are then evaluated through simulation to determine their optimal values.

In this chapter, a simplified example is used to demonstrate that optimizing the emergency operation of reservoirs can be an efficient non-structural risk mitigation measure for dam-reservoir systems. Furthermore, the results reveal that the optimal operation of reservoirs is strictly dependent on the particular system under study. The characteristics of the dam structure, the upstream and downstream regions topography, and the reservoir storage capacity determine the operation strategy to be adopted at each system. In cases in which high pool levels dictate the overall risk of the system, opening operation strategies with higher outflow rates are optimal, leading to higher risk mitigation. Meanwhile, when releases exceeding downstream channel capacities dominate the total risk of the system, closing flood control strategies are preferred under extreme circumstances.

The chapter is structured as follows: it begins with a brief description of the problem followed by a review on both, the methodologies currently used for the development of emergency operation schedules and the techniques concerning flood control operation optimization. The introductory

section concludes setting up the objectives of the chapter. Then, the architecture of the simulation approach, the proposed objective function for the optimization and the parametrization of the operating rule are presented. Finally, a simplified example is used to evaluate the performance of the suggested approach as compare to the deterministic and widely used USACE flood operation schedules. The chapter concludes with a summary of the main findings.

4.1 Literature Review

Dam-reservoir systems will never provide a complete protection against flooding, but when their capacity of storing excess water is properly managed [8] [9], they play an important role in flood management plans, offering efficient means of flood control and protection [10] [11]. They are responsible of reducing the risks of loss of life and structural damage in downstream regions by temporarily retaining water during storms and releasing it afterwards at admissible non-damaging rates. However, as pointed out by Valdes and Marco [12] and many other authors in the literature [152] [153] [154], dams also introduce important risk factors into the system, such as structural dam failure or inducing flooding due to uncontrolled dam spillage.

Generally, dams are designed to safely retain the local runoff from minor and moderate floods maximizing the storm peak attenuation at downstream locations. Nevertheless, as soon as the inflows are predicted to exceed the capacity of the reservoir, dam operators face an operational dilemma. As stated by Bianucci et. al [16], an important conflict of objectives emerges during emergency operations of reservoirs. Although the priority is to ensure the integrity of the dam, so as to prevent catastrophic damages downstream, maximizing the use of the flood control storage is also desired [23]. Indeed, this secondary objective is typically the reason that justified the construction of the project in first place [24]. Ideally, the required emergency release rate for a given reservoir state is that which, if maintained during the remainder of the flood, will exactly fill the residual flood control storage [155]. Nonetheless, in actual operations, a perfect forecast is a chimera, being that future inflows are either unknown or only partly forecasted. This uncertainty poses a serious conflict to the reservoir operator who must make decisions in an extremely short time frame under uncertain conditions and with limited information [14].

The adequate definition of flood control operation rules is, therefore, an essential component of flood risk management in dam-reservoir systems [16]. A common practice in reservoir management is to develop emergency operation schedules [15]. These operating rules in the form of equations or graphs provide the required guidance to the reservoir operators in charge of making real-time release decisions. Since they can be used by reservoir managers in complete isolation at the dam, a common situation under emergency operations, the importance of these curves has been recognized by the entire water management community [12].

Currently, the standard methodology for developing emergency operation schedules recommended by the USACE [24] is based on conservative estimates of expected inflow volumes. This conservative approach is adopted in an attempt to minimize the risk of committing an operational error in terms of excessive releases. According to the method, the scheduled releases should provide enough storage to accommodate the remainder of a flood speculating that the flows continue a receding trend as described by the recession constant of the Spillway Design Flood hydrograph. If, however, inflows continue increasing or if they recede slower than expected, even greater releases than those initially specified will be required. An important assumption made by this development methodology is that there will always be sufficient time to increase releases in a manner that is in accordance with the maximum allowable rate of change of release rates [15]. This assumption becomes less reasonable if the reservoir storage is close to its maximum capacity. Under this condition, if an increase in reservoir releases is required but

the specified rate cannot be attained quickly enough, the resulting increase in storage may be sufficiently large to cause dam overtopping, or, in the worse of the situations, dam breach [23].

While deterministic approaches do not consider the uncertainty of future inflows, other methodologies currently in use within the water resources literature incorporate external hydrologic variables uncertainties. To guarantee that the operation policies obtained with a given model are optimal, these should display fitting behavior for a wide array of flood events. The stochastic generation of inflow hydrographs and initial reservoir levels allows the ensemble of inputs to be representative of statistically possible future events [54] [55]. Rani and Moreira [48] presented a classification of the simulation-optimization modeling techniques differentiating between implicit stochastic programming (ISO) and explicit stochastic programing (ESO). More recently, Koutsoyiannis and Economou [69] proposed the Parametrization-Simulation-Optimization technique which yields solutions that are not inferior to those of benchmark methods and, simultaneously, presents several theoretical, computational, and practical advantages.

The problem of including inflow uncertainties in the optimization is typically addressed by Stochastic Dynamic Programming (SDP) [33]. SDP is the most popular type of explicit stochastic optimization, an approach that incorporates probabilistic inflow methods directly into the optimization problem. Approaches using the implicit stochastic programming are also available in the literature. Rivera and Wurbs [15] [23] proposed a methodology based on the implicit integration of historical inflow records for the development of emergency operation schedules. A few years later, Celeste and Billib [33], highlighted the advantages presented by Implicit Stochastic Programming and Parametrization-Simulation-Optimization techniques to obtain optimal rule curves in an arguably simpler way than Explicit Stochastic Programming approaches.

Despite the comprehensive research on the application of optimization models to reservoir systems, many authors have pointed out the continuous gap between theoretical progress and real world implementations. Among the reasons listed, Wurbs [19], Yeh [18], and Labadie [47], concur that many reservoir system operators are skeptical about models pretending to replace their judgment. In addition, optimization models are generally complex from a mathematical point of view and may be difficult to understand, especially when stochasticity is explicitly included in the optimization. In order to bring theory and practice back together, Koutsoyianis and Economou [69] formally presented the parametrization-simulation-optimization approach. The method parametrizes the flood control operation reducing the dimensions of the typical optimization models to a handful of variables [32]. The parametric rule is then linked to a simulation model which enables the evaluation of the performance of the system for given parameter values; and to heuristic optimization strategies to look for the optimal balance solution. This optimization procedure has successfully been applied in the literature [31] and includes the inflow and initial reservoir level uncertainties within the flood control optimization framework [33].

The aim of this chapter is to improve the existing methodologies for developing emergency operation schedules by including the concept of risk into the optimization of flood control operations. The chapter proposes a framework that combines a simulation-optimization model with a novel parametric flood control operating rule. The parameters of the rule are estimated by optimization, using a Monte Carlo simulation approach to evaluate the performance of the system in terms of overall risk. The rule is based on the concept of storage zoning and establishes a four-dimensional correlation between release, storage and inflow. For each parameter set, a series of simulations of the system operation and its response to an ensemble of flood events allows the system objective to be evaluated. For validation purposes, a simple hypothetical example is employed to test the proposed parametric rule against the emergency operation schedules utilized by the USACE. At the same time, to explore the influence of each of the proposed parameters on the overall risk and to gain insight into extreme event operations, a sensitivity analysis is conducted.

4.2 Proposed Methodology

The problem associated with the operation of a reservoir in the case of a flood event is fundamentally multi-objective. It involves a compromise between the released flows and the stored volumes, to neither damaging the urban areas downstream and upstream of the dam, nor endangering the safety of the structure [13]. The uncertainty regarding future inflow volumes makes reservoir regulation a challenging task. To facilitate the labor of dam operators in charge of making real-time release decisions, operating rules in terms of functions and graphs provide the guidance required during extreme situations.

A novel procedure is presented in this chapter for the development of emergency operation schedules applied to single dam-reservoir systems. The procedure combines a novel parametric operating rule, a heuristic optimization algorithm, and a Monte Carlo simulation approach for conducting risk analysis. As such, the concept of risk is directly included into the optimization of flood control operations. The parametrization-simulation-optimization framework is reduced to a four dimensional problem in which the optimal operation is determined in terms of the aggregated sum of three objectives: minimize flooding risks at the upstream region, minimize flooding risk at the downstream area and minimize the risk attributed to the structural failure of the dam. The suggested optimization approach includes three steps:

- **Step 1:** development of a parametric rule curve for emergency operations defined by a few operational parameters,
- **Step 2:** simulation for the synthesis of the system performance in terms of downstream flooding risk, $R_{SLS,O}$, dam failure risk, $R_{ULS,B}$, and upstream flooding risk $R_{SLS,h}$,
- **Step 3:** optimization of the set of parameters using a pattern search algorithm in which the objective function is equal to the overall risk of the system

The framework of the parametrization-simulation-optimization process is shown in Fig. 4.1. Parametrization-simulation-optimization starts with the shape of a operating rule defined by a few operational parameters, θ. The reservoir operation is then simulated under an ensemble of stochastically generated inflow hydrographs. The simulation culminates with the synthesis of the performance of the chosen set of parameters according to the downstream flooding risk, $R_{SLS,O}$, the dam failure risk, $R_{ULS,B}$, and the upstream flooding risk $R_{SLS,h}$. These three components of risk are aggregated into one single figure, the overall risk of the dam-reservoir system, R_T, which is selected as objective function for the optimization. The parameters are then changed applying a pattern search algorithm, and the reservoir is operated again for the same scenarios. This process goes on until the combination of parameters that minimizes the overall risk, θ_{opt}, is reached.

The risk assessment procedure developed in Chapter 3 is used for the synthesis of the performance of each trial set of operational parameters. The suggested simulation approach integrates the impacts of predefined operating rules within the risk identification and estimation process based on three ideas: one relating to the use of a structure-based approach for the interpretation of the external hydrologic loading return period; other to the simultaneous analysis of initial reservoir levels, inflow peaks and inflow volumes; and the last one to the representation of the probabilistic dependence between water levels and peak outflows through their quantile-quantile relationship. These three points allow to correctly consider the effect of the operational parameters on the objective function.

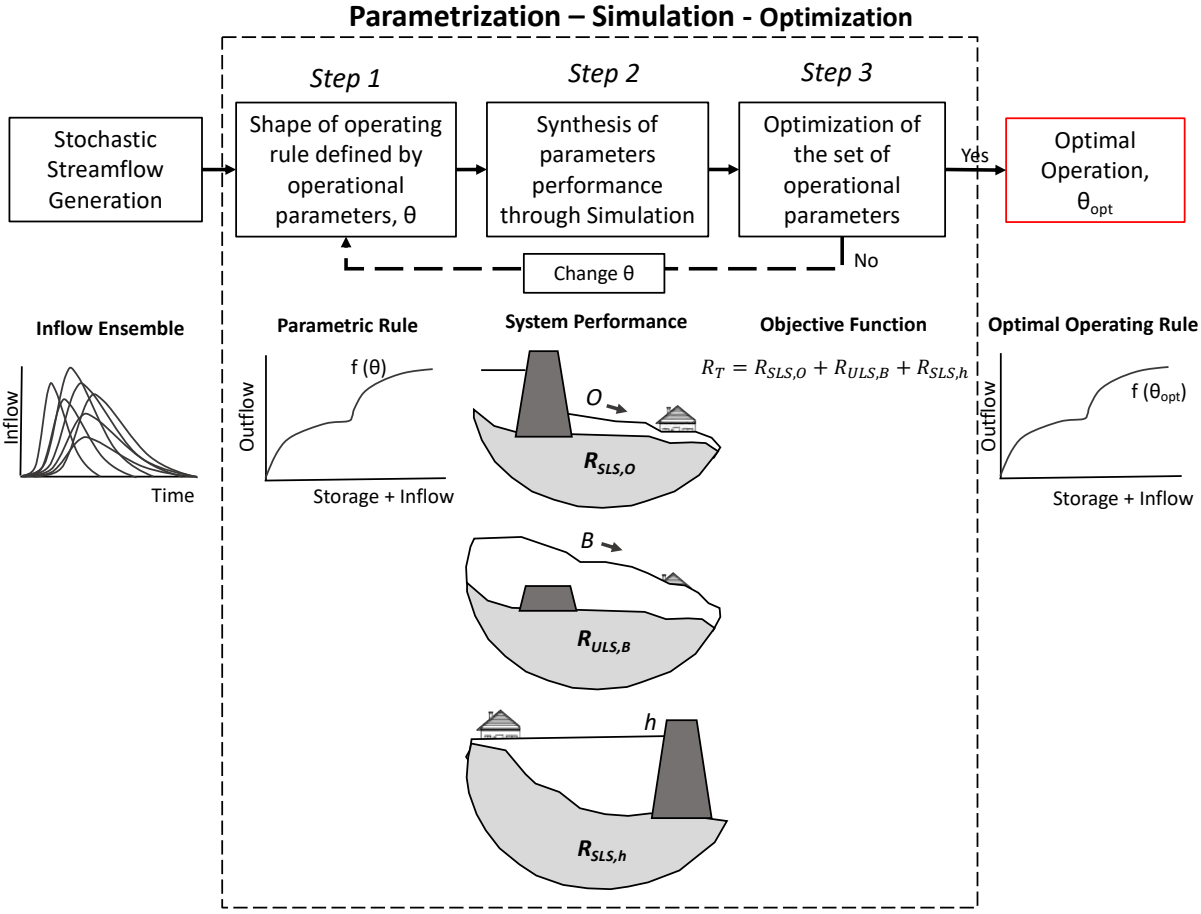

Figure 4.1: General framework of parametrization-simulation-optimization modeling approach for emergency reservoir operations: (1) define the shape of a parametric rule, (2) measure the performance of the set of parameters through simulation, and (3) optimize the parameters to obtain the best overall performance of the system, R_T

4.2.1 Parametrization

Most common methods used in the optimization of flood control operations require of a large number of control variables. These are typically the sequences of outflows at every time step of the control period [69]. In order to facilitate the application of the optimization framework to different case studies and simplify the resolution of the problem, the flood control operating rule has been parametrized. This way, the optimization process is transformed into a low-dimensional problem with fewer computational inconveniences.

It was concluded from the previous chapter that the normal flood control operation presents a better overall performance for small, moderate and large floods as compared with the emergency operation schedules. Waiting until the last moment for making releases results in a large increase of the serviceability limit state risk at downstream locations. However, it was also indicated that in extreme circumstances, releases at higher than normal rates are necessary to guarantee the integrity of the structure and reduce the risk due to the structural failure of the dam.

Based on these two principles, a novel parametric rule is proposed for the management of single dam-reservoir systems during extreme hydrological conditions. The suggested rule combines the concept of storage zoning with a four-dimensional correlation between storage, inflow and outflow, being the discharges expressed as a function of four operational parameters denoted

as $\theta = \{m_1, m_2, s_1, s_2\}$. The first two parameters, m_1 and m_2, are responsible for limiting the releases at each storage level; whereas, s_1 and s_2, are related to the separation levels between the three different storage zones illustrated in Fig. 4.2. Releases in a future time step, O_{j+1}, are determined by the prior state of the reservoir, S_j, the inflow rates entering the reservoir, I_j and I_{j+1}, the maximum released capacity of the outlet works, $O_{max,j}$, and the set of operational parameters $\theta = \{m_1, m_2, s_1, s_2\}$.

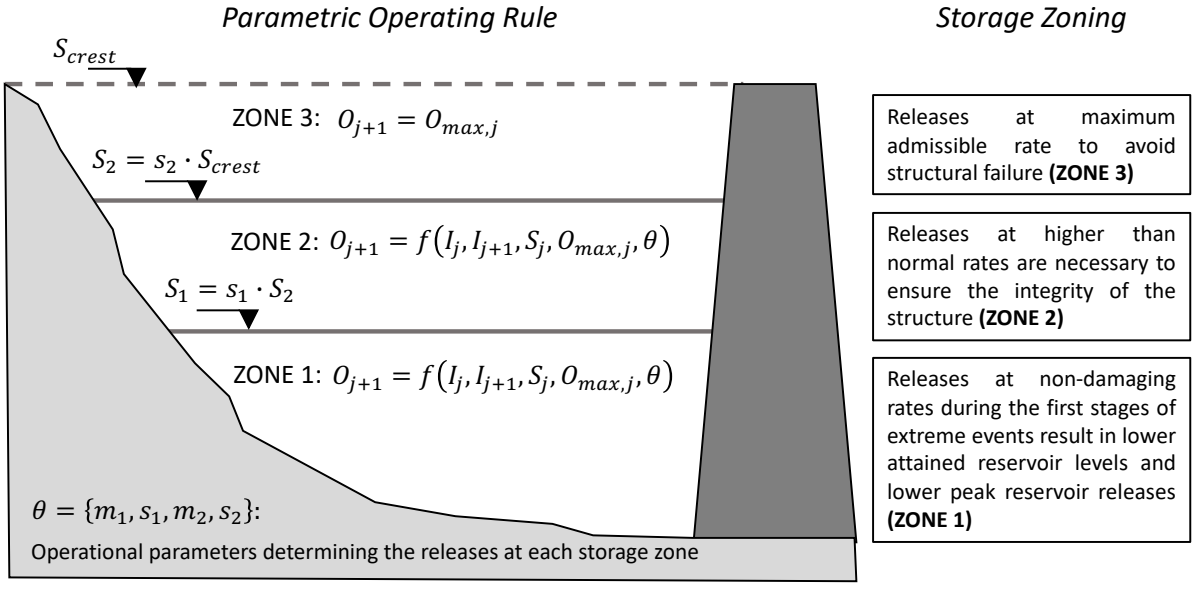

Figure 4.2: Sketch of the three storage zones and the parameters influencing the releases

The separation between ZONE 1 and ZONE 2 is determined by the storage value $S_2 = s_2 \cdot S_{crest}$. Meanwhile, the limit between ZONE 1 and ZONE 2 is expressed as a function of S_2, being $S_1 = s_1 \cdot S_2$. Depending on the storage zone at which the pool level is at each time step, the proposed operating rule can be expressed as in Eq. (4.1):

$$O_{j+1} = \begin{cases} \text{ZONE 3: } O_{max,j} & \text{if } \sqrt{S_j^2 + I(t)^2} > S_2 \\ \text{ZONE 2: } O_{max,j} \cdot \left[\dfrac{\sqrt{S_j^2 + I(t)^2}}{S_2} \right]^{m_2} & \text{if } S_1 \leq \sqrt{S_j^2 + I(t)^2} \leq S_2 \\ \text{ZONE 1: } O_{max,j} \cdot \left[\dfrac{S_1}{S_2} \right]^{m_2} \cdot \left[\dfrac{\sqrt{S_j^2 + I(t)^2}}{S_1} \right]^{m_1} & \text{if } \sqrt{S_j^2 + I(t)^2} \leq S_1 \end{cases} \tag{4.1}$$

where $I(t)$ symbolizes the total inflow volume entering the reservoir at each time step $I(t) = (I_j + I_{j+1})/2 \cdot \Delta t$, $O_{max,j}$ is the maximum discharge permitted at each time step, S_j is the active storage, S_1 the activation level for ZONE 2, S_2 the activation level for ZONE 3, and $\theta = \{m_1, m_2, s_1, s_2\}$ the parameters to be optimized.

The equation describing the releases for the suggested operating rule changes depending on whether the combination of active storage and inflow, $S^* = \sqrt{S_j^2 + I(t)^2}$, is above $S_2 = s_2 \cdot S_{crest}$

(ZONE 3), below $S_1 = s_1 \cdot S_2$ (ZONE 1), or within S_2 and S_1 (ZONE 2). Releases at low rates in ZONE 1 are permitted within this formulation. This way the ultimate limit state risk and the serviceability limit state risk associated with upstream flooding are reduced. These releases are controlled by parameter m_1 and parameter m_2. To control the rate of change between reservoir zones, the coefficient between S_2 and S_1 has been included in the operating equation. When the combination of active storage and inflow, S^*, equals S_1, the last release on ZONE 1 equalizes the first outflow rate of ZONE 2. The release policy changes in ZONE 2 and ZONE 3 where releases at higher rates are conducted to ensure the integrity of the structure, to avoid uncontrolled overflows and to limit the increasing upstream flooding risk observed during normal flood control operations.

4.2.2 Simulation

The simulation approach for conducting risk analysis developed in Chapter 3 provides the perfect means of evaluation of each set of operational parameters, θ. The stochastic flood scenario generator, the reservoir flood control model, and the risk estimator model are included within the parametrization-simulation-optimization framework to synthesize the performance of the system in terms of the overall risk. Figure 4.3 displays the architecture of the simulation approach. The figure includes all the information required for the assessment of risk where each variable is represented by a node and each relationship by an arc. The analysis is divided into four sections corresponding with the four terms of the definition of risk.

- Analysis corresponding to the modeling of loads
- Analysis corresponding to the modeling of the effects of reservoir operations
- Analysis corresponding to the response of the system
- Analysis corresponding with the modeling of the consequences

The first node introduces the inflow hydrographs entering the reservoir. Following the indications from Mediero et. al [8], the synthetic generation of inflow hydrographs is based on three aspects: the analysis of the marginal distribution function of inflow peaks; the analysis of the statistical dependence between the inflow volumes and inflow peaks through a linear regression analysis; and the study of characteristic hydrograph shapes of the watershed. These hydrographs are assumed as being the expected annual maximum hydrologic forcing acting on the dam-reservoir system.

The next node refers to the generation of random initial water levels in the reservoir. The node represents the pool level prior to the arrival of the largest flood wave of the year. In this study, the variability of the initial reservoir level is addressed following the procedure recommended by Carvajal et. al [141]. The authors propose the statistical analysis of reservoir stage records to elaborate an empirical cumulative distribution function. The importance of including the stochastic nature of the initial water level within the simulation approach resides in the objective function chosen for the optimization. Assuming that the dam is always at its maximum Flood Control Level [117] [92] would lead to a set of optimal operational parameters that release larger rates than the strictly required, ultimately increasing the risk of downstream flooding.

The maximum water levels are achieved by routing the synthetic series of inflow hydrographs through the reservoir where each simulation starts at the corresponding random value of initial reservoir level. The mass balance equation is solved using the Modified Puls Method [39] which requires of some additional information such as the set of operational parameters, the storage-elevation curve and the storage-release curve of the outlet works. Following the definition of

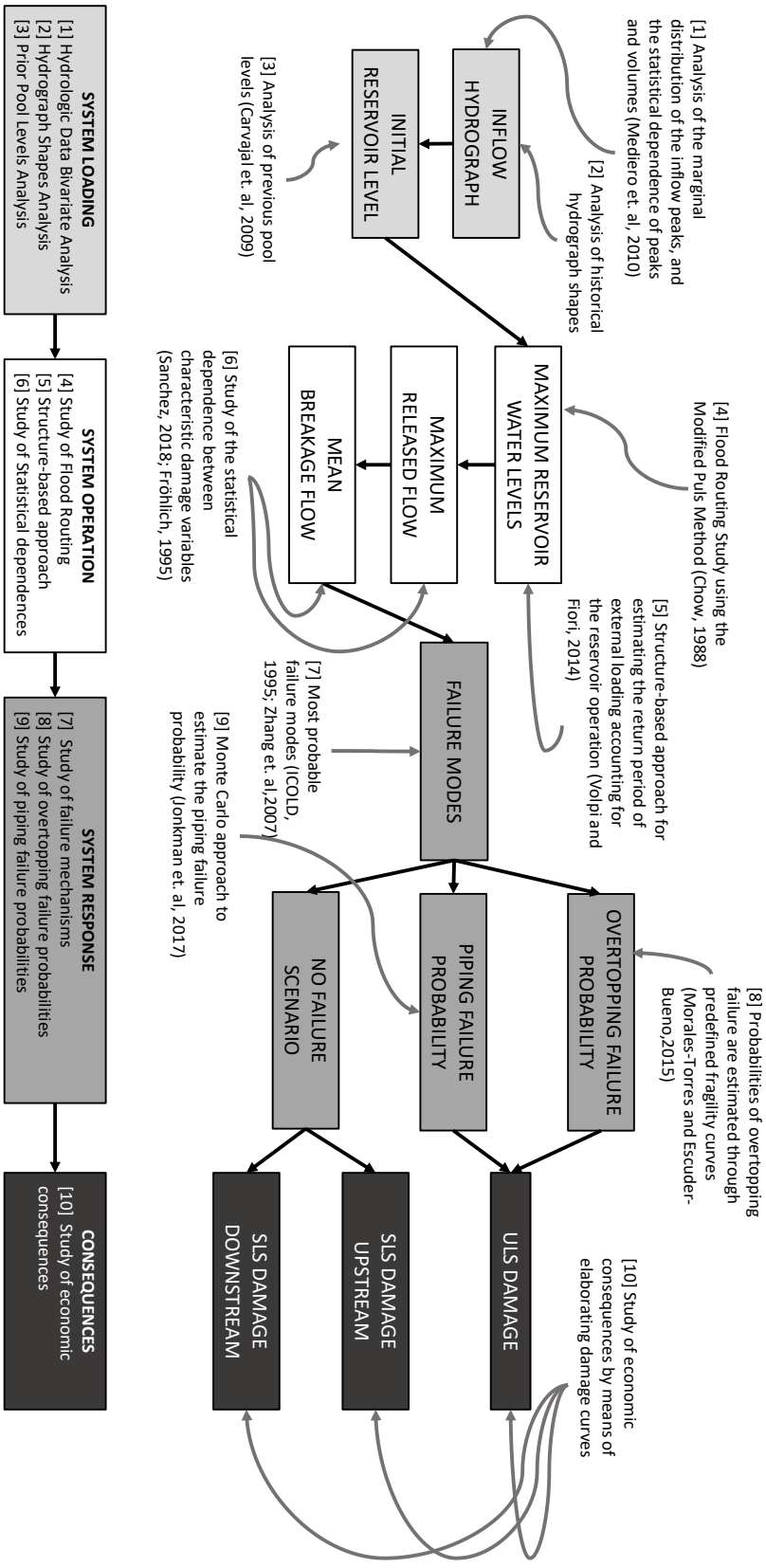

Figure 4.3: Influence Diagram of the simulation approach showing the works to be done to define each of the variables and their interrelations. The variables are represented by nodes and the relationships by arcs

risk proposed in the previous chapter, the return period of the set of generated flood scenarios is calculated as the total number of events divided by the number of events that reach a maximum water level higher than a chosen threshold [116] [139]. The statistical analysis of the maximum reservoir water level is, therefore, a key component for the assessment of risk, the probabilities of failure of the system, and the potential damages at upstream and downstream areas.

The following two nodes refer to the maximum released flows and the mean breakage flows. They include the analysis of the statistical dependence between the two characteristics damage variables and the maximum water levels. The effects the dam operation has on the released flows and magnitudes is expressed through the quantile-quantile relationship between reservoir levels and reservoir releases. It was demonstrated in the previous chapter that this statistical relation representing the most likely outflow peak for each maximum reservoir level is unique for each operating rule. Furthermore, the conditional probability between maximum reservoir levels and peak breakage flows is obtained applying the results from the multiple linear regression analysis carried out by Frölich [128].

The next node in dark gray contains the information of the failure modes. According to the report on dam failure statistics developed by the International Commission on Large Dams (ICOLD) [144] and the works from Zhang et. al [145] presented in the First International Symposium on Geotechnical Safety and Risk celebrated in Shanghai in 2007, piping and overtopping comprise the two most frequent causes of embankment dam failure. As such, both failure mechanisms are included and combined through a common caused adjustment for the evaluation of the system response against the external hydrological loading [146].

First, the overtopping failure probability is implemented using a predefined fragility curve proposed by Escuder-Bueno and Morales-Torres [149] in which the structural failure probability is expressed as a function of the overtopping depth (Fig. 3.19). The curve encompasses the outcome from a combined effort made during the 13^{th} ICOLD Workshop on Probability of Failure of Embankment Dams due to Slope Stability and Overtopping [148] [147]. Meanwhile, the piping failure probability is assessed by means of a Monte Carlo probabilistic approach. The methodology follows the procedures contemplated by Jonkman et. al [81] in which the piping failure is considered as a parallel system comprised of uplift, heave and piping.

Moreover, since the failure of the system does not only refer to the catastrophic breakage of the structure, the serviceability limit state risk considering the non-failure scenarios causing damages upstream and downstream of the dam are also taken into account. Their probability of occurrence results from the combination of the occurrence probability of the maximum reservoir levels, the conditional probability of having a peak outflow for that reservoir level and the conditional probability of non-structural failure for the attained reservoir stage.

Finally, there are nodes of consequence estimation where the relationship between the economic damages and the three characteristic damage variables associated with each component of the overall risk, i.e. peak reservoir stages, h, peak outflow rates, O, and peak breakage flows, B, are contemplated. The damage curves are elaborated combining 1D steady state hydraulic modeling, predefined depth-damage curves for residential buildings [129], and Geographic Information Systems for terrain data processing. First, the hydraulic modeling calculates the flooding depths at each parcel. Then, the depth-damage curves are used to estimate the percentage of structural damages as a function of the flood depth. Finally, the construction of consequence curves culminates with the determination of affected residential properties and their values using ArcGIS.

4.2.3 Optimization

During extreme hydrological conditions, dam operators face an operational dilemma: how much water to release and at what rate. On one hand, flood control operations should minimize flood damages at downstream locations; on the other hand, operations must ensure the integrity of the structure by preventing the reservoir water levels from reaching threatening levels. Finally, in some cases, urban development upstream from the reservoir also poses a limiting constraint to be considered during flood control operations. Figure 4.4 represents the objectives that are formulated in the risk-based parametrization-simulation-optimization framework:

- **Objective 1:** Minimize the risk of releasing rates larger than the downstream non-damaging capacity should the dam not collapse. Also denoted as serviceability limit state risk of downstream flooding, this objective aims at minimizing downstream damages and their probabilities of occurrence motivated by flawed outlet works operation.

$$R_{SLS,O} = \sum_{h} p(h) \cdot p(nf|h) \cdot \left\{ \sum_{O} p(O|h) \cdot D_{nf,O} \right\} \tag{4.2}$$

  where $p(h)$ is the occurrence probability of reaching certain water level in the reservoir and $p(nf|h)$ is the conditional probability of non-structural failure of the dam for the attained reservoir stage. The last terms of the equation represents the sum of the peak outflow probabilities expressed through their conditional probability for the given reservoir stage, $p(O|h)$, and their associated damages $D_{nf,O}$.

- **Objective 2:** Minimize the risk posed by the retaining structure to the downstream floodplain properties that is attributed to dam failure. This objective aims to ensure the integrity of the structure during extreme events. The ultimate limit state risk is not limited to one single failure mechanism like dam overtopping, but, instead, to the combination of all possible ways in which a dam could fail using a common cause adjustment [146].

$$R_{ULS,B} = \sum_{h} p(h) \cdot p(f|h) \cdot \left\{ \sum_{B} p(B|h) \cdot D_{f,B} \right\} \tag{4.3}$$

  where $p(f|h)$ is the probability of structural failure of the dam for a given reservoir level, $p(B|h)$ is the conditioned probability of breakage peakflow with respect to the reservoir level, and $D_{f,B}$ the damages associated to the breakage peakflow values.

- **Objective 3:** Minimize the risk of flooding upstream properties should the dam not fail. This objective has been previously referred as serviceability limit state risk of upstream flooding, and aims to keep the water levels from reaching pool elevations above which the residential and commercial properties located upstream from the reservoir are susceptible to flooding.

$$R_{SLS,h} = \sum_{h} p(h) \cdot p(nf|h) \cdot D_{nf,h} \tag{4.4}$$

  where $p(h)$ is the probability that a reservoir pool elevation, h, may occur; $p(nf|h)$ is the conditional probability of non-failure of the structure given a the reservoir stage, h; and $D_{nf,h}$ symbolizes the consequences derived from the water levels reached.

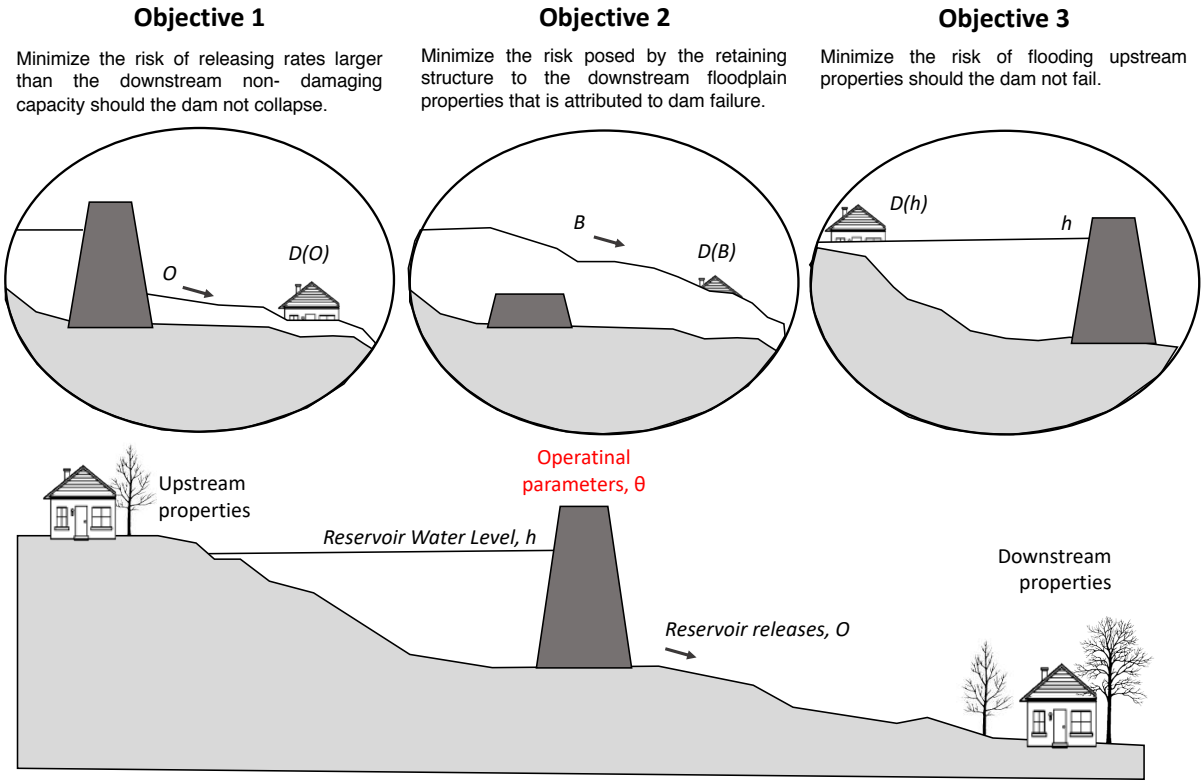

Figure 4.4: Graphical representation of the three objectives of the parametrization-simulation-optimization framework. Objective 1: minimize the risk of releasing rates larger than the downstream non-damaging capacity should the dam not collapse; Objective 2: minimize the risk attributed to dam failure; Objective 3: minimize the risk of flooding upstream properties should the dam not fail

The damages are expressed in monetary terms whereas the probabilities are given in yearly units. From among the multi-objective optimization approaches available in the literature [63], the weighted sum aggregation is chosen. The synthesis of the performance of each combination of operational parameters is evaluated through the overall risk of the system, R_T, Eq. (4.5). To put it another way, the objective function for the optimization results from the summation of: (1) the serviceability limit state risk downstream of the reservoir due to outflow rates larger than the non-damaging capacity of downstream reaches, $R_{SLS,O}$, (2) the risk associated with the failure of the structure, $R_{ULS,B}$, and (3) the serviceability limit state risk upstream of the dam motivated by high pool levels, $R_{SLS,h}$. Since all the elements of the overall risk are commensurable and at the same time are expressed in the same units, equal levels of priority or relevance are ascribed to the three components.

$$R_T = R_{SLS,h} + R_{SLS,O} + R_{ULS,B} \tag{4.5}$$

Furthermore, following the works from Celeste and Billib [33], this research uses a pattern search method as optimization model. Pattern search algorithms are optimization strategies that, unlike other optimization methods, do not require any information about the gradient or higher derivatives of the objective function to search for an optimal point. At each optimization step, the pattern search algorithm searches a set of points, called a mesh, for a point that improves the objective function. The algorithm forms the mesh by multiplying the default pattern vectors from MATLAB by a scalar ε, called the mesh size, Eq. (4.6):

$$\theta_i = \theta_0 + \varepsilon \cdot v_i \tag{4.6}$$

in which θ_i and θ_k are the new and the previous set of operational parameters, respectively; and v_i is a pattern vector which takes values ranging from minus one to one. The algorithm polls the points in the current mesh by computing their objective function values. If it finds a point whose objective function value is lower than that of the current simulation, the poll is called *successful*, and the point that has been found becomes the new point at the next iteration. In contrast, if the algorithm fails to find a point that improves the objective function, the poll is called *unsuccessful* and the current point stays the same for the next iteration. At the first iteration, the mesh size is 1. By default, the pattern search doubles the mesh size after each successful poll and halves it after each unsuccessful poll.

4.3 Results and Discussions

The optimization framework presented in this chapter has been applied in the study of the hypothetical single-purpose dam-reservoir system presented in Chapter 3. The system is comprised of three elements: a 9.5 m height embankment dam with gated outlets and uncontrolled spillways constructed with the main purpose of flood control; a downstream region where flooding occurs if flows exceed the non-damaging channel capacity of $CC = 200m^3/s$; and an upstream region where residential properties are susceptible to flooding when pool levels reach $H_{res} = 7.5m$. The reader may refer to Chapter 3 for further details concerning the utilized damage curves, system response curve and hydrological loading conditions affecting the hypothetical reservoir.

The goal of this section is to improve the understanding of the system's behavior when the proposed method for developing emergency operation schedules is adopted for the management of floods. The four operational parameters, $\theta = \{m_1, m_2, s_1, s_2\}$, and their impact on the overall risk have been evaluated using a sensitivity analysis. In the following, the evaluation method used and the most important conclusions are briefly explained. The study reveals that the optimal operation strategy is strictly related to the particular system under study, leading to significantly different combinations of parameters depending on the characteristics of the structure, the reservoir capacity and the topography of upstream and downstream regions.

Additionally, under the same hydrological loading conditions, the performance of the parametric operating rule resulted from the proposed risk-based optimization framework is compared against the USACE emergency operation schedules. The results show that the optimization of the flood control operations reduces the total risk of the system by almost 70%. Furthermore, the optimum set of parameters displays a 35 % decrease on the structural failure risk under extreme circumstances.

4.3.1 Sensitivity Analysis of the Proposed Parametrized Rule

In order to improve the operations during extreme hydrological conditions in terms of overall risk of the system, a parametric operating rule has been proposed in Section 4.2.1. The suggested operating rule divides the reservoir into three storage zones, and establishes a four-dimensional correlation between releases, storage and inflows. This has been achieved through a handful set of four operational parameters that determine the releases from the reservoir at each time step, $\theta = \{m_1, m_2, s_1, s_2\}$. The first two parameters, m_1 and m_2, are responsible for limiting the outflow rate at each storage level. On the other hand, s_1 and s_2, are related to the division of the reservoir pool into three different storage zones (Fig. 4.2).

The evaluation of each parameter has been conducted maintaining the remaining variables untouched. With the aim of having representative results, the same 10.000 stochastic flooding

scenarios have been used for each evaluation. Herein, Tab. 4.1, Fig. 4.5 and Fig. 4.6 display the results from the analysis of the parameter s_2. The reader may refer to Appendix C for further details concerning the results obtained for the remaining parameters.

	$R_{SLS,H}$ [M$/yr]	$R_{SLS,O}$ [M$/yr]	$R_{ULS,B}$ [M$/yr]	R_T [M$/yr]
$s_2 = 0.1$	0,0468	1,1003	3,6311E-4	1,1475
$s_2 = 0.3$	0,0574	1,0447	0,0011	1,1031
$s_2 = 0.5$	0,0684	0,5332	0,0020	0,6036
$s_2 = 0.7$	0,0853	0,2807	0,0038	0,3698
$s_2 = 0.9$	0,1033	0,1817	0,0057	0,2907

Note: Sensitivity analysis with $m_1 = 0.5$; $m_2 = 0.8$; $s_1 = 0.5$

Table 4.1: Serviceability limit state, ultimate limit state and overall risk results for a range of values of the operational parameter s_2. The analysis was conducted with the remaining parameters being: $m_1 = 0.5$, $m_2 = 0.8$ and $s_1 = 0.5$

The results are plotted in Fig. 4.5 and Fig. 4.6. The first image illustrates the values of the different objectives of the optimization as well as their aggregated sum for a range of s_2 magnitudes. The analysis has been carried out being the remaining parameters $m_1 = 0.5$, $s_1 = 0.5$ and $m_2 = 0.8$. Figure 4.5 shows how, in this case study, the overall risk is strongly related to the serviceability limit state risk of downstream flooding. Combinations of parameters that minimize this operation objective will lead to better performances of the system.

Figure 4.6 depicts the cumulative frequency at which the estimated level of damages are caused. The area under the curve symbolizes the overall economic risk of the system. Five frequency-damage curves are plotted corresponding to the different values of the studied parameter s_2. It is inferred from the figure that, although the annualized structural failure probability of the dam increases for larger values of the parameter, the probability of having larger damages decreases. This nicely confirms that risk during extreme events is not exclusively related with the catastrophic breakage scenarios, but also on releases at higher than normal rates.

The results obtained coincide with the general reasoning. Let analyze two distinct parameters, $s_2 = 0.7$ and $s_1 = 0.1$. The former implies that the limit between ZONE 2 and ZONE 3 is closer to the crest level, whereas the latter corresponds to very small storage capacity at ZONE 1 and ZONE 2. Releases at maximum capacity start at very low levels for $s_2 = 0.1$, decreasing the attained pool levels and increasing the magnitudes and frequencies of damages downstream of the reservoir. In contrast, larger values of s_2 will decrease the outflows leading to upstream flooding and higher structural failure risk.

Similar outcomes have been achieved with the sensitivity analysis of the parameter m_2. Although increasing the upstream flooding risk and the structural failure probabilities, larger values of m_2 led to lower values of the overall risk and the serviceability limit state risk of downstream flooding. This has been attributed to the fact that larger values of m_2 reduce the outflow rates. Important features concerning the parameters s_1 and m_1 have also been inferred from the analyses. A behavior very similar to an "opening strategy" [12] is observed when the reservoir is managed with low values of m_1. The flood is more efficiently dampened but its delay downstream is reduced. This practice is safer from the point of view of dam collapse as well as upstream flooding. Furthermore, since the non-exceeding downstream channel capacity is very large in the considered case study, lower values of m_1 also lead to better performance in

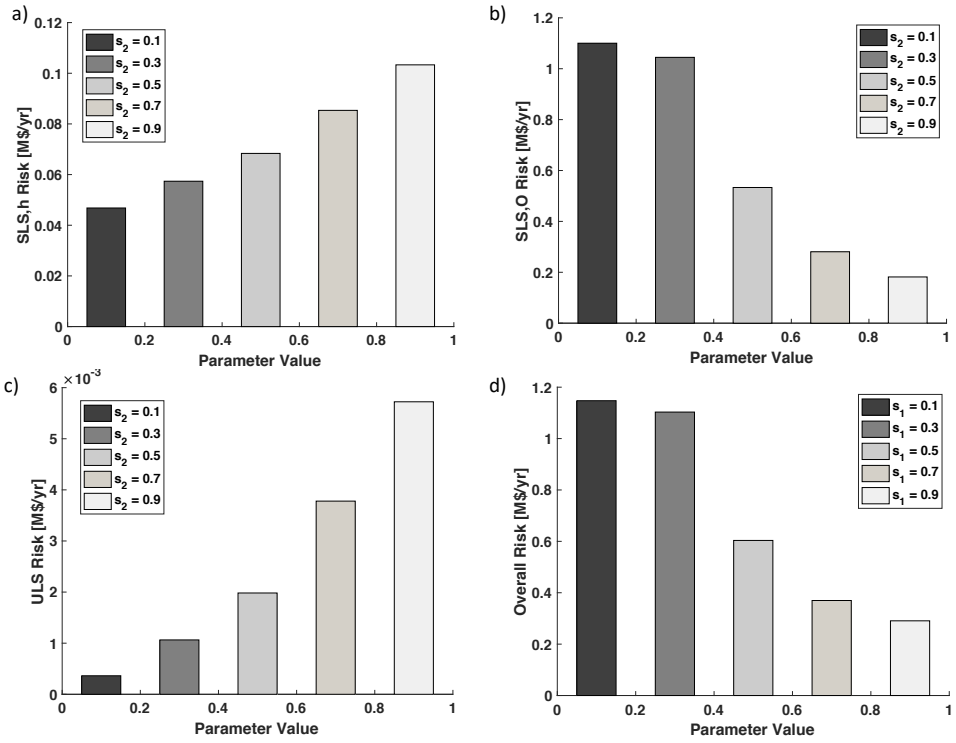

Figure 4.5: Bar diagrams representing the performance of the system under diverse values of s_2 in terms of: (a) upstream flooding risk, (b) downstream flooding risk, (c) dam break risk, and (d) aggregated sum risk

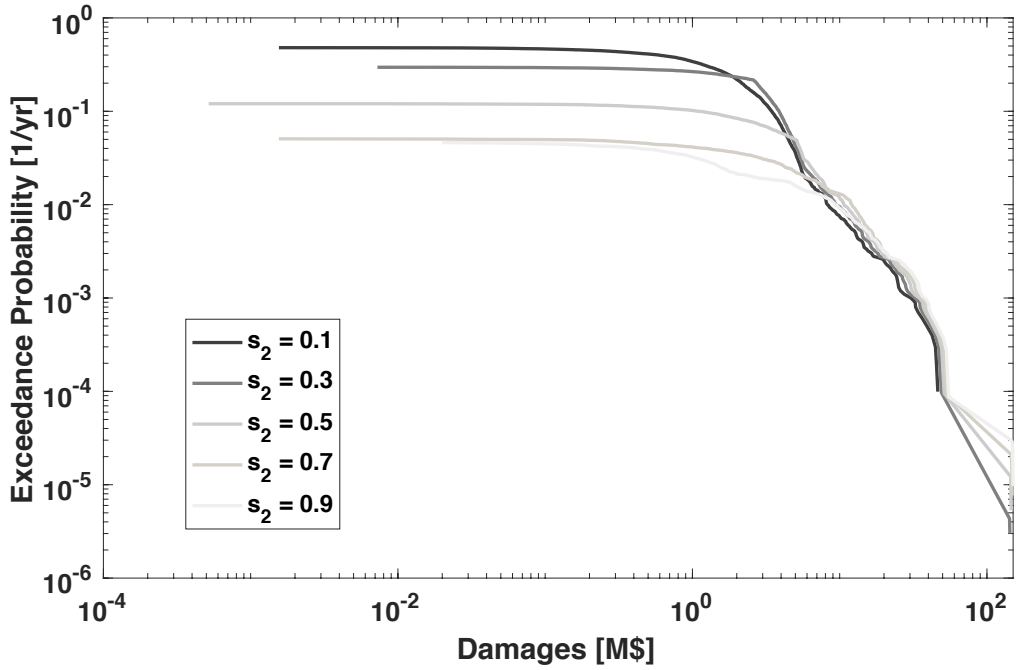

Figure 4.6: Frequency-damages curves representing the performance of the system in terms of overall risk under diverse values of s_2

terms of downstream flooding risk. Meanwhile, the parameter s_1 depends on the downstream capacity threshold, with optimal performances achieved for values in the range of $s_1 = 0.7$.

4.3.2 Evaluation of the Optimal Set of Operational Parameters

As discussed throughout this chapter, little research has been published related to the optimization of release and store decisions including the expected annual damage in their objective function. A novel optimization framework to develop emergency operating rules has been proposed in this chapter to improve the deterministic standard U.S. Army Corps of Engineers method [24]. First, through an stochastic approach the suggested optimal performance of the system under a wide range of flooding scenarios is guaranteed; second, the methodology includes the concept of risk as crucial component for operation decision-making; and lastly, it reduces the complexity of other optimization processes focusing exclusively on four variables describing a simple operating rule that is valid through the entire control period, and determines the releases at each time step.

Under similar loading conditions, the performance of the suggested parametric operating rule obtained using the proposed risk-based optimization framework has been compared with the emergency operation schedules developed following the guidelines from the USACE [24]. Table 4.2 displays the results for each optimization objective as well as their aggregated sum in terms of the overall risk. The parametric rule with operational parameters equal to $\theta = \{0, 0.695, 1, 1\}$, mitigated by almost 70% the total risk of the system as compare to the USACE emergency operation schedule. Furthermore, the ultimate limit state is diminished by a 35%. This results nicely demonstrates that optimizing the emergency flood control operation of reservoirs can be an efficient non-structural risk mitigation measure.

	USACE OPERATION [M$/yr]	PARAMETRIZED RULE [M$/yr]	RISK REDUCTION [%]
$R_{SLS,H}$	0.1662	0.0653	60.7
$R_{SLS,O}$	0.3592	0.1019	71.6
$R_{ULS,B}$	0.0049	0.0017	34.7
R_T	0.5303	0.1688	68.1

Table 4.2: Summary of the risk values attained by operating the hypothetical dam-reservoir system following the USACE method and the proposed operating rule

The magnitudes from Tab. 4.2 are represented in Fig. 4.7. The illustration depicts the Frequency-Damage curves of the system adopting both operation strategies. The curves suggest better performances during extreme hydrological conditions following the proposed operating rule. The also show two interesting aspects concerning the optimal operation of reservoirs. First, opening strategies with non-damaging rates at the first stages of extreme events results in lower attained reservoir levels, ultimately decreasing the upstream flooding risk as well as the structural failure risk (ZONE 1). Second, as water levels increase inside the reservoir and under extreme circumstances, releases at higher than normal rates are necessary to ensure the integrity of the structure (ZONE 2).

4.3.3 Classification of Dam-Reservoir System According to the Proposed Optimization Objectives

According to the parametrization-simulation-optimization framework proposed in this chapter, the performance of each set of predefined parameters is evaluated through the aggregation of

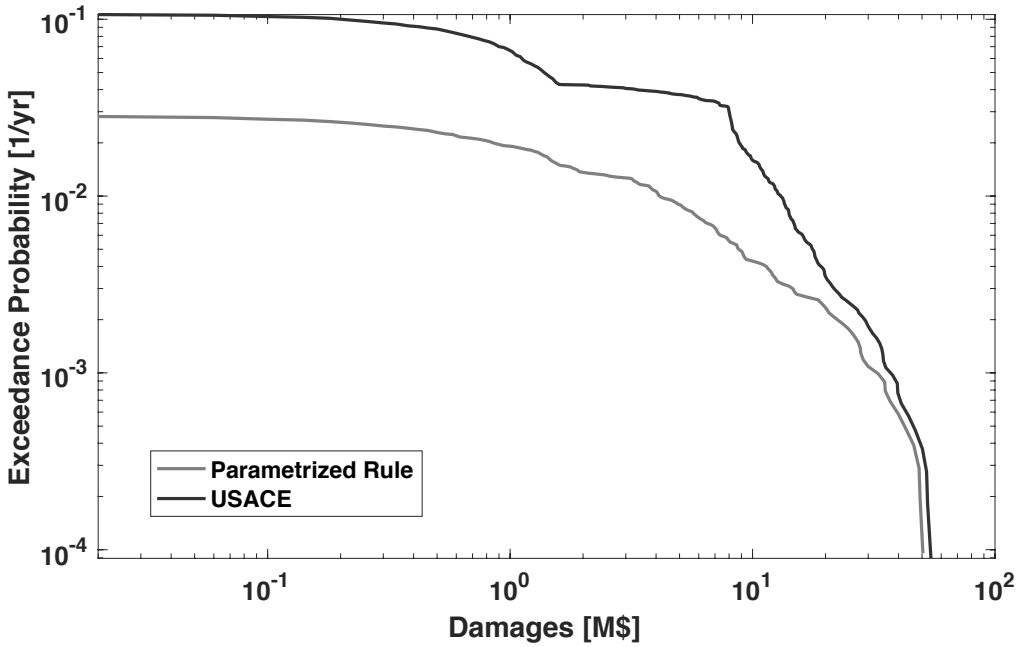

Figure 4.7: Frequency-Damage curves representing the performance of the system in terms of overall risk under the proposed operating rule and the emergency operation schedules recommended by the USACE

three risk components: (1) the serviceability limit state risk downstream of the reservoir due to outflow rates exceeding the stream banks, (2) the risk associated with the failure of the structure, and (3) the serviceability limit state risk upstream of the dam motivated by high pool levels. A conflict of interests is observed between the three objectives. Reducing the outflow rates, that is, minimizing the first objective will lead to higher values for objectives two and three. On the other hand, maximizing the releases will lead to minimal ultimate limit state risk and serviceability limit state risk of upstream flooding.

The optimal set of parameters will result from the specification of the threshold between released flows and stored volumes that best complies with the three objectives. For instance, in the simplified example used in this chapter, minimizing the releases leads to a significant improvement of the performance of the system. Since the outflows are the main responsible for increasing the total risk, the system presented for this study is classified as "release dominated". Nonetheless, this could be different if higher damages are expected due to dam breach or upstream flooding. In addition, potential failure at lower storage levels will also increase the ultimate limit state risk requiring larger releases through the outlet works. This second type of systems are "storage dominated".

When the characteristics of the reservoir, the topography of upstream and downstream regions, the external loading conditions or the dam structure response change, it is to be expected that what is optimal for one system could be not capital for other. Acknowledging that the optimal operation strategy of reservoirs is strictly dependent on the particular system under study, similarities regarding optimal flood control operation strategies between diverse systems can also be recognized. As such, this graduation project suggests the classification of dam-reservoir systems according to their dominant risk objective (Fig. 4.8):

- **Release Dominated Systems (RDS)**: Within this category fall all the systems in which lower releases are preferred to low storage values. That is, systems which overall risk is

dominated by the peak outflows. Small downstream channel capacities, large reservoir storage capacity and low structural failure probabilities are some of the characteristics of this type of systems. Other factors pertain to the characteristics of the regions downstream of the dam. Urban development in flat lowlands adjacent to river systems will increase the vulnerability and exposure of downstream communities. This increases the importance of the risk associated with downstream flooding.

- **Storage Dominated Systems (SDS)**: This category comprises systems whose overall risk presents a high dependence with the ultimate limit state risk and the risk of upstream flooding. Contrary to release dominated systems, SDS are characterized by: large downstream channel capacities, elevated failure probabilities before reaching the crest levels, large values of expected damages within the reservoir area and enormous damages in case of structural dam failure.

From the point of view of the four parameters that determine the releases at each time step in the proposed framework, release dominated systems mitigate risk better for larger values of s_2 and larger values of m_2. Operation policies showing similarities with closing strategies and normal flood control schedules are preferred. Meanwhile, in cases in which high pool levels dictate the overall risk of the system, opening operation strategies with high outflow rates lead to higher risk mitigation.

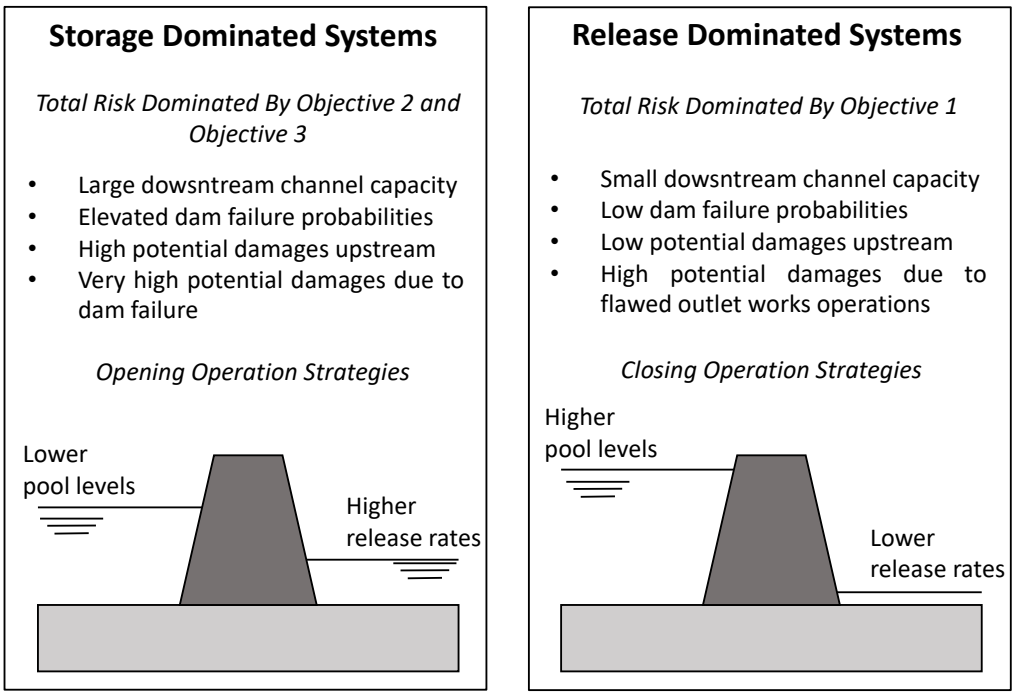

Figure 4.8: Classification of dam-reservoir systems according to their dominant risk objective: storage dominated (SDS), and release dominated (RDS); including the optimal operation strategy for each type under extreme events

If the type of system is known, recommendations regarding the optimal emergency operations could be made without requiring detailed analysis of the dam-reservoir system. Furthermore, it could be of great help for the optimization framework given that the four initial operational parameters can be more or less estimated. Since the threshold between the two types of systems is not always clear, a simple sensitivity analysis similar to the herein exposed could be carried to determine the dominant risk objective of the system.

4.4 Conclusions

A novel optimization framework based on the Parametrization-Simulation-Optimization technique has been introduced in this chapter. The suggested approach aims to improve the existing methods for developing emergency operation schedules applied to single dam-reservoir systems. The procedure combines a novel parametric operating rule, a heuristic optimization algorithm and a Monte Carlo simulation approach for conducting risk analysis. As such, the concept of risk is directly included into the optimization of flood control operations under extreme circumstances. The parametrization-simulation-optimization framework is reduced to a four dimensional problem in which the optimal operation is determined in terms of the aggregated sum of three objectives: minimize flooding risks at the upstream region, minimize flooding risk at the downstream area and minimize the risk attributed to the structural failure of the dam.

A simplified example has been used to demonstrate that changing the emergency operation of reservoirs can be an efficient non-structural risk mitigation measure. The total risk of the system has been estimated for two emergency operation procedures: (1) the emergency operation schedules in which the operation depends on the state of the reservoir, and (2) emergency operation schedules in which the overall risk determines the releases. The results showed that adopting an alternative operation strategy different than the U.S. Army Corps of Engineers deterministic operation schedules can greatly mitigate risk in a dam-reservoir system. This generic insights could be employed in the last chapter of the report in which the novel risk-based framework is applied to the study of the Barker Reservoir system in Houston, Texas.

Furthermore, the analysis of the results revealed that the optimal flood control operation of reservoirs depends on the characteristics of the dam structure, the upstream and downstream regions attributes, and the reservoir storage capacity. Although the optimal operations are strictly dependent on the particular system under study, similarities can be recognized between different systems. As such, a classification of dam-reservoir systems according to their dominant risk objective has been proposed in this chapter. In cases in which high pool levels dictate the overall risk of the system, opening operation strategies with higher outflow rates are optimal, leading to higher risk mitigation (storage dominated systems). Meanwhile, when releases exceeding downstream channel capacities dominate the total risk of the system, closing flood control strategies are preferred (release dominated).

Finally, this study marks a significant step towards improving the procedures for developing emergency flood control operations of reservoir, and introduces their efficiency to mitigate risk in dam-reservoir systems. Simultaneously, the difficulties in fully addressing the problem using a simplified example are acknowledged, and in consequence, continued investigations of this important subject are advocated. Future comparison of different real life case studies could strengthen the results herein obtained and might further reveal additional properties of the management of extreme events using the combination of probabilities and consequences. *Is the proposed framework valid for every system?*, *Is the risk of the system reduced equally for different types of systems? How does each particular characteristics of the system influence the optimal operation strategies? How can the threshold between release dominated and storage dominated systems be determined?*.

Chapter 5

Case Study: Barker Reservoir System

The proposed risk-based optimization framework has been applied in a study of the Barker Reservoir located in Buffalo Bayou Watershed, on the western edge of Harris County and the city of Houston, Texas (Fig. 5.1). Together with the Addicks Reservoir, the two structures comprise a parallel flood control reservoir system responsible for the protection of downtown Houston and the west side of Buffalo Bayou from flooding. Susceptible to Hurricanes and Tropical Storms, the Barker Reservoir system presents a unique operational dilemma requiring trade-offs between released flows and stored volumes in order to:

1. minimize flooding risks at the upstream region;
2. minimize flooding risk at the downstream area;
3. minimize structural dam failure risk

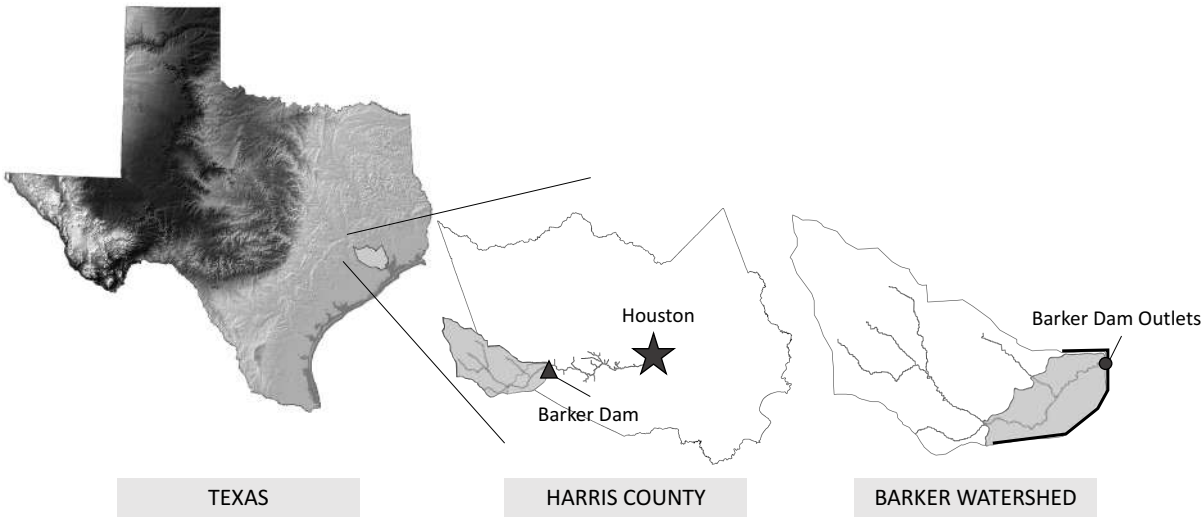

Figure 5.1: Barker Reservoir location map

After a National Cadre initiated a Potential Failure Analysis in September 2009, the Barker Reservoir was categorized as one of the six most dangerous dams in the U.S., requiring immediate engineering intervention due to the high combination of life an economic consequences and probability of failure of the structure resulted in the study. In addition to its elevated annualized probability of structural failure [156], the recent urban development in the upstream area

affected by high pool levels minimizes the storing non-damaging capacity of the system. Besides, urban encroachment in the floodplain along Buffalo Bayou has reduced the non-damaging downstream channel capacity which nowadays is one third of the original project design. This limits the possible release rates and increases the risk of having an appreciable portion of the flood storage capacity filled when a subsequent flood occurs.

The chapter is structured following the four steps contemplated in a standard risk analysis procedure. First, a description of the system is provided, where important information concerning the location, history, structure, streamflows and operational constrains are examined. Then, possible hazards, failure modes and potential economic damages are identified. Following the qualitative analysis, the quantification of the current level of risk of the system is discussed. The obtained overall risk is compared against risk estimations given optimized emergency operation schedules. The chapter ends up with a summary of the results and the discussion of future risk mitigation solutions in the Barker Reservoir system.

5.1 Barker Reservoir System Description

Addicks and Barker Reservoirs are located in the Buffalo Bayou Watershed of the San Jacinto River basin, approximately 25 kilometers west of downtown Houston. The dams were strategically constructed in parallel above the confluence of Buffalo Bayou and South Mayde Creek. Beyond this confluence, Buffalo Bayou continues east through central Houston, where it joins with White Oak Bayou, and eventually becomes the Houston Ship Channel, which flows into Galveston Bay (Fig. 5.2). Although the two reservoirs are operated as a single system, for the sake of simplicity, this project will focus exclusively on the operation and optimization of just one of the two reservoirs, the Barker Reservoir.

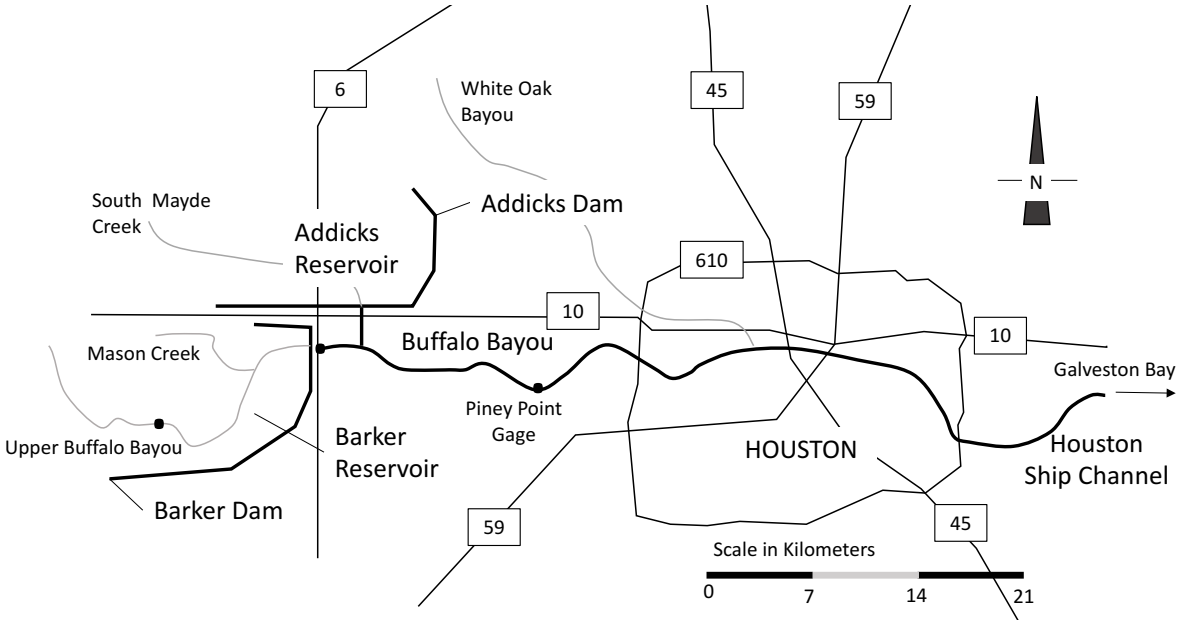

Figure 5.2: Buffalo Bayou through city of Houston

The Barker Dam-Reservoir system is comprised of three elements: the Barker Dam, the Barker Watershed located upstream of the reservoir, and the Buffalo Bayou Watershed, on the downstream side. Operated by the USACE, the reservoir has a drainage area of 337 km^2 and is supplied by about 76 km of open streams, including secondary channels and the two primary

tributaries: Upper Buffalo Bayou and Mason Creek (Fig. 5.2). When originally constructed, the dam was located 20 km west of the city limits. Nowadays, the reservoir lands are part of Houston, and substantial residential and commercial development are located upstream adjacent to the federal reservoir lands as well as along the channel below the dams and scattered throughout the Buffalo Bayou Watershed. Figure 5.3 and Fig. 5.4 display the 2011 National Land Cover Database (NLCD) maps at the upstream and downstream regions from Barker Reservoir [157]. The figures show the elevated urbanized areas both at the reservoir area and along Buffalo Bayou.

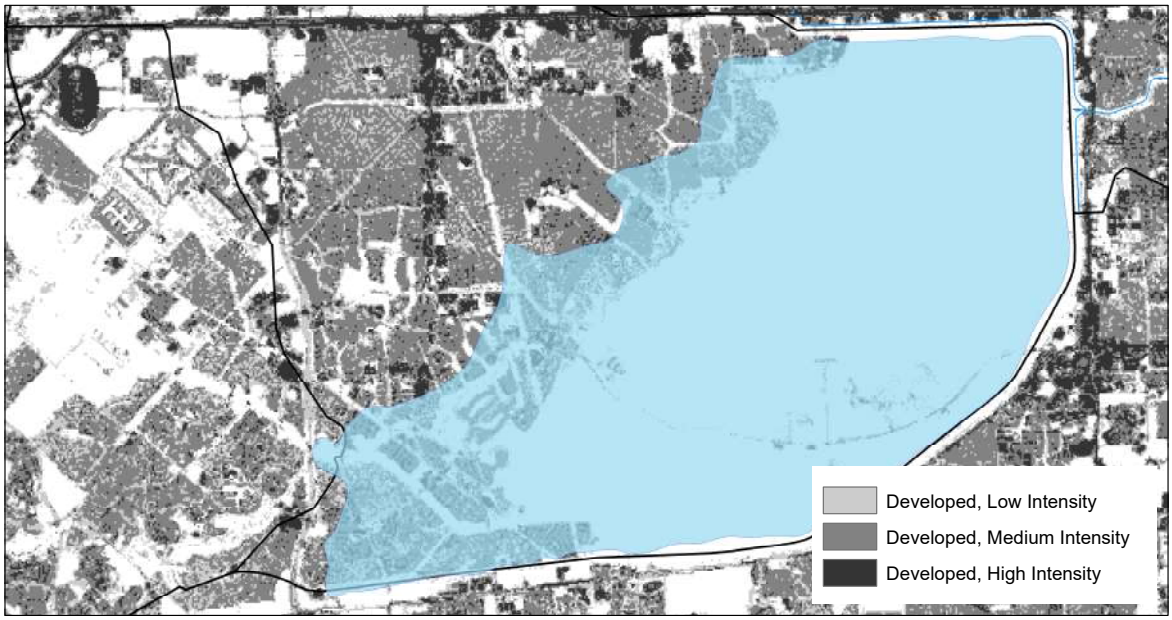

Figure 5.3: NLCD 2011 land cover at Barker Watershed [157]

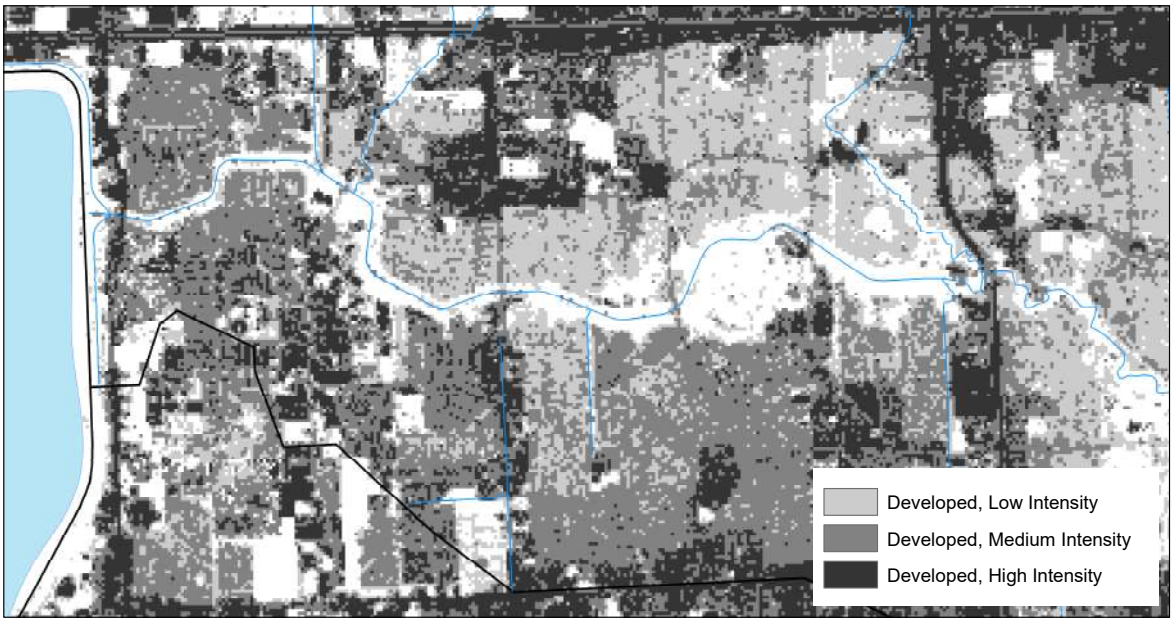

Figure 5.4: NLCD 2011 land cover at Buffalo Bayou Watershed [157]

5.1.1 Structural Characteristics

The earthen dam structure consists of an unzoned, random fill embankment constructed across the valley of Buffalo Bayou, on the south side of IH-10, and west of SH 6 (Fig. 5.2). The 22 kilometers long earth embankment rises 13 m above the original stream bed with a crest level ranging from 33.5 to 34.5 m NAVD88. The outlet works have five 2.7 m by 2.15 m concrete conduits controlled by sluice gates. Originally, only one of the five outlet conduits was gated, with the other conduits being uncontrolled. Two gates were added in 1948, and gates were installed in the remaining uncontrolled conduits in 1963. Additionally, both ends of the dam are armored with roller compacted concrete that serve as uncontrolled auxiliary spillways in case of emergency operations. Existing ground at both ends is at elevation 31.7 m NAVD88. Meanwhile, the spillway crest at the North and South ends are at elevation 32.16 m NAVD88 and 32.52 m NAVD88 respectively. Figure 5.5 sketches typical cross sections of the structure.

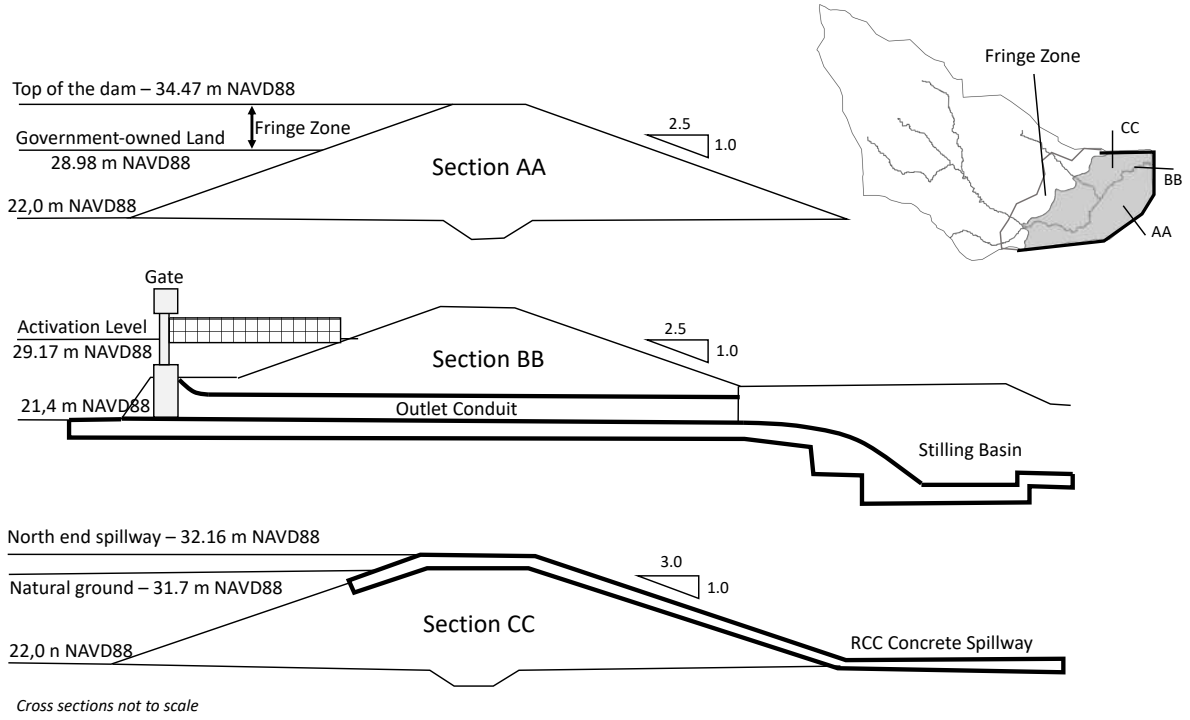

Figure 5.5: Representative cross sections Barker Dam: (AA) Barker Dam typical cross section, (BB) Barker Dam outlets cross section, (CC) Barker Dam spillway cross section

Since the majority of the originally proposed channel improvements on Buffalo Bayou were not implemented, the downstream channel capacity is much less than envisioned when the reservoirs were designed and constructed. Commercial and residential development along Buffalo Bayou has also constrained its non damaging rates that have been significantly reduced relative to the original project design. Furthermore, the changes in the dam's operation motivated by the installation of gates in all outlet structures led to significant structural problems. The embankment material which was considered suited for short time detention, was not adequate for the prolonged ponding in the reservoirs. For instance, several subsequent floods in the 1970's caused seepage through and under the dam embankments [158].

The storage versus elevation curve for the reservoir is depicted in Fig. 5.6a. The curve has been extended to 36 m NAVD88 due to computational issues regarding the future calculation of risk. However, the maximum storage capacity is set by the natural ground at the end of

the dam which is 31.7 m NAVD88. At that elevation, the maximum release rate through the outlet works is 250 m^3/s. That release rate is increased until the elevation of 33.2 m NAVD88 above which the release rate is maintained at 266.5 m^3/s due to possible problems at the outlet conduits. The outlet works rating curve for the reservoir is shown in Fig. 5.6b. It can be inferred from Fig. 5.6a that flood damages would occur within the reservoir area before reaching the natural grounds. Other significant elevations used as hydrological design criteria are those that would result from the Standard Project Flood (SPF) equivalent to a 1.000 year return period event [159] and the Probable Maximum Flood (PMF) which reaches an elevation of 32.9 m NAVD88 [156]. The values of both design events have been updated in the "Statistical Analysis of Reservoir Pool Elevations" report carried out by the USACE in 2008 [160], and the 2013 "Addicks and Barker Dam Safety Modification Report" [156].

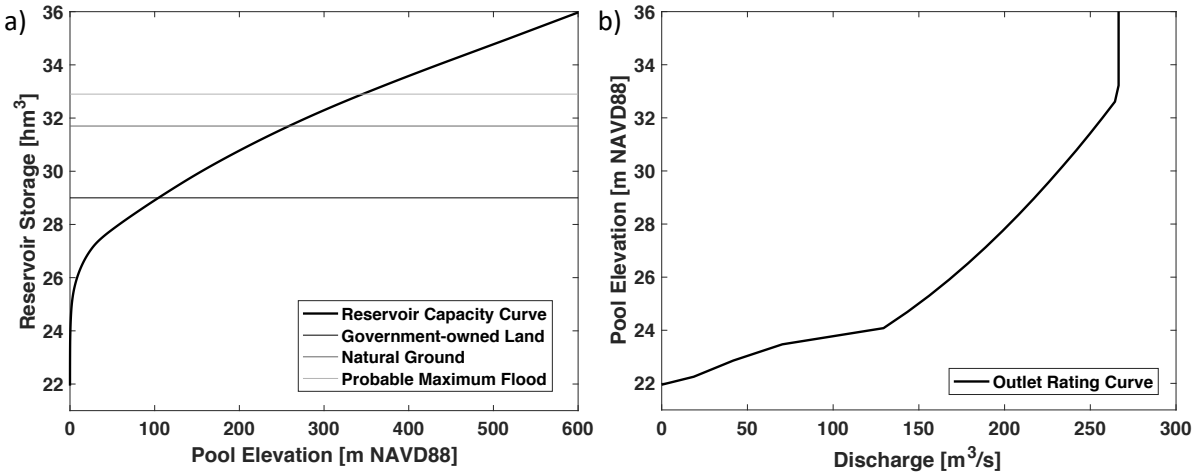

Figure 5.6: (a) Barker Reservoir Capacity Curve, (b) Barker Reservoir rating curve

5.1.2 Reservoir Pool Elevation and Operating Rules

Under normal conditions without precipitation, with negligible ponding in the reservoirs, gates are set with small openings to pass the environmental low flows. When rains occur or are expected to produce significant runoff, the gates are closed following the "Normal Flood Control Operations" contemplated in the 2012 *Water Control Manual* [158]. The gates remain closed until local flows at the control gaging station at Piney Point Road peak and then recede to a level such that reservoir releases can be made without the risk of contributing to flows at the gage exceeding 56.6 m^3/s. The controlled storage capacity is set by the elevation of the natural ground at the end of the dams. Before even reaching the auxiliary spillways, if the water surface rises above 31.7 m NAVD88, uncontrolled discharges around the ends of the dam will occur. These uncontrolled discharges compromise the safety of the structure and are to be avoided. Furthermore, the upper limit of government-owned land at 29 m NAVD88 represents the key elevation above which the residential and commercial properties are susceptible to flooding.

In cases in which the reservoir pool equals or exceeds 29.2 m NAVD88, the rate of rise (RoR) of pool levels and the storage state determine the reservoir releases. The emergency operation schedules are then activated. The downstream conditions at Piney Point are no longer the main constraint and the operations aim at guaranteeing the safety of the structure by avoiding uncontrolled spills around the edge of the dam and over the auxiliary spillways. Releases through the outlet works are made in accordance with the emergency operation curves shown in Fig. 5.7. The curves were constructed following the standard procedures from the USACE explained

in Chapter 2.2. The graph is read as follows: if the pool elevation monitoring at the reservoir indicates that the water surface level is, for instance, at 30 m NAVD88 with a rate of rise of 0.095 m/h, the conduits are to be opened to discharge 125 m^3/s. The gates should remain at the maximum opening attained from the emergency regulation schedules until reservoir levels fall below the government-owned land limits.

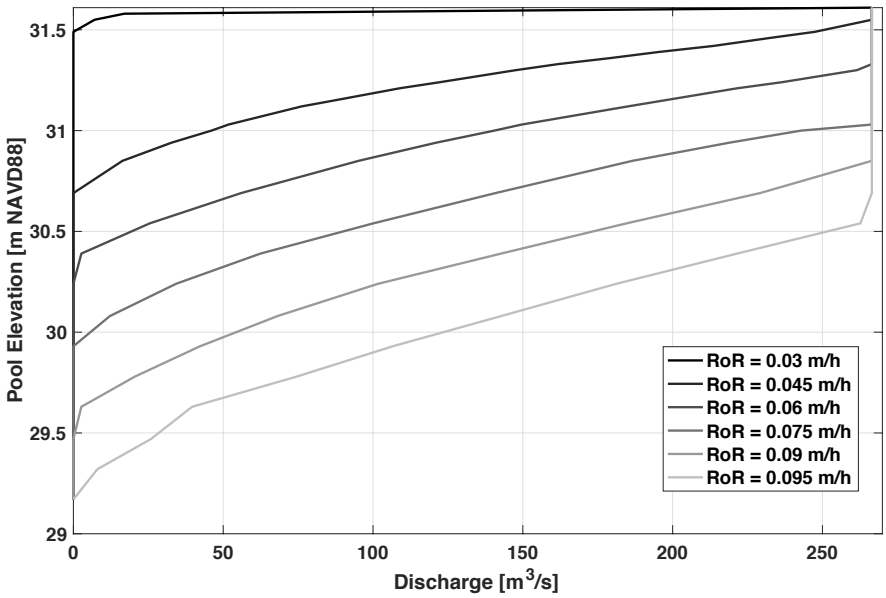

Figure 5.7: Emergency operation schedule Barker Reservoir

The reader should note that an original non-damaging downstream channel capacity of 170 m^3/s was reduced during the 1960s to 56.6 m^3/s due to encroachment by urban development. This relative small discharge rate has given rise to a phenomenon referred as "ratcheting" effect. As the region experiences a wet season over a long period, the reservoir pool level slowly increases even though no single large event may occur. The probability of reaching high pool levels that could jeopardize the safety of the structure raises and accordingly the probability of failure of the structure. Furthermore, as ponded water surfaces in the reservoirs increase, upstream flooding within the fringe areas start causing significant economic damages and traffic mobility problems. This is why, regulation procedures aim at emptying the reservoir as quickly as possible once the storms have passed until reservoir levels fall below the government-owned land limits. After that, the emergency flood control schedule is deactivated and releases at higher rates than the maximum allowable flow rate of 56.6 m^3/s are not conducted.

5.1.3 Hurricane Harvey

After making landfall near Corpus Christi on Friday August 25^{th}, 2017, Category 4 Hurricane Harvey continued to move inland hovering over southeastern Texas and bringing calamitous rainfall and historical life-threatening flooding to Houston and surrounding areas for days. Up to now, the total damages caused by Harvey still uncertain. Back in September Texas Governor Greg Abbott estimated damage from Hurricane Harvey varying between $150 billion and $180 billion, calling it more costly than epic Hurricanes Katrina or Sandy, which devastated New Orleans in 2005 and New York City in 2012 [161]. Another estimate released in 2017 fall evaluated the damages caused by Hurricane Harvey to be upward of $200 billion in southeastern Texas [162]. However, the latest NOAA damage estimate from Harvey is a bit more conservative ranging the damages to $ 125 billion [4].

In addition to the billions in economic damages, Harvey has directly or indirectly taken the lives of at least 88 Texans according to the Department of State Heath Services [163]. A post-event analysis carried out by Jonkman et. al [164] pointed out that most of the 70 studied fatalities occurred outside the designated 100 and 500 year flood zones in the greater Houston area. A total of 36 of those victims died within Harris County border [165] being 7 of them reported at the Addicks ad Barker Reservoir systems watersheds.

Due to Harvey's record-smashing rainfall, substantial flooding occurred both upstream and downstream of the Barker Reservoir. The unprecedented magnitude of the upstream inflows led to record pool elevations raising all the emergency operational alarm bells. For the first time in the reservoir service life, the USACE was forced to open the gates in order to avoid uncontrolled releases and dam failure. Figure 5.8 illustrates the inflow hydrograph recorded at the reservoir during the Hurricane as well as the water surface elevation time series during the event. On August 25^{th}, following the "Normal Flood Control Regulation" stated in the Water Control Manual [158], the USACE had closed the gates prior to a predicted rainfall event.

In the following days, between August 25^{th} and 28^{th}, approximately 457 mm of rain fell in the contributing areas upstream of the Barker Reservoir [166]. Water rose inside the reservoir, exceeding the record levels recorded during the Tax Day Flood (2016) and reaching Government-Owned-Land levels around midnight on August 27^{th}. At that moment, the Army Corps of Engineers announced that it would begin controlled releases in the early morning hours on August 28^{th} at 'higher-than-normal' rates to prevent uncontrolled and even catastrophic releases from the dams. It is inferred from Fig. 5.9 that Barker releases peaked on August 29^{th} at 141.0 m^3/s tripling the non-damaging channel capacity on Buffalo Bayou. The reader should note that by that time, areas directly downstream of the dams were already flooded with water levels overflowing the banks and reaching 19.5 m NAVD88 at the operations control point Piney Point. Despite the controlled releases, the reservoirs continued to rise until August 30^{th}, peaking at 30.95 m NAVD88. A cross section of the reservoir with the most important data concerning the system response, system loading and consequences is depicted in Fig. 5.10.

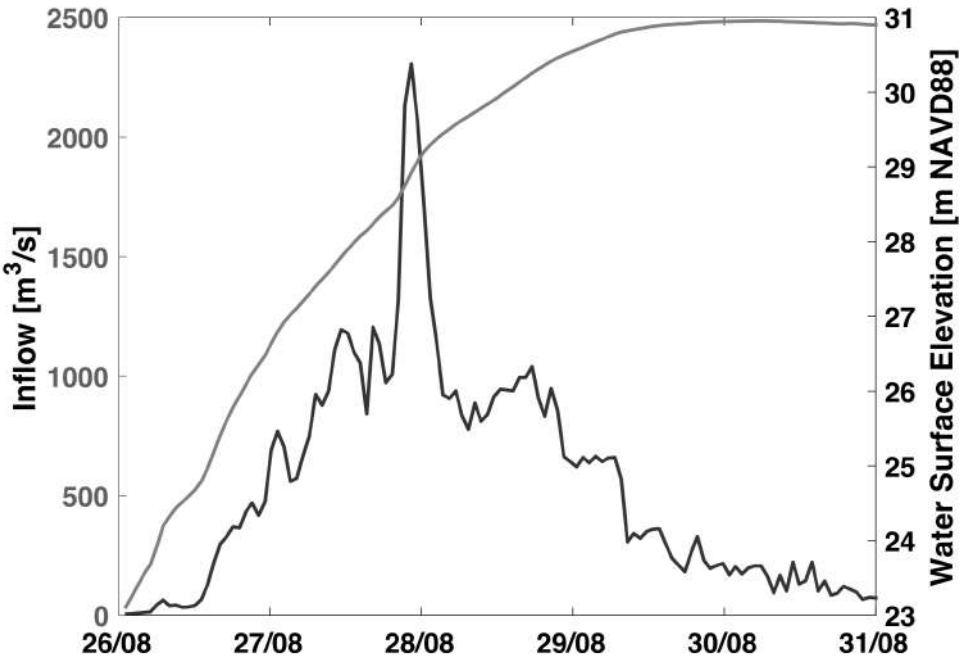

Figure 5.8: Inflow and water surface elevation time series of Barker Reservoir during Hurricane Harvey (USACE ResSIM)

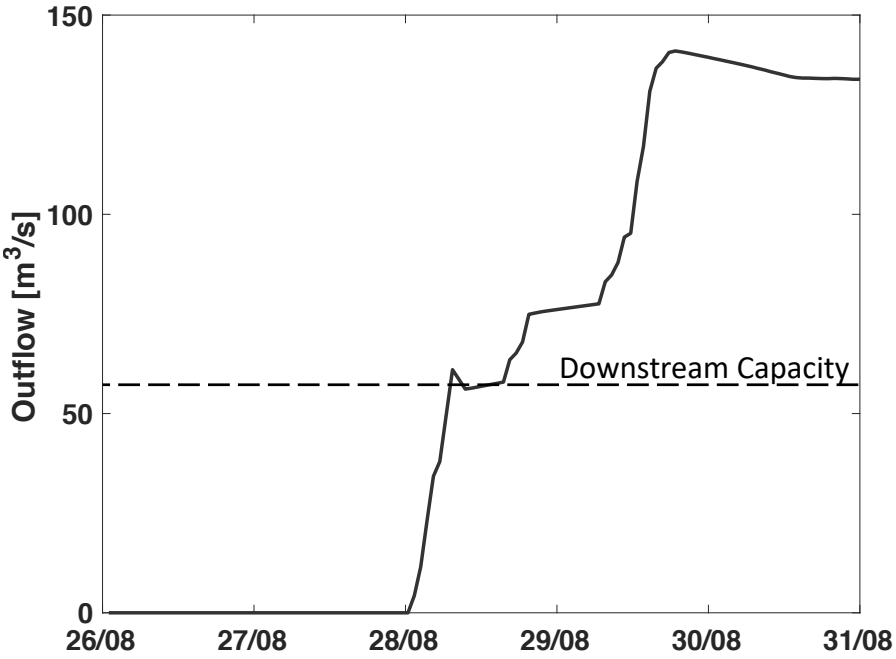

Figure 5.9: Outflow time series of Barker Reservoir during Hurricane Harvey (USACE ResSIM)

5.2 Identification of the Risks

Since the objective of this study is to optimize the operations during episodes of extreme events like hurricanes and tropical storms, the risk analysis carried out in this chapter will only focus on hazards, consequences and failure modes related to hydrological loading scenarios. To address the identification of the risks posed by the construction of the dam to the reservoir area and the downstream floodplains, the qualitative study has been divided into three subsections:

- **Hazard Identification:** study of yearly maximum inflows and initial water levels.
- **Failure Modes Identification:** study of the most probable failure modes.
- **Receptor Identification:** study of potential structural damages.

The analysis of consequences has been limited to structural damages to residential properties. Economic damages to other building types or potential life loss are out of the scope of this study. Moreover, due to Expert Judgment considerations, the failure modes contemplated within the simulation approach explained in Chapter 3 do not apply for the Barker Reservoir Case. First, it is believed that the reservoir levels will never reach the top of the structure due to the high rates of uncontrolled releases over the emergency spillways as well as around the natural ends of the dam. Second, it is considered that enough measures have been taken to provide protection of the embankment against piping. The response of the structure against the flood scenarios has been circumvented by the use of the fragility curves held by the USACE. These curves were obtained from the Potential Failure Modes Analysis conducted in 2009 and 2010 [156].

5.2.1 Hazard Identification

Precipitation in the Barker Reservoir area is well distributed throughout the year. Summer precipitation typically results from intense, short, isolated convective cells, while winter and

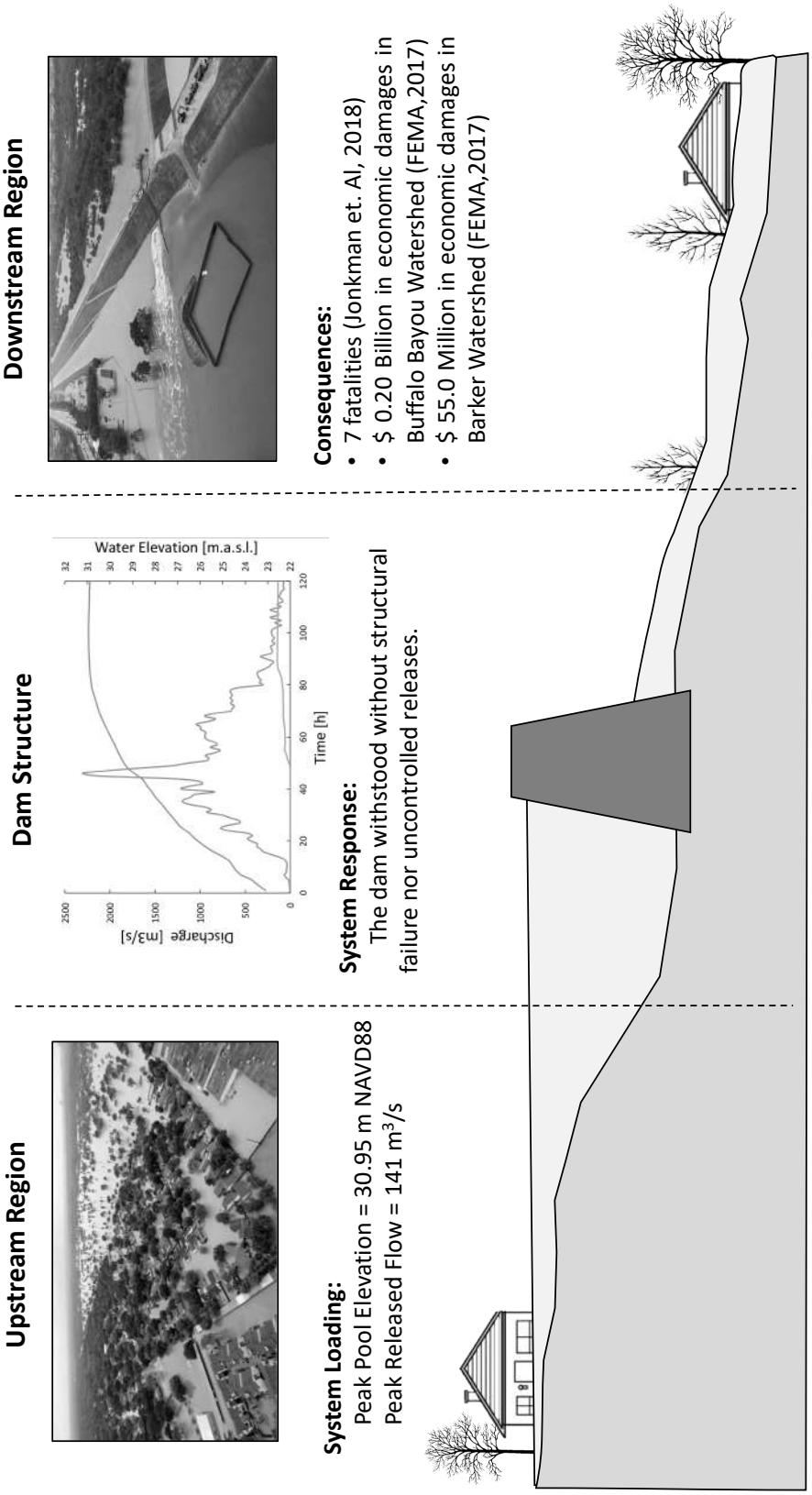

Figure 5.10: Graphical representation of the Barker Reservoir performance during Hurricane Harvey including the most relevant data concerning the system loading, system response and consequences

spring precipitation is generally produced by more widespread frontal events. The area is also affected by torrential rainfall associated with hurricanes and other tropical disturbances like Hurricane Harvey (2017). Furthermore, in this study, it is recognized that an extreme flood event does not only refer to a large magnitude inflow. Indeed, a flood (not necessarily of a large magnitude) occurring before the entire flood control capacity has been emptied may comprise serviceability or ultimate limit state failure. Consequently, the hazard analysis carried out in this study consists of:

1. Statistical analysis of reservoir stages prior to each yearly maximum flood wave
2. Statistical analysis of the maximum yearly inflows arriving to the reservoir

Reservoir daily mean stage data from 1973 to 2018 at the USGS 08072500 gage station located in the reservoir has been collected in order to develop an empirical cumulative distribution of the reservoir stages. The study has been conducted according to the methodology proposed by Carvajal et. al [141]. The reader may refer to Appendix E.2 for further details concerning the empirical cumulative density function of initial reservoir pool levels as well as the empirical distribution plot of the annual maximum reservoir levels.

Moreover, the gage station USGS 08072300 situated upstream from the reservoir with mean daily discharge data from 1977 to 2018 and maximum daily data from 2008 to 2018 has been used as input for the generation of synthetic series of inflow hydrographs entering the reservoir. Instantaneous peak flow data and hydrograph volumes were obtained from the analysis of daily mean series. First, the maximum daily annual flow was converted to maximum annual peak following the indications from Appendix B. Regression analysis between maximum daily and mean daily data at the gage station has been developed. A peak flow coefficient of $k = 1.37$ showed the best fit with the available instantaneous data. Second, the local minimum method for baseflow separation was utilized for the estimation of the hydrograph volume. As the study begins with the annual maximum discharge frequency curve, the volumes linked to these peaks were identified and assumed to be the largest of the year in accordance with the synthetic hydrograph generation methodology developed by Mediero et. al [114].

Flood Frequency Distribution

In order to proceed with the stochastic generation of inflow hydrographs, first the marginal distributions from the flood peaks and the statistical dependence between peaks and volumes was determined. As such, the recommendations of the *USGS Bulletin 17 C* for flood frequency analysis [167] have been followed. The outliers of the observed data series have been identified, the corresponding statistical tests have been conducted and the annual maximum analysis has been carried out for the hydrograph volumes and the peak flows.

No autocorrelation was observed in the correllogram from the data series. In addition, both the run test and the Mann-Kendal test resulted negative, meaning that no trends were found and that the studied data is random. Figure 5.11 and Fig. 5.12 display the results from the annual maximum marginal distribution of peak flows and volumes. The analysis was conducted considering the observations recorded during Hurricane Harvey (2017) as historical.

Figure 5.11 and Fig. 5.12 show the curves representing all the distributions implemented in the model. The parameters of each distribution function were estimated using the L-Mom adjustments proposed by Hosking and Wallis [168]. The observed data is depicted by the blue diamonds in accordance with the empirical frequency formulation presented in Appendix B. The results from the hydrograph volumes analysis are consistent with the ones from the peak flows, being the Generalized Logistic function the one giving the best fit.

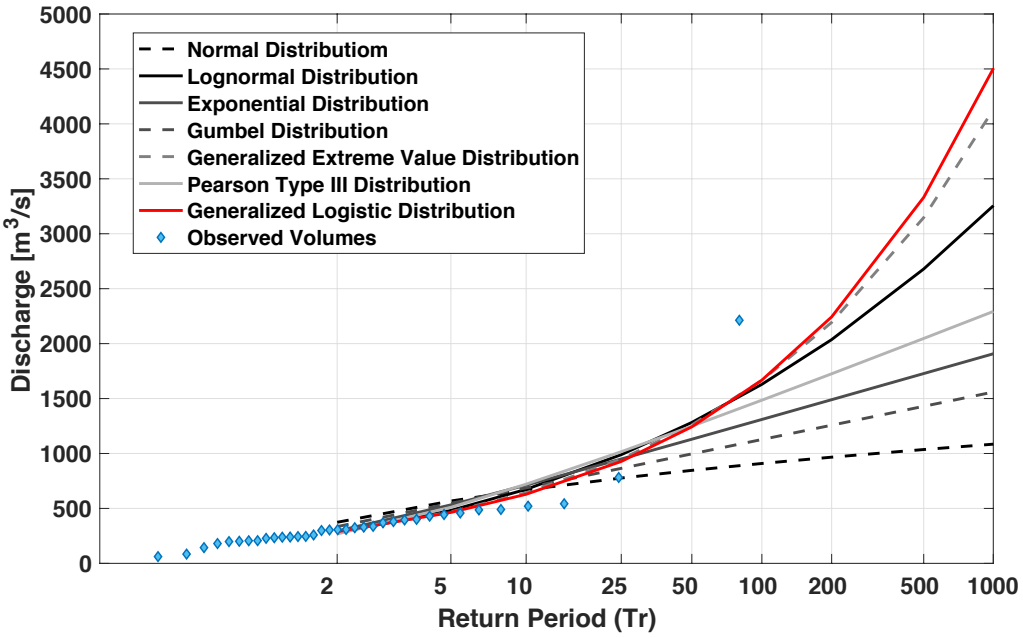

Figure 5.11: Maximum Annual Peak Flow Analysis. The best fit is represented by the Generalized Logistic distribution function with location parameter $u = 288.1060$, scale parameter $\alpha = 91.7061$ and shape parameter $k = -0.4434$

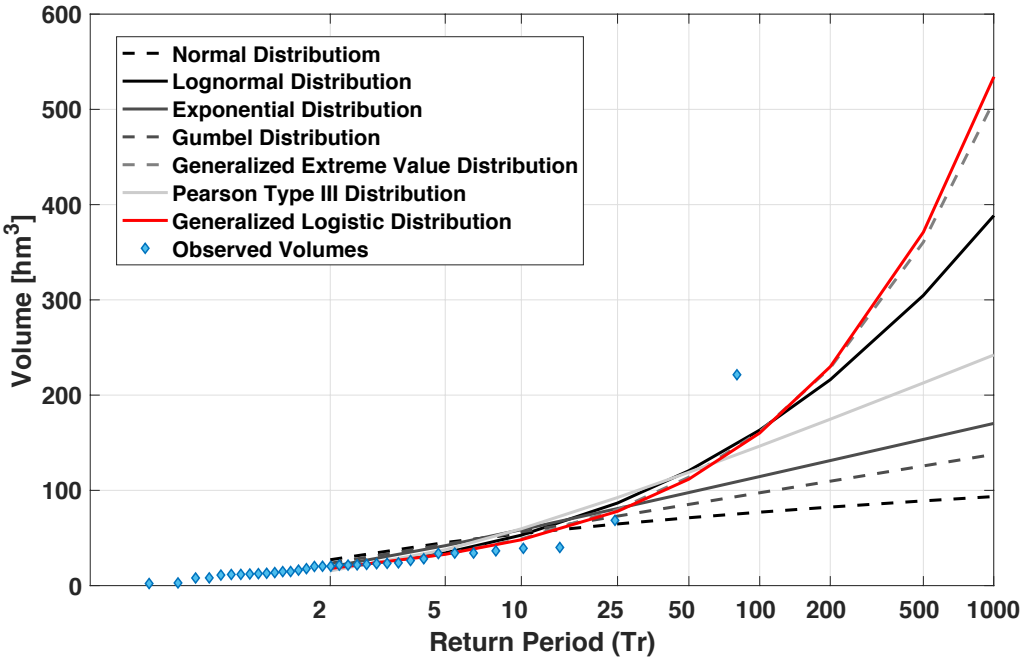

Figure 5.12: Maximum Annual Inflow Volume Analysis. The best fit is represented by the Generalized Logistic distribution function with location parameter $u = 17.9946$, scale parameter $\alpha = 7.2612$ and shape parameter $k = -0.5288$

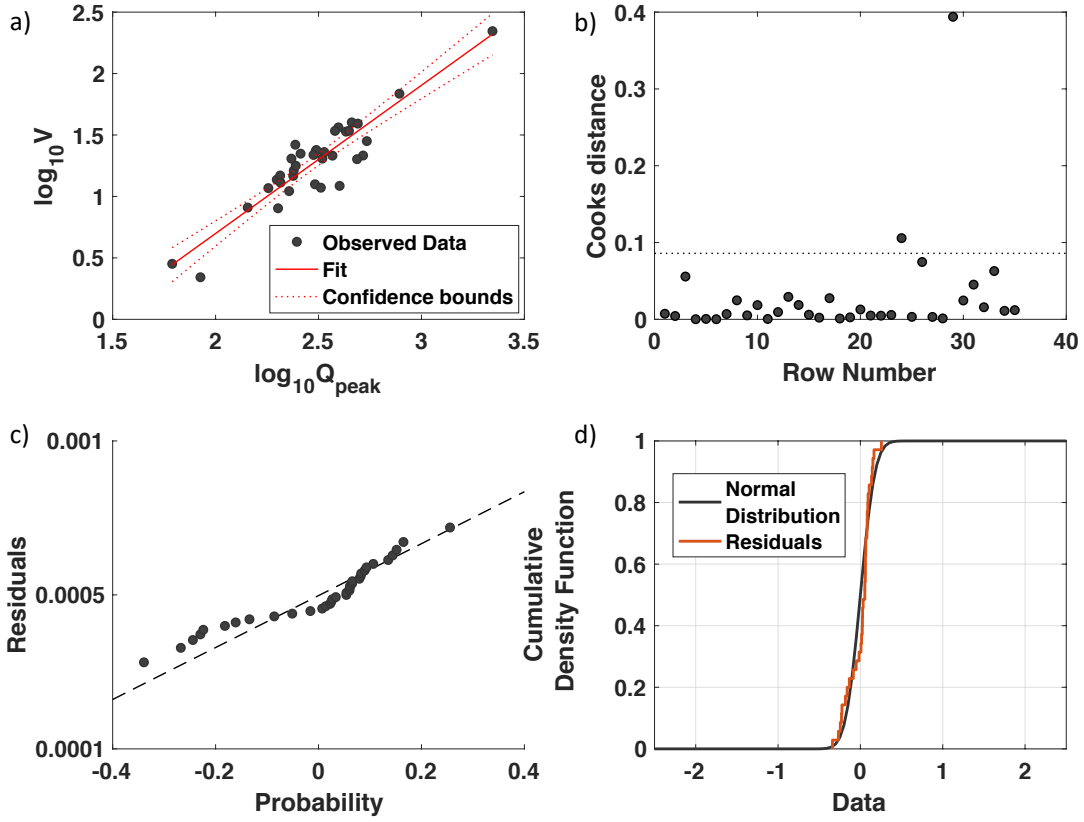

Figure 5.13: Linear regression analysis between peak flows and hydrograph volumes. (a) Relationship between observed volumes and observed peaks; (b) Cook's distance test for outliers detection; (c) (d) Normality tests of the residuals

Statistical Dependence Between Peak Flows and Volumes

A linear regression analysis was conducted to develop an equation for predicting hydrograph volumes from stochastically generated peak inflows. Logarithmic transformation of all variables was found to provide the best linear relation:

$$log_{10}V = a \cdot log_{10}Q + b = 1.2056 \cdot log_{10}Q - 1.7123 \tag{5.1}$$

where V is the predicted mean hydrograph volume and Q is the peak inflow at each simulation. The regression could have been improved by introducing data from the neighbor gage stations. However, this study has been limited to local data analysis. The correlation coefficient of Eq. (5.1) is 0.839, and the standard error from the predicted logarithmic is 0.1401. Taking the logarithms out, Eq. (5.1) yields:

$$V = 10^{-1.7123} \cdot Q^{1.2056} \tag{5.2}$$

Figure 5.13 plots the results from the linear regression analysis. The Cook's distance test for the estimation of regression outliers showed that only one peak-volume pair behaves differently as the statistical dependence achieved using the regression analysis. Furthermore, normality tests of the residuals show that the conditional distribution function of the volume with respect to the peak flow can be defined by a log-normal distribution [114] [115]. Its average is determined from the regression equation, and its standard deviation is equal to the standard deviation of the regression's adjustment.

5.2.2 Failure Modes Identification

After the National Cadre initiated a Potential Failure Mode Analysis in September 2009, the structure was reclassified as DSAC I (Urgent and Compelling) and 23 PFMs were identified for Barker Dam. The reader may refer to the *Addicks and Barker Dam Safety Modification Report Phase I* developed in 2013 by the U.S. Army Corps of Engineers from the Galveston District [156] for detailed explanations regarding the performed failure mode analysis. In this study, the five most significant failure modes have been considered.

- PMF 1 - "Seepage flow along or beneath the outlet works structure due to voids or low stress areas leads to head-cut then backward erosion piping beneath the outlet works".
- PFM 7 – "Seepage and piping in the foundation at the old Buffalo Bayou channel beneath the existing cutoff wall and exiting at the end of the stilling basin".
- PFM 8 – "Seepage and piping at the end of the cutoff trench at Noble Road".
- PFM 21 – "'Hydraulic pressure in the conduit exceeds pressure outside the conduit which leads to seepage through conduits joints and erosion along conduits".
- PFM 23 – "Instability of the outlet works parabolic chute slab and stilling basin retaining walls due to uplift caused by excessive seepage and/or tailwater".

The fragility curves are shown in Fig.5.14a and Appendix E.5. In addition, Fig. 5.14b displays the maximum and minimum bounds of the total failure probability in scenarios resulting from a common cause. According to the Theorem of the unequivocal limits, the total probability of failure lies within the probability of the most likely failure mode and the probability obtained assuming that all failure are independent:

$$max(p_j) \leq P_f \leq 1 - \prod_{j=1}^{k}(1 - p_j) \tag{5.3}$$

where p_j is the unadjusted failure probability for the potential failure mode j, and P_f is the total probability of failure of the structure. Within this study, the simplified approach proposed by Hill et. al [146] for adjusting the system response probabilities for each potential failure mode has been applied (Section 3.3.3).

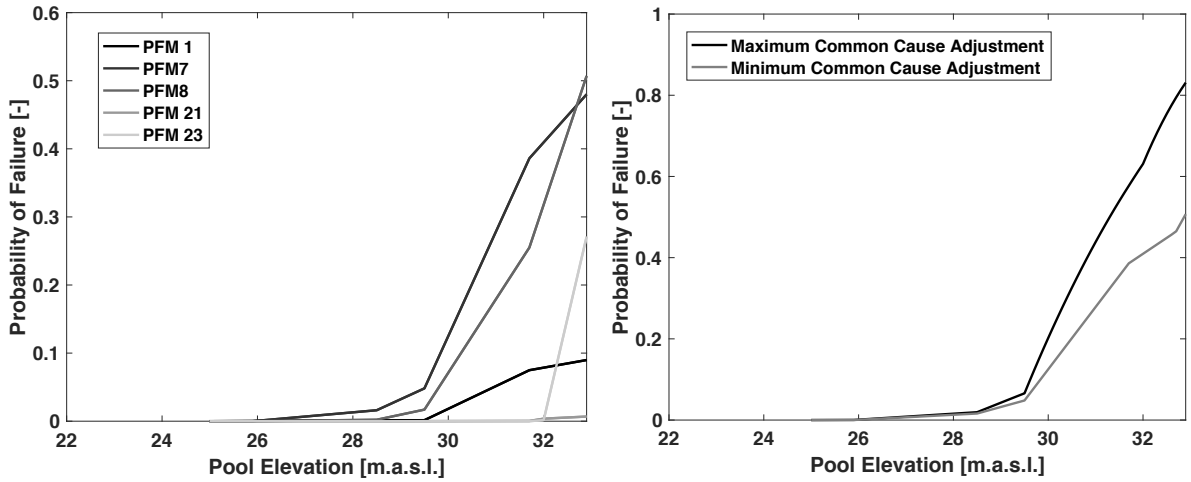

Figure 5.14: (a) Potential Failure Modes Barker Dam [156] (b) Adjusted system response curve

5.2.3 Receptor Identification

The last component of the quantitative analysis of risk comprises the identification of potential damages. As previously stated, the scope of this study is limited to the estimation of consequences related to structural damages in residential properties. Potential economic damages to industrial and commercial buildings have been disregarded due to its minor weight within the Barker Reservoir and Buffalo Bayou areas. According to the statistical analysis carried out at both watersheds and presented in Appendix E.6 and Appendix E.7, residential buildings constitute approximately the 95 % of the potentially affected parcels. To conduct the risk analysis of the Barker Reservoir system, three consequence curves have been developed:

- Consequence curve relating the structural damages upstream of the reservoir and reservoir pool levels (Fig.5.15a)
- Consequence curve relating the structural damages downstream of the reservoir and peak outflows (Fig.5.15b)
- Consequence curve relating the structural damages downstream of the reservoir and breach scenarios (Fig.5.15c)

Since the construction of the dam, extensive residential development has occurred in the fringe area affected by maximum pool levels. The upper limit of governmental-owned land at 28.98 m NAVD88 represents the elevation above which residential structures are susceptible to flooding. Starting at this level, an event-based damage curve has been elaborated for the estimation of upstream damages. Based on total parcel values [30] and depth-damages curves from the 2017 report on "Global Flood Depth-Damage Functions" developed by the European Joint Research Center [129], the residential structural damage costs have been computed for four different reservoir levels: (a) 100 yr. floodplain elevation, (b) elevation attained inside the reservoir during Hurricane Harvey, (c) North end spillway elevation, and (d) dam crest elevation.

The damage curves downstream of the reservoir have been computed combining HEC-Ras 1D steady state hydraulic modeling, predefined depth-damage curves for residential buildings [129], and Geographic Information Systems for terrain data processing. A total of six flood scenarios with different maximum peak discharges have been considered. Important features concerning downstream riverine protections have been inferred from the analysis. As shown in Fig. 5.15b, at 170 $m3/s$ there is a sudden increase of the potential damages. The value coincides with the original non-damaging downstream channel capacity. Releases above this value are to be avoided to keep downstream risk at acceptable levels.

Finally, the damages curves provided by the USACE concerning dam collapse scenarios have been included in the estimations [156]. The numbers herein represented include costs related to the reconstruction of the dam as well as the annual project benefit lost. The curves were calibrated using Hurricane Harvey damages estimates from the Harris County Flood Control District (HCFCD), the U.S. Army Corps of Engineers and Federal Emergency Management Agency (FEMA). The reader may refer to Appendix E.8 for more information regarding the damages curves and their calibration.

5.3 Risk Estimation

The risk posed by the Barker Dam to the reservoir area and the downstream floodplain has been estimated applying the procedure developed in Chapter 3. Based on a Monte Carlo simulation framework, the hydrologic event tree presented in Fig. 5.16 has been used to conduct the risk

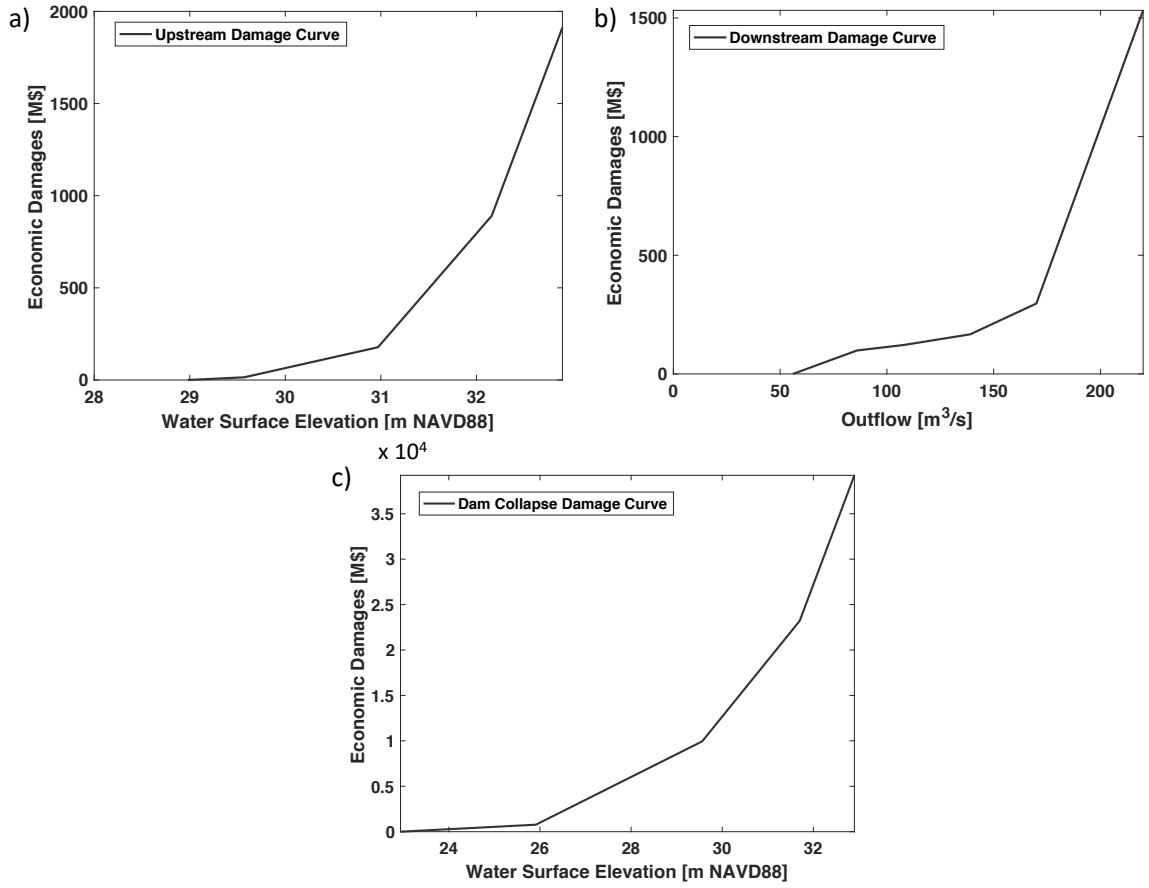

Figure 5.15: Barker Reservoir system damage curves: (a) upstream damages as a function of reservoir water levels, (b) downstream damage as a function of peak releases, (c) dam breach damage curve as a function of upstream reservoir levels

analysis of the system. In this study, the risk has been quantified using the total expected annual damages, R_T, the Annualized Failure Probability (AFP) and the Frequency-Damage curve. Furthermore, for validation purposes, the model has been calibrated using the observed storage, volume and peak flow data.

The total risk of the system is assessed as the summation of of serviceability limit state risk (SLS) and ultimate limit state risk (ULS). In the case of the Barker Reservoir system, the serviceability limit state risk includes expected annual damages at the upstream and downstream areas during the normal and emergency operation of the dam: damages caused by water levels above the governmental-owned land at a elevation of 28.98 m NAVD88, and reservoir releases exceeding the downstream channel capacity of 56.6 m^3/s; whereas the ultimate limit state refers to the probability and consequences of the structural failure of the dam calculated through the system response curves and the damage curves provided by the U.S. Army Corps of Engineers.

Level 1 contains a continuous branch type representing the peak reservoir stage, which values can be related to their annual exceedance probability. Level 2 is a state function branch included to compute the upstream flooding depths from the peak reservoir pool level. Level 3 contains the structural failure branches for the system response curves and the non-structural failure branch. Potential failure modes 1, 7, 8, 21 and 23 are considered to be similar enough that the same breach characteristics and location have been used. Level 4 contains the peak discharges and peak breakage flows which relation with the branches on the left is based on conditional

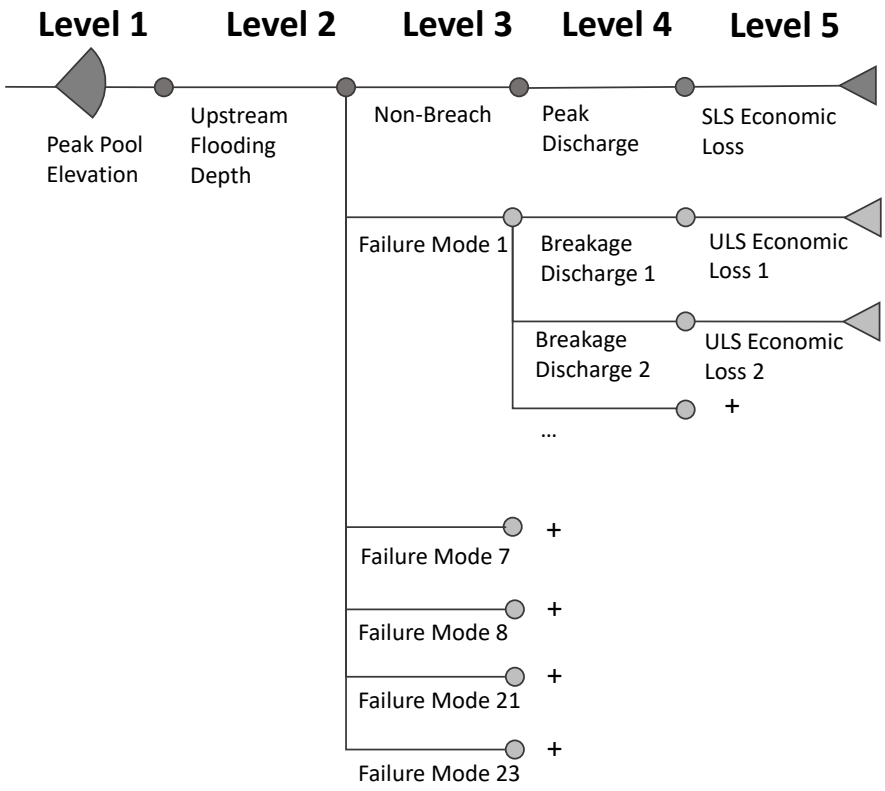

Figure 5.16: Event tree showing the risk assessment of the Barker Dam-Reservoir system

probability estimates. Finally, the estimated values of economic consequences for combinations of pool level intervals, peak outflows, peak breakage flows and failure modes are assigned to the consequence branches represented in Level 5.

The effects the dam operation has on the estimation of risk are included in Level 1 and Level 4 of the event tree. First, the input for the event tree is not directly related to the external hydrological loading, but to the attained water level annual exceedance probabilities. This way, the interplay between the external loading conditions, the characteristics of the reservoir, the attributes of the structure and the operation are considered. Second, the released flows are expressed through a quantile-quantile relationship between reservoir levels and reservoir releases obtained by simulation. This statistical relationship represents the most likely outflow peak for each water level interval. Additionally, the conditional probability between reservoir levels and breakage peakflows is implemented applying the results from the multiple linear regression analysis carried out by Fröhlich [128].

The baseline total Annual Probability of Failure (APF) was estimated to be 0.013. Under the USACE tolerable risk guidelines, a total Annual Probability of Failure (APF) greater than 0.0001 per yr. is considered unacceptable. The result shows disagreement with the estimations carried out by the USACE [156]. Back in 2013, the "Addicks and Barker Dam Safety Modification Report" concluded that the APF for the Barker Dam was 0.00443. The differences may be motivated by the fact that the statistical analyses of streamflows have changed after the flood events from the last years: the Tax Day storm (2016) and Hurricane Harvey (2017). The peak flows, hydrograph volumes, and reservoir pool levels recorded at both episodes underscored a new reality for the Barker Watershed.

5.3.1 Risk Model Calibration

In order to simulate all the possible scenarios leading to the failure of the system, 10.000 flood events, assumed as being representative of the external loads affecting the system, have been stochastically generated and routed through the reservoir according to the emergency operation schedules shown in Fig. 5.7. As stated in Chapter 3, the synthetic hydrograph generation always follows the same scheme [8]:

1. Generation of a set of synthetic peak flows arriving to the reservoir in accordance with the marginal probability density function shown in Fig. 5.11.
2. Generation of a hydrograph volume value for each synthetic peak flow relying on the linear regression analysis displayed in Fig. 5.13.
3. Generation of a hydrograph shape for each synthetic pair of peak and volume rescaling patterned and design hydrographs.

To validate the results from the model, first, the ensemble of inflow hydrographs must show fitting behavior with the statistical properties of the observed maximum yearly data. Fig. 5.17 compares the generated values of peak flows and hydrograph volumes to test their capability of preserving the statistical properties of the Barker Watershed. Both variables retain the statistics fairly well following the frequency curve up to the return period of 1000 yr., but, for higher return periods the synthetic volumes are smaller than the theoretical distribution.

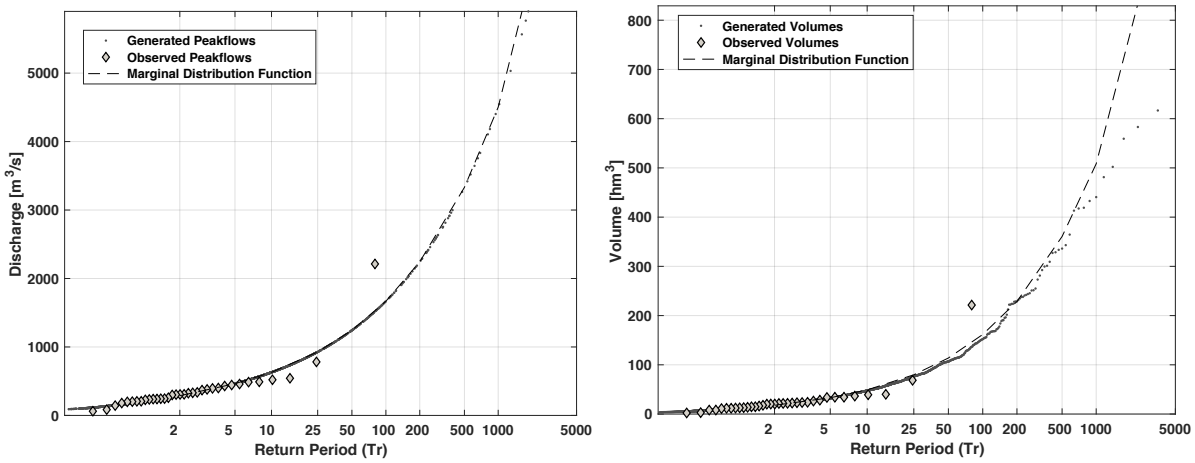

Figure 5.17: Plot showing the capability of the simulated values of preserving the statistical properties of the observed data: (a) peak discharges (b) volumes

Additionally, Fig. 5.18 ascertained that the characteristic hydrograph shapes as well as the reservoir flood control operation model throughly keep the empirical annual maximum reservoir level frequency curve. The simulated values show good fit in the intermediate part of the curve, however, the accuracy is reduced at the low and high frequency tails. First, since the aim of this project is to optimize emergency flood control operations, no attention has been directed towards higher tail events. Characteristic shapes of hydrographs corresponding to lower return periods could improve the adequacy of the model.

In the upper tail of the curve, differences with the USACE estimates are observed. This is attributed to the change in the streamflow statistics motivated by recent volume and peak flow values. This has an influence on the final results being larger magnitudes of reservoir storage

more frequent than anticipated by the risk analysis studies carried out by the USACE is 2013. Simultaneously, since only 35 years of recorded data are available, the difficulty of making a good estimate of low frequency inflow hydrographs is acknowledged. Other procedures such as paleoflood studies or regional data analysis could help improve the estimates of theoretical distribution functions. Furthermore, expert judgment might also be required for the correct interpretation of Hurricane Harvey historical values.

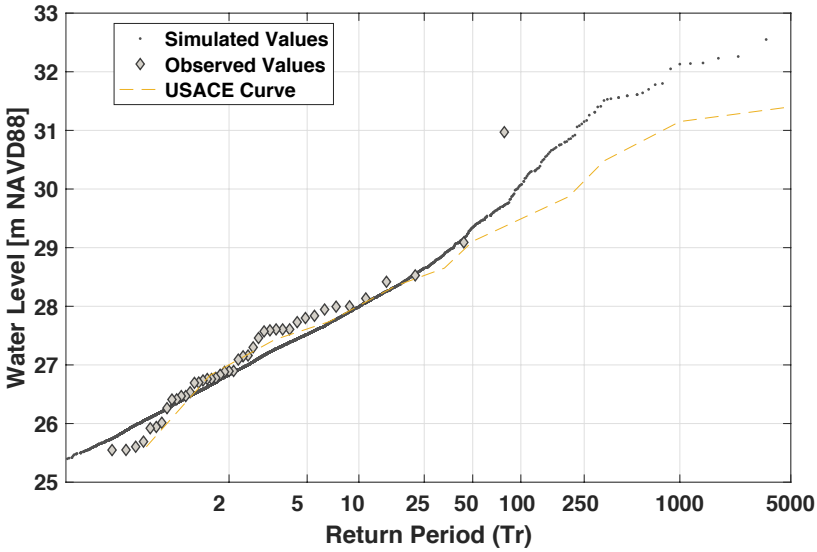

Figure 5.18: Barker Reservoir annual maximum water surface elevation frequency curve including the observed annual maximum water elevations and the frequency curve used by the U.S. Army Corps of Engineers to assess the risk of the system [156]

5.3.2 Dam Safety Analysis

Since releases are not made until pool levels reach the activation level at 29.17 m NAVD88, the properties located close the upper government owned land limit at 28.98 m NAVD88 and within the 100 yr. floodplain at 29.57 m NAVD88 are susceptible to frequent flooding. The potential damages to upstream structures are represented in the high frequency-low damage tail of the serviceability limit state frequency-damage curve in Fig. 5.19. In contrast, due to the operational strategy followed in the Barker Reservoir, the potential damages to downstream properties are very rare with frequencies in the order of 10^{-3}. Their influence in the serviceability limit state risk can be appreciated as a ledge in the frequency-damage curve. Finally, the risk of downstream flooding motivated by the collapse of the structure is portrayed at the low frequency-high damage part of the ultimate limit state frequency-damage curve which is expected with an exceedance probability of 10^{-2} because of the elevated failure probabilities of the structure at low reservoir pool levels.

Figure 5.20 illustrates the estimated level of economic damages, being the area under the curve the total economic risk of the system. The table under the figure outlines the results obtained for each risk component, i.e. flooding risks at the upstream region, $R_{SLS,h}$, flooding risk at the downstream area, $R_{SLS,O}$ and risk attributed to the structural failure of the dam, $R_{ULS,B}$; as well as their contribution to the overall risk of the system, R_T. Although the downstream channel capacity along Buffalo Bayou is very low, it is inferred from this analysis that the level of risk posed by the failure of the structure is the dominating risk component. This clearly exemplifies one of the main drawbacks from the U. S. Army Corps of Engineers emergency

operation schedules. The conservative approach adopted for its development aims to minimize the risk of committing an operational error in terms of excessive releases. The serviceability limit state of downstream flooding is therefore reduced at the expense of increasing the structural failure risk of the system.

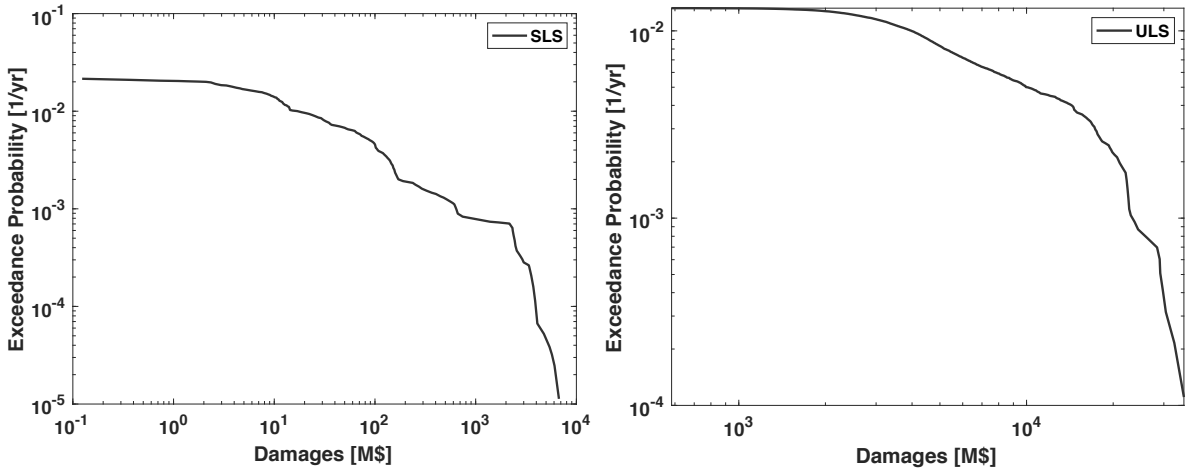

Figure 5.19: Plot showing the frequency-damage curves for: (a) Serviceability Limit State (b) Ultimate Limit State

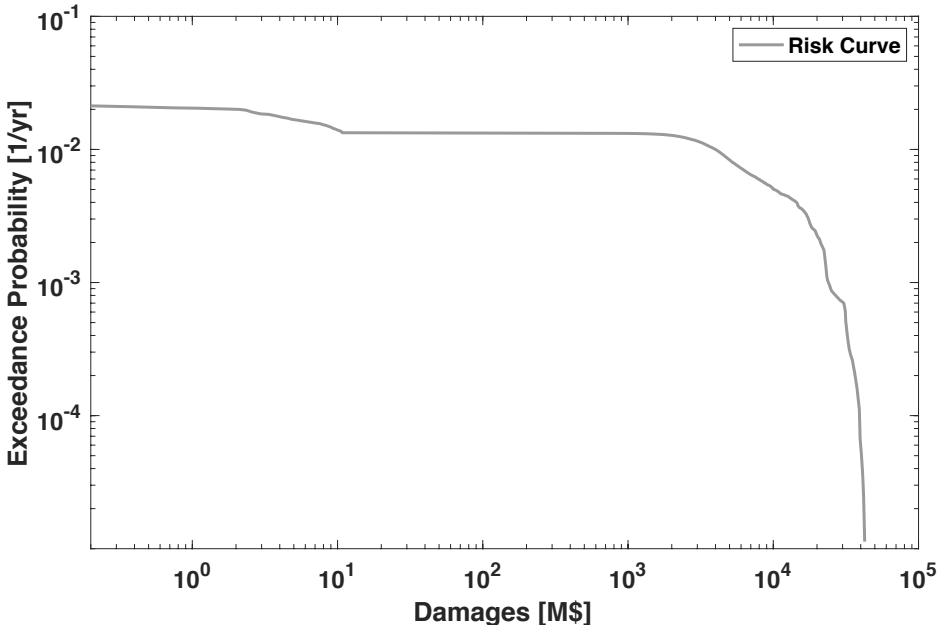

	R, SLSh	R, SLSO	R, ULSB	RT
Expected Annual Damage	1.72	1.9	141.42	145.04
Percentage of Total [%]	1.2	1.3	97.5	-

Note:

R, SLSh = Serviceability Limit State Risk of upstream flooding

R, SLSO = Serviceability Limit State Risk of downstream flooding

R, ULSB = Ultimate Limit State associated to structural failure of the dam

RT = Total risk of the system

Figure 5.20: Frequency-Damage curve of the Barker Dam-Reservoir System

5.4 Risk Mitigation Measures for Barker Reservoir

The parametrization-simulation-optimization framework proposed in Chapter 4 has been applied in the Barker Dam-Reservoir system to generate an optimal emergency operation schedule. Under similar loading conditions, the performance of the parametric operating curve obtained using the proposed risk-based optimization framework has been compared with the emergency operation schedules currently followed in the Barker Reservoir.

According to the classification proposed in Chapter 4, the Barker Reservoir is storage dominated, meaning that high pool levels inside the reservoir dominate the overall risk. This is attributed to the elevated probability of structural failure obtained through the adjustment of the system response curves handed over by the USACE. The optimal operational parameters obtained are in accordance with the expectations for a storage dominated system:

- Low value of s_2 prevents reservoir levels to reach elevations that might jeopardize the integrity of the structure and avoids releases over the uncontrolled spillways.
- Low value of m_1 increases the releases at the first stages of the event which is safer from the point of view of dam collapse as well as upstream flooding.
- Low value of s_1 reduces the releases in the first storage zone to avoid rates exceeding the non-damaging capacity of the downstream channel, but also increases the overall releases by increasing the second storage zone.
- High value of m_2 implies that at some point the reservoir releases could cause high impact on the overall risk. This value coincides with the original non-damaging release rate of 170 m^3/s above which the damages in downstream floodplain escalate quickly for small increases of discharge (Fig. 5.15).

The obtained optimal emergency operating rule is presented in Eq. 5.4:

$$O_{j+1} = \begin{cases} \text{ZONE 3: } O_{max,j} & \text{if } \sqrt{S_j^2 + I(t)^2} > 221.4 \\ \text{ZONE 2: } O_{max,j} \cdot \left[\dfrac{\sqrt{S_j^2 + I(t)^2}}{221.4} \right]^{0.92} & \text{if } 57.3 \leq \sqrt{S_j^2 + I(t)^2} \leq 221.4 \\ \text{ZONE 1: } O_{max,j} \cdot 0.287 & \text{if } \sqrt{S_j^2 + I(t)^2} \leq 57.3 \end{cases} \tag{5.4}$$

The cross section sketched in Fig. 5.21 illustrates the three storage zones in which the reservoir is divided according to the optimal operation strategy. Maximum release rates (ZONE 3) are required before reaching the spillway and the natural ground ends elevations to avoid uncontrolled outflows. Moreover, although downstream damages are exacerbated with this new strategy, releases in ZONE 1 and ZONE 2 before reaching the previous activation level at a elevation of 29.17 m NAVD88 will reduce the reservoir levels attained by extreme events, ultimately reducing the ultimate limit state risk and the risk of upstream flooding.

Figure 5.22 represents the frequency of the damages upstream and downstream of the reservoir. The curves compare the performance under the current emergency operation schedule and the optimized emergency operation schedule of different components of risk. It is inferred that the new operation reduces both, the risk at the upstream region (Fig. 5.22a) and the

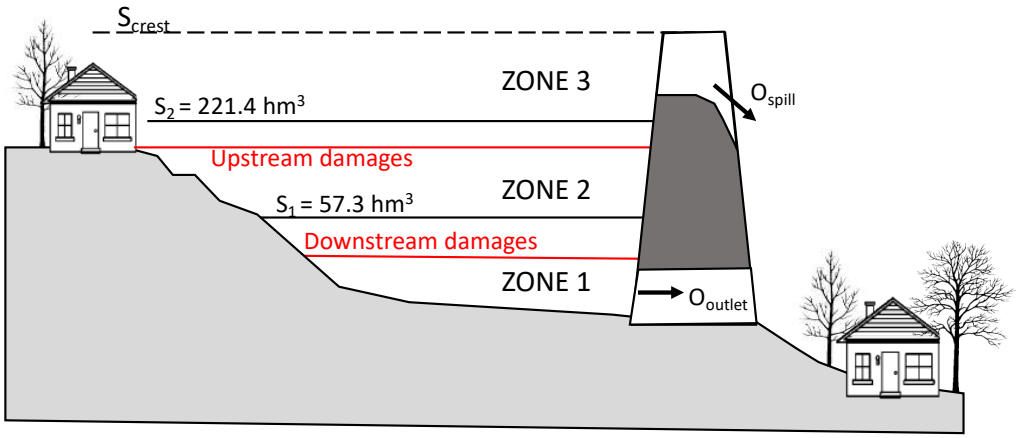

Figure 5.21: Cross section of the Barker Dam showing the different storage zones in which the optimize operating rule has divided the reservoir

damages associated with the structural failure of the dam (Fig. 5.22c). However, the risk at the downstream region in non-breach scenarios is exacerbated (Fig. 5.22b).

Finally, the Frequency-Damage curves comparing the total risk of the system under the current emergency operation schedule and the optimized emergency operation schedule are plotted in Fig. 5.23. The figure has been divided in two parts corresponding to low and high frequency events. The new operation strategy adopted as non-structural risk mitigation measure reduces the total risk for extreme hydrological events but increases the risk for failure scenarios with return periods below 100 yr. This nicely confirms that for minor and moderate flood events, a closing operation strategy is preferred since the releases are dominating the risk; nonetheless, as soon as reservoir levels rise inside the reservoir, the importance of structural failure becomes the driving optimization objective, requiring releases at first stages of the event to ensure the integrity of the structure.

Although optimal from an overall risk point of view, the new operation strategy might be socially unacceptable because it increases the frequency of downstream flooding and could also be questionable for the engineering practice since it is highly dependent on uncertain estimates of fragility curves for structural failure. The author recommends the application of the suggested parametric operating rule only in cases of extreme events like Harvey (2017) which probability of occurrence is still very low. Furthermore, further risk mitigation measures should be contemplated to reduce the structural failure probabilities and the potential economic damages:

1. Strengthen the dam structure to reduce the structural failure probability that caused this reservoir to be classified as one of the six most dangerous flood control dams in the United States.

2. Establish a buy-out program for houses located nearby the upper limit of governmental-owned land and along the Buffalo Bayou channel to increase the channel capacity which now is one third of the ambitioned in the original designs.

3. Revision of the system response curves after Harvey to display a more realistic estimate of the structure's strength against high reservoir levels.

4. Raise the population's awareness of the risks of living nearby the reservoir and limit the future urban development.

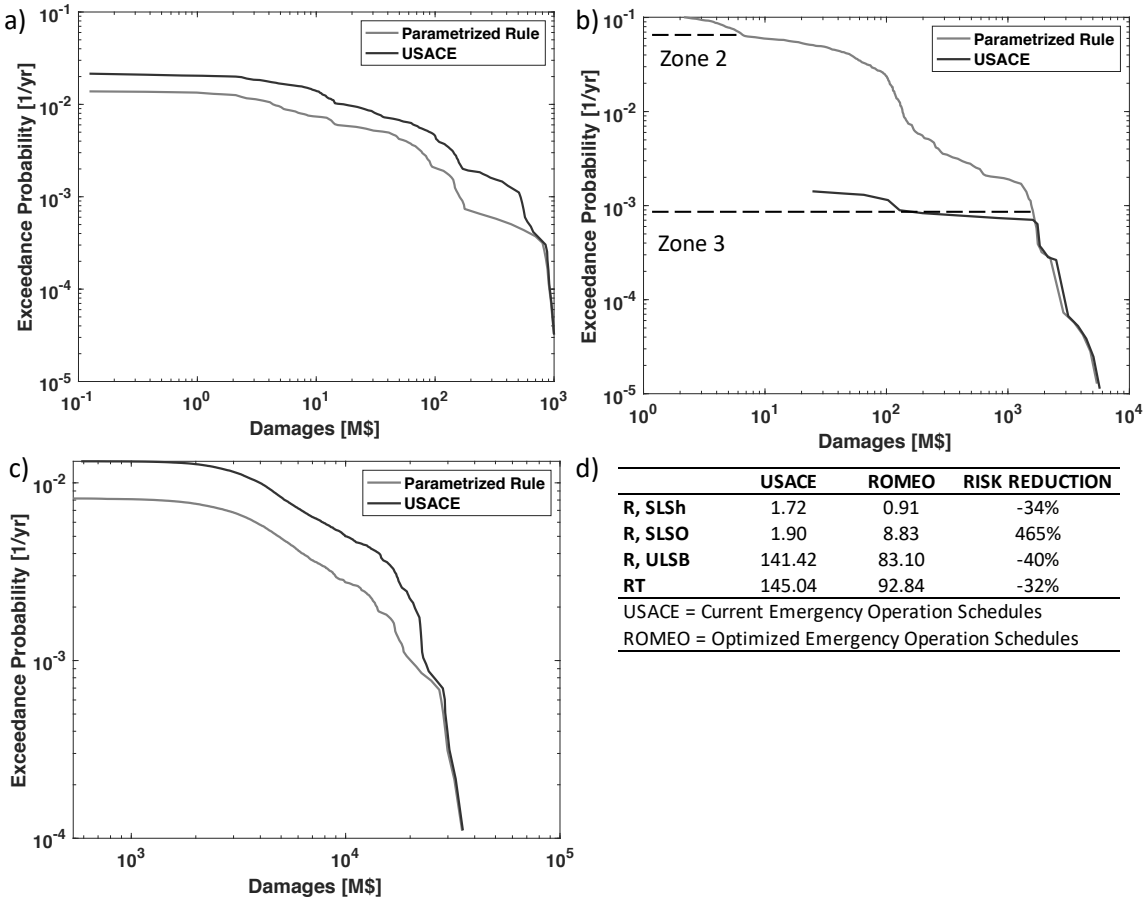

	USACE	ROMEO	RISK REDUCTION
R, SLSh	1.72	0.91	-34%
R, SLSO	1.90	8.83	465%
R, ULSB	141.42	83.10	-40%
RT	145.04	92.84	-32%

USACE = Current Emergency Operation Schedules
ROMEO = Optimized Emergency Operation Schedules

Figure 5.22: Frequency-Damage curves comparing the system performance under the current emergency operation schedule (USACE) and the optimized emergency operation schedule (Parametrized rule) for: (a) upstream risk, (b) downstream risk due to dam spillage, (c) downstream risk due to dam collapse, and (d) table summarizing the results and the percentage of risk mitigation

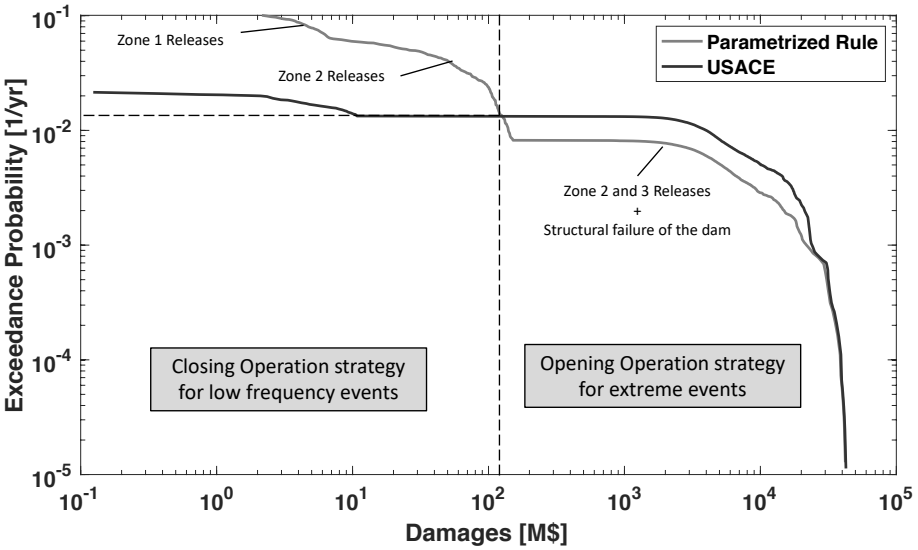

Figure 5.23: Frequency-Damage curves representing the risk mitigation effects resulted from the optimization of the emergency operation schedule in the Barker Dam-Reservoir system

5.5 Conclusions

The thesis culminates with the application of the Risk-based Optimization of Reservoir Emergency Operations model in a study of the Barker Reservoir system in Houston, Texas. Susceptible to hurricanes and intense precipitation events, the Barker system presents a unique operational dilemma requiring trade-offs between released flows and stored volumes. In addition to its low structural resistance, urban development in the reservoir area affected by high pool levels as well as urban encroachment along Buffalo Bayou have constraint the operations of the system. Furthermore, over the lifetime of the structure, several circumstances related with changes in extreme rainfall patterns and watershed runoff characteristics have increased the vulnerability and exposure of both upstream and downstream communities to flooding.

The qualitative risk analysis of the system has revealed important aspects concerning the hazards, the resistance and the potential consequences of the system. First, the flood frequency analysis carried out in this report showed that larger magnitudes of reservoir storage are to be expected more frequently than anticipated by previous risk studies. Second, the common cause adjustment of the five most probable failure modes resulted in a elevated probability of failure for reservoir levels not even reaching the emergency spillway elevations. Finally, it has been observed that, although downstream flooding damages start at a release rate of 56.6 m^3/s, outflows above the original non-damaging capacity of $170m^3/s$ represent the key discharge to be avoided to keep the risk at acceptable levels.

Using the methods developed in Chapter 3 and Chapter 4 of this thesis, it is concluded that an opening strategy during extreme events can effectively reduce the total risk of the Barker Reservoir system. The results have shown that the overall risk could be reduced almost by a 32% as compared with the current closing operation strategy. This is attributed to the high annualized failure probability of the structure and the escalated urban development at downstream regions. The new operating policy, however, increases the frequency of downstream damages during non-structural low frequency failure scenarios which might be socially unacceptable. Therefore, an increase of the downstream channel capacity along Buffalo Bayou, the arrangement of a buy-out program for houses located nearby the upper limit of governmental-owned land and the Buffalo Bayou channel; and adequate measures to strengthen the dam are recommended to reduce downstream damaging flooding and diminish the failure probabilities of the structure.

Finally, the behavior of the structure during Hurricane Harvey (2017) have raised some questions regarding the resistance of the embankment. Since lower structural probabilities would give more importance to downstream flooding risk, the system response curves should be revised to display a more realistic estimate of the structure's strength against high reservoir levels. Simultaneously, since only 35 years of recorded data are available, the difficulty of making a good estimate of low frequency inflow hydrographs is acknowledged. Other procedures such as paleoflood studies or regional data analysis could help improve the estimates of theoretical distribution functions.

Chapter 6

Conclusions & Suggestions for Future Research

As population levels protected by large dams have risen in the last decades, accurately assessing flood hazard and risk will become increasingly important for developing and sustaining flood mitigation policies. Recent research has shown that the degree of control and protection offered by retaining structures largely depend on their operation strategies. However, the operation schedules currently use in the engineering practice lack on mechanisms for evaluating and balancing the potential risks associated with storage and release decisions. This results in reservoir flood control strategies that, from the perspective of flood risk mitigation, are distant from the optimal. This graduation project provides methodological developments for assessing risk in existing dam-reservoir systems and explores the importance of optimized system emergency operations as non-structural risk mitigation measures.

Based on a generalized event tree framework, a novel procedure for conducting risk analysis applied to single dam-reservoir system is presented in Chapter 3. The proposed methodology includes the system operation as an essential component in the quantification of risk. It is found that both **the reservoir water surface elevation and the peak outflow frequency curves highly depend on the flood control operation procedure**, ultimately altering the total risk of the system. Furthermore, the results demonstrate that the **approaches currently applied in engineering practice oversimplify the complex processes associated with dam-reservoir system operations**, leading to incorrect estimations of the overall risk. However, the analysis presented using a simple hypothetical example stops short of evaluating the influence of important hydrological system characteristics such as different hydrograph shapes, or the flooding conditions at the downstream regions. In that sense it is recommended that future work should be carried out to assess the underlaying copula structure for the variables in the network and improve the assumptions made concerning the statistical dependences between diverse system variables. Finally, this study highlights the necessity of finding optimal reservoir operations and prompted its analysis in subsequent chapters.

Chapter 4 presents a parametrization-simulation-optimization procedure for the development of optimal emergency operation schedules applied to single dam-reservoir systems. The method is computationally efficient and it includes the total expected annual damage as objective function for the optimization. Its application into a simplified example shows that **adopting an operation strategy in which the overall risk determines the releases could effectively reduce the level of risk** posed by the retaining structure to the reservoir area and the downstream floodplain properties. Furthermore, similarities between systems are recognized and reveal that **operation strategies should be formulated in accordance with the system's dominant risk component**. It is concluded that in cases in which high pool levels

dictate the overall risk of the system, opening operation strategies with higher outflow rates are optimal (storage dominated systems); whereas closing flood control strategies are preferred when releases exceeding downstream channel capacities dominate (release dominated). However, future research should further assess the effects of the different system characteristics on the outcomes of the developed framework. To improve the understanding on how the mitigation effects of optimized operations fluctuate from system to system, the implementation of the approach into diverse real-life case studies is recommended. Finally, this study also advocates for future addition of individual and societal risks into the framework to be in accordance with tolerability guidelines.

In Chapter 5 the methodologies proposed in this thesis are used in a study of the Barker Dam-Reservoir system in the heavily urbanized area of Buffalo Bayou in the west side of Houston, Texas. Over the lifetime of the structure, changes in the release policies and the watershed runoff characteristics have increased the vulnerability and exposure of both upstream and downstream communities to flooding. The flood frequency analysis carried out in this report shows that recent flood events have significantly modified the streamflow statistics, implying that **larger magnitudes of reservoir storage are more frequent than anticipated by previous risk studies**. The results indicate that **releasing at early stages during extreme events could drastically reduce the overall risk of the system**. This new operation strategy, however, increases the frequency of downstream flooding which might entail low social acceptability. Therefore, the operating rule is only recommended in cases of extreme events like Harvey (2017). Furthermore, measures should be taken to increment **the downstream channel capacity, which now is one third of the ambitioned in the original designs**, and reduce the downstream damages by **establishing a buy-out program** to remove and relocate all those properties that are most likely to suffer flooding in the upstream and downstream regions. The dam safety analysis shows that the elevated probability of structural failure dominates the optimization framework. However, the behavior of the structure during the last hurricane have raised some questions regarding the resistance of the embankment. Since lower structural probabilities would lead to different optimal operations, the system response curves should be revised to display a more realistic estimate of the structure's strength against high reservoir levels. Finally, future work should also be undertaken to improve the flood frequency analysis of reservoir inflows by including regional and paleoflood information.

The models developed in this thesis can be used to assess and mitigate economical flood risk of single dam-reservoir systems where operational effects play a crucial role. Furthermore, the novel procedure for developing emergency operation schedules helps update and adapt reservoir systems to new loading conditions which probabilities and consequences are being increased by changes in climate extreme patterns and increasing urban development. The methods presented in this study have important implications for the development of flood mitigation strategies in dam-reservoir systems and informing future risk-informed dam safety management policies.

Bibliography

[1] J. Blackburn, "Hurricane/Tropical Storm Harvey: Policy Perspectives," tech. rep., Rice University's Baker Institute for Public Policy, Houston, Texas, September 2017.

[2] J. Eerdman, "Is Houston America's Flood Capital?," *The Weather Channel*, August 2017.

[3] WCR, "Weather Research Ceneter: Significant Houston Area Floods." `http://www.wxresearch.com/almanac/houflood.html`, 2016.

[4] E. S. Blake and D. A. Zelinsky, "Hurricane Harvey - Tropical Cyclone Report," Tech. Rep. AL092017, National Hurricane Center, January 2018.

[5] A. Sebastian, K. Lendering, B. Kothuis, N. Brand, S. Jonkman, P. van Gelder, M. Godfroij, B. Kolen, T. Comes, and S. Lhermitte, "Hurricane Harvey Report - A fact-finding effort in the direct aftermath of Hurricane Harvey in the Greater Houston Region," tech. rep., Delft University of Technology, Delft, October 2017.

[6] P. Bedient, J. Blackburn, A. Gori, and A. Juan, "Tropical Storm Harvey Summary Report - No.1," tech. rep., SSPEED Center, Rice University, September 2017.

[7] KHOU, "Buffalo Bayou to remain at record level: Barker, Addicks Reservoirs have peaked," *KHOU.com*, 2017.

[8] L. Mediero, L. Garrote, and F. Martin-Carrasco, "A probabilistic model to support reservoir operation decisions during flash floods," *Hydrological Science Journal*, vol. 52, no. 3, pp. 523–537, 2010.

[9] A. Sordo-Ward, L. Garrote, M. Dolores-Bejarano, and L. G. Castillo, "Extreme flood abatement in large dams with gate-controlled spillways," *Journal of Hydrology*, vol. 498, pp. 113 – 123, 2013.

[10] ICOLD, *Dams and floods, Guidelines and cases histories, Bulletin 125*. International Comission of Large Dams, La Chapelle Montligeon, France, 2003.

[11] ICOLD, *Role of dams in risk mitigation, Bulletin 131*. International Comission of Large Dams, La Chapelle Montligeon, France, 2006.

[12] J. Valdes and J. Marco, "Managing reservoir for flood control," in *US-Italy research workshop on the hydrometeorology, Impacts and Management of extreme floods*, (Perugia, Italy), November 1995.

[13] R. Wurbs, "Comparative evaluation of generalized river/reservoir system models," tech. rep., Texas Water Resources Institute, 2005.

[14] A. Sordo-Ward, I. Gabriel-Martin, P. Bianucci, and L. Garrote, "A Parametric Flood Control Method for Dams with Gate-Controlled Spillways," *Water*, vol. 9, pp. 219–237, March 2017.

[15] H. R. Ramirez, *Flood Control Reservoir Operations for Conditions of Limited Storage Capacity*. PhD thesis, Texas A&M University, 2004.

[16] P. Bianucci, A. Sordo-Ward, J. Perez, J. Garcia-Palacios, L. Mediero, and L. Garrote, "Risk-based methodology for parameter calibration of a reservoir flood control model," *Natural Hazards and Earth System Sciences*, vol. 13, pp. 1–17, January 2013.

[17] R. Wurbs, *State-of-the-art Review and Annotated Bibliography of Systems Analysis Techniques Applied to Reservoir Operation*. Technical report, Texas Water Resources Institute, Texas A&M University, 1985.

[18] W. Yeh, "Reservoir management and operations models: A state-of-the-art review," *Water Resources Research*, vol. 21, no. 12, pp. 1797–1818, 1985.

[19] R. A. Wurbs, "Reservoir-System Simulation and Optimization Models," *Journal of Water Resources Planning and Management*, vol. 119, no. 4, pp. 455–472, 1993.

[20] O. Prakash, K. Srivasan, and K. Sudheer, "Simulation-Optimization Framework for the Optimal Flood Mitigation Operation of Multi-Reservoir System," *Journal of Civil Enginering and Architecture Research*, vol. 1, pp. 300–311, November 2014.

[21] USACE, "Safety of Dams - Policy and Procedures," Tech. Rep. ER 1110-2-1156, U.S. Army Corps of Engineers, Washington D.C., March 2014.

[22] Bureau of Reclamation and U.S. Army Coprs of Engineers, Denver, Colorado, *Best Practices in Dam and Levee Safety Risk Analysis*, July 2015.

[23] H. Rivera-Ramirez and R. Wurbs, "Flood Control Reservoir Operations for Conditions of Limited Storage Capacity," in *ASCE Fall 2004 Meeting*, (Texas), September 2004.

[24] USACE, "Management of Water Control Systems," Engineering and Design ER 1110-2-3600, U.S. Army Corps of Engineers, Washington D.C., October 2017.

[25] N. Santella, L. J. Steinberg, and G. Andrea-Aguirra, "Empirical Estimation of the Conditional Probability of Natech Events within the United States," *Risk Analysis*, vol. 31, no. 6, pp. 951–968, 2011.

[26] NOAA, "Billion-dollar weather and climate disasters: Mapping." `https://www.ncdc.noaa.gov/billions/mapping`, 2017.

[27] A. G. Sebastian, *Quatifying Flood Hazard and Risk in Highly Urbanized Coastal Watersheds*. PhD thesis, Rice University, September 2016.

[28] K. Kunkel, P. Bromirski, H. Brooks, T. Cavazos, A. Douglas, D. Easterling, K. Emanuel, P. Groisman, G. Holland, T. Knutson, J. Kossin, P. Komar, D. Levinson, and R. Smith, "Observed changes in weather and climate extremes," tech. rep., U.S. Climate Change Science Program, 2008.

[29] T. Madsen and E. Figdor, "When it rains it pours: Global warming and the rising frequency of extreme precipitation in the united states," tech. rep., Boston Environmental America Research and Policy Center, 2007.

[30] H-GAC, "H-gac regional growth forecast 2017." http://www.h-gac.com/community/socioeconomic/2040-regional-growth-forecast/default.aspx, 2017.

[31] I. Nalbantis and D. Koutsoyiannis, "A parametic rule for planning and management of multiple-reservoir systems," *Water Resources Research*, vol. 33, no. 9, pp. 2165–2177, 1997.

[32] D. Koutsoyiannis and A. Economou, "Evaluation of the parametrization-simulation-optimization approach for the control of reservoir systems," *Water Resources Research*, vol. 39, June 2003.

[33] A. B. Celeste and M. Billib, "Evaluation of stochastic reservoir operation optimization models," *Advances in Water Resources*, vol. 32, pp. 1429 – 1443, 2009.

[34] F. Correia, M. Saraiva, F. D. Silva, and I. Ramos, "Floodplain management in urban development areas, Part 1, Urban Growth scenarios and land-use controls," *Water Resources Management*, vol. 13, pp. 1–21, 1999.

[35] S. Jonkman, "Global perspectives on loss of human life caused by floods," *Natural Hazards*, vol. 34, pp. 151–175, 2003.

[36] M. Fiorentini and S. Orlandini, "Robust numerical solution of the reservoir routing equation," *Advances in Water Resources*, vol. 59, pp. 123–132, May 2013.

[37] E. Laurenon, "Variable time-step nonlinear flood routing," in *Hydrosoft 86: hydrauli engineering software* (M. R. an C. Maksimovic and C. Brebbia, eds.), (Berlin, Germany), pp. 61–72, Springer Verlag, 1986.

[38] D. Peligrim, "Flood routing," in *Australian rainfall and runoff: a guide to flood estimation* (D. Peligrim, ed.), vol. 1, (Australia, Barton), pp. 129–149, ACT, Australia:The Institution of Engineers, 1987.

[39] V. Chow, D. Maidment, and L. Mays, *Applied Hydrology*. New York: Mc Graw Hill, 1988.

[40] J. Cash and A. Karp, "A variable order Runge-Kutta method for initial volume problems with rapidly varying right-hand sides," *ACM Trnsactions on Mathematical Software*, vol. 16, no. 3, pp. 201–222, 1990.

[41] R. E. Horton, "The role of infiltration in the hydrologic cycle," *Transactions, American Geophysical Union*, vol. 14, pp. 446–460, 1993.

[42] L. W. Mays, *Water Resources Engineering*. USA: John Wiley and Sons Inc, 2nd ed., 2011.

[43] R. A. Sloto and M. Y. Cruise, "HYSEP: a computer program for streamflow hydrograph separation and analysis," tech. rep., U.S.G.S., Lemoyne, Pennsylvania, 1996.

[44] W. A. Pettyjohn and R. Henning, "Preliminary Estimate of Ground-Water Recharge Rates, Related Streamflow and Water Quality in Ohio," Tech. Rep. 552, Water Resource Center - The Ohio State University, 1979.

[45] R. Wurbs, *Modeling and Analysis of Reservoir System Operations*. Prentice Hall PTR, 1996.

[46] J. Windsor, "Optimizaion model for the operation of flood ontrol systems," *Water Resources Research*, vol. 9, no. 5, pp. 1219–1226, 1973.

[47] J. W. Labadie, "Optimal operation of multireservoir systems: State-of-the-art review," *Journal of Water Resources Planning and Management*, vol. 130, no. 2, pp. 93–111, 2004.

[48] D. Rani and M. M. Moreira, "Simulation-Optimization Modeling: A Survey and Potential Applicatio in reservoir Systems Operation," *Water Resources Management*, vol. 24, pp. 1107–1138, 2010.

[49] A. Maas, "Design of water resources systems," *Harvard University Press*, 1962.

[50] D. Hydraulics, "RIBASIM - River Basin Planning and Management Simulation Program." https://www.wldelft.nl/soft/ribasim/int/index.html, 1985.

[51] J. Klipsch and M. Hurst, "HEC-ResSim Reservoir System Simulation User's Manual Version 3.0. ASCE-HEC." https://www.hec.usace.army.mil/software/hec-ressim/documentation.html, 2007.

[52] D. H. Institute, "MIKE 11 - Modelizacion de rios, canales y embalses." https://www.dhi.es/Software/RecursosH%C3%ADdricos/MIKE11.aspx, 2008.

[53] R. T. Inc, "RES-J - Joint Reservoir Regulation Operation. Hydrologic Software Engineering Branch." https://www.nws.noaa.gov/oh/hrl/nwsrfs/users_manual/part8/_pdf/833resj.pdf, 2007.

[54] E. Alemu, R. Palmer, A. Polebitski, and B. Meaker, "Decision support system for optimizing reservoir operations using ensemble of streamflow predictions," *Journal of Water Resources Planning and Management*, vol. 137, pp. 72–82, 2011.

[55] A. Faber and J. Stedinger, "Reservoir optimization using sampling SDP with esemble streamflow prediction (ESP) forecast," *Journal of Hydrology*, vol. 249, pp. 113–133, 2001.

[56] X. Mei, *Probability Analysis of Floods in Catchments With Dams*. PhD thesis, Delft University of Technology, 2013.

[57] J. Needham, "Linear programming for flood control in the Iowa and Des Moines rivers," *Journal of Water Resources Planning and Management*, vol. 126, no. 3, pp. 118–127, 2000.

[58] R. Teegavarapu and S. Simonovic, "Short-term operation model for coupled hydropower reservoirs," *Journal of Water Resources Planning and Management*, vol. 126, no. 2, pp. 98–106, 2000.

[59] L. Mays and Y. Tung, *Hydrosystems Engineering and Management*. Water Resources Publications, 2002.

[60] L. Chen, "Real coded genetic algorithm optimization of long term reservoir operation," *J. American Water Resources Association*, vol. 39, no. 5, pp. 1157–1165, 2003.

[61] F. Chang, L. Chen, and L. Chang, "Optimizing the reservoir operating rule curves by genetic algorithms," *Hydrological Processes*, vol. 19, no. 11, pp. 2277–2289, 2005.

[62] L. L. Ngo, *Optimizing reservoir operation: A case study of the Hoa Binh reservoir, Vietnam*. PhD thesis, Institute of Environment and Resources - Technical University of Denmark, Copenhagen, October 2006.

[63] S. Khu and H. Madsen, "Multiobjective calibration with Pareto preference ordering: An application to rainfall-runoff model calibration," *Water Resources Research*, vol. 41, no. 3, 2005.

[64] C. Cheng and K. Chau, "Fuzzy iteration methodology for reservoir flood control operation," *J. American Water Resources Association*, vol. 37, pp. 1381–1388, 2001.

[65] E. Can and M. Houck, "Real-time reservoir operation by goal programming," *Journal of Water Resources Planning and Management*, vol. 110, pp. 297–309, 1984.

[66] B. Malekmohammadi, B. Zahraie, and R. Kerachian, "Ranking solutions of multi-objective reservoir operation optimization models using muti-criteria decision analysis," *Expert Systems Applications*, vol. 38, pp. 7851–7863, 2011.

[67] D. Loucks, J. Stedinger, and D. Haith, *Water resources systems planning and analysis*. Prentice-Hall. Englewood Cliffs, 1981.

[68] M. Karamouz and M. Houck, "Comparison of stochastic and deterministic dynamic-programming for reservoir operating rule generation," *Water Resources Bulletin*, vol. 23, no. 1, pp. 1–9, 1987.

[69] D. Koutsoyiannis, A. Estratiadis, and G. Karavokiros, "A decision support tool for the management of multi-reservoir systems," *Am Water Resour Assoc*, vol. 38, no. 4, pp. 945–958, 2002.

[70] *Directive 2007/60/EC of the European Parliament and of the Council of 23 October 2007 on the assessment and management of flood risks*, 2007.

[71] *Directive 2008/114/EC of the European Parliament and of the Council of 8 December 2008 on the identification and designation of European critical infrastructures and the assessment of the need to improve their protection*, 2008.

[72] S. Jonkman, *Loss of life estimation in flood risk assessment: theory and application*. PhD thesis, Delft University of Technology, 2007.

[73] CRUE, "Synthesis Report No. I-2009, Addressing the key findings of reseacrh, Risk Assessment and Risk Management: Effectiveness and Efficiency of Non-structural Flood Risk Management Measures," Tech. Rep. ERAC-CT-2004-515742, CRUE Research Funding Initiative, 2009.

[74] J. Schanze, G. Hutter, A.Olfert, E. Penning-Rowsell, D. Parker, T. Harries, A. Werritty, H. Nachtnebel, H.Holzman, C. Neuhold, V. Meyer, C. Kuhlicke, A. Schildt, B. Jessel, and P. Königer, "CRUE Research Report I-1: Systematisation, evaluation and context conditions of structural and non-structural measures for flood risk reduction," FLOOD-ERA Joint Report Project Contract No. ERAC-CT-2004-515742, CRUE Funding Iniciative on Flood Risk Management Research, London, 2008.

[75] W.C.D., *Dams and Development - A New Framework for Decision-Making*. Sterling, VA, USA: Earthscan Publications Ltd, November 2000.

[76] B. Gouldby and P. Samuels, "Lenguage of risk: Project definitions," report: t32-04-01, FLOODste project, HR Wallingford, UK, 2005.

[77] S. Kaplan and B. J. Garrick, "On the quantitative definition of risk," *Risk Analysis*, vol. 1, no. 1, pp. 11–27, 1981.

[78] B. Merz, H. Kreibich, R. Schwarze, and A. Thieken, "Review article - Assessment of economic flood damage," *Natural Hazards and Earth System Sciences*, vol. 10, pp. 1697–1724, 2010.

[79] S. Jonkman, P. van Gelder, and J. Virjling, "An overview of quantitative risk measures for loss of life and economic damage," *Journal of Hazardous Materials*, vol. A99, pp. 1–30, 2003.

[80] E. van Berchum, *Flood Risk Reduction System Optimization - Interim report*. PhD thesis, Delft University of Technology, 2017.

[81] S. Jonkman, R. Jorissen, T. Schweckendieck, and J. van den Bos, "Flood defences - lecture notes cie5314," tech. rep., Delft University of Technology, 2017.

[82] I. 31010:2009, *ISO International Standard: Risk management - Risk assessment techniques*, 2009.

[83] I. Escuder-Bueno, A. Morales-Torres, and S. Perales-Momparler, "Characterization as a tool for planning and managing," in *Exploration of Torerable Risk Guyidelines for Levee Systems*, (Washington D.C. (USA)), March 2010.

[84] I. Escuder-Bueno, J. Castillo-Rodriguez, S. Zechner, C. Jöbstl, S. Perales-Momparler, and G. Petaccia, "A quantitative flood risk analysis methodology for urban areas with integration of social research data," *Natural Hazards and Earth System Sciences*, vol. 12, pp. 2843–2863, 2012.

[85] S. Jonkman, R. Steenbergen, O. Morales-Napoles, A. Vrouwenvelder, and J. Vrijling, "Probabilistic Design: Risk and Reliability. Analysis in Civil Engineering - CIE4130 Lecture Notes," tech. rep., Delft University of Technology, 2016.

[86] J. Castillo-Rodriguez, I. Escuder-Bueno, L. Altarejos-Garcia, and A. Serrano-Lombillo, "The value of integrating information from multiple hazards for flood risk analysis and management," *Journal of Natural Hazards and Earth System Sciences*, vol. DOI: 10.5194/nhess-14-379-2014, 2014.

[87] A. Serrano-Lombillo, I. Escuder-Bueno, M. de Membrillera, and L. Altarejos-Garcia, "ipresas: software for risk analysis," in *23rd International Congress on Large Dams*, (Brasilia), 2009.

[88] D. Munger, D. Bowles, D. Boyer, D. Davis, D. Margo, D. Moser, and P. Regan, "Interim tolerable risk guidelines for us army corps of engineers dams," in *USSD Conference*, 2009.

[89] J. Virjling and P. van Gelder, "A framework for risk evaluation," *Journal of Hazardous Materials*, no. 43, pp. 245–261, 1995.

[90] M. Barnes, "Famous Failure: Revisiting Major Dam Catastrophes," in *ASDSO Annual Conference* (H. R. Magazine, ed.), (Baltimore), Association of State Dam Safety Officials, 1992.

[91] A. Srivastava, "Generalized Event Tree Algorithm and Software for Dam Safety Risk Analysis," Master's thesis, Utah State University, Utah, 2008.

[92] SPANCOLD, "Risk Analysis Applied to Management of Dam Safety," tech. rep., Spanish National Committee on Large Dams, 2012.

[93] I. Escuder-Bueno, A. Serrano-Lombillo, and L. Altarejos-Garcia, "Una visión integral de la seguridad de presas, la mitigación del riesgo de inundación y la gestion de las infrastructuras criticas a traves del analis de riesgos," tech. rep., Universidad Politécnica de Valencia, 2012.

[94] F. E. M. A. FEMA, "Federal guidelines for dam safety risk management," Tech. Rep. P-1025, FEMA, Washington D.C., January 2015.

[95] D. Bowles, "Risk assessment in dam safety decision making," in *Risk-based decision making in water resources*, pp. 254–283, American Society of Civil Engineers, 1990.

[96] U. S. D. of the Interior and U. S. B. of Reclamation, *Guidelines for Achieving Public Protection in Dam Safety Decision Making*. U.S. Department of the Interior, Bureau of Reclamation, 2003.

[97] ANCOLD, "Guidelines on risk assessment," tech. rep., Australian National Committee on Large Dams, Sydney, New South Wales, Australia, October 2003.

[98] N. S. W. D. S. Committee, *Risk Management Policy Framework For Dam Safety*, August 2006.

[99] S. Kaplan, "The words of rik analysis," *Risk Analysis*, vol. 17, no. 4, pp. 407–417, 1997.

[100] D. S. Bowles, "Evaluation and Use of Risk Estimates in Dam Safety Decisionmaking," in *20-Year Retrospective and Prospective of Risk-Based Decision-Making*, vol. United Engineering Foundation Conference on Risk-Based Decision-Making in Water Resources IX, (Santa Barbara, California), American Society of Civil Engineers, August 2001.

[101] EAUK, "Guide to risk assessment for reservoir safety management," Report - SC090001/R2 Volume 2, UK Environmental Agency, 2013.

[102] Bureau of Reclamation, "Dam Safety Public Protection Guidelines," interim, Bureau of Reclamation, Denver, Colorado, August 2011.

[103] HSE, "Reducing risks, protecting people - hse's decision-making process," tech. rep., Health and Safety Executive, 2001.

[104] I. Escuder-Bueno, J. Castillo-Rodriguez, S. Perales-Momparler, and A. Morales-Torres, "A complete and quantitative tool for flood risk analysis in urban areas: river and pluvial flooding," in *UFRIM Conference*, (Graz (Austria)), September 2011.

[105] A. Serrano-Lombillo, *Development of a Complete Tool of Risk Analysis and Assesstment in Dam Safety*. PhD thesis, Universidad Politécnica de Valencia, 2011.

[106] D. Bowles, S. C. amd D. Jams, and B. Dustson, *ResRisk UU Version 1.0 User Guide. Report 8, Developmet of Reservoir Safety Porfolio Risk Assessment (PRA) Stage 3 Sofware and Enhancement of PRA Stage-2 Functionallity*. Institute for Dam Safety Risk Management, URWRL, USU, Logan and RAC Engineers and Economists, Providenc, UT, prepared for united utilities water plc ed., October 2008.

[107] G. Baxter, T. Adrysewski, J. Banks, P. Sayers, J.-D. Simm, and M. Wallis, "Performance-based Asset Management (PAMS) project - What has it delivered? How will we use it? Where next?," in *45th Flood and Coastal Risk Management*, (Telford, UK), Jun 29 - Jul 1 2010.

[108] A. Srivastava and D. S. B. abd Sanjay S. Chauhan, "DAMRAE-U: A tool for incudin uncertainty in dam safety risk assessment," in *ASDSO 2012 Conference on Dams*, 2012.

[109] A. Srivastava, *A Computational Framework for Dam Safety Risk Assessment with Uncertainty Analysis*. PhD thesis, Utah State University, Utah, 2013.

[110] I. Escuder-Bueno, M. de Membrillera, M. Meghella, and A. Serrano-Lombillo, "Damse: a european methodology for risk based security assessment of dams," in *Twenty Third International Congress on Large Dams*, May 2009.

[111] C. D. Michele, G. Salvadori, M. Canossi, A. Petaccia, and R. Rosso, "Bivariate statistical approach to check adequacy of dam spillway," *Journal of Hydrologic Engineering*, vol. 10, no. 1, pp. 50–57, 2005.

[112] B. Klein, M. Pahlow, Y. Hundecha, and A. Schumann, "Probability analysis of hydrological loads for the design of flood control systems using copulas," *Journal of Hydrologic Engineering*, vol. 15, pp. 360–369, May 2010.

[113] F. Serimaldi and S. Grimaldi, "Synthetic Design Hydrographs Based on Distribution Functions with Finite Support," *Journal of Hydrologic Engineering*, vol. 16, pp. 434–446, May 2011.

[114] L. Mediero, A. Jimenez, and L. Garrote, "Design Flood Hydrographs from the Relationship between Flood Peak and Volume," *Hydrology and Earth System Sciences*, vol. 14, pp. 2495 – 2505, 2010.

[115] A. Jimenez, *Desarrollo de Metodologías para mejorar la Estimación de los Hidrogramas de Diseño para el Cálculo de los Órganos de Desagüe de las Presas*. PhD thesis, Universidad Politécnica de Madrid, 2015.

[116] E. Volpi and A. Fiori, "Hydraulic structures subject to bivariate hydrological loads: Return period, design, and risk assessment," *Water Resources Research*, vol. 50, pp. 885 – 897, 2014.

[117] D. Goldman, "Quatifying uncertainty in estimates of regulated flood frquency curves," in *World Water and Environmental Resources Congress*, (Reston, VA), ASCE, 2001.

[118] P. Arnaud and J. Lavabre, "Coupled rainfall model and discharge model for flood frequency estimation," *Water Resources Research*, vol. 38, no. 6, 2002.

[119] A. Loukas, "Flood frequency estimation by a derived distribution procedure," *Journal of Hydrology*, vol. 255, no. 1, pp. 69 – 89, 2002.

[120] J. England, "Probabilistic extreme flood hydrographs that use peleoflood data for dam safety application," Tech. Rep. DSO-03-03, Department of Interior Bureau of Reclamation, 2003.

[121] G. Aronica and A. Candela, "Derivation of flood frequency curves in pooly gauged mediterranan catchments uing a simple stochastic hydrological rainfal-runoff model," *Journal of Hydrology*, vol. 347, no. 1-2, pp. 132–142, 2007.

[122] S. Yue, "The bivariate lognormal distribution to model a multivariate flood episode," *Journa of Hydrological Processes*, vol. 14, pp. 1464–1477, 2000.

[123] C. D. Michelle and G. Salvadori, "A generalized Pareto intensity-duration model of storm rainfall exploring 2-copula," *Journal of Geophysical Research*, vol. 108, no. D2, 2003.

[124] A. Favre, S. E. Adlouni, L. Perreault, N. Thiemonge, and B. Bobee, "Multivariate hydrological freuency analysis using copulas," *Water Resources Research*, vol. 40, no. W01101, 2004.

[125] I. Flores-Montoya, A. Sordo-Ward, L. Mediero, and L. Garrote, "Fully stochastic distributed methodology for multivariate flood frequency analysis," *Water*, vol. 8, 225, no. DOI: 10.3390/w8060225, 2016.

[126] USACE, "Des Moines River Regulated Flow Frequency Study," tech. rep., US Army Corps of Engineers Rock Island District, Rock Island, Ilinois, November 2010.

[127] T. Wahl, "Prediction of embankment dam breach parameters - a literature review and needs assessmn," tech. rep., Dam Safety Office - U.S. Bureau of Reclamation, 1998.

[128] D. Froehlich, "Embankment dam breach parameters revisited," in *1995 ASCE Conference on Water Resources Engineering*, (San Antonio, Texas), pp. 887–891, 1995.

[129] J. Huizinga, H. de Moel, and W. Szewczyk, "Global flood depth-damage functions," jrc technical report, European Commission, Sevilla, Spain, 2017.

[130] R. Hui and J. Lund, "Flood Storage Allocation Rules for Parallel Reservoirs," *Water Resources Management*, vol. 141, August 2014.

[131] A. Sordo-Ward, L. Garrote, F. Martín-Carrasco, and M. Dolores-Bejarano, "Extreme flood abatement in large dams with fixed-crest spillways," *Journal of Hydrology*, vol. 466, pp. 60 – 72, 2012.

[132] T. B. Ayalew, W. F. Krajewski, and R. Mantilla, "Exploring the Effect of Reservoir Storage on Peak Discharge Frequency," *Journal of Hydrologic Engineering*, vol. 18, pp. 1697–1708, 2013.

[133] I. Gabriel-Martin, A. Sordo-Ward, L. Garrote, and L. G. Castillo, "Influence of initial reservoir level and gate failure in dam safety analysis. stochastic approach," *Journal of Hydrology*, vol. 550, pp. 669 – 684, 2017.

[134] B. Graeler, M. van der Berg, S. Vandenberghe, A. Petroselli, S. Grimaldi, B. D. Baets, and N. Verhoest, "Multivariate return periods in hydrology: a critical and practical review focusing on synthetic design hydrograph estimation," *Hydrology and Earth System Sciences*, vol. 17, pp. 1281–1296, 2013.

[135] D. Nijsen, A. Schumann, M. Pahlow, and B. Klein, "Planning of technical flood reention measures n large river basins under consideration of imprecise probabilities of multivariate hydrological loads," *Natural Hazards and Earth System Sciences*, vol. 9, pp. 1349–1363, 2009.

[136] G. Salvadori, C. D. Michelle, and F. Durante, "On the return period and design in a multivariate framework," *Hydrology and Earth System Sciences*, vol. 15, pp. 3293–3305, 2011.

[137] E. Volpi and A. Fiori, "Design event selection in bivariate hydrological frequency analysis," *Hydrological Science Journal*, vol. 57, pp. 1506–1515, March 2012.

[138] A. Requena, L. Mediero, and L. Garrote, "A bivariate return period based on copulas for hydrologic dam design: accounting for reservoir routing in risk estimation," *Hydrology and Earth System Sciences*, vol. 17, August 2013.

[139] A. Jimenez and L. Mediero, "Combined treatment of peak flow and volume for estimating design flood hydrographs of dams," *CEDEX - Ingeniería Civil*, vol. 174/2014, no. ISSN 0213-8468, 2014.

[140] S. Yue, T. B. M. J. Ourda, B. Bobee, P. Legendre, and P. Bruneau, "Approach for Describing Statistical Properties of Flood Hydrograph," *Journal of Hydrologic Engineering*, vol. 7, pp. 147–153, March 2002.

[141] C. Claudio, P. Laurent, A. Patrick, B. Daniel, and R. Paul, "Probabilistic modeling of floodwater level for dam reservoirs," *Journal of Hydrologic Engineering*, vol. 14, pp. 223–232, 2018/04/23 2009.

[142] C. Cunnane, "Unbiased Plotting Positons - A review," *Journal of Hydrology*, vol. 37, pp. 205–222, 1978.

[143] J. Stedinger, R. Vogel, and G. Foufoula, *Handbook of Applied Hydrology*. No. Chapter 18 : Frequency Analysis of Extreme Events, New York: Mc Graw Hill Book Co., 1993.

[144] ICOLD, "Dam failures: statistical analysis," Tech. Rep. Bulletin 99, Internation Comission on Large Dams, Paris, 1995.

[145] L. Z. an Y. Xu and J. Jia, "Analysis of earth failures: A database approach," in *Fisrt International Symposium on Geotechnical Safety and Risk*, (Shanghai, China), pp. 293–302, Tongji University, 2007.

[146] P. Hill, D. Bowles, P. Jordan, and R. Nathan, *Estimating Overall Risk of Dam Failure: Practical Considerations in Combining Failure Probabilities*. ANCOLD, 2003.

[147] S. Andreev and A. Z. Zhelyazkov, "Probability of Failure of an Embankment Dam Due to Slope Instability and Overtopping: First Order Second Method for Assessmentof Uncertainty," in *13th ICOLD Benchmark Workshop on Numerical Analysis of Dams* (A. Morales-Torres and I. Escuder-Bueno, eds.), (Lausanne, Switzerland), ICOLD, 2015.

[148] A. Morales-Torres and I. Escuder-Bueno, "Theme B: Probability of failure of an embankment dam due to slope instability and overtopping," in *13th ICOLD Benchmark Workshop on Numerical Analysis of Dams* (A. Morales-Torres and I. Escuder-Bueno, eds.), (Lausanne, Switzerland), ICOLD, 2015.

[149] iPresas Risk Analysis, Valencia, *iPresas Calc Version 1.0.2 - Manual de Usuario*, 2017.

[150] A. S. W. L. G. A. Jimenez, *El Efecto Laminador de los Embalses en Avenidas Extraordinarias*, vol. CEDEX: Sección de Edición. Centro de Publicaciones Secretaría General Técnica Ministerio de Fomento, 2012.

[151] United States Bureau of Reclamation, *Design of Small Dams*. United States Department of Interior, third edition ed., 1987.

[152] A. Serrano-Lombillo, I. Escuder-Bueno, M. de Membrillera, and L. Altarejos-Garcia, "Modelos de Riesgo para la Ayuda a la Toma de Decisiones en Gestion de Seguridad de Presas," in *IX Jornadas Espanolas de Presas* (SPANCOLD, ed.), 2010.

[153] M. Anhalt and G. Meon, "Risk-Based Procedure for Design and Verification of Dam Safety," in *4th International Symposium on Flood Defence: Managing Flood Risk, Reliability and Vulnerability*, (Toronto, Ontario, Canada), May 2008.

[154] Y. Chen and P. Lin, "The Total Risk Analysis of Large Dams under Flood Hazards," *Water*, vol. 10, no. 140, 2018.

[155] J. Connaughton, N. King, L. Dong, P. Ji, and J. Lund, "Comparing Simple Flood Reservoir Operation Rules," *Water*, vol. 6, pp. 2717–2731, September 2014.

[156] U.S. Army Corps of Engineers Galveston District, "Addicks and Barker Dam Safety Modification Report," tech. rep., U.S. Army Corps of Engineers, Houston, Texas, May 2013.

[157] NLCD, "National land cover database." https://catalog.data.gov/dataset/national-land-cover-database-nlcd-land-cover-collection, 2018.

[158] USACE, *Water Control Manual Addicks and Barker Reservoirs*. USACE, November 2012.

[159] USACE, "Reconnaissance Report - Section 216 Study: Addicks and Barker Reservoirs, Houston, TX," tech. rep., USACE Galveston District, Houston, Texas, October 1995.

[160] U.S. Army Corps of Engineers Galveston District, "Statistical Analysis of Reservoir Pool Elevations," summary report (draft), USACE Galveston District, Galveston, Texas, December 2008.

[161] Reuters, "Hurricane harvey damages could cost up to $180 billion." http://fortune.com/2017/09/03/hurricane-harvey-damages-cost/, September 2017.

[162] J. Belles, "Harvey could be america's first $200 billion hurricane," *The Weather Channel*, November 2017.

[163] G. Afiune, "Sate says harvey's death toll has reached 88," *The Texas Tribune*, October 2017.

[164] S. Jonkman, M. Godfroy, A. Sebastian, and B. Kolen, "Brief Communication: Loss of Life due to Hurricane Harvey," *Natural Hazards and Earth System Sciences*, vol. 18, pp. 1073–1078, 2018.

[165] L. A. Sanchez, "Hurricane harvey - storm related deaths." Harris County Institute of Forensic Sciences, September 2017.

[166] HCFCD, "Stormwater rising into neighborhoods near Addicks, Barker Reservoirs in west Harris County," August 2017.

[167] USWRC, *Guidelines for Determinig Flood Flow Frequency - Bulletin 17C*. U.S. Water Resources Council, 2015.

[168] J. R. M. Hosking and J. R. Wallis, *Regional Frequency Analysis: An Approach Based on L-Moments*. Cambridge University Press, 1997.

[169] H. D. Fill and A. A. Steiner, "Estimating Instantaneous Peak Flow from Mean Daily Flow Data," *Journal of Hydrologic Engineering*, vol. 8, pp. 365–369, November 2003.

[170] J. Salas, "Analysis and modelling of hydrologic time series," in *Handbook of hydrology* (D. Maidment, ed.), pp. 19.1 – 19.72, McGraw Hill Inc., 1993.

[171] D. Helsel and R. M. Hirsch, *Statistical Methods in Water Resources Investigations*, ch. chapter A3, p. 522 p. No. Book 4, U.S. Geological Survey, 2002.

[172] J. Hosking, "L-Moments: analysis and estimation of distributions using linear combinations of order statistics," *Journal of Royal Statistical Society*, vol. 52, pp. 105–124, 1990.

[173] A. J. L. M. C. García, "Análisis y selección de modelos estadísticos para el ajuste de la ley de frecuencia de caudales máximos anuales en españa," *CEDEX - Ingeniería Civil*, vol. 174/2014, no. ISSN 0213-8468, 2014.

[174] R. M. Hirsch, "Probability plotting position formulas for flood records with historical information," vol. 96, no. 1-4, pp. 185–199, 1987.

Vita

Pablo Sanchez Gomez was born in Madrid, Spain in 1993. He was raised in Majadahonda, Madrid, and graduated from Escuelas Pias de San Fernando in 2011. After high school, Pablo was awarded with the "Madrid Excellent Student Scholarship" to start his studies in the Polytcnic University of Madrid as an undergraduate. Parallel to his studies on Civil Engineering, Pablo followed his music career at the Alfredo Kraus Music School were he finished the clarinet middle grade of music. On his fourth year, Pablo was awarded with a Erasmus Scholarship to finish his Bachelor degree at the "Karlruher Institut für Technology" where he completed his Bachelor thesis tutored by Dr. ir. Andreas Bieberstein on partially overflow dams with open stone asphalt revetments. After four years Pablo concluded his Bachelor of Science degree in Civil Engineering in 2015 with a focus on Structures, Geotechnique and Civil Constructions.

During the year after graduation, Pablo stayed in Germany where he worked for the companies "Roth und Partner" and "Unger Ingenieure" gaining great experience in different fields of the Civil and Environmental Engineering world. Finally, in 2016, Pablo entered the graduate program at Delft University of Technology where he pursued his interests in hydraulic structures and flood risk. During his Masters, Pablo carried out an internship in the Hydraulics Laboratory of CEDEX, where he had the opportunity to work closely with Dr. ir. David Lopez and to participate in the publication of two academic papers.

Appendix A

Structure-based Framework for Risk Assessment

Standard procedures mostly refer to cases in which the hydrological load is represented by a single environmental variable and by its cumulative density function. This approach, however, has a series of shortcomings which might not adequately represent the complexity of the hydrological processes affecting a dam-reservoir system. It assumes that by characterizing the flood events with a unique variable, the other hydrological parameters are perfectly known. While in reality, the association between hydrological variables is, in general, not unique. The magnitude of a flood and its consequences not only depends on the peaks but also on the volume, duration and temporal distribution of the hydrograph. Jimenez et. al [115] demonstrated that in cases of large reservoir storage, the statistical dependence between peakflows and volumes plays a crucial role. The univariate analysis of peak inflows or inflow volumes does not suffice for the study of the hydrological safety of the structure.

In the proposed methodology, the term risk refers to the occurrence probability of those variables that measure the effect of the hydrological loads on the structure. These parameters, denoted as *characteristic damage variables* from now on, include all those variables directly associated with the potential damages such as the water reservoir elevation which is responsible for upstream flooding damages, the released flows exceeding non-damaging downstream reaches capacities, and the breakage flows derived from the structural failure of the dam.

As pointed out by Mediero et. al [114] and Volpi and Fiori [116], the relationship between the sources of hazard and the damage variable becomes complex when performing a multivariate analysis [116]. The system may fail if some combination of the associated hydrological variables exceeds a certain return period. If, for instance, Q and V is the pair of random variables which measure the hydrological processes acting on the structure (where Q is the peak inflow and V the inflow volume), $F_{Q,V}$ represents their joint cumulative probability distribution function, Eq. (A. 1):

$$F_{Q,V}(q,v) = Pr[(Q \leq q) \cap (V \leq v)] \tag{A. 1}$$

and $f_{Q,V}$ the related joint probability density function (Eq. (A. 2)):

$$f_{Q,V}(x,y) = \frac{\partial^2 F_{Q,V}(q,v)}{\partial q \partial v} \tag{A. 2}$$

The characteristic damage variable Z representing, in this case, the reservoir water surface elevation does not depend on just one variable, being $Z = g(Q,V)$. Denoted as structure function by Volpi and Fiori [116], $g(.)$ is a function that accounts for the interactions among the structure characteristics, the reservoir operation procedures and the hydrological variables

acting on it. The probability distribution function of Z can be derived using classical statistics as the integral of the joint distribution function of peakflows and volumes over the region of the discharge-volume plane in which the structure function has values $g(q, v) \leq z$:

$$F_Z(z) = \int_{D_z} f_{Q,V}(q, v) dq dv \tag{A. 3}$$

To calculate the cumulative distribution function of the characteristic damage variable, $F_Z(z)$, it is sufficient to find the region D_z for which the value of z equals that of a pool elevation causing upstream damages. The return period of upstream system failure can be easily computed by applying the standard univariate frequency analysis to the random variable Z:

$$T(z) = \frac{1}{1 - F_Z(h)} \tag{A. 4}$$

This return period is the inverse of the probability of having events belonging to the supercritical region $\hat{D}_z$ [136] which comprises all those combinations of Q and V that lead to a value of Z larger than the "damage theshold levels". Figure A. 1a represents the integration region D_z, its boundary or structure function $g(q, v) = z$, and the supercritical region $\hat{D}_z$. This methodology is denoted as the *structure-based* approach [116] or *routed return period* [138]. The structure function can be very complex and its evaluation should be based on simulated experiments [116].

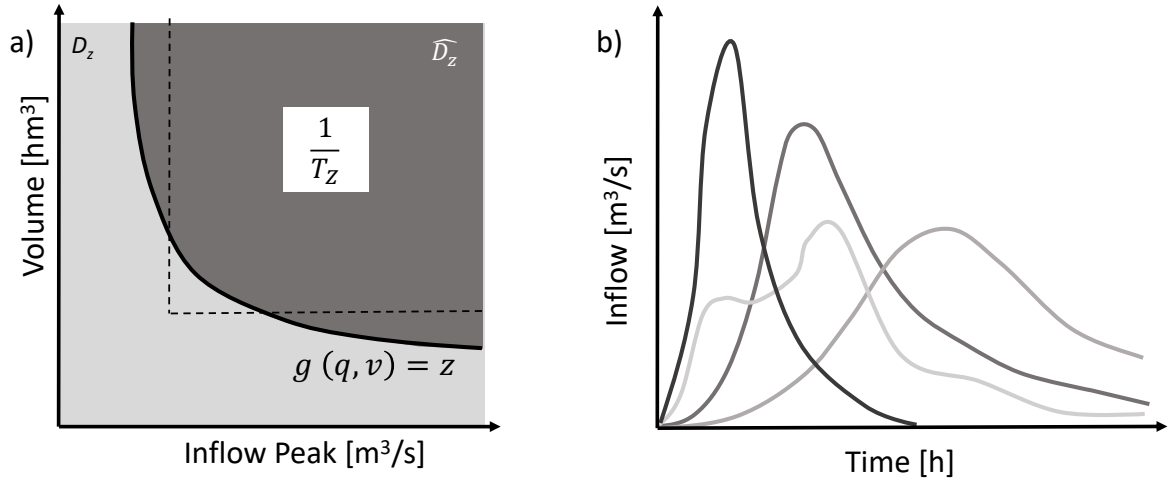

Figure A. 1: Plot showing a graphical representation of: (a) the structure-based bivariate return period; and (b) the family of hydrographs representing all those inflow hydrographs which reach the same maximum water level in the reservoir, $g(Q, V) = z$.

Consequently, instead of using the inverse of the probability of exceeding a specific peakflow or volume, the return period of the hydrological loading is to be understood as the inverse of the probability of exceeding a pre-determine reservoir level, which is directly related to the potential probability of structural failure and to the flooding damages in the reservoir area. When applying that return period definition, a family of hydrographs which generate the same maximum reservoir level and thus pose the system to the same level of risk is obtained. This family is represented by the structure function in the plane peak-volume and depends upon the dam's features such as the reservoir storage capacity, the spillway length, and above all, the reservoir operating policy. Figure A. 1b symbolizes this *family of hydrographs* [139].

The above example refers to a bivariate analysis of inflow volumes, V, and peaks, Q. In this research, however, a third external variable has been included for the study of the system loading,

the initial water level in the reservoir, H_0. Figure A. 2 illustrates how the curve representing the family of hydrographs in the discharge-volume plane (points B and C) is extrapolated to a surface in the three dimensional discharge-volume-initial water level space. The figure displays the situation in which high frequency values of volume and peak, represented by point A, can reach the same maximum water level as lower frequency values (points B and C) due to a higher initial water level.

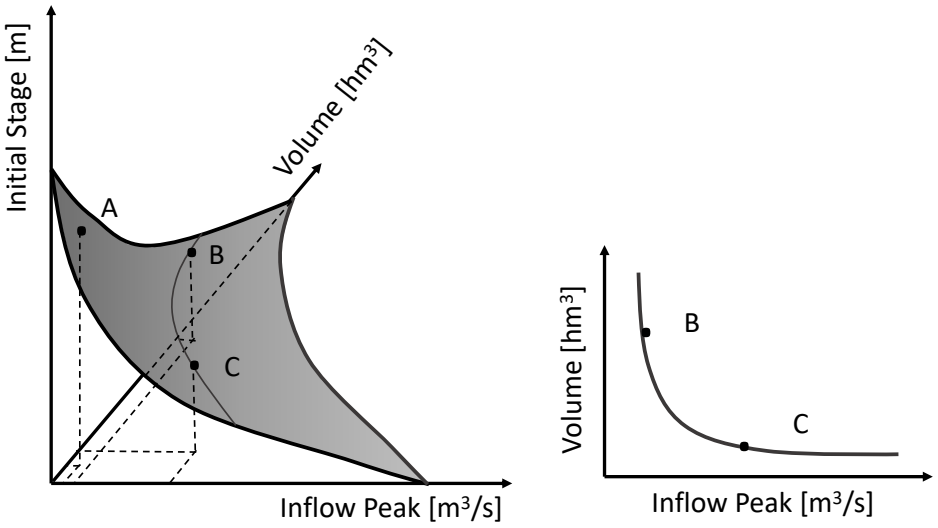

Figure A. 2: Plot representing the plane in the space peak-volume-initial reservoir stage for flood events reaching the same water level in the reservoir including the curve in the peak-volume plane for an equal reservoir stage

Appendix B

Statistical Analysis of Hydrological Variables

Hydrographs may be characterized by several variables such as peak flows, volume, and total duration, among others. The methodology adopted for the estimation of the overall risk takes into account the statistical dependence between peak flows and hydrograph volumes by means of the marginal distribution for maximum peak flow, and the conditioned distribution of the volume with respect to the flow [115]. As previously stated, the inflow hydrograph generation always follows the same scheme [8]: (1) generation of a set of synthetic peak flows, (2) generation of a hydrograph volume value for each peak flow, (3) generation of a hydrograph shape for each synthetic pair of peak and volume. In order to conduct the stochastic generation of inflow hydrographs, first, the marginal distributions from the flood peaks and volumes and their statistical dependence are to be determined.

This appendix comprises a review of the methodology applied for flood frequency analysis. The reader should note that within the technical literature, there is a wide variety of methods concerning the statistical study of flood peaks and volumes. The procedure presented herein is limited to local hydrological analysis and follows the recommendations from the *USGS Bulletin 17 C* [167] and the works carried out by Hosking and Wallis regarding frequency analysis procedures [168]. To clarify the concepts, data analysis examples of the gage station USGS 08072300 located upstream from the Barker Reservoir have been included in this appendix.

Flood Frequency Analysis

Flood frequency analysis is used to predict a possible flood magnitude corresponding to a given return period of occurrence. Due to the limited number of hydrological observations and the rare occurrences of extreme floods, a good estimate of flood frequency is not an easy task. This problem is overcome by fitting sufficiently long series of observed data to distribution functions. The technique of flood frequency analysis involves the following steps:

- Data selection
- Statistical tests and homogeneity analysis.
- Suggestion of theoretical probability distribution for the hydrological observations.
- Estimation of parameters for the selected distribution based on the recorded data set.
- Computation of empirical frequency based on the plotting position formula.
- Comparison between the estimate curve and the observed data plotted.

Peak Flow and Volume Data Selection

The flood frequency analysis starts with the selection of the data required to characterize the hydrological loads affecting the reservoir. As such, synthetic data series records from gage stations at the upstream and downstream regions or reservoir stage measurements are crucial for the hydrologic safety evaluation of dam. In the common practice, in absence of instantaneous data, the daily mean time series are used to estimate the maximum yearly peak flows and hydrograph volumes.

Usually, agencies in charge of evaluating an maintaining hydrologic data publish only the mean daily flow data. The direct use of these time series in flood studies may lead to underestimation of the magnitudes of the inflows with a potential increase of the risk of failure of the structure. Methods to estimate the peak flow based on mean daily data have been study by many authors in the literature. Fill and Steiner in their research on instantaneous peak flow estimation from daily mean data [169] distinguished between two main approaches: one relating to the estimation of the relation between instantaneous flow and the daily mean flow through the peak flow coefficient; and the other to the use of sequences of mean daily flow data from posterior and anterior days to estimate the peak flow. Table B. 1 summarizes several formulas proposed in the literature.

Proponent	Formula
Fuller (1914)	$Q_{max} = Q_d(1 + 2.66\ A^{-0.3})$
Gray (1973)	$Q_{max} = Q_d 10\ A^{*-0.46}$
Sangal (1983)	$Q_{max} = (4Q_2 - Q_1 - Q_3)/2$
Dieter and Steiner (2003)	$Q_{max} = [aQ_2 + b(Q_1 + Q_3)]/k$

A = drainage area (km2)
A* = drainage area (mi2)
Q1 and Q3: mean daily flow for the posterior and anterior day
a , b and k: numerical coefficients determined by regression

Table B. 1: Summary of formulations used to estimate instantaneous peak flow from mean daily flow data (adapted from Fill and Steiner [169])

In this study, it has been decided to follow the first procedure due its broader use in the technical literature [139] [115]. The maximum daily annual flow is converted into maximum annual peak flow according to the Eq. (B. 1):

$$Q_{max} = \left(1 + \frac{a}{A^b}\right) \cdot Q_d = k \cdot Q_d \tag{B. 1}$$

where Q_{max} is the maximum annual peak flow, Q_d is the maximum daily annual discharge, A is the watershed area expressed in km^2, and a and b are parameters that depend on the physical characteristics of the basin.

Chapter 2 addressed some of the available techniques to determine the start and end of storm hydrographs. Applying the local minimum method for baseflow separation recommended by the USGS HYSEP program [43] and introduced by Pettyjohn [44], the duration of surface runoff is calculated from the empirical relation showed in Eq. (B. 2):

$$N = A^{0.2} \tag{B. 2}$$

where N is the number of days after which surface runoff ceases, and A is the drainage area of the watershed in square miles. The local-minimum method checks each day of the anterior and posterior $0.5 \cdot [2N - 1]$ days to determine if it is the lowest discharge before and after the maximum peak flow day [44]. Figure B. 1 presents an schematic of the local minimum baseflow separation method. The local minimums are then connected by straight lines, being the base flow values for each day between local minimums estimated using linear interpolation.

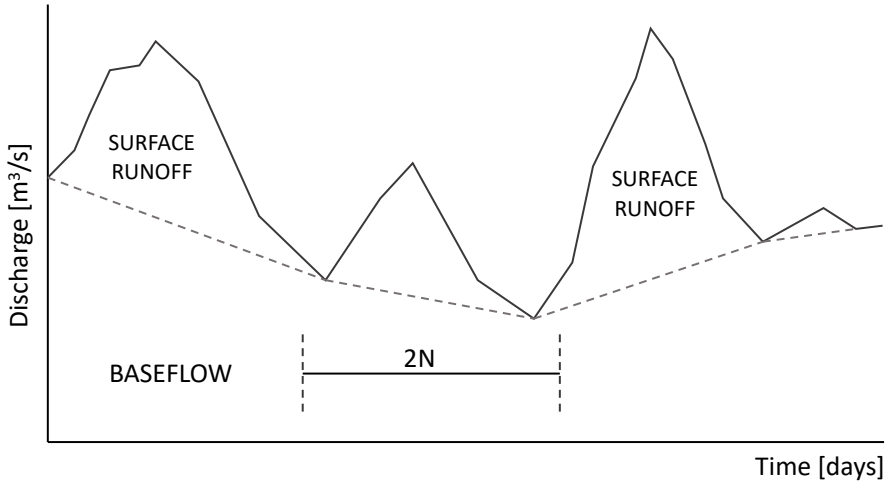

Figure B. 1: Baseflow separation according to the local-minimum method [43]

Statistical Test and Homogeneity Analysis

Hydrological data for any flood frequency analysis should in theory be random, independent and identically distributed. The observations should be originated from the same hydrologic process and be representative of it. Since the data are collected over time, the series should not show any time trend nor abrupt change to satisfy the basic requirement of stationary. When analyzing a set of synthetic records, the above mentioned requirements can be statistically evaluated using randomness, trend and autocorrelation tests.

First, it is recommended by the USGS Bulletin 17C [167] that an annual flood series is must examined for autocorrelation through the use of a correlogram [170]. In an autocorrelated time series, the value in one time step is correlated with the value in a previous (and future) time step. Second, the run test is suggested when it is necessary to test whether a set of data is from a random sequence. A "run" is defined as a set of components sharing the same characteristic. The theory behind the run test states that the probability that one observation is larger or smaller than the previous observation follows a binomial distribution.

Finally, changes in peak-flow generation processes can lead to gradual trends or abrupt shifts in the peak-flow time series. Statistical tests for trends and shifts can be useful for detecting such changes in the peak-flow time series. A common test for trends is the Mann-Kendall test. This test uses Kendall's τ as the test statistic to measure the strength of the monotonic relationship between annual peak streamflow and the year in which it occurred. The Mann-Kendall test is nonparametric and does not require that the data conform to any specific statistical distribution [171]. Figure B. 2 displays the results obtained when conducting the Mann Kendall test for the maximum reservoir stages at the Barker reservoir with a 5% significance level. The graph shows an increasing trend. Nonetheless, the Mann Kendall test suggested that the trend does not alter the stationarity of the series.

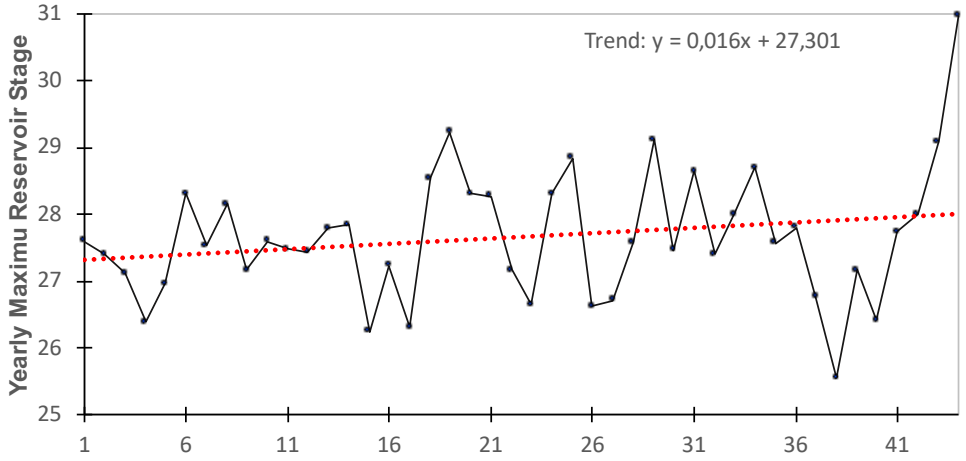

Figure B. 2: Mann Kendall trend test conducted for the analysis of the maximum reservoir levels at the Barker Reservoir

Probability Distribution Function in Flood Frequency Analysis

Once the data has been tested against randomness, autocorrelation and trends, in hydrology, future floods are predicted with probability concepts. By analyzing the sample data, a probability distribution is defined and then is used to estimate the likelihood of a future flood event. This distribution can take many forms and its choice differs from place to place. For instance, the generalized extreme value is commonly used in Europe, whereas the Pearson Type III distribution with a curve fitting method is suggested by the Ministry of Water Resources in China. Hosking and Wallis [168] presented an extensive review of distributions that have been commonly used in hydrology. Herein, the small group of distributions that has been included in the hydrologic data analysis time series have been included: (1) Normal distribution, (2) Log-Normal distribution, (3) Extreme Value Type I (Gumbel) distribution, (4) Exponential distribution, (5) Generalized Extreme Value distribution, (6) Generalized Logistic distribution, and (7) Pearson Type III distribution.

The formulas below show the general form of the Probability Density Functions, $f(x)$, and the Cumulative Density Functions, $F(x)$ included in this thesis for the analysis of annual maximum peak flows and annual maximum hydrograph volumes [168]:

- **Normal Distribution:**

  Parameters (2): μ (location), σ (scale)

  Range of x: $-\infty \leq x \leq \infty$

$$f(x) = \frac{1}{\sqrt{2\pi}} \cdot \frac{1}{\sigma} \cdot e^{\{-(x-\mu)^2/2\sigma^2\}} \tag{B. 3}$$

$$F(x) = \Phi\left(\frac{x-\mu}{\sigma}\right) \quad | \quad \Phi(x) = \int_{-\infty}^{x} f(x)dx \tag{B. 4}$$

- **Log-Normal Distribution:**

  Parameters (3): ξ (location), α (scale), k (shape).

  Range of x: $-\infty \leq x \leq \xi + \alpha/k if k > 0$; $-\infty < x < \infty if k = 0$; $\xi + \alpha/k \leq x < \infty if k < 0$

$$f(x) = \frac{e^{ky-y^2/2}}{\alpha\sqrt{2\pi}} \tag{B. 5}$$

$$y = \begin{cases} -k^{-1}log\{1-k(x-\xi)/\alpha\} & k \neq 0 \\ (x-\xi)/\alpha & k = 0 \end{cases} \tag{B. 6}$$

$$F(x) = \Phi(y) \quad | \quad \Phi(x) = \int_{-\infty}^{x} f(x)dx \tag{B. 7}$$

- **Extreme Value Type I (Gumbel):**

  Parameters (2): ξ (location), α (scale)

  Range of x: $-\infty < x < \infty$

$$f(x) = \alpha^{-1} \cdot \exp\{-(x-\xi)/\alpha\} \exp[-\exp\{-(x-\xi)/\alpha\}] \tag{B. 8}$$

$$F(x) = \exp[-\exp\{-(x-\xi)/\alpha\}] \tag{B. 9}$$

- **Exponential Distribution:**

  Parameters (2): ξ (lower endpoint of the distribution), α (scale).

  Range of x: $\xi \leq x < \infty$.

$$f(x) = \alpha^{-1} \cdot exp\{-(x-\xi)/\alpha\} \tag{B. 10}$$

$$F(x) = 1 - exp\{-(x-\xi)/\alpha\} \tag{B. 11}$$

- **Generalized Extreme Value Distribution:**

  Parameters (3): ξ (location), α (scale), k (shape).

  Range of x: $-\infty \leq x \leq \xi + \alpha/k$if $k > 0$; $-\infty < x < \infty$if $k = 0$; $\xi + \alpha/k \leq x < \infty$if $k < 0$

$$f(x) = \alpha^{-1} \cdot \exp\{-(1-k)y\} \exp[-\exp\{-y\}] \tag{B. 12}$$

$$y = \begin{cases} -k^{-1}log\{1-k(x-\xi)/\alpha\} & k \neq 0 \\ (x-\xi)/\alpha & k = 0 \end{cases} \tag{B. 13}$$

$$F(x) = \exp[-\exp\{-y\}] \tag{B. 14}$$

- **Generalized Logistic Distribution:**

  Parameters (3): ξ (location), α (scale), k (shape).

  Range of x: $-\infty < x < \xi + \alpha/k$if $k > 0$; $-\infty < x < \infty$if $k = 0$; $\xi + \alpha/k \leq x < \infty$if $k < 0$

$$f(x) = \frac{\alpha^{-1} \cdot \exp^{-(1-k)y}}{(1+\exp^{-y})^2} \tag{B. 15}$$

$$y = \begin{cases} -k^{-1}log\{1-k(x-\xi)/\alpha\} & k \neq 0 \\ (x-\xi)/\alpha & k = 0 \end{cases} \tag{B. 16}$$

$$F(x) = 1/(1+\exp^{-y}) \tag{B. 17}$$

- **Pearson Type III Distribution:**

  Parameters (3): μ (location), σ (scale), γ (shape).

  If $\gamma \neq 0$, let $\alpha = 4/\gamma^2$, $\beta = 0.5\sigma\gamma$, and $\xi = \mu - 2\sigma/\gamma$. If $\gamma > 0$, then the range of x is $\xi \leq x < \infty$ and

$$f(x) = \frac{(x-\xi)^{\alpha-1}e^{-(x-\xi)/\beta}}{\beta^{\alpha}\Gamma(\alpha)} \tag{B. 18}$$

$$F(x) = G\left(\alpha, \frac{x-\xi}{\beta}\right)/\Gamma(\alpha) \tag{B. 19}$$

  If $\gamma = 0$, then the distribution is Normal, the range of x is $-\infty < x < \infty$ and

$$f(x) = \phi\left(\frac{x-\mu}{\sigma}\right) \quad | \quad F(x) = \Phi\left(\frac{x-\mu}{\sigma}\right) \tag{B. 20}$$

  If $\gamma < 0$, then the range of x is $-\infty < x \leq \xi$ and

$$f(x) = \frac{(x-\xi)^{\alpha-1}e^{-(x-\xi)/\beta}}{\beta^{\alpha}\Gamma(\alpha)} \tag{B. 21}$$

$$F(x) = G\left(\alpha, \frac{x-\xi}{\beta}\right)/\Gamma(\alpha) \tag{B. 22}$$

  where

$$G(\alpha, x) = \int_0^x t^{\alpha-1}e^{-t}dt \quad | \quad \Gamma(x) = \int_0^{\infty} t^{x-1}e^{-t}dt \tag{B. 23}$$

Parameters Estimation

Each of the listed probability distribution function contains two to three parameters that must be determined. In the technical literature, there are many different methodologies to estimate the parameters of distribution functions. Three of the most used ones are the Moments Method (Mom), the Maximum Likelihood Method (ML) and the L-Moments Method (L-Mom). The first one is a very simple and sound procedure based on the computation of the traditional mean, variance coefficient (CV) and the skewness parameter (CS). This method is very suitable for symmetrical distribution functions, such as the Normal Distribution. Environment Canada uses, and recommends the MOM technique to estimate the parameters for Extreme Value Type I distributions. However, it leads to inappropriate results for skewed distributions.

In order to addressed the skewed distributions, Hosking and Wallis [168] developed the L-Mom method. The L-Moment estimators are desired because they are easy to work with, and more

reliable as they are less sensitive to outliers [172]. As such, this procedure has been used in this thesis for the assessment of the different distribution function parameters.

The Empirical Distribution

When making flood frequency analysis, it is necessary to compare the assumed distribution with the sample data. Generally, the sample values are plotted in a figure by assigning each of them an exceedance probability based on a plotting position formula showed in Eq. (B. 24):

$$p_i = \frac{i - a}{N + 1 - 2a} \tag{B. 24}$$

where p_i is the annual exceedance probability of the i ranked observed data, N is the total number of values and a is the plotting position parameter. Table B. 2 summarizes the main plotting position formulas reported by Cunnane [142] and Stedinger et. al [143]. As previously stated, in this thesis, the Weibull plotting position formula has been used for the estimation of the water level annual exceedance probability (AEP) [22], and the Gringorten plotting parameter was utilized for the extreme analysis of volumes and peaks [173]. This implies that in Eq. (B. 24) a equals 0 and 0.44 [142].

Proponent	Formula	a	Parent Distribution
Weibull (1939)	$\frac{i}{n+i}$	0	All distributions
Beard (1943)	$\frac{i - 0.3175}{n + 0.365}$	0.3175	All distributions
Blom (1958)	$\frac{i - 3/8}{n + 1/4}$	0.375	Normal Distributions
Cunnane (1977)	$\frac{i - 0.4}{n + 0.2}$	0.4	GEV and PIII distributions
Gringorten (1963)	$\frac{i - 0.44}{n + 0.12}$	0.44	Exponential, EV1 and GEV distributions
Hazen (1914)	$\frac{i - 0.5}{n}$	0.5	Extreme Value Distributions

Table B. 2: Plotting position formulas [143] [142]

In the majority of the situations, plotting positions only need to deal with a systematically recorded annual flood series. However, in some specific occasions, like in the case of the Barker Reservoir, in addition to the data measured during the period of record, a number of extra-large floods which occurred during an extended historical period are also available. According to the USGS Bulletin 17 C, high outliers should also be included as historical data for the empirical study of the annual exceedance probability [167]. The plotting position formula when including historical flood data is presented in Eq. (B. 25):

$$p_i = \begin{cases} \dfrac{i - a}{k + 1 - 2a} \cdot \dfrac{k}{n} & i = 1, ..., k \\ \dfrac{k}{n} + \dfrac{n - k}{n} \cdot \dfrac{i - k - a}{s - e + 1 - 2a} & i = k + 1, ..., g \end{cases} \tag{B. 25}$$

where in a total of g known floods, k of them are known to be the k largest in a period of n years. The n year period contains within it some systematic record period of s years. Finally, of

the k largest floods, e of them occurred during the systematic record [174], being the remaining floods either historical or high outliers.

Statistics to Compare Empirical Frequency with Theoretical Frequency

To specify the marginal distribution function that best fits within the empirical analysis of the observed data, various statistical methods are available in the literature [56]. In this study, the mean square deviation, Eq. (B. 26), the Kolmogorov-Smirnov test, Eq. (B. 27), and the dimensionless difference between the observed and estimated values, Eq. (B. 28), have been taken as selection criteria:

$$MSD = \sqrt{\frac{\sum_{i=1}^{n}(x_i - y_i)^2}{n}} \tag{B. 26}$$

$$KS = max \mid x_i - y_i \mid \tag{B. 27}$$

$$e = \frac{1}{n}\sum_{i=1}^{n}\frac{x_i - y_i}{x_i} \tag{B. 28}$$

where x_i is the theoretic frequency for observation and y_i is the corresponding empirical frequency. An example summarizing the steps required for the estimation of the most appropriate marginal distribution is shown in Fig. B. 3. The illustration reflects the statistical analysis of the peak inflow volumes arriving to the Barker Reservoir. The analysis was conducted considering the volume recorded during Hurricane Harvey as a historical observation. The observed data depicted by the blue diamonds was plotted in accordance with Eq. (B. 25). Meanwhile, the best fit is represented by the Generalized Logistic distribution function with location parameter $\xi = 17.99$, scale parameter $\alpha = 7.26$ and shape parameter $k = -0.523$.

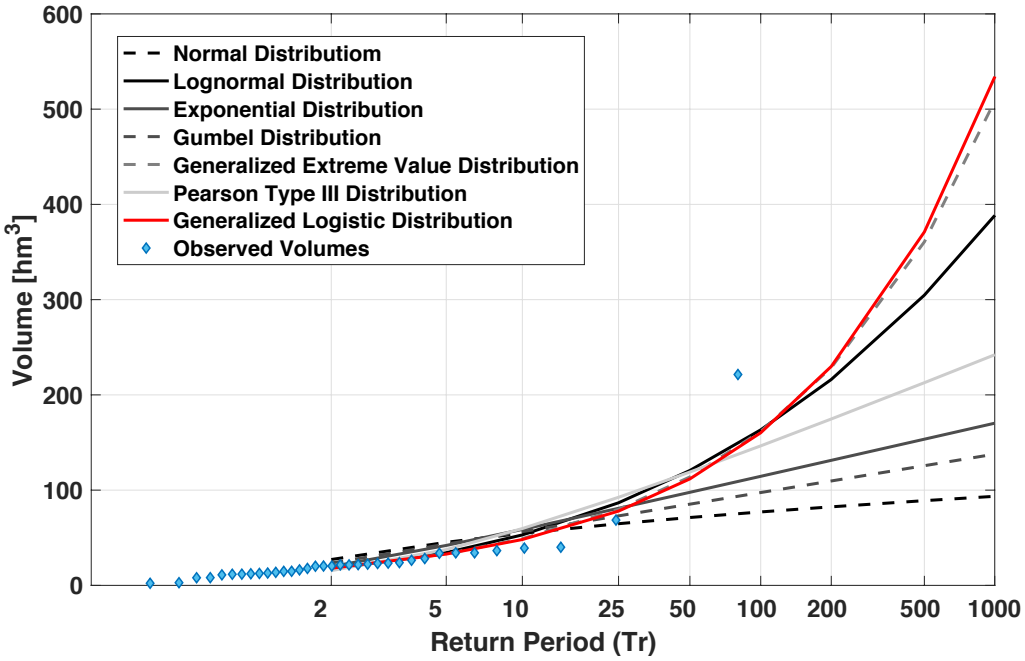

Figure B. 3: Maximum annual peak volume analysis for the Barker Reservoir without Hurricane Harvey volume. The best fit is represented by the Generalized Logistic distribution function with location parameter $\xi = 17.9946$, scale parameter $\alpha = 7.2612$ and shape parameter $k = -0.5288$

Appendix C

Reservoir Routing Modified Puls Method

To transform inflow hydrographs to outflow hydrographs the continuity equation of the system needs to be solved. The Modified Puls Method, also known as Level Pool Routing method [39], has been employed for the implementation of the proposed overall risk definition. The Level Pool Routing calculates outflow hydrograph from a reservoir with horizontal water surface given its inflow hydrograph and storage-outflow characteristics. In their study Fiorentini and Orlandini [36] stated that the Modified Puls Method solves the system continuity equation with an acceptable degree of accuracy. Due to its ease of use, the method has been adopted by many other authors for studies concerning the hydrological safety of dams. For instance, Sordo-Ward et. al [131] [9] proposed its application in their investigations concerning extreme flood abatement in large dams with fixed-crested and gated spillways. The continuity equation for storage in a reservoir is a first order differential equation which is generally expressed as:

$$\frac{dS}{dt} = I(t) - O(t) \tag{C. 1}$$

where $\mathrm{d}S/\mathrm{d}t$ symbolizes the change in volume of water stored in the reservoir during the time t, $I(t)$ is the inflow rate arriving to the reservoir as a function of time; and $O(t)$ the releases from the reservoir. Using the Modified Puls Method, the time horizon is divided into intervals of duration Δt, and the continuity equation, Eq. (C. 1) is integrated over each time interval as shown in Eq. (C. 2). The smaller the time step the higher the accuracy of the method. However, smaller time steps imply higher computational cost which could slow down the calculations since a large number of flood events is also desired. For the implementation of the methodology a time step of an hour has been selected.

$$\int_{S_j}^{S_j+1} dS = \int_{j\Delta t}^{(j+1)\Delta t} I(t)dt - \int_{j\Delta t}^{(j+1)\Delta t} O(t)dt \tag{C. 2}$$

The inflow values at the beginning and end of the j-th time interval are I_j and I_{j+1}, respectively, and the outflows are O_j and O_{j+1}. If the variation of inflow and outflow over a time interval is approximated as linear, the change in storage over the interval $S_{j+1} - S_j$, can be found by discretizing Eq.(C. 1) as:

$$S_{j+1} - S_j = \frac{I_j + I_{j+1}}{2} \cdot \Delta t - \frac{O_j + O_{j+1}}{2} \cdot \Delta t \tag{C. 3}$$

Assuming that the values of I_j and I_{j+1} are forecasted, and Q_j and S_j are known, Eq. (C. 3) contains two unfamiliar variables, which can be isolated by multiplying Eq. (C. 3) by $2/\Delta t$. Rearranging the result Eq. (C. 3) yields:

$$\left(\frac{2S_{j+1}}{\Delta t} + O_{j+1}\right) = (I_j + I_{j+1}) + \left(\frac{2S_j}{\Delta t} + O_j\right) \tag{C. 4}$$

In order to calculate the outflow O_{j+1}, a storage-outflow-function relating $2S/\Delta t + O$ and O is needed. A method for developing this function using elevation-storage and elevation-outflow relationships was explained by Chow [39] and is shown in Fig. C. 1. For a given value of water surface elevation, the values of storage and outflow are determined. Then, the value of $2S/\Delta t + O$ is calculated and plotted in the horizontal axis of a graph with the value of outflow O in the vertical axis. In routing the flow through time interval j, all terms on the right side of Eq. (C. 4) are known. Consequently, the values $2S_{j+1}/\Delta t + O_{j+1}$ can be computed. To set up the data required for the next time interval, the value of $2S_{j+1}/\Delta t - O_{j+1}$ is calculated by:

$$\left(\frac{2S_{j+1}}{\Delta t} + O_{j+1}\right) = \left(\frac{2S_{j+1}}{\Delta t} + O_{j+1}\right) - 2O_{j+1} \tag{C. 5}$$

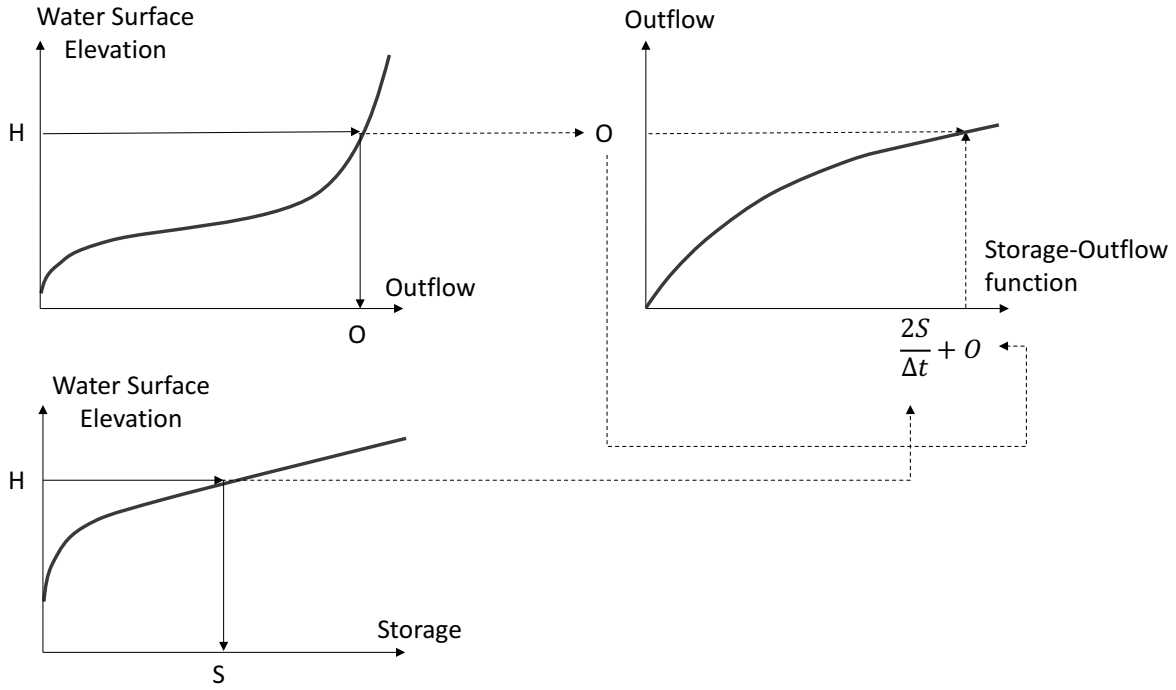

Figure C. 1: Development of the storage-outflow function on the basis of storage-elevation and elevation-outflow curves adopted from Chow 1988 [39]

Appendix D

Sensitivity Analysis of the Parametric Rule

Analysis of the Parameter m_1

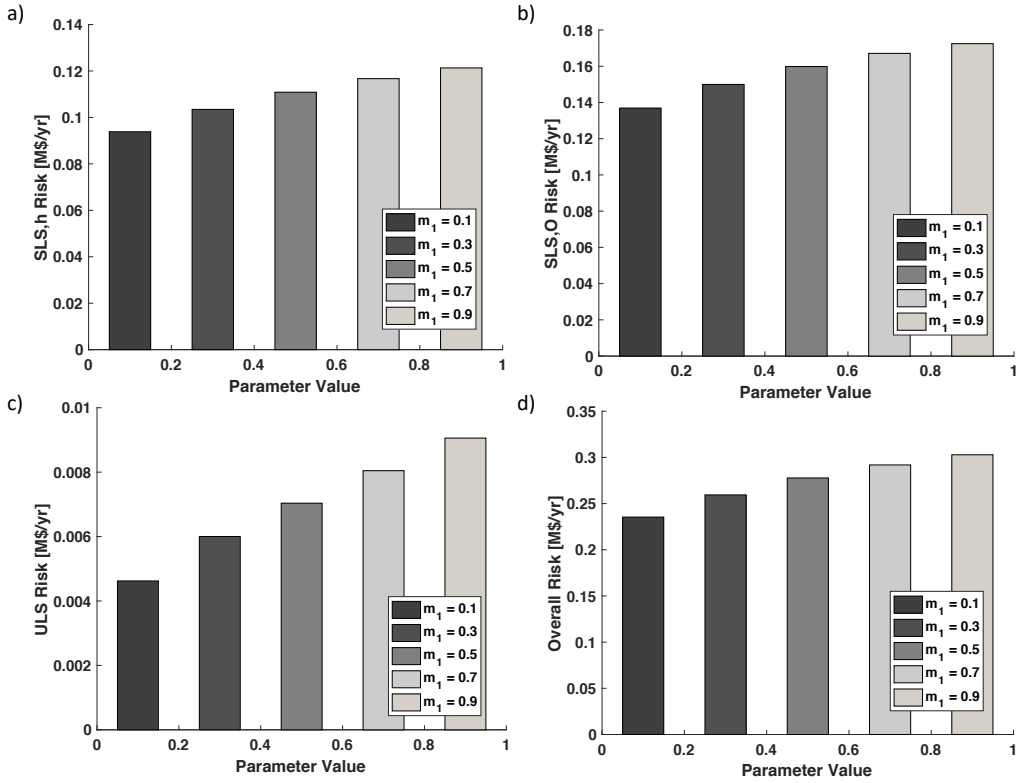

Figure D. 1: Bar diagrams representing the performance of the system under diverse values of m_1 in terms of: (a) upstream flooding risk, (b) downstream flooding risk, (c) dam break risk, and (d) aggregated sum risk

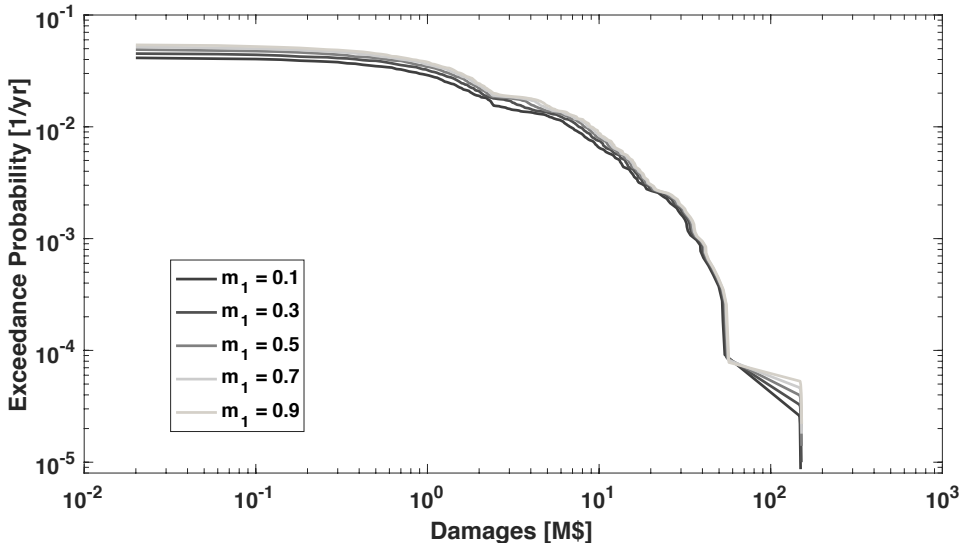

Figure D. 2: Frequency-damages curves representing the performance of the system in terms of overall risk under diverse values of m_1

Analysis of the Parameter m_2

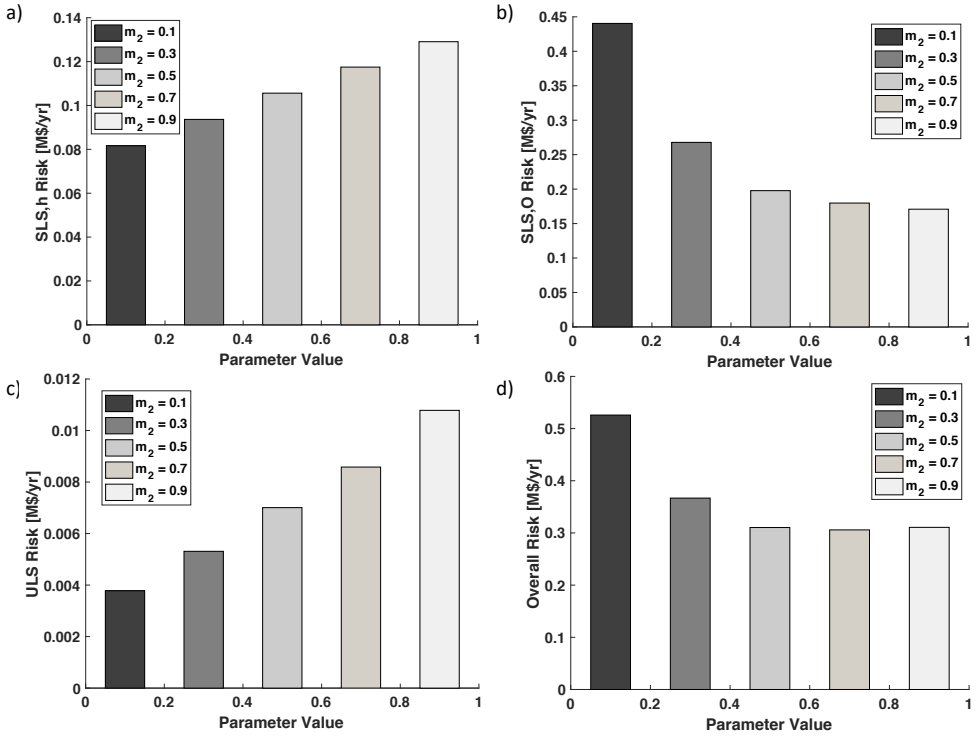

Figure D. 3: Bar diagrams representing the performance of the system under diverse values of m_2 in terms of: (a) upstream flooding risk, (b) downstream flooding risk, (c) dam break risk, and (d) aggregated sum risk

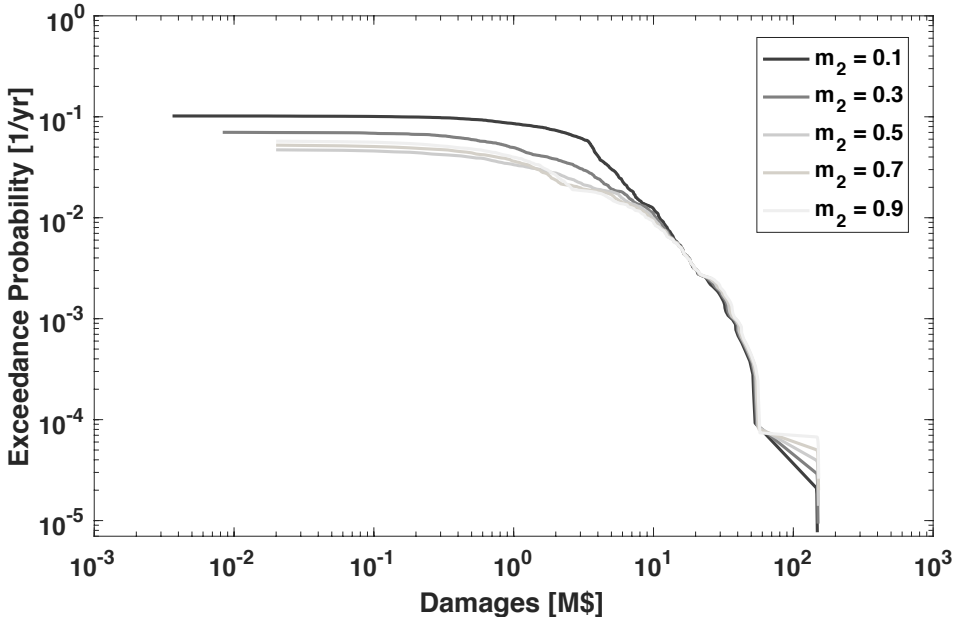

Figure D. 4: Frequency-damages curves representing the performance of the system in terms of overall risk under diverse values of m_2

Analysis of the Prameter s_1

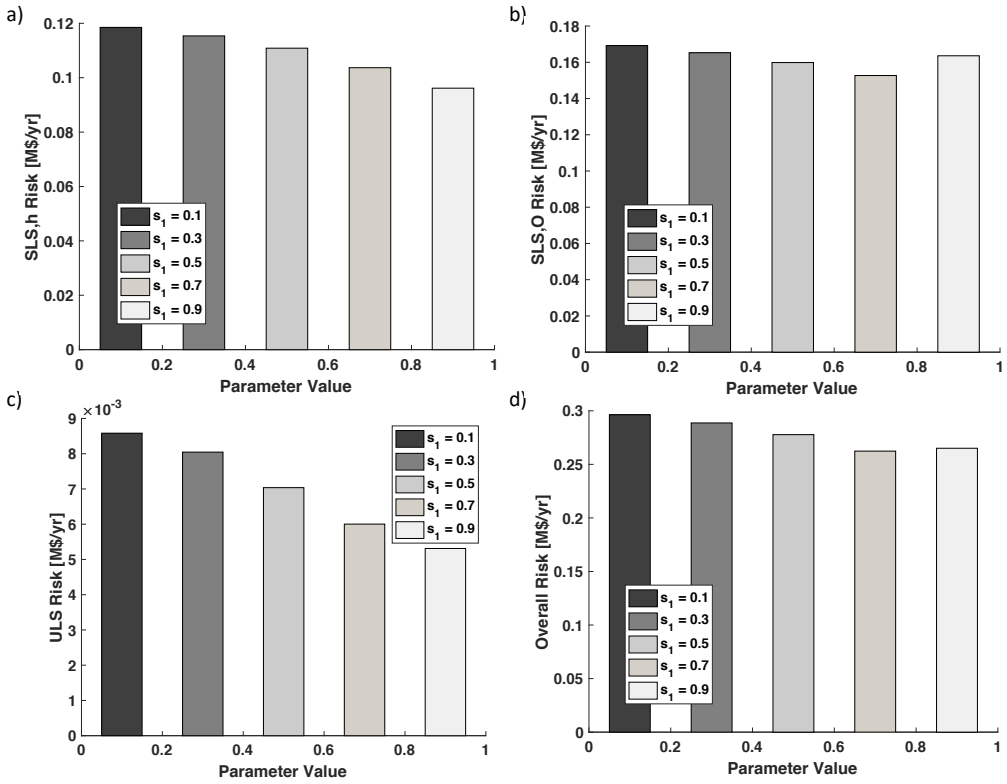

Figure D. 5: Bar diagrams representing the performance of the system under diverse values of s_1 in terms of: (a) upstream flooding risk, (b) downstream flooding risk, (c) dam break risk, and (d) aggregated sum risk

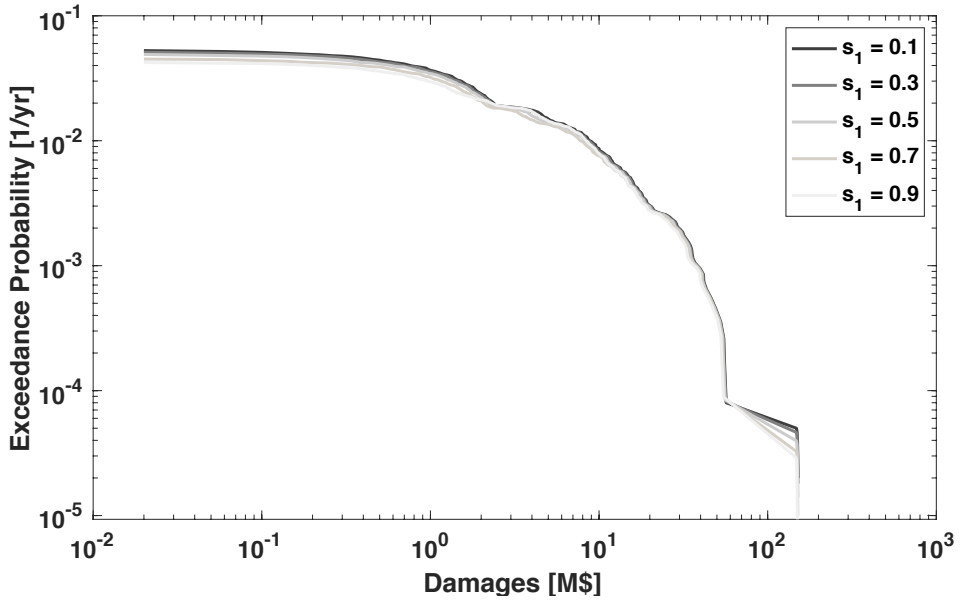

Figure D. 6: Frequency-damages curves representing the performance of the system in terms of overall risk under diverse values of s_1

Appendix D

Barker Reservoir System Results

The proposed risk-based optimization framework has been applied in a study of the Barker Reservoir located in Buffalo Bayou Watershed. This appendix comprises the main characteristics of the system as well as the main results obtained.

- **Appendix E.1:** Barker Dam-Reservoir Characteristics
- **Appendix E.2:** Statistical Analysis of Reservoir Pool Elevations
- **Appendix E.3:** Statistical Analysis of Peak Inflows
- **Appendix E.4:** Statistical Analysis of Hydrograph Volumes
- **Appendix E.5:** Barker Dam System Response Curves
- **Appendix E.6:** Barker Dam System Upstream Consequence Curve
- **Appendix E.7:** Barker Dam System Downstream Consequence Curves
- **Appendix E.8:** Inundation Maps During Hurricane Harvey
  - Appendix E.8.1: Flooding Map Barker Reservoir during Hurricane Harvey
  - Appendix E.8.2: Flooding Map Buffalo Bayou with Releases from Barker Reservoir during Hurricane Harvey
- **Appendix E.9:** Risk Assessment Barker Dam-Reservoir System
- **Appendix E.10:** Risk Mitigation Measure Barker Dam-Reservoir System

Barker Dam-Reservoir System Characteristics

Main Characteristics of the Barker Dam-Reservoir System

BARKER RESERVOIR

DRAINAGE AREA	337 square kilometers		*DOWNSTREAM CHANNEL CAPACITY*	56,6 m3/s	
DAMS			*Construction period*	1942 - 1945	
Type	Rolled earth embankment		*Gating of two additional conduits*	1948 - 1949	
Length	22000 m		*Gating of last uncontrolled conduits*	1962 - 1963	
Height (above stream bed)	13,0 m				
			EMERGENCY OPERATION SCHEDULE		
RESERVOIR	[m NAVD88]	[hm3]	Activation Level (USACE,2012)	29,17 m NAVD88	
Conduit Invert	21,40	0	Deactivation Level (USACE,2012)	28,92 m NAVD88	
Limits of Government Land	28,96	102,3			
100-Year Flood (USACE,2012)	29,57	132,6	*REPRESENTATIVE FLOODS*	Peak Flow	Volume
Standard Project Flood	29,96	154,3	100 yr. HEC-HMS (HCFCD,2018)	725,4	70,6
Natural ground at the end of the dam	31,70	258,5	500 yr. HEC-HMS (HCFCD,2018)	1190,5	113,9
North End Spillway	32,16	290,4	Hurricane Harvey	2305,0	237,0
South End Spillway	32,52	316,5	Standard Project Flow	2462,5	154,3
Top of the dam	34,47	-	Spillway Design Flood	7242,8	344,2
CONDUITS	5 gated concrete box culvert conduits, 2,7 m wide x 2,15 m high x 58,0 m long		MAXIMUM ALLOWED RELEASES	266,5 m3/s	

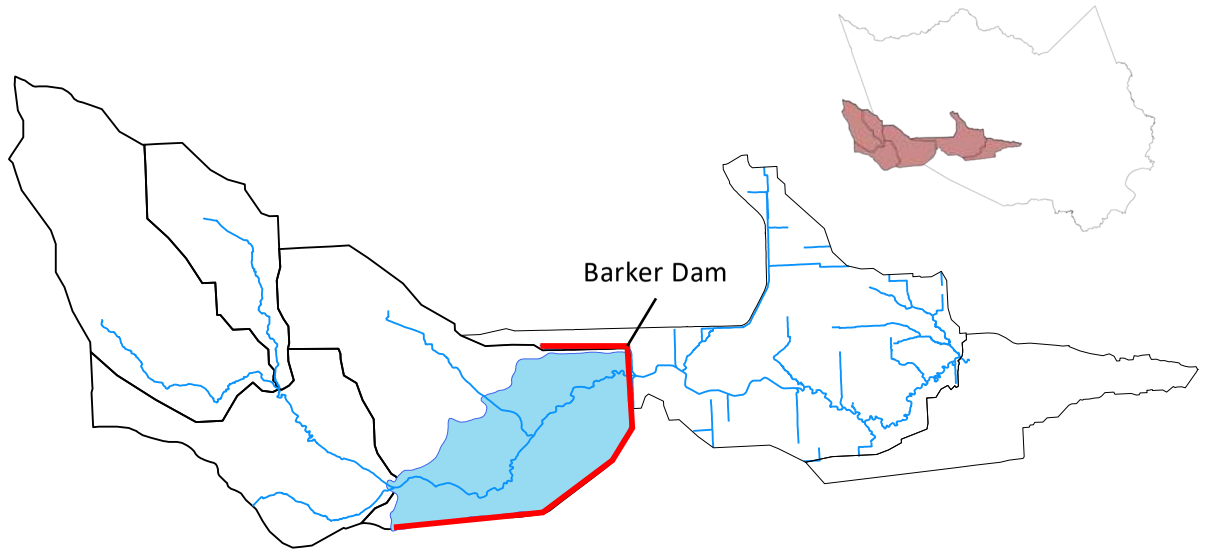

Barker and Buffalo Bayou Watersheds

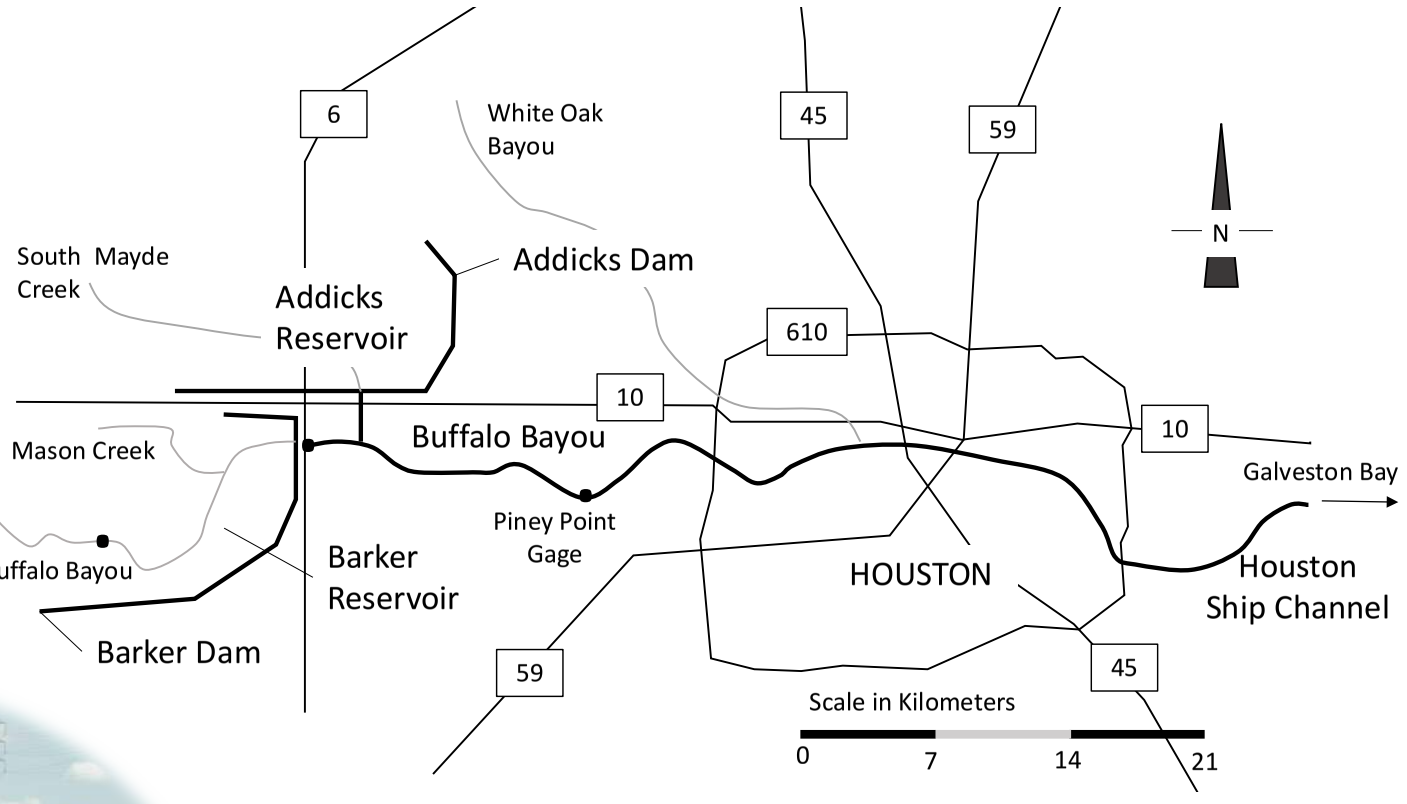

Barker Dam-Reservoir System Location Map

Barker Dam North end auxiliary spillway

Barker Dam outlet conduits releasing wáter towards Buffalo Bayou

TUDelft	DELFT UNIVERSITY OF TECHNOLOGY DEPARTMENT OF HYDRAULIC STRUCTURES AND FLOOD RISK
TITLE OF THE PROJECT: **RISK-BASED OPTIMIZATION OF RESERVOIR EMERGENCY OPERATION**	APPENDIX: E.1
NAME OF THE APPENDIX: **BARKER RESERVOIR CHARACTERITICS AND LOCATION**	SCALE:

Statistical Analysis Reservoir Levels

Order	Water Level [m NAVD88]	AEP (a = 0)	T [yr.]
1	30,97	0,02222	88,0000
2	29,23	0,04444	45,0000
3	29,12	0,04494	22,2529
4	29,09	0,06715	14,8923
5	28,83	0,08936	11,1908
6	28,69	0,11157	8,9630
7	28,65	0,13378	7,4749
8	28,54	0,15599	6,4106
9	28,31	0,17820	5,6116
10	28,31	0,20041	4,9897
11	28,31	0,22262	4,4919
12	28,29	0,24483	4,0844
13	28,16	0,26705	3,7447
14	28,00	0,28926	3,4571
15	28,00	0,31147	3,2106
16	27,85	0,33368	2,9969
17	27,8	0,35589	2,8099
18	27,79	0,37810	2,6448
19	27,73	0,40031	2,4981
20	27,60	0,42252	2,3667
21	27,59	0,44473	2,2485
22	27,58	0,46694	2,1416
23	27,57	0,48915	2,0444
24	27,53	0,51136	1,9556
25	27,48	0,53357	1,8742
26	27,46	0,55579	1,7993
27	27,43	0,57800	1,7301
28	27,40	0,60021	1,6661
29	27,39	0,62242	1,6066
30	27,23	0,64463	1,5513
31	27,17	0,66684	1,4996
32	27,17	0,68905	1,4513
33	27,16	0,71126	1,4060
34	27,11	0,73347	1,3634
35	26,96	0,75568	1,3233
36	26,76	0,77789	1,2855
37	26,71	0,80010	1,2498
38	26,64	0,82231	1,2161
39	26,62	0,84452	1,1841
40	26,41	0,86674	1,1538
41	26,39	0,88895	1,1249
42	26,30	0,91116	1,0975
43	26,25	0,93337	1,0714
44	25,55	0,95558	1,0465

Annual Maximum Reservoir Level Empirical Distribution

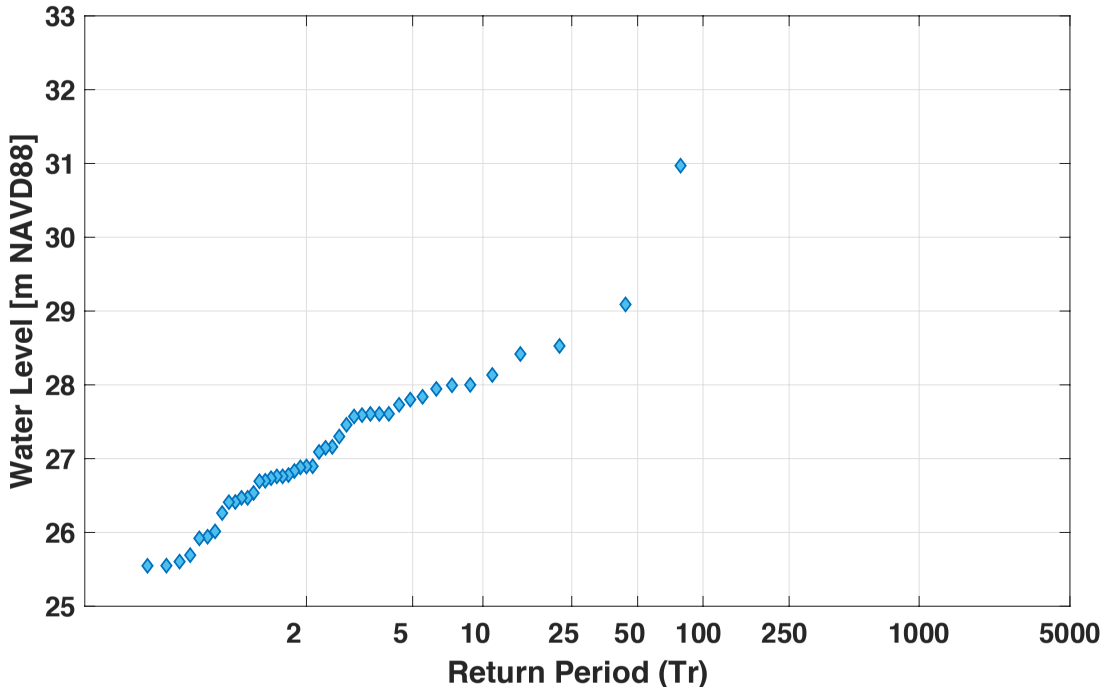

Initial Reservoir Level Exceedance Probability Curve

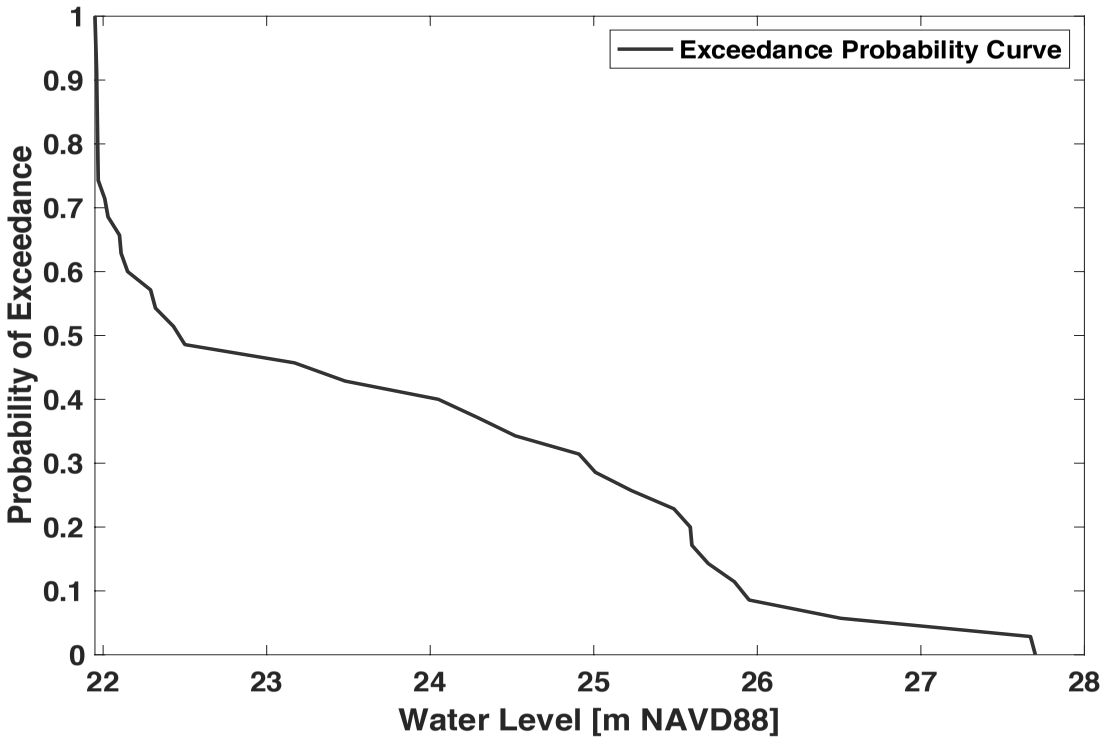

TUDelft

DELFT UNIVERSITY OF TECHNOLOGY

DEPARTMENT OF HYDRAULIC STRUCTURES AND FLOOD RISK

TITLE OF THE PROJECT:
RISK-BASED OPTIMIZATION OF RESERVOIR EMERGENCY OPERATION

APPENDIX: E.2

NAME OF THE APPENDIX:
STATISTICAL ANALYSIS OF RESERVOIR LEVELS

SCALE:

Statistical Analysis Peak Flows

Order	Date [dd/mm/yy]	Month	Qmax	AEP (a = 0,44)	T [yr.]
1	28/8/17	8	2212,522	0,01429	70,0000
2	18/4/16	4	781,618	0,04452	22,4643
3	21/2/94	2	542,696	0,07299	13,7012
4	14/9/08	9	520,581	0,10146	9,8564
5	23/11/04	11	490,522	0,12993	7,6966
6	26/5/15	5	486,595	0,15840	6,3132
7	4/11/02	11	458,572	0,18687	5,3513
8	28/4/09	4	444,380	0,21534	4,6438
9	20/9/79	9	429,794	0,24381	4,1015
10	16/10/06	10	400,413	0,27228	3,6727
11	22/12/91	12	395,029	0,30075	3,3250
12	27/5/14	5	380,255	0,32922	3,0374
13	4/4/93	4	369,467	0,35770	2,7957
14	14/5/82	5	336,849	0,38617	2,5896
15	31/8/81	8	330,016	0,41464	2,4117
16	9/1/13	1	324,568	0,44311	2,2568
17	4/2/92	2	308,423	0,47158	2,1205
18	9/6/86	6	306,526	0,50005	1,9998
19	11/2/85	2	303,938	0,52852	1,8921
20	15/3/07	3	298,927	0,55699	1,7954
21	12/6/87	6	258,676	0,58546	1,7080
22	1/2/05	2	245,113	0,61393	1,6288
23	21/1/80	1	243,880	0,64240	1,5567
24	28/3/01	3	239,647	0,67088	1,4906
25	10/2/83	2	238,251	0,69935	1,4299
26	11/3/12	3	233,425	0,72782	1,3740
27	25/10/84	10	227,557	0,75629	1,3222
28	12/2/10	2	206,692	0,78476	1,2743
29	18/5/89	5	205,901	0,81323	1,2297
30	21/2/90	2	201,069	0,84170	1,1881
31	19/1/78	1	198,223	0,87017	1,1492
32	18/11/03	11	180,388	0,89864	1,1128
33	24/11/00	11	143,213	0,92711	1,0786
34	5/1/11	1	84,389	0,95559	1,0465
35	18/3/88	3	61,535	0,98406	1,0162

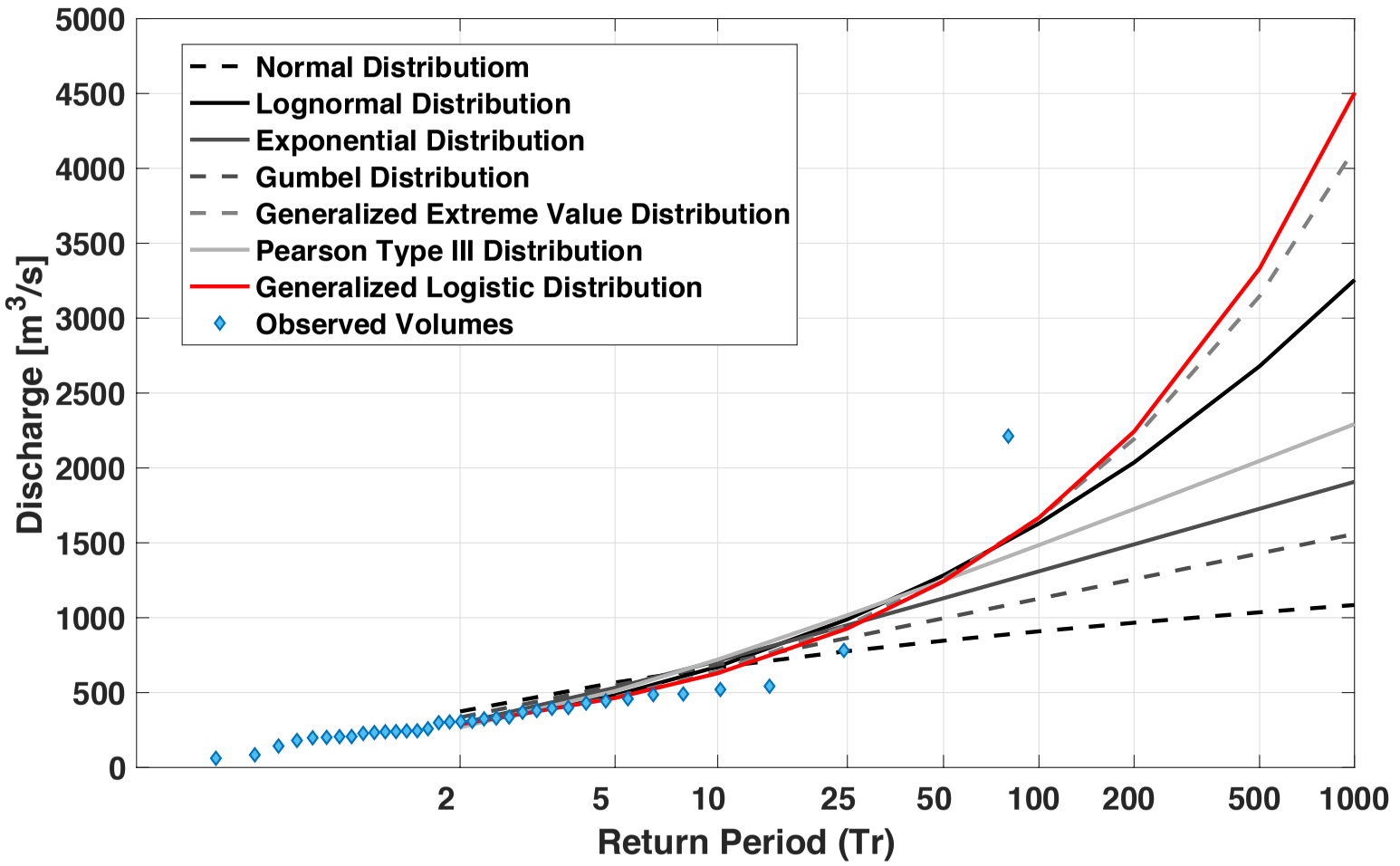

T	F	NORM	LOG	EXP	EV1	GEV	GL	PEAR
2	0,5000	374,00	279,10	294,30	334,50	285,2	288,1	267,7
5	0,8000	567,60	482,00	532,20	546,80	468,6	463,7	510,2
10	0,9000	668,80	673,60	712,10	687,30	642,5	629,20	720,8
25	0,9600	776,70	989,30	949,90	864,80	948,3	927,70	1016,6
50	0,9800	846,40	1282,60	1129,90	996,50	1259,7	1242,70	1248,5
100	0,9900	909,10	1629,50	1309,80	1127,20	1664,8	1667,70	1485,2
200	0,9950	966,50	2036,60	1489,70	1257,50	2193,1	2243,30	1725,4
500	0,9980	1096,10	2679,30	1727,50	1429,30	3147,1	3331,30	2047
1000	0,9990	1084,90	3254,40	1907,50	1559,20	4129,3	4502,50	2292,6
5000	0,9998	1188,30	4937,40	2325,20	1860,60	7732,9	9109,4	2869

NOTE:
NORM = Normal distribution function
LOG = Lognormal distribution function
EXP = Exponential distribution function
EV1 = Gumbel distribution function
GEV = Generalized Extreme Value
GL = Generalized Logistic
PEAR = Pearson Type III distribution function

Best-Fit Tests

	NORM	LOG	EXP	EV1	GEV	GL	PEAR
e	0,35	0,1588	0,1811	0,2144	0,1272	0,1167	0,2157
KS	0,4415	0,00079144	0,6403	0,8389	0,9672	0,9672	0,6403
MSD	241,9	136,8409	180,2459	204,68	129,1767	127,7696	160,9145

NOTE:
e = Dimensionless difference between the observed and estimated values
KS = Kolmogorov-Smirnov test
MSD = Mean Square Deviation

TU Delft

DELFT UNIVERSITY OF TECHNOLOGY

DEPARTMENT OF HYDRAULIC STRUCTURES AND FLOOD RISK

TITLE OF THE PROJECT:
RISK-BASED OPTIMIZATION OF RESERVOIR EMERGENCY OPERATION

APPENDIX: E.3

NAME OF THE APPENDIX:
STATISTICAL ANALYSIS PEAK FLOWS

SCALE:

Statistical Analysis Peak Volumes

Order	Date [dd/mm/yy]	Month	Duration [days]	Volume [hm3]	AEP (a = 0.44)	T [yr.]
1	28/8/17	8	5	221,40	0,01429	70,0000
2	18/4/16	4	4	68,55	0,04452	22,4643
3	4/11/02	11	4	40,05	0,07299	13,7012
4	23/11/04	11	4	39,14	0,10146	9,8564
5	22/12/91	12	5	36,48	0,12993	7,6966
6	28/4/09	4	4	34,18	0,15840	6,3132
7	27/5/14	5	4	34,16	0,18687	5,3513
8	20/9/79	9	4	33,69	0,21534	4,6438
9	21/2/94	2	3	28,20	0,24381	4,1015
10	21/1/80	1	5	26,37	0,27228	3,6727
11	4/2/92	2	4	23,89	0,30075	3,3250
12	9/6/86	6	4	23,34	0,32922	3,0374
13	14/5/82	5	5	22,98	0,35770	2,7957
14	12/6/87	6	4	22,29	0,38617	2,5896
15	15/3/07	3	4	21,77	0,41464	2,4117
16	14/9/08	9	3	21,53	0,44311	2,2568
17	4/4/93	4	3	21,48	0,47158	2,1205
18	31/8/81	8	4	20,33	0,50005	1,9998
19	11/3/12	3	5	20,31	0,52852	1,8921
20	26/5/15	5	3	20,11	0,55699	1,7954
21	1/2/05	2	5	17,79	0,58546	1,7080
22	28/3/01	3	4	16,25	0,61393	1,6288
23	18/5/89	5	4	14,80	0,64240	1,5567
24	10/2/83	2	4	14,71	0,67088	1,4906
25	12/2/10	2	4	12,97	0,69935	1,4299
26	11/2/85	2	3	12,55	0,72782	1,3740
27	16/10/06	10	3	12,19	0,75629	1,3222
28	9/1/13	1	4	11,78	0,78476	1,2743
29	18/11/03	11	4	11,70	0,81323	1,2297
30	19/1/78	1	3	11,18	0,84170	1,1881
31	25/10/84	10	3	11,05	0,87017	1,1492
32	24/11/00	11	4	8,12	0,89864	1,1128
33	21/2/90	2	4	8,01	0,92711	1,0786
34	18/3/88	3	3	2,83	0,95559	1,0465
35	5/1/11	1	3	2,20	0,98406	1,0162

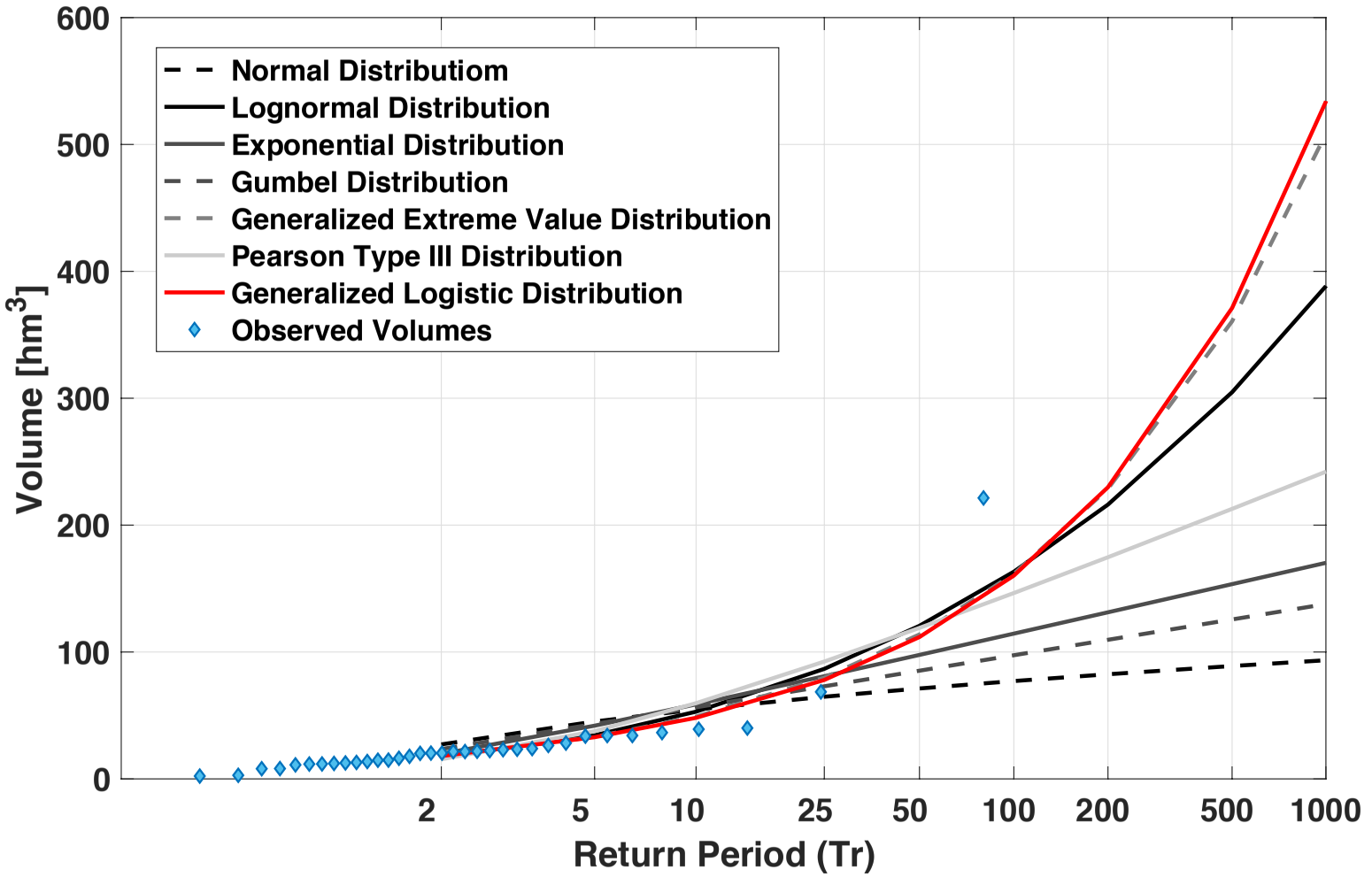

T	F	NORM	LOG	EXP	EV1	GEV	GL	PEAR
2	0,5000	27,17	17,04	19,73	23,48	17,8	18	15,46
5	0,8000	45,23	34,40	41,93	43,29	33,1	32,8	37,57
10	0,9000	54,68	52,98	58,72	56,40	49	48,1	59,66
25	0,9600	64,75	86,71	80,91	72,97	79,8	78	92,48
50	0,9800	71,25	120,64	97,71	85,26	113,8	111,8	118,99
100	0,9900	77,11	163,30	114,50	97,46	161,6	160,2	146,47
200	0,9950	82,46	216,17	131,29	109,62	228,6	29,9	174,68
500	0,9980	88,96	304,71	153,48	125,66	360,6	371,1	212,8
1000	0,9990	93,51	388,32	170,27	137,78	508,4	533,8	242,12
5000	0,9998	103,17	651,51	209,26	165,91	1125,9	1245	311,37

NOTE:
NORM = Normal distribution function
LOG = Lognormal distribution function
EXP = Exponential distribution function
EV1 = Gumbel distribution function
GEV = Generalized Extreme Value
GL = Generalized Logistic
PEAR = Pearson Type III distribution function

Best-Fit Tests

	NORM	LOG	EXP	EV1	GEV	GL	PEAR
e	0,7959	0,2611	0,268	0,476	0,1945	0,1871	0,3765
KS	0,0937	0,005	0,6403	0,4415	0,8389	0,8389	0,4415
MSD	26,7686	13,8787	20,6741	23,202	13,8232	13,9798	16,7441

NOTE:
e = Dimensionless difference between the observed and estimated values
KS = Kolmogorov-Smirnov test
MSD = Mean Square Deviation

TUDelft

DELFT UNIVERSITY OF TECHNOLOGY

DEPARTMENT OF HYDRAULIC STRUCTURES AND FLOOD RISK

TITLE OF THE PROJECT:
RISK-BASED OPTIMIZATION OF RESERVOIR EMERGENCY OPERATION

APPENDIX: E.4

NAME OF THE APPENDIX:
STATISTICAL ANALYSIS VOLUMES

SCALE:

System Response Curves

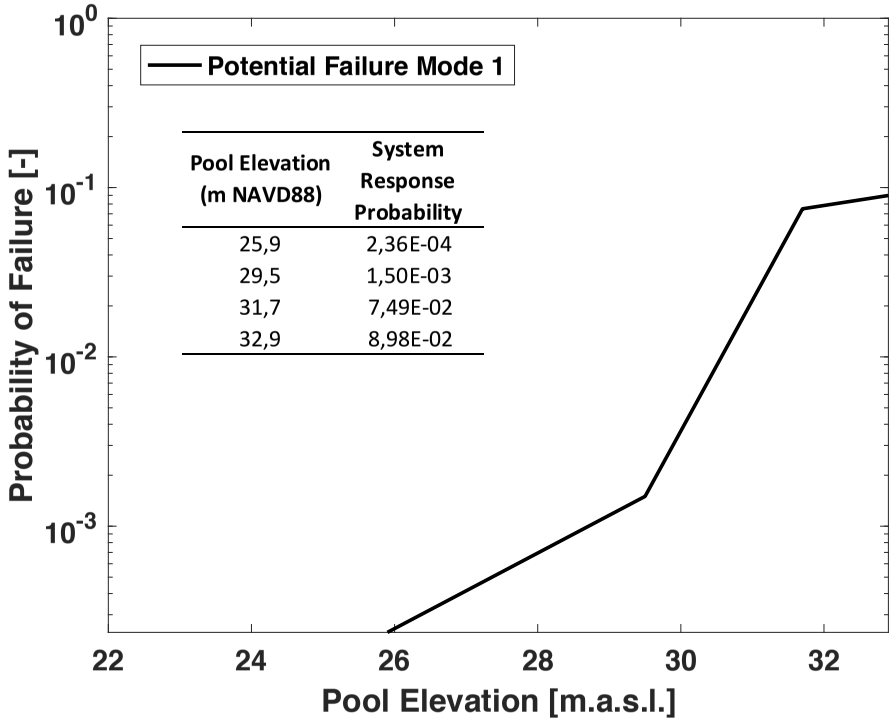

Pool Elevation (m NAVD88)	System Response Probability
25,9	2,36E-04
29,5	1,50E-03
31,7	7,49E-02
32,9	8,98E-02

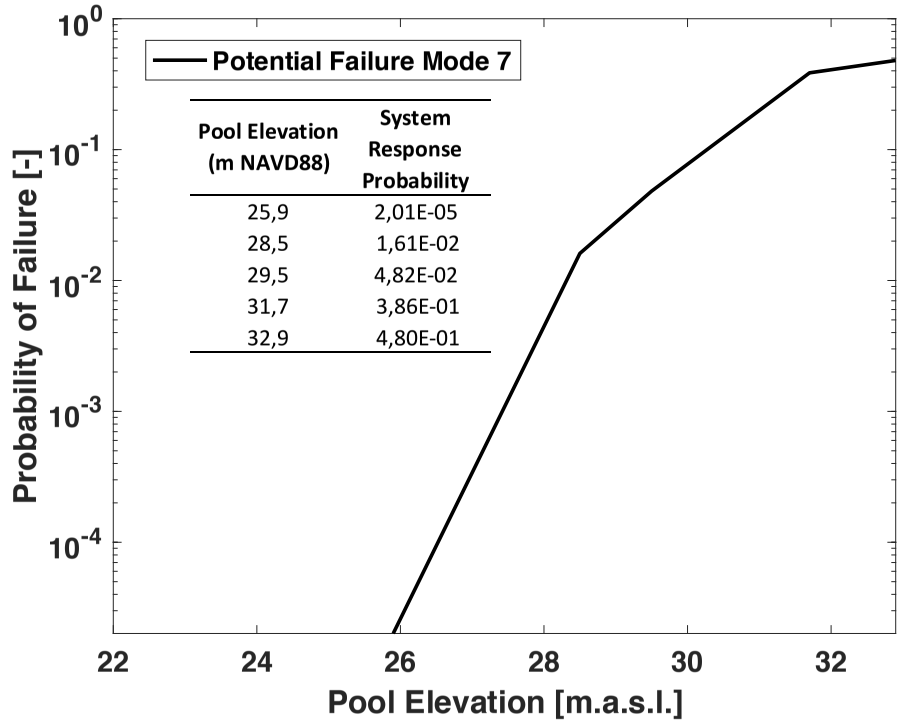

Pool Elevation (m NAVD88)	System Response Probability
25,9	2,01E-05
28,5	1,61E-02
29,5	4,82E-02
31,7	3,86E-01
32,9	4,80E-01

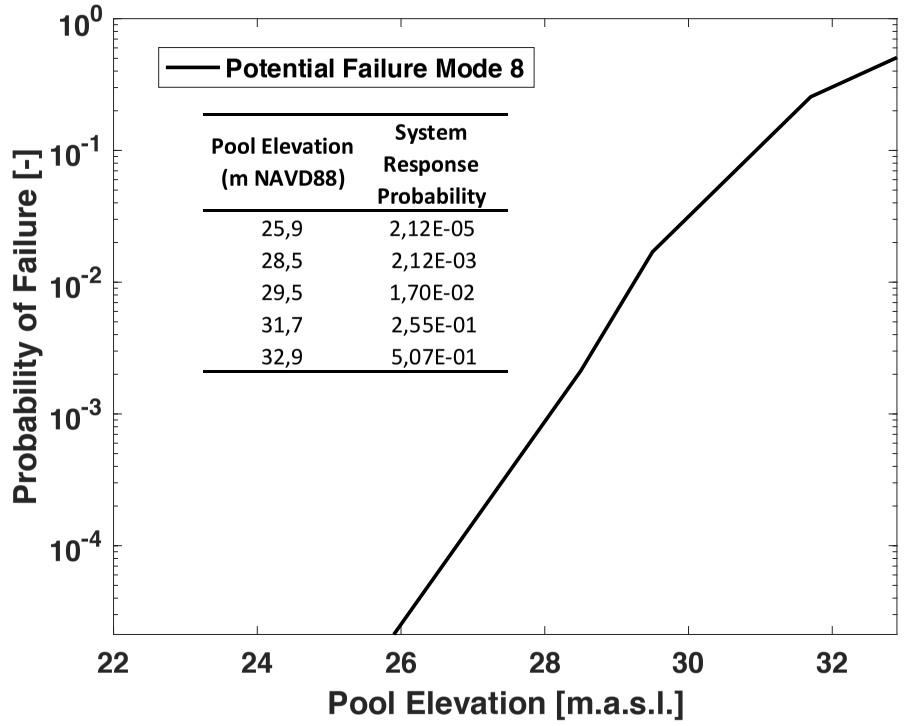

Pool Elevation (m NAVD88)	System Response Probability
25,9	2,12E-05
28,5	2,12E-03
29,5	1,70E-02
31,7	2,55E-01
32,9	5,07E-01

- **PMF 1** - ``Seepage flow along or beneath the outlet works structure due to voids or low stress areas leads to head-cut then backward erosion piping beneath the outlet works structure''.
- **PFM 7** – ``Seepage and piping in the foundation at the old Buffalo Bayou channel beneath the existing cutoff wall and exiting at the end of the stilling basin''.
- **PFM 8** – ``Seepage and piping in the foundation at the end of the cutoff trench at Noble Road''.
- **PFM 21** – ``'Hydraulic pressure in the conduit exceeds pressure outside the conduit which leads to seepage through conduits joints and erosion along conduits''.
- **PFM 23** – ``Instability of the outlet works parabolic chute slab and stilling basin retaining walls due to uplift caused by excessive seepage and/or tailwater''.

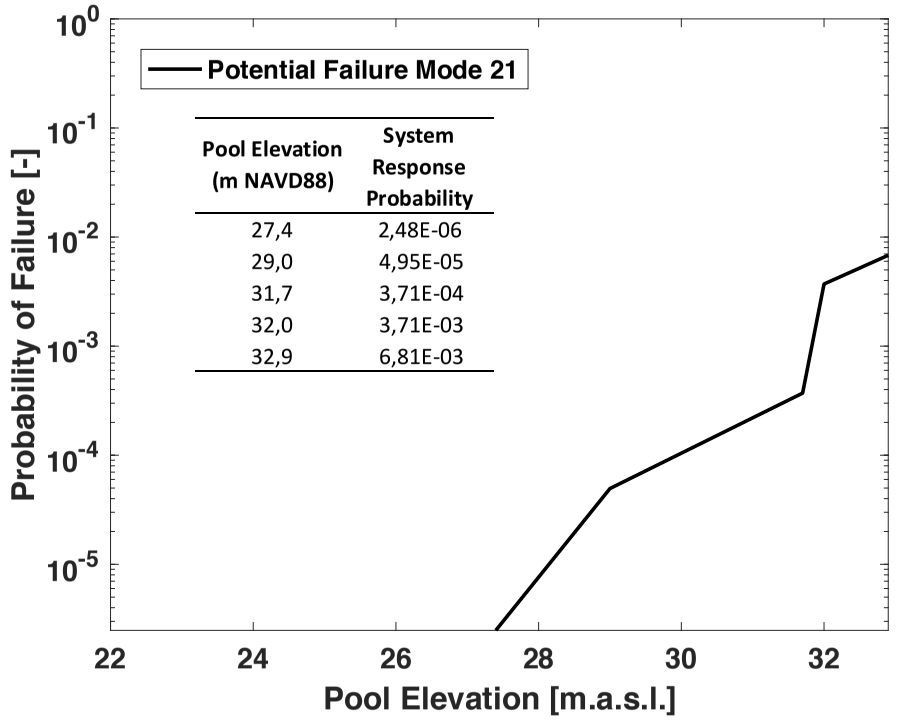

Pool Elevation (m NAVD88)	System Response Probability
27,4	2,48E-06
29,0	4,95E-05
31,7	3,71E-04
32,0	3,71E-03
32,9	6,81E-03

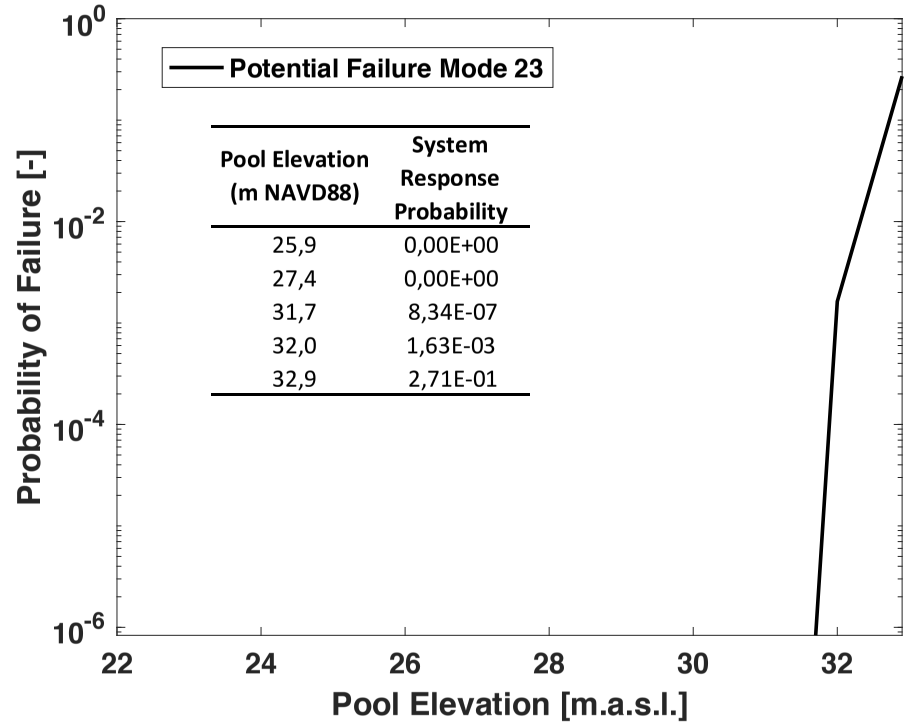

Pool Elevation (m NAVD88)	System Response Probability
25,9	0,00E+00
27,4	0,00E+00
31,7	8,34E-07
32,0	1,63E-03
32,9	2,71E-01

Source: ``Addicks and Barker Dam Safety Modification Report, USACE (2013)''

TUDelft

DELFT UNIVERSITY OF TECHNOLOGY

DEPARTMENT OF HYDRAULIC STRUCTURES AND FLOOD RISK

TITLE OF THE PROJECT:
RISK-BASED OPTIMIZATION OF RESERVOIR EMERGENCY OPERATION

APPENDIX: E.5

NAME OF THE APPENDIX:
BARKER DAM SYSTEM RESPONSE CURVES

SCALE:

Consequence Curve Upstream Flooding

Parcel Data Statistics Buffalo Bayou

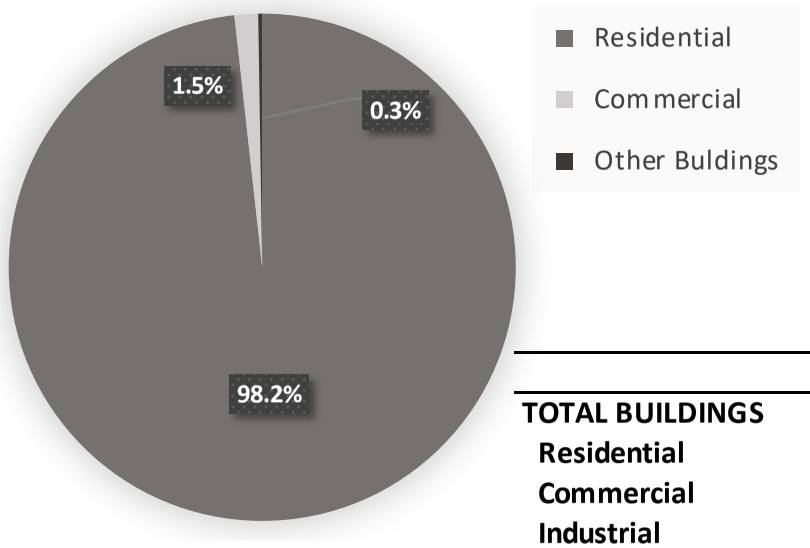

	Parcels	*% Total*	% Building
TOTAL BUILDINGS	11176	95,2	-
Residential	10980	93,5	98,2
Commercial	168	1,4	1,5
Industrial	0	0,0	0,0
Other Buldings	28	0,2	0,3
TOTAL OTHERS PARCELS	565	4,8	-

Damage Curve Barker Reservoir

	Water Surface Elevation [m NAVD88]	Property Damage (Total) [Millions $]
Government-owned Land	28,98	0
100 yr. Floodplain	29,57	14,6
Hurricane Harvey	30,97	177,7
Spillway Elevation	32,16	890,8
Dam Crest Elevation	34,47	4078,8

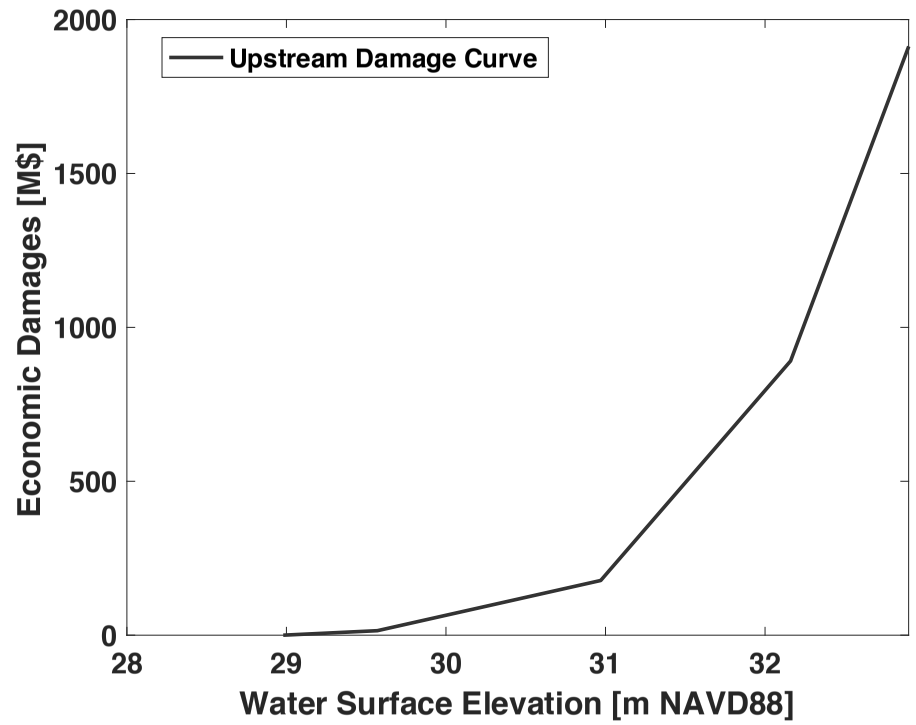

Depth-Damage Curve (JRC,2017)

Depth [m]	Damage [%]
0	0,00
0,5	0,25
1	0,40
1,5	0,50
2	0,60
3	0,75
4	0,85
5	0,95
6	1,00

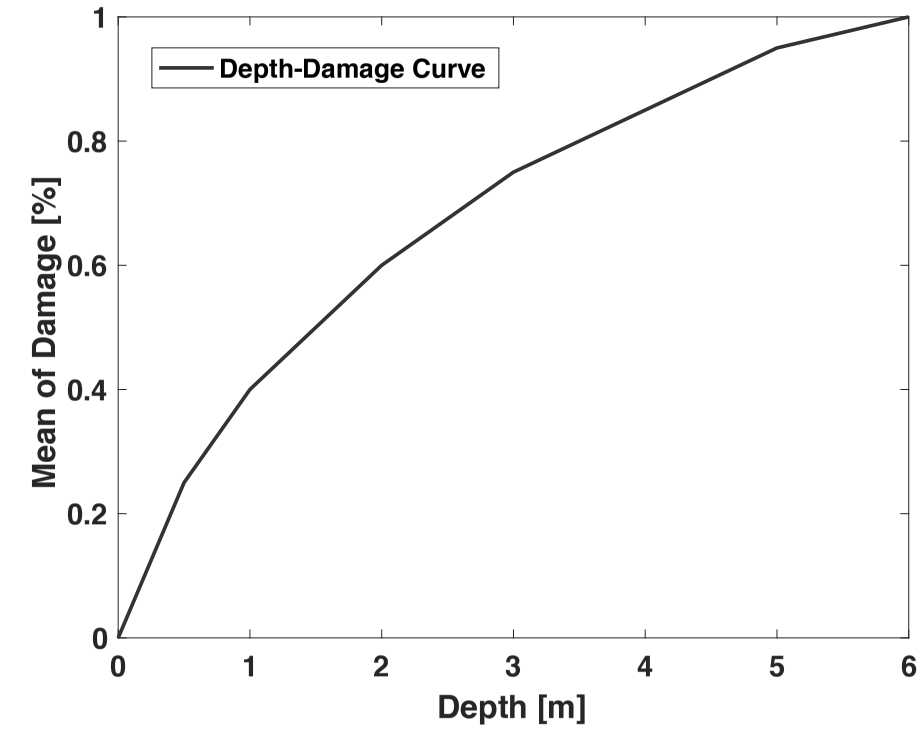

Flood Events used for the development of the Damage Curves

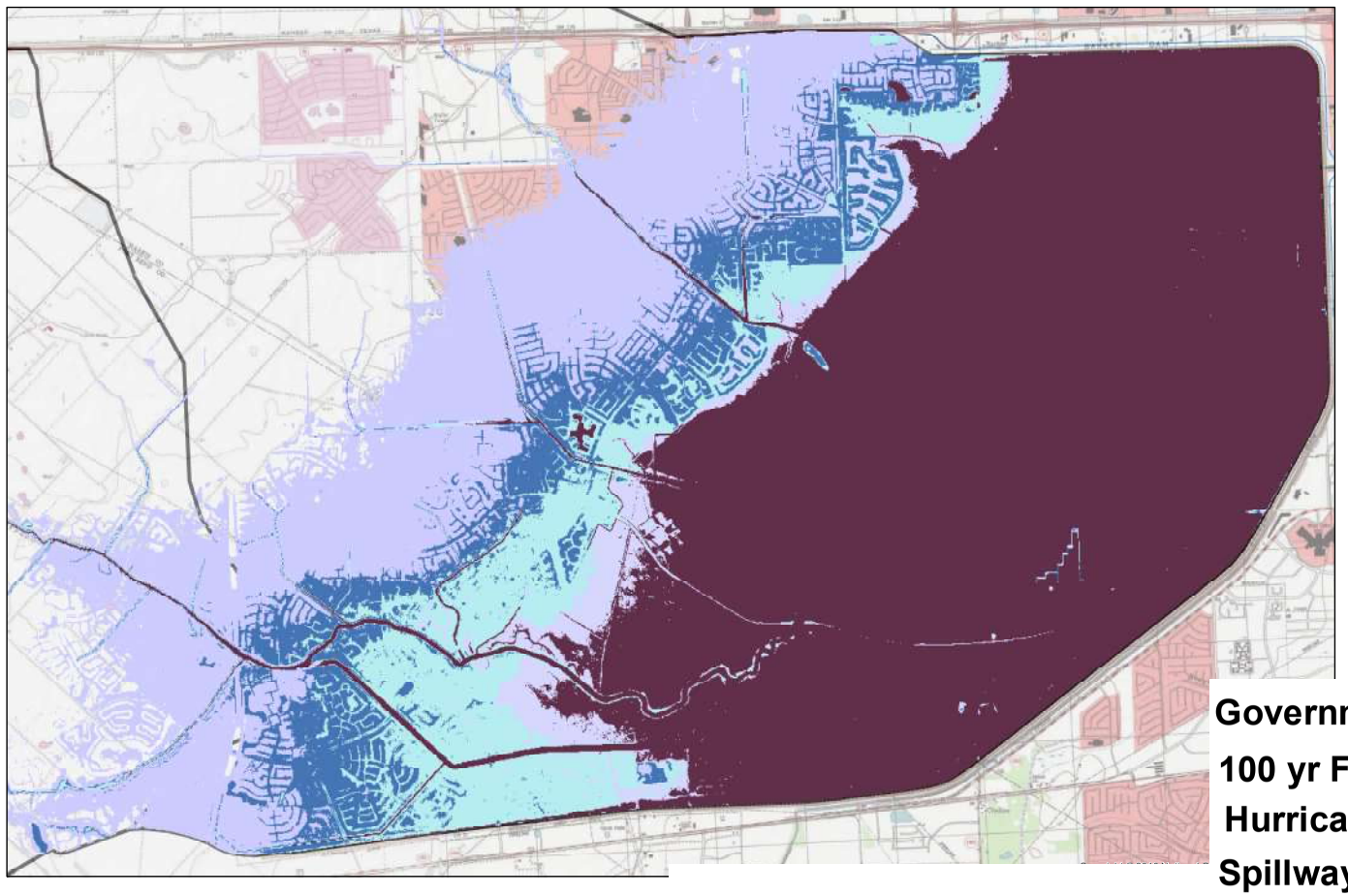

TUDelft

DELFT UNIVERSITY OF TECHNOLOGY

DEPARTMENT OF HYDRAULIC STRUCTURES AND FLOOD RISK

TITLE OF THE PROJECT:
RISK-BASED OPTIMIZATION OF RESERVOIR EMERGENCY OPERATION

APPENDIX: E.6

NAME OF THE APPENDIX:
UPSTREAM CONSEQUENCE CURVE

SCALE:

Consequence Curves Downstream Flooding

Parcel Data Statistics Buffalo Bayou

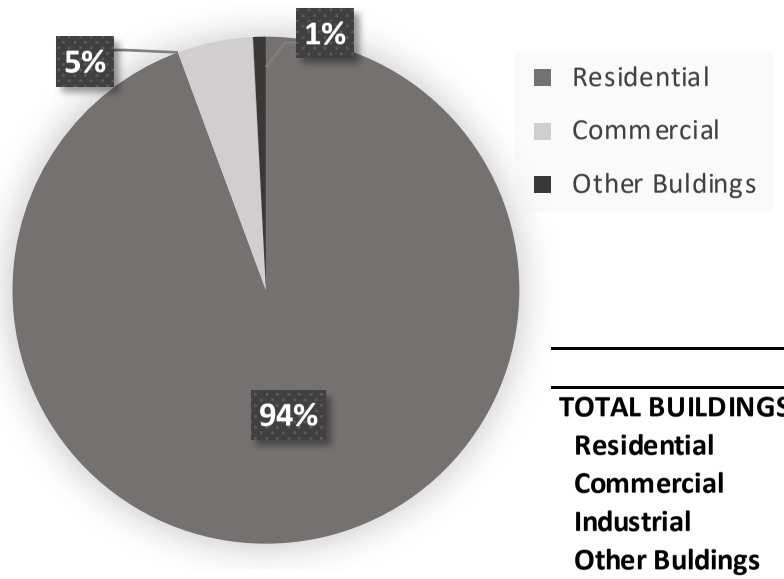

	Parcels	*% Total*	% Building
TOTAL BUILDINGS	96506	92,8	-
Residential	91061	87,5	94,4
Commercial	4627	4,4	4,8
Industrial	35	0,0	0,0
Other Buldings	783	0,8	0,8
TOTAL OTHERS PARCELS	7543	7,2	-

Damage Curve Buffalo Bayou Dam Breach Scenarios

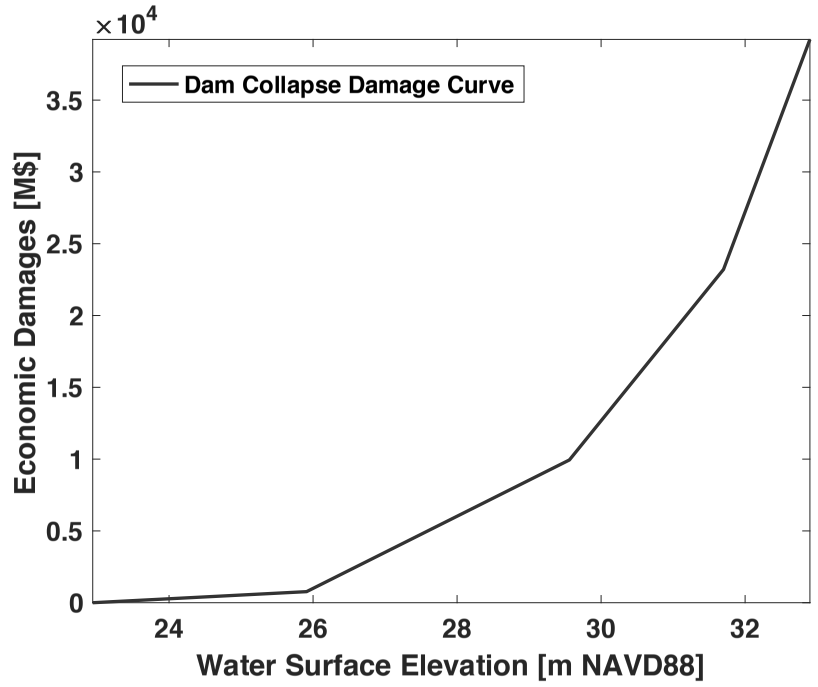

Water Surface Elevation [m NAVD88]	Property Damages [Million $]
25,91	771
29,56	9942
31,7	23208
32,9	39227

Source: ``Addicks and Barker Dam Safety Modification Report, USACE (2013)''

Flood Events used for the development of the Damage Curves

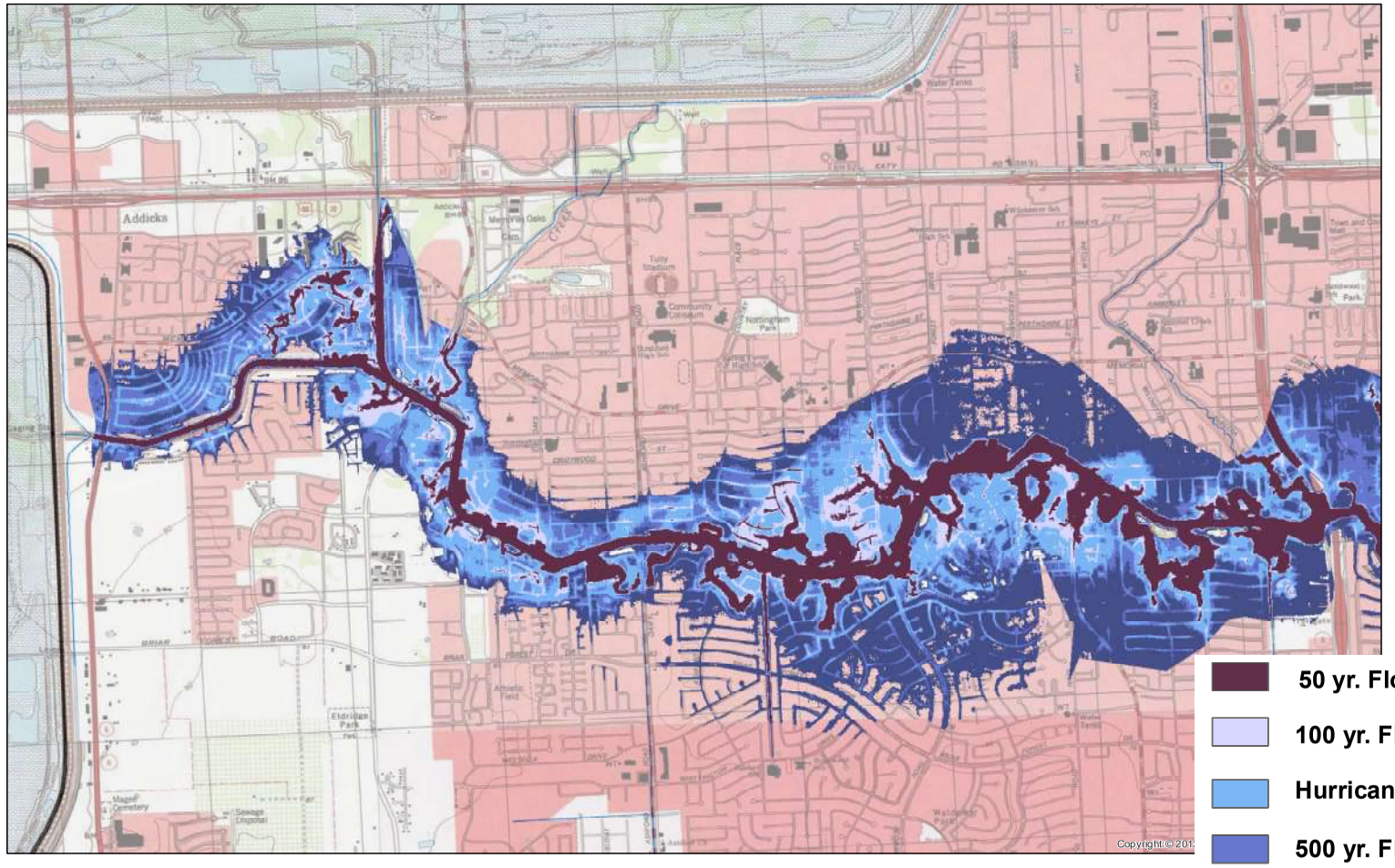

Damage Curve Buffalo Bayou Dam Outlet Works Releases Scenarios

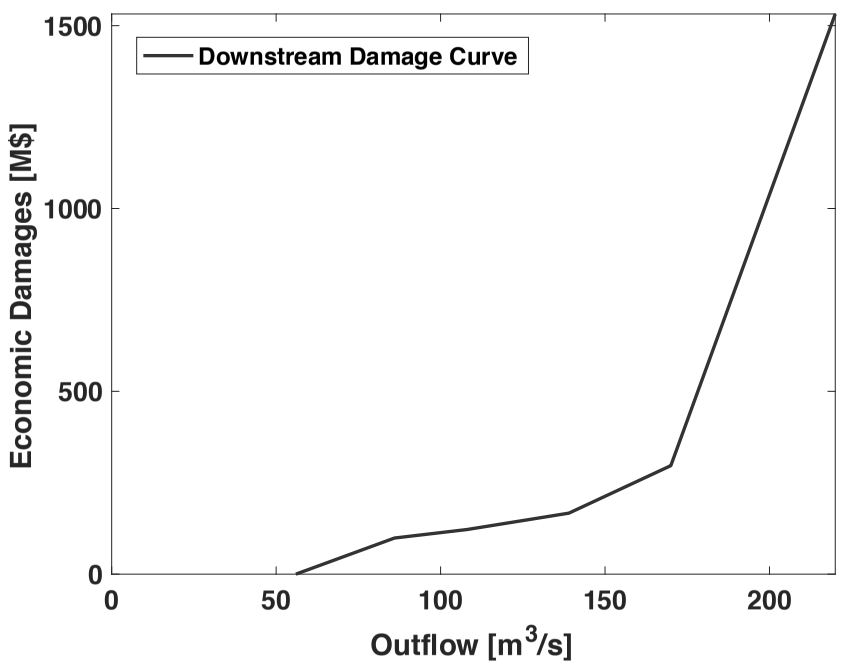

Outflow Discharge [m3/s]	Property Damages [Million $]
56	0
86	99
108	122
141	167
170	297
220	1532
2322	14190

TU Delft

DELFT UNIVERSITY OF TECHNOLOGY

DEPARTMENT OF HYDRAULIC STRUCTURES AND FLOOD RISK

TITLE OF THE PROJECT:
RISK-BASED OPTIMIZATION OF RESERVOIR EMERGENCY OPERATION

APPENDIX: E.7

NAME OF THE APPENDIX:
DOWNSTREAM FLOODING CONSEQUENCE CURVE

SCALE:

Inundation Map Barker Reservoir - Hurricane Harvey (2017)

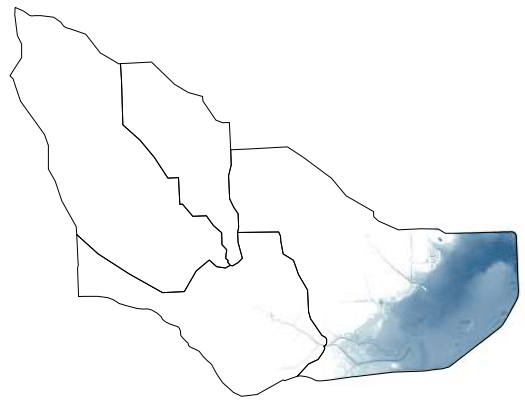

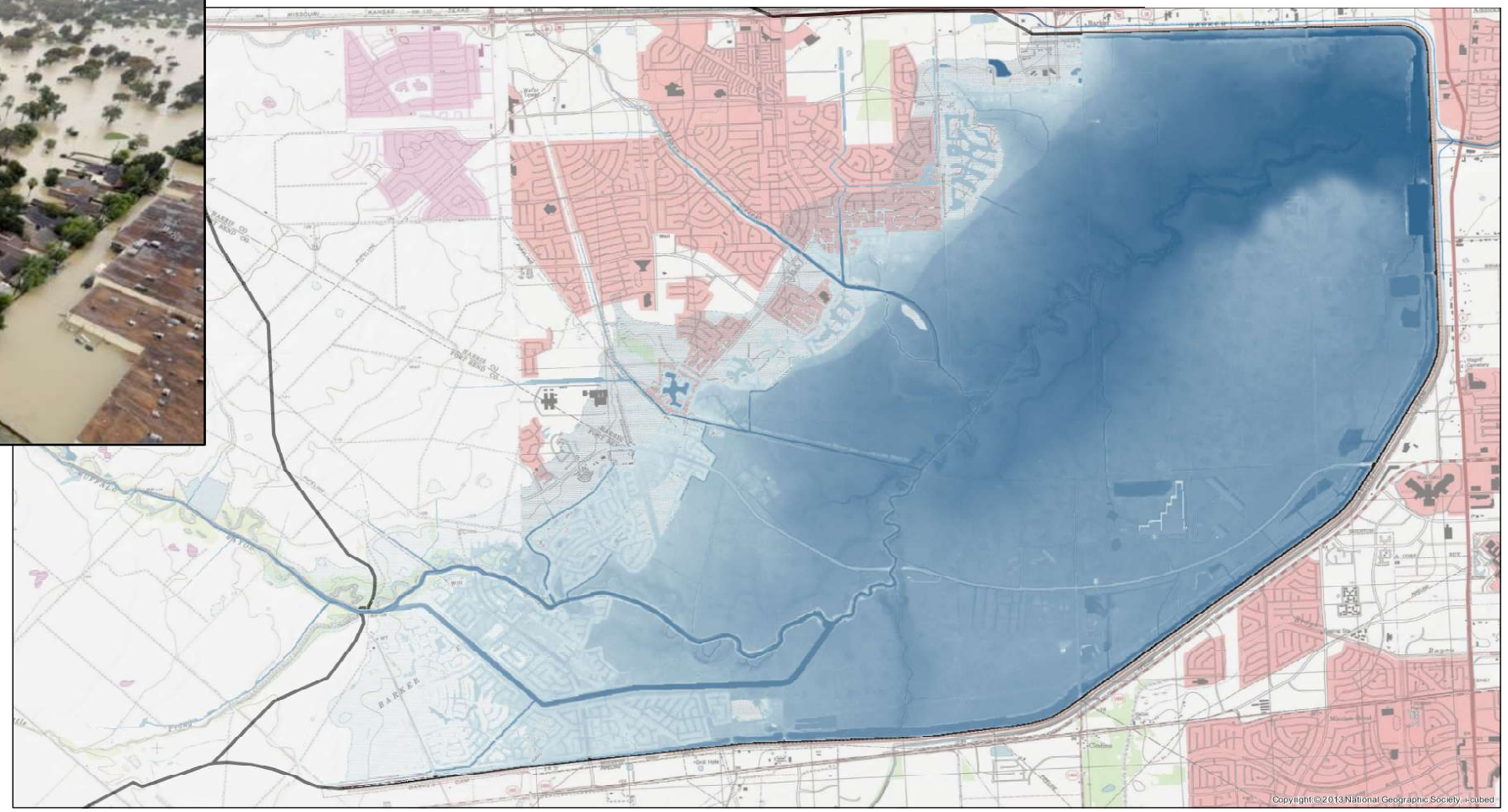

Kilometers
0 0.9 1.8 2.7 3.6 4.5

ESTIMATES	AFFECTED HOMES		ECONOMIC DAMAGES	
	HARRIS COUNTY	FORT BEND COUNTY	HARRIS COUNTY	FORT BEND COUNTY
USACE	6380		-	
FEMA	1910	-	M$ 55	-
CLAIMS	4136		M$ 183	
OBTAINED	1381	3178	M$ 92	M$ 85

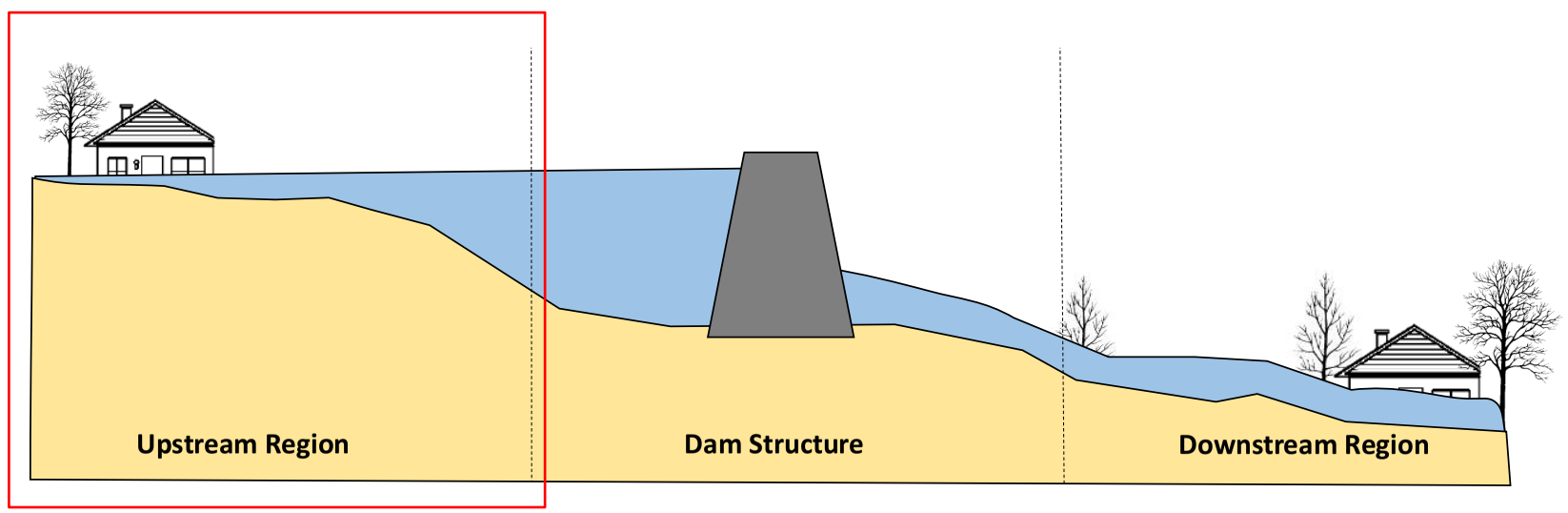

TUDelft

DELFT UNIVERSITY OF TECHNOLOGY

DEPARTMENT OF HYDRAULIC STRUCTURES AND FLOOD RISK

TITLE OF THE PROJECT:
RISK-BASED OPTIMIZATION OF RESERVOIR EMERGENCY OPERATION

APPENDIX: E.8.1

NAME OF THE APPENDIX:
FLOODING MAP HARVEY AT BARKER RESERVOIR AREA

SCALE:

Inundation Map Buffalo Bayou – Hurricane Harvey Releases (2017)

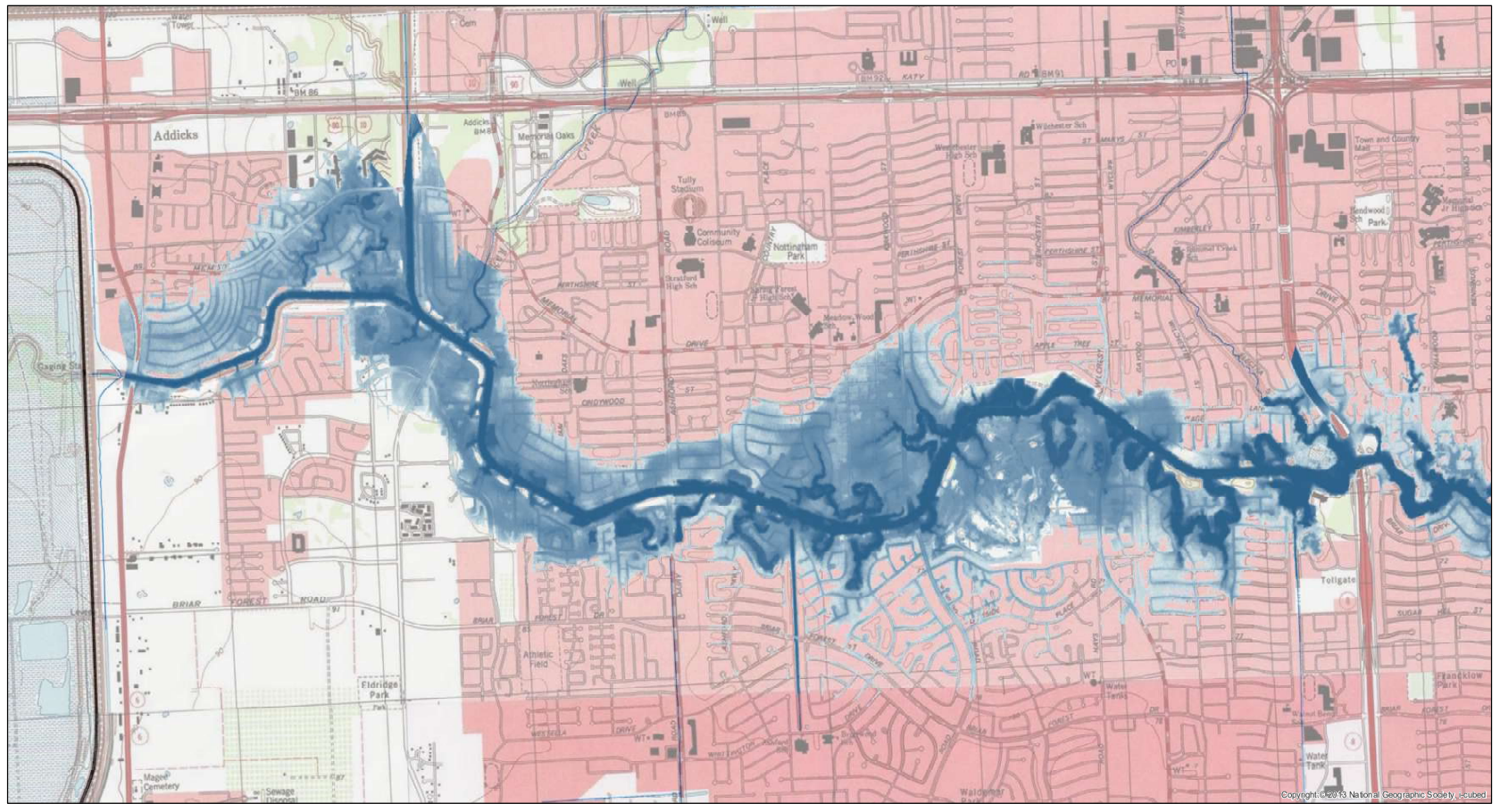


Houston Chronicle, September 2017

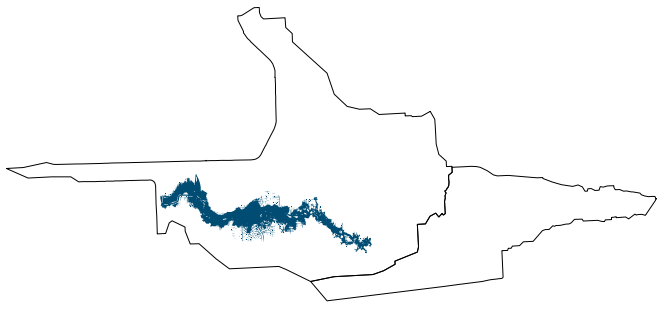

Kilometers
0 0.5 1 1.5 2 2.5

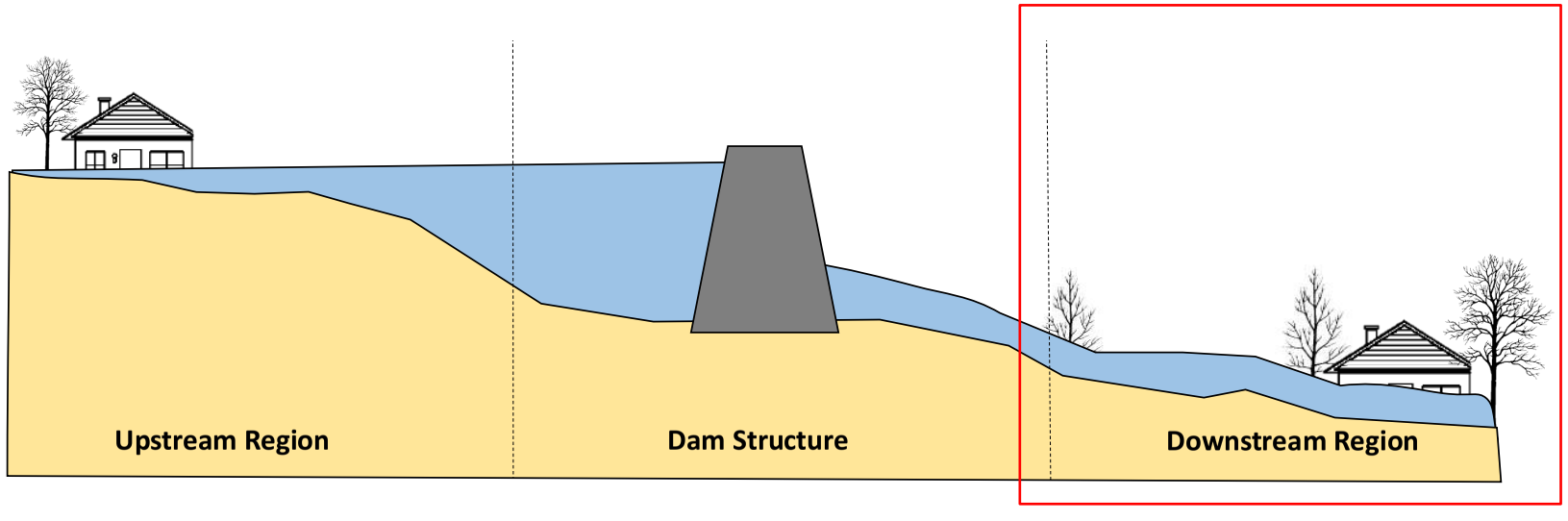

ESTIMATES	AFFECTED HOMES	ECONOMIC DAMAGES
USACE	20108	-
FEMA	17090	B$ 0.2
OBTAINED	12343	M$ 166

TUDelft

DELFT UNIVERSITY OF TECHNOLOGY

DEPARTMENT OF HYDRAULIC STRUCTURES AND FLOOD RISK

TITLE OF THE PROJECT:
RISK-BASED OPTIMIZATION OF RESERVOIR EMERGENCY OPERATION

APPENDIX: E.8.2

FLOODING MAP BUFFALO BAYOU WITH RELEASES FROM BARKER RESERVOIR DURING HARVEY

SCALE:

Risk Assessment Barker Dam-Reservoir System

Frequency-Damage Curve Barker Dam-Reservoir System

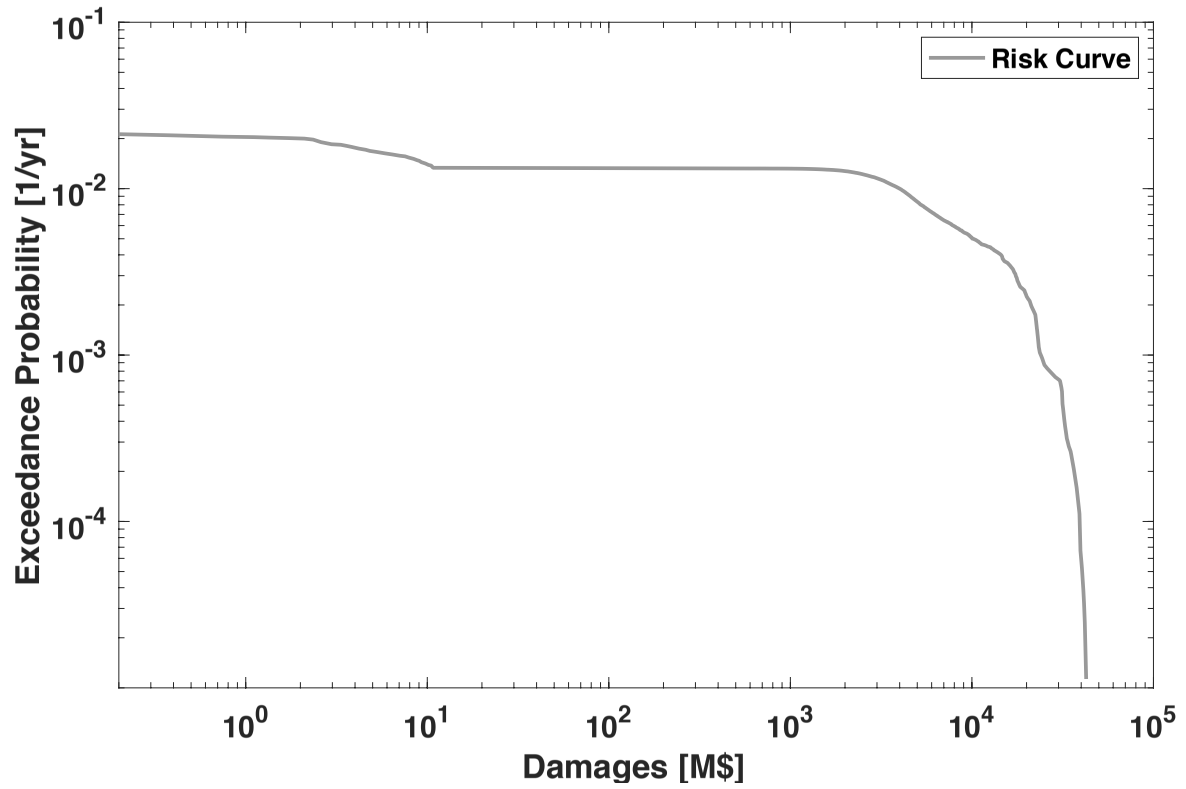

Hydrologic Event Tree Barker Dam-Reservoir System

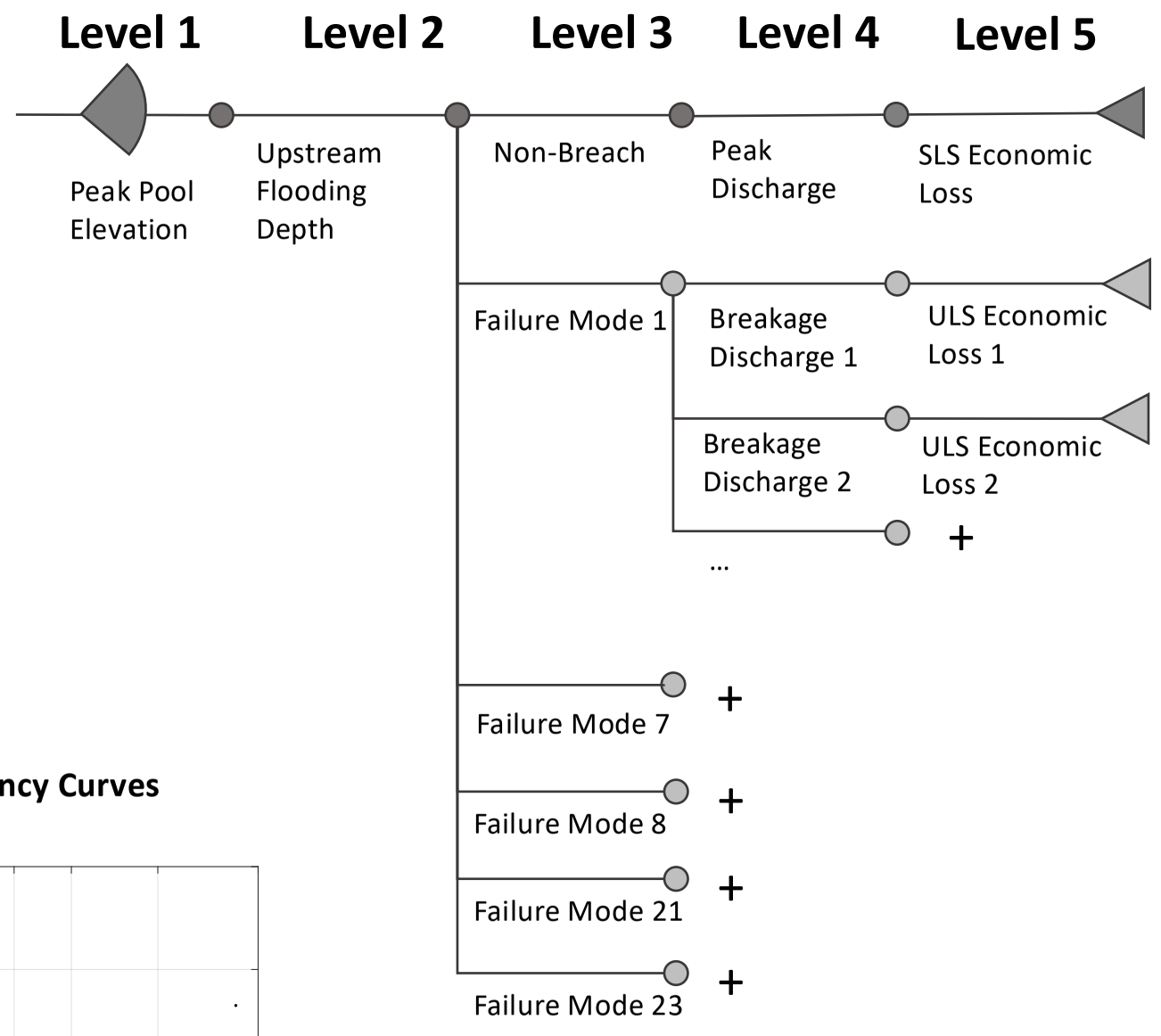

Reservoir Annual Maximum Water Surface Elevation and Reservoir Releases Frequency Curves

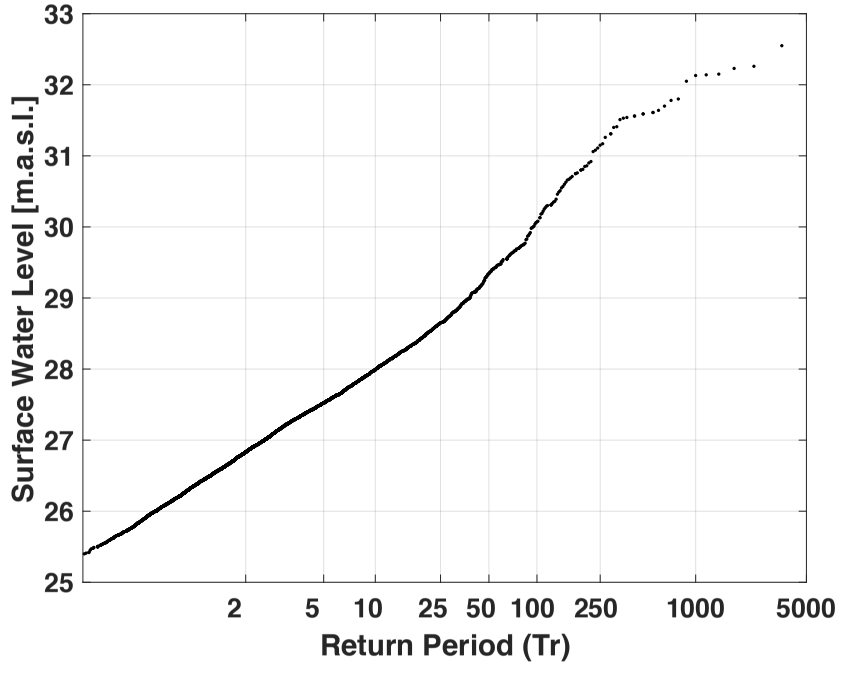

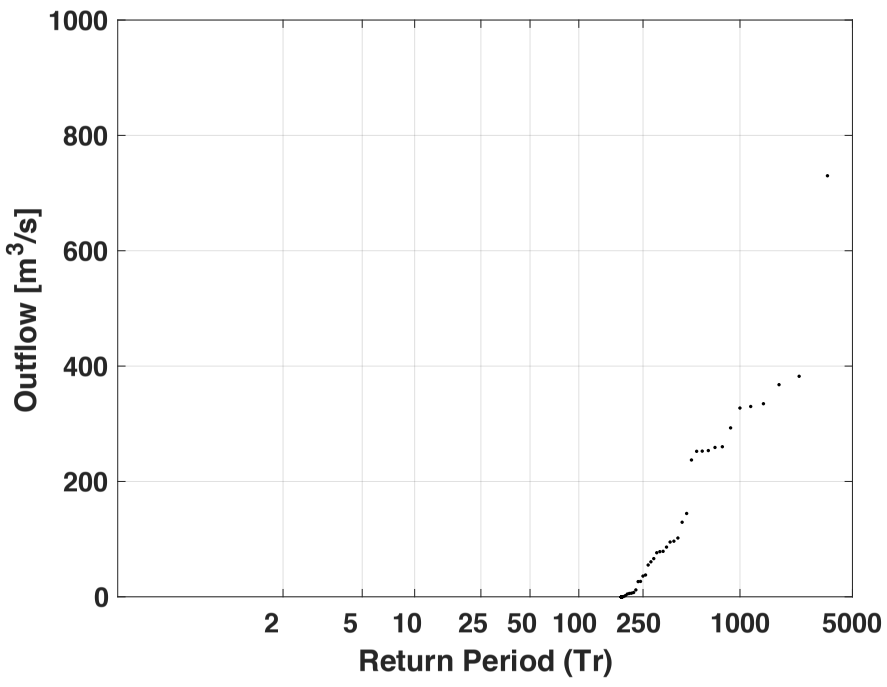

TU Delft

DELFT UNIVERSITY OF TECHNOLOGY

DEPARTMENT OF HYDRAULIC STRUCTURES AND FLOOD RISK

TITLE OF THE PROJECT:
RISK-BASED OPTIMIZATION OF RESERVOIR EMERGENCY OPERATION

APPENDIX: E.9

NAME OF THE APPENDIX:
RISK ASSESSMENT BARKER DAM-RESERVOIR SYSTEM

SCALE:

Risk Mitigation Measure Barker Dam-Reservoir System

Frequency-Damage Curve Barker Dam-Reservoir System

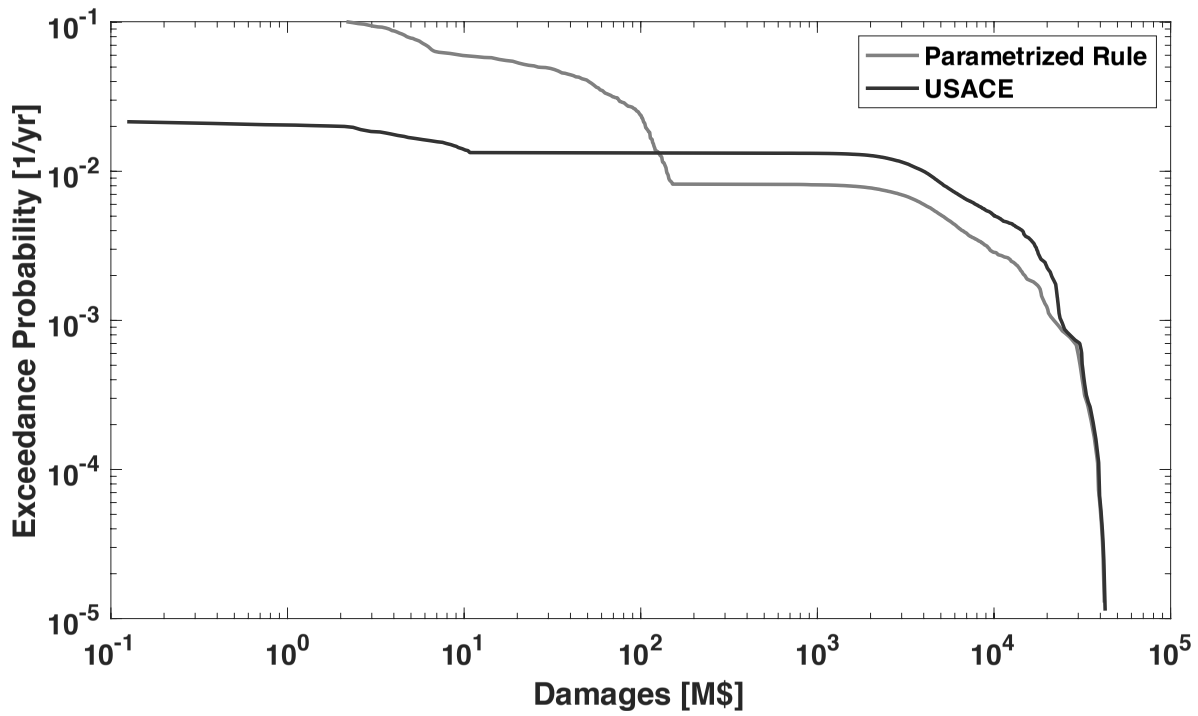

New Operating Rule for Barker Dam-Reservoir System

$$O_{j+1} = \begin{cases} \text{ZONE 3: } O_{max,j} & \text{if } \sqrt{S_j^2 + I(t)^2} > 221.4 \\ \text{ZONE 2: } O_{max,j} \cdot \left[\dfrac{\sqrt{S_j^2 + I(t)^2}}{221.4} \right]^{0.92} & \text{if } 57.3 \leq \sqrt{S_j^2 + I(t)^2} \leq 221.4 \\ \text{ZONE 1: } O_{max,j} \cdot 0.287 & \text{if } \sqrt{S_j^2 + I(t)^2} \leq 57.3 \end{cases}$$

ACTIVATION LEVEL ZONE 2: 31.12 m NAVD88
ACTIVATION LEVEL ZONE 3: 27.98 m NAVD88

FD Curve Upstream Flooding Risk

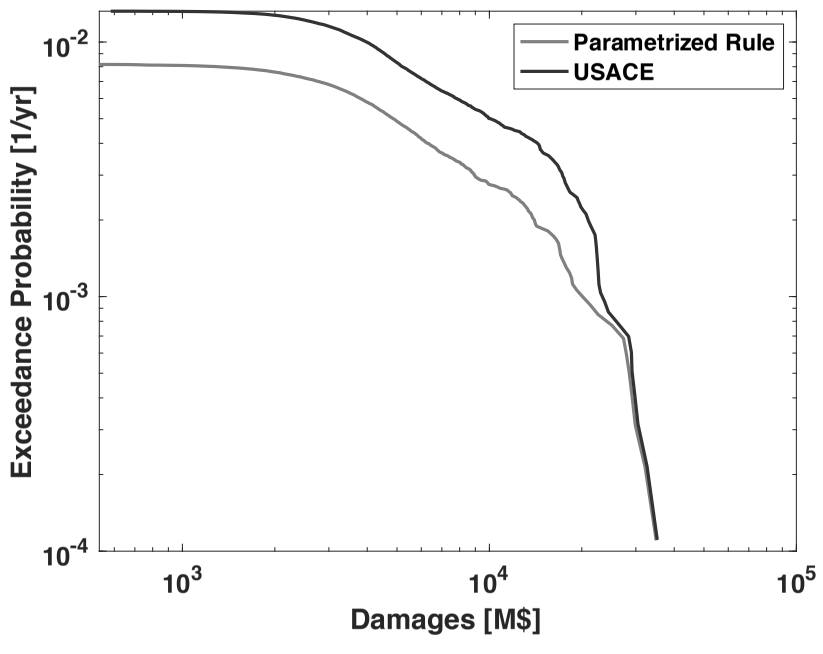

FD Curve Downstream Flooding Risk

FD Curve Structural Failure Risk

	USACE	ROMEO	RISK REDUCTION
R, SLSh	1.72	0.91	34%
R, SLSO	1.90	8.83	-
R, ULSB	141.42	83.10	40%
RT	145.04	92.84	32%

Adopting an opening strategy against extreme flood events is beneficial for the Barker Reservoir system

TU Delft

DELFT UNIVERSITY OF TECHNOLOGY

DEPARTMENT OF HYDRAULIC STRUCTURES AND FLOOD RISK

TITLE OF THE PROJECT:
RISK-BASED OPTIMIZATION OF RESERVOIR EMERGENCY OPERATION

APPENDIX: E.10

NAME OF THE APPENDIX:
RISK MITIGATION MEASURE BARKER DAM-RESERVOIR SYSTEM

SCALE: